

State of the Art and Practice in Fatigue Cracking Evaluation of Asphalt Concrete Pavements



State of the Art and Practice in Fatigue Cracking Evaluation of Asphalt Concrete Pavements

Version 1.0

An experimental and numerical synthesis from the mid-1990s to 2016

Edited by:

Andrew Braham, University of Arkansas
B. Shane Underwood, Arizona State University

October 2016

This document represents the combined efforts of over fifty leaders in academia, industry, and government agencies. While the document was compiled by Andrew Braham and Shane Underwood, with assistance from the Association of Asphalt Paving Technologists (AAPT) board members, most work was performed by the people listed in the table on the next page. This document went through a full review by all contributing authors before release.



NC STATE UNIVERSITY



THE UNIVERSITY OF
TENNESSEE

TEXAS A&M
UNIVERSITY



UF UNIVERSITY OF
FLORIDA

THE UNIVERSITY OF
KANSAS

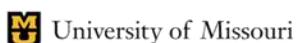


Table of Contributing Authors

Author	Affiliation	Section(s)
Imad Al-Qadi	University of Illinois Urbana Champaign	5.2.2
L. Babadopoulos	University of Lyon	6.3.2
Andrew Braham	University of Arkansas	5.2.4, 6.1, 6.4.1
Bill Buttlar	University of Missouri	5.1.3
Brian C. Hill	Illinois Department of Transportation	5.1.3
Bernardo Caicedo	Universidad de los Andes	5.1.4
Wei Cao	Louisiana Transportation Research Center	5.2.1
Silvia Caro	Universidad de los Andes	5.1.4
Daniel Castillo	Universidad de los Andes	5.1.4
Cassie Castorena	North Carolina State University	2.2.2
Don Christensen	Advanced Asphalt Technologies	6.3.3
Herve Di Benedetto	University of Lyon	6.3.2
Samuel Cooper, III	Louisiana Transportation Research Center	5.2.1
Masoud Darabi	University of Kansas	6.3.4
Mostafa Elseifi	Louisiana State University	5.2.1
Fan Gu	Texas Transportation Institute	5.1.5, 6.4.2, 7.2
Padmini Gudipudi	Arizona State University	5.1.2
David Hernando	University of Florida	2.1.3
Sheng Hu	Texas Transportation Institute	5.1.5
Baoshan Hao	University of Tennessee	5.1.7
Carl Johnson	Stark Pavement Corp.	2.1.1
Kamil Kaloush	Arizona State University	6.4.3
Richard Kim	North Carolina State University	6.3.1
Chulseung Koh	Korean Intellectual Property Office	5.1.6
Dallas Little	Texas A&M University	6.3.4
George Lopp	University of Florida	5.1.6
Xue Luo	Texas Transportation Institute	5.1.5, 6.4.2, 7.2
Robert Lytton	Texas A&M University	5.1.5, 6.4.2, 7.2
Eyad Masad	Texas A&M University at Qatar	6.3.4
Louay Mohammad	Louisiana State University	5.2.1
Carl Monismith	Retired – University of California Berkeley	5.1.1
Airam Morales	University of Arkansas	5.2.3
Hasan Ozer	University of Illinois Urbana Champaign	5.2.2
Adriaan Pronk	Retired	6.2.4
Reynaldo Roque	University of Florida	2.1.3, 5.1.6, 6.2.2
Geoff Rowe	Abatech	5.1.1, 6.2.1
Tom Scullion	Texas Transportation Institute	5.1.5
Yongguk Seo	Kennesaw State University	5.2.5
Cedric Sauzeat	University of Lyon	6.3.2
Shihui Shen	Pennsylvania State University, Altoona	5.1.3, 6.2.3
Sadie Smith	University of Arkansas	5.2.3
Jeff Stempihar	Arizona State University	6.4.3
Shane Underwood	Arizona State University	2.1.2, 2.2.1, 2.2.2, 6.3.1, 7.1
Shenghua Wu	University of Illinois Urbana Champaign	5.1.3
Yu Yan	University of Florida	2.1.3
Waleed Zeiada	University of Sharjah	5.1.2
Weiguang Zhang	University of Florida	6.2.3
Yuqing Zhang	Aston University	5.1.5, 6.4.2, 7.2
Fujie Zhou	Texas Transportation Institute	5.1.5
Jian Zou	University of Florida	6.2.2

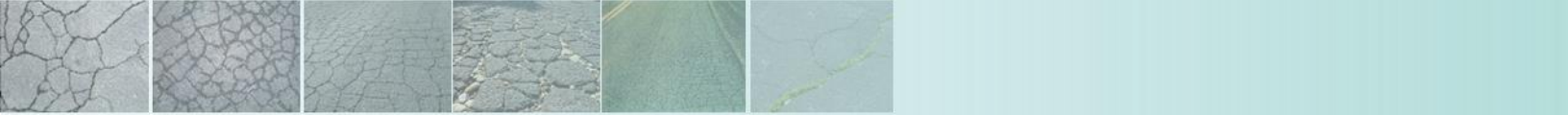


Table of Contents

1.	Introduction.....	1
2.	Asphalt Binder Studies	3
3.	Crack Process, Damage Growth, and Macrocracking.....	17
4.	Structural Influence on Cracking and Pavement Fatigue Analysis Techniques.....	17
5.	Material Fatigue Assessment	18
6.	Asphalt Mixture Analysis Theory.....	68
7.	Healing.....	118
8.	Going Forward.....	125
9.	References.....	128



Executive Summary

This document intends to summarize the current body of knowledge of fatigue cracking. It is not intended to be a comprehensive document that answers all questions, but more a resource that gives a summary of the different experimental and numerical options available to understand fatigue cracking. These summaries provide a review of the development of each option and provide reference for further examination.

Chapter 1 provides an introduction to fatigue cracking. This includes a background of existing fatigue cracking resources, a context of cracking, the influence of cracking, and the increased relevancy of cracking. Chapter 2 begins with the experimental perspective of fatigue cracking of asphalt binders. This includes the repeated loading test, the double edge notched test, and the binder fracture energy test. Chapter 2 continues with a numerical perspective of fatigue cracking, discussing rheological linkages, the linear amplitude sweep (LAS) procedure, and the continuum damage model. Chapters 3 and 4 provide a bridge between binder and mixture work. Chapter 3 discusses crack process, damage growth, and macrocracking, while Chapter 4 examines the structural influence of pavements on cracking and fatigue.

Chapter 5 begins the discussion of asphalt mixtures with the experimental approach, beginning with the traditional four-point bending beam test, followed by the cylindrical geometry. Next, the indirect tension test is covered. While this configuration was originally designed for low temperature cracking, it has also been adapted to capture fatigue properties. The trapezoidal test has been used outside of the United States and is followed by the overlay tester. Chapter 5 finishes by covering the dogbone test configuration, and the loaded wheel tester. All of these asphalt mixture tests do not have notches, but there are a number of tests that have been developed that require the insertion of a notch. These tests include the Semi-Circular Bend test (both the LTRC and I-FIT configuration), the Disk-Shaped Compact Tension, the Single-Edge Notch Beam, and the Double Edge Notch Prism test. While some of these tests were originally developed for monotonic loading (often low-temperature or reflective cracking related), there are possibilities and have been applications for these tests to move into the realm of fatigue cracking.

Chapter 6 moves into the theory behind fatigue cracking. This chapter starts with a general fatigue and empirical fatigue approach, and then moves into energy and energy inspired methods. Energy methods include dissipated energy, energy ratio, ratio of dissipated energy change, and the asphalt concrete pavement fatigue model. The next section of theory focuses on continuum damage methods. This section begins with the viscoelastic continuum damage model, and then moves into the French method, the reduced cycles approach, and the Texas A&M University approach. The final section of Chapter 6 covers fracture methods involving fatigue cracking. First, a review of the roots of elastic fracture mechanics is provided, followed by the distributed continuum fracture and the C^* fracture test.

The final chapter of the existing work, Chapter 7, reviews the concept of healing of fatigue cracks. First, the continuum damage healing is reviewed, followed by distributed continuum healing. Finally, the document concludes by discussing the work that needs to be done. This includes diving deeper into the relationship to the binder structure and composition (referred to as genome), the sensitivity of both experimental and numerical methods, and the dearth of comparisons across multiple geometries and models. The final chapter of the document, Chapter 8, discusses limitations of this document and areas that should be considered in future research of fatigue cracking.

It is hoped that this document is a living document, and is updated on a regular basis in order to stay up to date and current. With over one hundred pages of text, there has been a significant amount of work performed on fatigue cracking, but it is fully acknowledged that there is still much to do.



1. Introduction

While research on asphalt materials (also known as asphalt concrete, bituminous concrete, Hot Mix Asphalt, etc.) is a dynamic process, the overall goals of these efforts have not changed over the years. Engineers and researchers attempt to make infrastructure last longer while balancing economic and social impacts. With the increased interest in sustainability, these goals also include reducing emissions (by using technologies such as Warm Mix Asphalt) and reusing materials (by utilizing materials such as Recycled Asphalt Pavements). As new technologies and materials are introduced through research and practitioners, issues may occur with long term performance, and the cycle repeats with more research providing solutions. With asphalt materials, long term performance is described according to different metrics. The FHWA Distress Identification Manual lists and describes fifteen common distresses in asphalt concrete pavements and among these, one of the most significant groups is cracking, specifically fatigue cracking (Miller and Bellinger, 2003). This document looks to synthesize the current state of the art of research and knowledge in fatigue cracking, to help us better understand what we have used in the past, what we are currently using, and what we could use in the future to extend the life of our pavement infrastructure.

There have been several documents over the years that have synthesized the state of the art of research and knowledge with asphalt materials. In 1999, the Association of Asphalt Paving Technologists (AAPT) put together a 75th anniversary compilation of papers that included:

- A history of AAPT
- Additives in asphalt
- Materials, design, and characterization of asphalt mixes
- Developments in the structural design and rehabilitation of asphalt pavements
- Producing and placing hot mix asphalt
- Quality initiatives
- Pavement management, maintenance, and rehabilitation

This series of papers were published in a special volume (68A) that acts as a strong reference to the state of the art in asphalt mixtures in the late 20th century. Around the same time, the Superpave mix design was also being introduced in the United States, leading to a series of in-depth reviews of asphalt mixtures. While AAPT provided a slightly broader approach, covering almost all bases of asphalt mixtures, the Superpave reports drilled deeply into many areas of asphalt mixtures with the publication of dozens of reports and summaries. From binder characterization and evaluation, to low-temperature cracking, to performance prediction models, the SHRP reports provide a wealth of information. There have been many advances in the intervening years since the conclusion of SHRP and an in-depth synthesis of this information has been lacking. The objective of this document is to provide this synthesis. The document itself loosely begins where SHRP-A-404 (Fatigue Response of Asphalt-Aggregate Mixes) ends and therefore, there is very little information on fatigue cracking pre-1994, where the University of California Berkeley left off upon publication of SHRP-A-404 (Monosmith, 1994). Intermediate documents of note since this work in the 1990s including RILEM in 2004, which synthesized various test methods and models, but acknowledged that more investigations are needed (Di Benedetto *et al.*, 2004), Andre Molenaar in 2007 (Molenaar, 2007) who reviewed various tests and determined that the method of analysis should be independent of the test, and NCHRP 9-57, which recommended a suite of tests depending on the type of cracking of interest (Zhou *et al.*, 2016).

This document will not promote any one fatigue cracking testing geometry, or any one fatigue cracking model. In addition, it will not delve into proper construction practices to minimize the potential of fatigue cracking, or how to track fatigue cracking over the long-term. This document is meant to be a resource for those interested in learning about the different approaches to quantifying, capturing, and predicting fatigue cracking that have been attempted in the laboratory and on the computer. In addition, plenty of references have been provided for those wishing to dig deeper into any one topic area. Each section was written by the experts in that particular area in order to provide the reader with the most accurate and up to date information on that topic and to provide both a basic understanding, and additional resources for further learning.

1.1. Context of Cracking

Pavements are design to provide the following: 1) a safe traveling surface, 2) the structural capacity for loads applied, 3) smoothness, 4) drainage of water, and 5) surface friction to prevent vehicle slippage. There have been several structural pavement design strategies available over the years, from the Group Index Method to the Transport and Road Research Laboratory in the UK to Pavement-ME (Monismith and Brown, 1999). Pavement



deterioration can quickly occur if the structural pavement design is inadequate. If loads that exceed the design limits are applied to a road, severe rutting and cracking can quickly occur. If the roadway is not properly rehabilitated, the continued application of these loads will turn the road into essentially a gravel surface.

In addition to the importance of structural adequacy for pavements, the mixture properties of asphalt concrete are also critical and may not be separable from the structural design. Similar to structural pavement design, there have been several mix design strategies available over the years, including the Marshall Method, the Bailey Method, the BS EN 13108-1 (British Standard/European Standard), and the Superpave Mix Design Method. While there are pros and cons to each one of these methods, each essentially provide the same guidance for the same goal; ensure that the proper blend of asphalt binder and aggregates exist to provide a durable mixture. It is often the case though that explicit experimentation to ensure resistance to cracking and permanent deformation is not part of the mix design process.

Through the proper structural and mixture design, and with proper maintenance, asphalt concrete roads should provide all five design parameters discussed above through their service life. However, one of the challenges of roads is that not only are they exposed to both natural and extreme weather events day after day, but they also are exposed to repeated loads. Some of these loads may be above the design limit, whether by an individual truck or by the millions of repetitions of vehicles, and when this occurs, the pavement may begin cracking.

1.2. Influence of Cracking on Pavements

There are two primary types of cracking in asphalt concrete pavements. One type of cracking is load related, meaning the traffic the travels over the pavement causes the pavement to crack. This type of cracking can manifest itself in two ways, through fatigue cracking or through reflective cracking. Fatigue cracking, whether bottom up or top down, reflects the repeated loads causing incremental damage that over time accumulates into a macro crack, while reflective cracking is when there is an existing flaw in the underlying layers that reflects up through a newly placed asphalt concrete layer. The second type of cracking is non-load associated, and is generally referred to as low-temperature cracking. A low-temperature crack occurs when the temperature drops, the pavement shrinks, and eventually the stress in the pavement exceeds the strength, causing a transverse crack to form. Cracking is detrimental to asphalt concrete pavements for two primary reasons. First, it lowers the ride quality, and second, it introduces a vector for faster deterioration of the roadway.

Cracking reduces the ride quality by increasing the roughness of the road. A common form of quantification for ride quality is the International Roughness Index, or IRI. The IRI, in short, calculates the deviation from a smooth surface by measuring the vertical deflections of a road over a distance, whether inches/mile or meters/kilometer. Once a crack is formed in an asphalt concrete pavement, the pavement begins to move both horizontally and vertically, thus increasing the IRI. This movement also creates a less pleasant driving experience, as vehicles begin moving up and down and the noise level is increased. Unfortunately, once a crack starts, if it is not properly maintained, it can increase in severity quickly.

If a crack is very quickly cleaned and filled with a sealant, in theory, it should not cause further problems. But if it is not sealed, or if the sealant pops out due to lack of cohesion to the existing pavement, water and debris enter the crack. If water enters the crack, it can freeze and expand, thus increasing the size of the crack. If debris enters the crack, it prevents the pavement from being able to expand and contract, which cause more cracking to occur. Either way, the roadway deteriorates rapidly, thus reducing the service life and reducing the ride quality to the driver.

1.3. Increased Relevancy of Cracking

In addition to lowering the ride quality and increasing deterioration of a road, design strategies have also caused an increase of cracking on asphalt concrete roads. On a national level in the United States, the Superpave Mix Design Method replaced the Marshall Mix Design Method in the late 1990s. This transition continues at a state and local level. However, one of the weaknesses of the Marshall Mix Design Method is that the mixtures tended to rut over time. The Superpave Mix Design Method was developed to balance the rutting and cracking characteristics of asphalt concrete, but some believe that it went a bit too far and has produced dry mixtures, that are highly resistant to rutting but are susceptible to cracking. While the pendulum continues to swing and the mix designs are believed to be more balanced after small changes to the Superpave Mix Design Method, balancing rutting and cracking continues to be a challenge for the asphalt concrete industry.

In addition to changing mix design methods, a second design strategy has led to an increase in cracking, the addition of recycled materials. Asphalt binder is the most expensive component of asphalt concrete, so agencies and industry are constantly looking for ways to optimize the amount of asphalt binder put into mixtures. With the



addition of Recycled Asphalt Pavement (RAP) and Recycled Asphalt Shingles (RAS), the amount of virgin asphalt binder has been decreased in asphalt concrete mixtures. However, this decrease of virgin asphalt binder has occasionally produced dry mixtures, and with the new Superpave Mix Design, increased the amount of cracking. Again, over time, these issues have been addressed but continue to emphasize the importance of recognizing cracking as a relevant topic.

2. Asphalt Binder Studies

Except for extreme cases when weak or broken aggregates are used, the actual failure due to continuous loading occurs at either the asphalt-to-aggregate interface (adhesive) or within the asphalt itself (cohesive). It is not surprising then that research shows that fatigue cracking performance of asphalt mixture is largely influenced by the properties of the asphalt binder (Soenen *et al.*, 2003). So although the focus of this paper is a review of cracking principles in asphalt concrete mixtures, the very fact that these cracks originate and propagate through the asphalt cement binder suggests that this discussion should include at least a broad overview of the state of the knowledge in asphalt binder cracking.

At a basic level, cohesive and adhesive failures can be understood by using the concept of surface energy, which explains and quantifies the amount and origins of the energy available at the surface of solids and liquids. In asphalt concrete, the amount of this energy available in on the surface of asphalt cement governs the cohesive phenomena and the combined amounts at the asphalt and aggregate surface govern the adhesive phenomena. Bhashin *et al.* (2006) developed methodologies to reliably measure the surface energy of both asphalt and aggregate. They also applied these methodologies to characterize asphalts and asphalt-aggregate combinations and showed correlations between fatigue, moisture damage, and fracture (Little *et al.* 2006). Others have followed similar approaches to and demonstrated connections between surface energy and asphalt mixture performance (Wasiuddin *et al.*, 2006; Bhasin *et al.*, 2007; Arabani and Hamed, 2010; Wei and Zhang, 2014; Grenfell *et al.*, 2015; Aguiar-Moya *et al.*, 2015; Cong *et al.*, 2016).

Surface energy approaches offer scientific insight into the fatigue phenomenon, but the quantitative link between surface energy and cracking is not known. Hence many of the studies in this literature still rely on empirical correlations between surface energy behavior and fatigue performance. A much larger body of literature has been collected based on rheological investigations of asphalt cement binder and asphalt mastics, which consist of a blend of asphalt binder and filler-sized particles (generally passing the 75 μm sieve).

2.1. Test Method

2.1.1. Repeated Loading Test

Overview. The search for an improved asphalt binder fatigue test method is an on-going effort related to the improvement of asphalt specifications. The current specification practice of measuring linear viscoelastic dynamic shear modulus and phase angle does well to evaluate the effect of long-term aging on the material properties of asphalt, but it does not include actual evaluation of resistance to damage. Additionally, it does not account for the effect of pavement structure or traffic loading, as it is measured at only one load amplitude and frequency. During the National Cooperative Highway Research Program (NCHRP) Project 9-10, a test method was proposed that applies repeated cyclic loading to a binder specimen using the Dynamic Shear Rheometer (DSR), known as the time sweep (Bahia *et al.*, 2001). The new test was designed to mimic mixture testing and, although developed independently, has its basis in work done in the early 1960's (Pell, 1962). The main benefit to this test is a direct application of fatigue-type loading, and if performed at sufficient stiffness levels, relevant fatigue performance indicators can be measured (Anderson *et al.* 2001; Martono *et al.* 2007). However, the suitability of this test for use in specification is questionable due to the possibility of long testing times. Hence, recent work on binder fatigue has focused on the search for test procedures that can be used as "accelerated" fatigue tests (Andriescu *et al.*, 2004; Martono and Bahia, 2008; Johnson *et al.*, 2009). Multiple test procedures have been under investigation for their abilities to act as a surrogate to the time sweep test. These "accelerated" procedures take significantly less time to perform, but work to unite these methods to time sweep performance via a fundamental link continues to be a challenge. Recent work has suggested that these types of procedures may hold promise in the indication of fatigue performance of asphalt binders (Martono and Bahia, 2008; Johnson *et al.*, 2009).

Method Development. During the Strategic Highway Research Program (SHRP) efforts in the late 1980's and early 1990's, asphalt binder specifications transitioned from index properties to mechanical properties based on responses relevant to pavement performance; for example, the dynamic shear modulus of asphalt binder became of interest due to the tendency of aggregates to apply shear loads to the binder between them under dynamic loading from traffic. The result of this research was a new performance-based specification system for asphalt binder, now known as AASHTO M 320, or Superpave (Superior PERforming Asphalt PAVEments). Dynamic shear properties are measured using the Dynamic Shear Rheometer (DSR), as shown in Figure 1. As will be shown in detail in many of the following sections, testing and analysis methods have evolved in the intervening years since the initial development of Superpave, but the DSR remains a primary instrument to evaluate asphalt binder cracking.

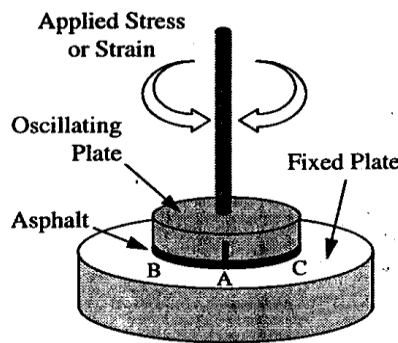


Figure 1. Schematic of the Dynamic Shear Rheometer.

Beginning in 1996, the National Cooperative Highway Research Program (NCHRP) sponsored research efforts to investigate the emerging practice of modifying asphalt binders and its effect on the current Superpave specifications. The research team was charged with the tasks of both identifying the shortcomings of the first iteration of Superpave, as well as suggesting improvements to better characterize modified asphalts. The findings from NCHRP Project 9-10 (*Superpave Protocols for Modified Asphalt Binders*) identified the general lack of correlation between mixture fatigue performance and $|G^*| \sin \delta$, therefore the development of improved binder fatigue testing procedures has been pursued. During NCHRP 9-10, the time-sweep (TS) test was introduced as a binder-specific fatigue test performed in the DSR, where the specimen is subjected to repeated cyclic shear loading, as shown in Figure 2, in either controlled-stress or controlled-strain mode (Bahia *et al.*, 2002; Bonnetti *et al.*, 2002). The TS allowed for the binder to go beyond linear viscoelastic behavior measured by Superpave and into the damage accumulation range. Results from this testing gave a much higher correlation with mixture fatigue performance ($R^2 = 0.84$), indicating that the TS was a promising procedure for evaluating binder fatigue characteristics. Upon the publication of *NCHRP Report 459* (Bahia *et al.*, 2001), further research was performed to evaluate the suitability of time-sweep testing for accurate characterization of binder fatigue. It was reported in subsequent studies (Anderson *et al.*, 2001; Shenoy, 2002) that at modulus values lower than 5 MPa, the outer edges of the binder specimen subjected to TS testing could become unstable and begin to flow. This “edge effect” can manifest itself as a drop in modulus due to changes in the sample geometry, which is indistinguishable from fatigue damage to the DSR data acquisition equipment.

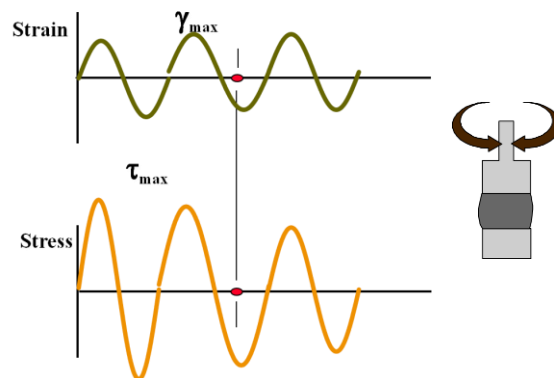


Figure 2. Schematic of time sweep load and response.



In response to this issue, additional research investigated these geometry effects by comparing the TS for binders against the torsion cylinder geometry (Martono *et al.*, 2007). The torsion cylinder geometry was established in earlier studies (Kim *et al.*, 2002; Kim *et al.*, 2006) and consists of a sand-asphalt mixture that is used to represent the thin-film behavior of asphalt binder within the mix. For the study performed by Martono *et al.* (2007), the torsion cylinder represented geometry unaffected by edge effect, as it was significantly stiffer and more resistant to unstable flow than binder alone. By subjecting parallel plate and torsion cylinder geometries to the same loading scheme, the effect of geometry on fatigue life was evaluated. The absolute dissipated energy was significantly different between the two geometries (as they consisted of fundamentally different materials), but when the dissipated energy was normalized to the unit volume of the sample and plotted against fatigue life, both geometries showed comparable fatigue trends. Extensive statistical modeling showed that geometry had little effect on fatigue behavior with respect to binder type and the applied loading, indicating that edge effects are not a significant factor in binder fatigue results.

Stress Sweep Developments. Following the work conducted to evaluate the time sweep as a valid binder fatigue testing procedure, researchers recognized that the time sweep is a very lengthy test, and thus began investigating a procedure to accelerate the damage accumulation in the binder specimens (Martono and Bahia, 2008). The procedure, known as the stress sweep, uses repeated cyclic loading at a constant frequency, but the controlled-stress level is increased incrementally over the duration of the test. By increasing the amount of applied energy from the DSR, the material accumulates damage much faster than the time sweep, leading to shorter times to binder failure. The binders used for the stress sweep study were used previously in a Federal Highway Administration (FHWA) Accelerated Loading Facility (ALF) fatigue study (Kutay *et al.*, 2007). The ALF test consisted of applying multiple passes of a simulated truck wheel load on full-scale pavements constructed using different types of binder. The fatigue crack length at 100,000 passes was measured for each section, and the binders were ranked accordingly.

The goal of Martono's stress sweep study was to first compare the results with those from time sweep testing, and evaluate the ability of each test to give the same ranking of the performance from the ALF test. As is common with most fatigue research, failure was defined as a 50% reduction in $|G^*|$ for both procedures, with the shear stress at failure (τ_f) being the parameter used to rank the materials' performance for stress sweep, and number of cycles to failure (N_f) used for the time sweep. The value of $|G^*|$ at failure for both test types correlated well, indicating a relationship between the two tests. The time sweep tests gave identical rankings to the ALF using N_f . This result was achieved by using strain-controlled testing at relatively high strain levels of 5% and 7% (for reference, the current Superpave fatigue specification typically uses 1% strain). The stress sweep was not completely accurate in its rankings of ALF performance using τ_f . However, it still showed some similarity in performance. While damage characteristics from the stress sweep correlated well with the time sweep, the ability of the stress sweep to indicate pavement fatigue performance needed further investigation. More details on the development of a formalized stress sweep experiment, the linear amplitude sweep (LAS) test is presented in Section 2.1.1.

2.1.2. Double Edge Notched Test

Queen's University researchers proposed evaluating the essential work of fracture (EWF) to obtain a measure of the fatigue and crack resistance behavior of asphalt binders (Broberg, 1975, Cotterell and Reddel, 1977, Andriescu *et al.*, 2004). Prior to the development of the EWF method, the fracture resistance of viscoplastic materials was largely evaluated by using laborious techniques requiring explicit measurements of a crack advancing through material. Within this technique, the work necessary to pull apart a pre-notched elastoplastic specimen is assumed to be divided in two parts: essential work performed in the local region of the advancing crack creating two surfaces and nonessential work away from the local region of cracking/tearing associated with ductility, plasticity, and yielding (Cotterell and Reddel, 1977).

The experimental determination of the essential and non-essential work of fracture involves the following steps. First, the total work of fracture is determined in simple direct tension tests of similar specimens with different ligament lengths. Double edged notched tension (DENT) are one means of performing this test. DENT is essentially a ductility test, but with two notches of controlled depth placed in the center of the specimen. Note that the DENT test geometry has also been applied to study low temperature fracture, but its importance here is the application to intermediate temperature fracture. The test itself is standardized in the Ontario Ministry of Transportation Test Method LS-299 (MOT LS-299, 2009). Figure 3 is a schematic of the sample in the DENT test defining ligament length, and Figure 4 shows the test samples in a computer-controlled force ductility instrument. Figure 5 provides an



example of raw force versus displacement data after a DENT test using three ligament lengths and two replicates for each ligament.

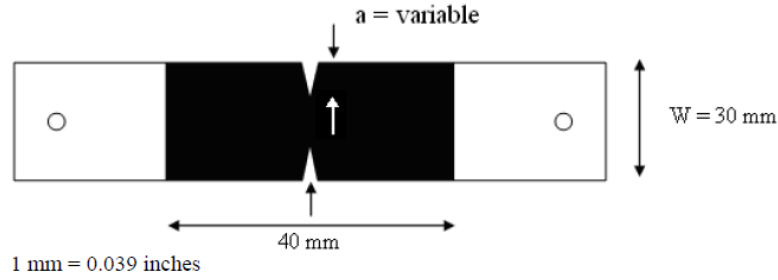


Figure 3. Schematic diagram of DENT test sample (Gibson et al., 2012).



Figure 4. DENT test specimens in ductiliometer (Gibson et al., 2012)..

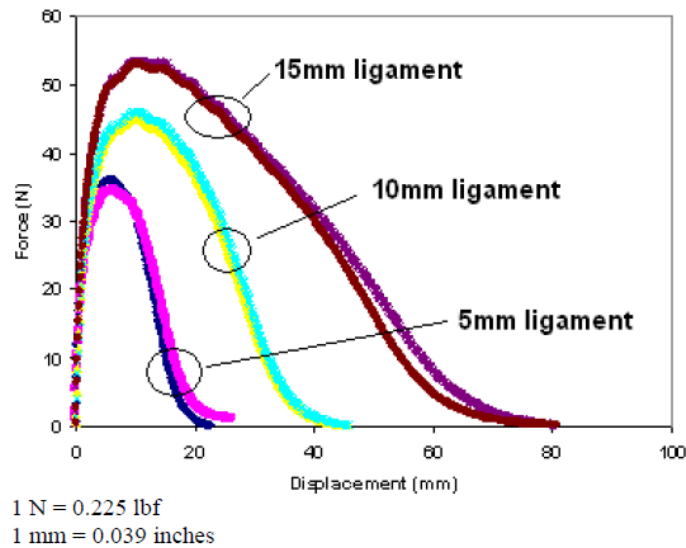


Figure 5. Typical test result from DENT experiment (Gibson et al., 2012)..

The EWF, W_e , is proportional to the fracture area (i.e., ligament length, ℓ , multiplied by thickness, B), while the non-essential or plastic work, W_p , is proportional to the volume of the plastic zone, which is the fracture area ($\ell \times B$) multiplied by the ligament length, multiplied with a factor. The factor depends on the shape of the plastic zone. Because the ligament length has major importance in determining the extent of plastic deformation, it is distinctly incorporated as ℓ and multiplied with the surface area to express the volume dependence of the plastic work of



fracture, W_p . The rather simple mathematical expression for the total work of fracture, W_f , is as shown in Equation [1].

$$W_f = W_e + W_p = (\ell \times B)w_e + 2(\beta \times \ell \times B)w_p \quad [1]$$

where; w_e = specific essential work of fracture and w_p = specific work of fracture. The β parameter is found by considering how close the geometry is to plane-strain or plane-stress conditions, Equation [2].

$$\beta = \frac{h\pi}{4L} \quad [2]$$

where; h = height of an assumed elliptic shape of the plastic zone and L = ligament length.

Experiments are performed at fixed displacement rates, but with different ligament lengths. The results are analyzed using a linear fitting procedure similar to the one employed for the EWF analysis. The calculated critical tip opening displacement (CTOD), δ , is the ultimate elongation for a zero ligament length, which represents the strain tolerance in the vicinity of a crack. Since a zero ligament length experiment is not reliable (e.g., it cannot be guaranteed that cracking will occur in the vicinity of interest, some approximation is necessary. For example, Gibson *et al.* (2012) approximated the tensile yield stress with the net section stress (peak load divided by the sectional area) for the smallest ligament length that they tested, 5 mm. This allowed an approximate CTOD to be calculated from the ratio between the essential work and the net section stress, Equation [3].

$$\delta = \frac{W_e}{\sigma} \quad [3]$$

Gibson *et al.* (2012) applied the DENT test to asphalt binders tested at the Federal Highway Administration's Accelerated Load Facility (FHWA ALF). The binders themselves were PAV-aged instead and were tested at 25°C, and an extension rate of 100 mm/min. The test was applied to the conventional asphalt and the modified asphalts. Ligament lengths were 5, 10, and 15 mm and the sample thickness was 6.5 mm. The areas underneath the force versus displacement curves, see Figure 5, represent the total work of fracture. It was found that the CTOD method was the most discriminating measure of mixture performance within the parameters evaluated. These parameters included binder yield energy, EWF, time sweep, strain sweep, and the standard $|G^*| \sin(\delta)$ parameter. Huber (2009) performed a similar study comparing several binder fatigue parameters using in-service pavements from Ontario, Canada. They also found that the CTOD parameter had the highest association with the CTOD parameter. Zhou *et al.* evaluated multiple binder fatigue tests for Texas materials and concluded that the CTOD parameter and LAS parameters yielded similar rankings as compared to mixture performance from the Overlay Tester (Zhou *et al.*, 2014). In a related study, Zhou *et al.* (2012) compared various binder fatigue measures to cylindrical push-pull mixture tests and concluded that CTOD and Elastic Recovery best matched the observed mixture performance.

2.1.3. Binder Fracture Energy Test

Overview. As the writing in Section 2 demonstrates, numerous tests have been developed in an attempt to provide a better evaluation of asphalt binder cracking performance. This is the case for the binder yield energy test (Johnson, Bahia and Wen, 2009) and linear amplitude sweep (LAS) test (Johnson, 2010), which are based on shear fatigue properties measured from DSR. However, it is difficult to apply the binder yield energy test analysis protocol to modified binders as a result of apparent polymer network interference (Johnson, 2010). Also, contradictory results have been reported regarding the correlation between binder fatigue resistance obtained from the LAS test and mixture fracture resistance. Whereas Hintz *et al.* (2011a; 2011b) found a fairly good relationship between LAS test results and field fatigue cracking data, Zhou *et al.* (2013) found the LAS test correlated poorly with push-pull mixture fatigue tests.

Another approach is the use of fracture energy as a potential indicator of asphalt binder cracking resistance. Ponniah, Cullen and Hesp (1996) and Hoare and Hesp (2000) measured fracture energy from a single-edge notch bending (SENB) test. Nonetheless, the purpose of the SENB test was to evaluate cracking performance at low temperature (below -10°C), where binder response is brittle and the principles of linear elastic fracture mechanics are applicable. Andriescu, Hesp and Youtcheff (2004) used a double-edge notched tension (DENT) test to determine the essential and plastic work required to fracture a binder specimen. Gibson *et al.* (2012) found that essential plastic work and critical tip opening displacement (CTOD) from the DENT test correlated well with FHWA-ALF mixture fatigue test results. However, they pointed out the required number of replicates and the scatter in the analysis as major drawbacks of the DENT test. More description of the DENT test is given in Section 2.1.2.

Recently, an effort has been placed on developing a binder fracture energy (BFE) test to quantitatively evaluate the fracture energy density (FED) of asphalt binders at intermediate temperature and to identify the presence of various modifiers (rubber, polymer and combinations of rubber and polymer) (Niu, Roque and Lopp, 2014). Encouraging results have been reported so far, and in addition, an AASHTO provisional standard has been proposed with detailed description of the testing equipment, data analysis procedure and typical FED values for a broad range of unmodified and modified binders.

The BFE test was developed to evaluate the potential fracture tolerance of asphalt binder in the intermediate temperature range (0-20°C). It is performed by pulling at a constant displacement rate on two loading heads attached to a binder specimen until fracture occurs at the middle section of the specimen. Compared to previous direct tension tests, the BFE geometry overcomes the deficiencies associated with the identification of the failure plane and provides accurate and reliable measurements of true stress and true strain on the fracture surface. For evaluation of relative cracking performance, it is recommended that this test procedure be used with asphalt binder conditioned according to AASHTO T240 (RTFOT) plus AASHTO R28 (PAV), which is considered to better represent long-term asphalt aging in the field. However, this test can be used for determination of binder fracture energy of any asphalt binder including unaged or aged neat binder and modified binder as well as binder extracted and recovered from the field. Additional details on specimen preparation can be found in Yan *et al.* (2015). A timeline of the model, key elements, and literature are presented in Figure 6.

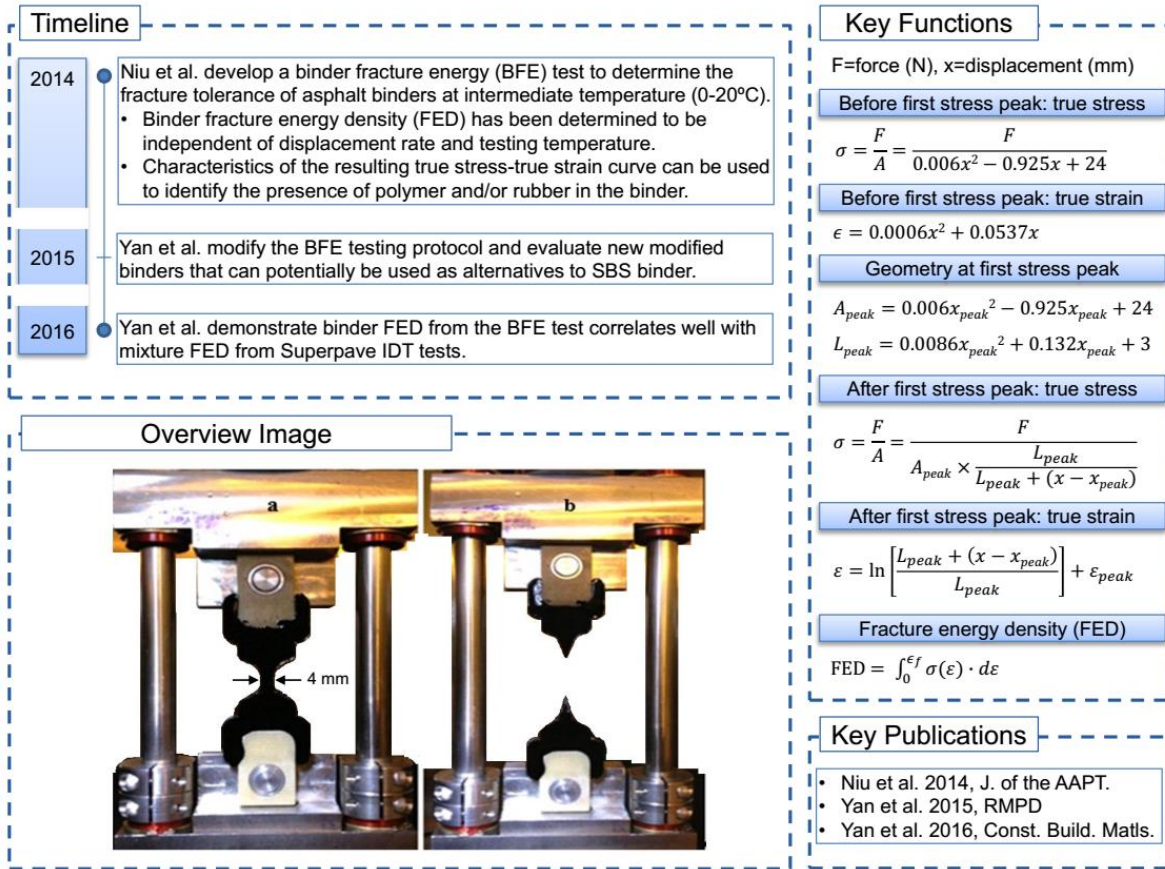


Figure 6. Summary of the BFE test.

Data Analysis Procedure. Fracture energy density (FED) is defined as the energy per unit volume required to initiate fracture (i.e., local failure). It is calculated as the area under the true stress-true strain curve up to the point at which stress peaks and drops. The post-peak energy is used to split the specimen in half after local fracture initiates and thereby, is not included in the calculation of FED. True stress and true strain refer to the local stress and strain on the failure plane and are determined from global force and displacement recorded during a test.

A finite element large deformation analysis was conducted by Niu *et al.* (2014) to relate global force and displacement reported by the data acquisition system to true stress and true strain on the failure plane (middle section of specimen). That analysis was revisited and simpler relationships were obtained, as described below:

- True stress is calculated as the ratio of global force to cross-sectional area of the middle section of the specimen. Equation [10] can be used to estimate the cross-sectional area as a function of measured displacement:

$$A = 0.006x^2 - 0.925x + 24 \quad [4]$$

where A is cross-sectional area (mm^2) and x is displacement (mm).

- True strain is obtained from measured displacement using Equation [5]:

$$\varepsilon = 0.0006x^2 + 0.0537x \quad [5]$$

where ε is true strain (dimensionless) and x is displacement (mm).

Equations [10] and [5] are applicable until a first peak in true stress is observed (note that stress peak and load peak may not necessarily coincide due to change in geometry). Beyond this point, significant reduction in cross-sectional area occurs and the finite element analysis becomes invalid. Consequently, a data analysis procedure was developed to account for the reduction in cross-sectional area that occurs at larger deformation levels, which is illustrated in Figure 7. Since Poisson's ratio of asphalt binder is generally close to 0.5, the volume of the middle part is assumed to remain constant during extension (i.e., binder is incompressible at the relatively low bulk stress associated with tensile testing at intermediate temperature). Furthermore, necking of the middle part of the specimen was observed after the first stress peak. Based on specimen geometry and observations during testing, the initial length of the middle part was designated to 3 mm.

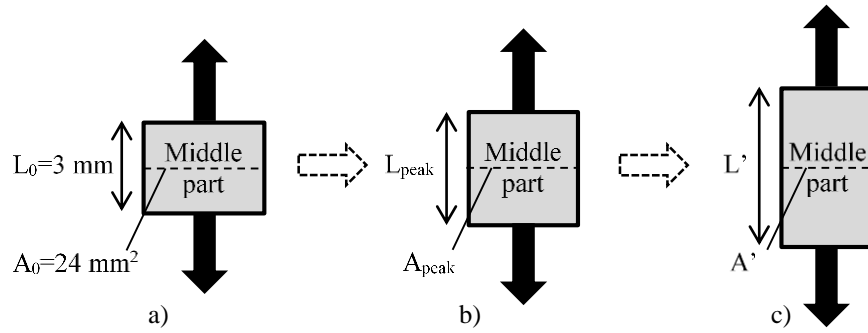


Figure 7. Dimensions of the 3-mm middle part of the BFE specimen at the beginning of the test (a), at first stress peak (b), and after first stress peak (c).

After identifying the first stress peak, the constant volume assumption is imposed:

$$A_{peak} \cdot L_{peak} = A' \cdot L' \rightarrow A' = A_{peak} \cdot \frac{L_{peak}}{L'} \quad [6]$$

in which; A' = central cross-sectional area after the first stress peak (mm^2) and A_{peak} = central cross-sectional area at the first stress peak (mm^2) (found by substituting the displacement level at the first stress peak (x_{peak}) into Equation [10]), L_{peak} = length of initial 3-mm middle part at the first stress peak (mm), Equation [7], and L' = length of initial 3-mm middle part after the first stress peak (mm).

$$L_{peak} = 0.0086x_{peak}^2 + 0.132x_{peak} + 3 \quad [7]$$

Once necking starts, it is assumed that increases in displacement takes place only in the 3-mm middle part of the specimen. Therefore, L' can be calculated as follows:

$$L' = L_{peak} \Delta x \quad [8]$$

where Δx (mm) is the increase in displacement after the first stress peak ($x - x_{peak}$). Then, true stress and true strain after the peak are determined as follows:

- True stress is calculated as the ratio of global force to the cross-sectional area provided by Equation [6].

- True strain can be obtained using a large strain formulation (Equation [9]):

$$\varepsilon = \ln \left(\frac{L_{peak} + \Delta x}{L_{peak}} \right) + \varepsilon_{peak} \quad [9]$$

in which L_{peak} and Δx are those defined above and ε_{peak} = strain at the stress peak calculated from Equation [5].

Related Applications. After extensive test results, the researchers concluded that the new fracture energy test and data interpretation system suitably measure unmodified and modified binder fracture energy density. Test results revealed that binder fracture energy is a fundamental property of asphalt binder and the characteristics of the true stress-true strain relationship are a good indicator of the presence and relative content of modifiers.

Yan *et al.* (2015) evaluated seven types of alternative PMA binders using different tests, including existing Superpave PG binder tests, the MSCR test, and the BFE test. Results showed that four alternative PMA binders (SBS plus polypropylene composite, terpolymer plus polypropylene composite, SBS plus oxidized polyethylene wax and a fourth non-SBS polymer of unknown composition) can potentially have equivalent performance to SBS binder. Three deficient binders (modified with plastomer, polyolefin and a third one unknown) were identified in both the MSCR and the BFE tests. However, Superpave PG binder tests distinguished only one as deficient. Compared to the MSCR test, which provides a qualitative assessment (pass/fail criterion), the BFE test brings the added advantage of providing a quantitative assessment of relative binder performance based on fracture energy density values. Findings appeared to indicate that the BFE test can be used as an effective tool for binder specification by state highway agencies.

Yan *et al.* (2016) extended prior efforts by assessing whether binder results would translate to improved cracking performance of resultant mixtures. Superpave indirect tension (IDT) tests were conducted to obtain the fracture properties of asphalt mixtures with the four alternative PMA binders, as well as a standard PG 76-22 (3% SBS) PMA binder and a PG 67-22 unmodified base binder. Results showed the alternative PMA binders (SBS plus polypropylene composite, terpolymer plus polypropylene composite, SBS plus oxidized polyethylene wax and a fourth non-SBS polymer of unknown composition) not only reduced the rate of damage accumulation but also improved the failure limit of the resultant mixtures. The energy ratio (ER) parameter, which has been closely tied to field pavement cracking performance (Roque *et al.*, 2004), showed the PMA binders exhibited equivalent or better cracking performance than PG 76-22 SBS PMA binder. Finally, binder fracture energy density (FED) results satisfactorily ranked mixture cracking performance thereby supporting the use of the binder fracture energy (BFE) test as an effective tool to quantitatively evaluate the relatively cracking performance of asphalt binder.

2.2. Analysis

2.2.1. Rheological Linkages

There have been numerous attempts to link asphalt binder rheology to fatigue performance, many of which have been reviewed by Glover *et al.* (2005). Hubbard and Gollomb (1937) reported that many well performing mixtures in an Ohio study showed a penetration of 30 or higher on recovered asphalts. Doyle (1958) showed correlation with fatigue performance of an Ohio test section with ductility as did Kandhal and others (1975, 1977, 1984). Skog (1967) examined the effect of aging and shear susceptibility and found materials that performed well in the field were less sensitive. Lee (1973) suggested a critical penetration of 20 and critical viscosity of 20-30 MPa at 25°C based on findings from lab aged asphalts in Iowa. The most widely used is the loss modulus at 10 radians per second and a temperature 4°C greater than the average of the high and low Superpave performance grading temperatures. In developing this parameter it was hypothesized that a lower amount of dissipated energy per cycle would result in a more fatigue resistant material. As shown in Equation [10] the dissipated energy is directly proportional to the loss modulus, which is mathematically determined as the product of the shear modulus and the sine of the phase angle.

$$W_d = \pi \gamma_0^2 [G^* \sin \delta] \quad [10]$$

Analysis of the Zaca-Wigmore field site and subsequent engineering adjustments led to the establishment of the 5 MPa limit on this quantity. While research has shown the capabilities of the mixture loss modulus to relate to the mixture fatigue life a generally poor correlation between the loss modulus of the binder and fatigue cracking of asphalt mixtures has been observed (Tayebali *et al.*, 1994; Deacon *et al.*, 1997). An alternative rheological index



based on the rate of change in complex viscosity and phase angle with respect to frequency was proposed by Reese and Goodrich (1993), but apparently failed to gain traction in the community as it did not explicitly include the influence of stiffness in the proposed parameter.

Glover *et al.* (2005), motivated by the historical data that showed a relationship between ductility and performance, propose an alternative rheological index defined based on the ratio of storage modulus (G') to the ratio of dynamic viscosity (η') to G' , Equation [11]. The historical correlation between performance and ductility coupled to the correlation between Glover's parameter and ductility suggested that the parameter would closely relate to field performance. Rowe simplified this parameter by applying the Cox-Merz approximation relating shear modulus and viscosity and then eliminating a constant (the angular frequency). The resulting parameter (referred to as the Glover-Rowe parameter, G-R) is given in Equation [12].

$$G = \frac{G'}{G'/\eta'} \quad [11]$$

$$G - R = \frac{|G^*|(\cos \delta)^2}{\sin \delta} \quad [12]$$

Anderson *et al.* (2011) evaluated the Glover parameter and confirmed its correlation to field performance and going further to propose that a value of 9×10^{-4} MPa/s (or an equivalent value of 180 kPa for the G-R parameter) indicated the onset of cracking.

2.2.2. Linear Amplitude Sweep (LAS) and Application of Continuum Damage Modeling to Asphalt Binder

Overview. The fatigue cracking resistance of an asphalt pavement is dictated by the structure (layer thickness), mixture type and volumetrics, and inherent fatigue cracking resistance of the asphalt binder. Asphalt binder is the weakest asphalt concrete constituent and, thus, fatigue cracks initiate and propagate primarily cohesively through the binder phase of asphalt mixtures in the absence of moisture (Lee and Kim 2014). Therefore, the ability to characterize and model the inherent fatigue performance of an asphalt binder is a necessary first step to design mixtures and pavements that are not susceptible to premature fatigue failure. Comprehensive understanding and prediction of asphalt binder fatigue performance require a suitable practical experiment coupled with a model to predict how the binder will perform under various traffic, temperature, and structural conditions encountered in the field.

Current asphalt binder Performance Graded (PG) specifications dictate that the parameter $|G^*|/\sin(\delta)$ is measured in a Dynamic Shear Rheometer (DSR) at a small strain level over a limited number of load cycles to evaluate fatigue resistance. This procedure lacks the ability to characterize damage resistance, as research conducted since the conclusion of the SHRP research has shown that the parameter lacks the ability to indicate resistance to fatigue damage (Bahia *et al.*, 2001; Bahia *et al.*, 2002; Tsai *et al.*, 2005). The primary concern is that $|G^*| \sin \delta$ is merely an initial measure of undamaged linear viscoelastic properties, and it may be unsuitable to extrapolate this property to predict damage after the multiple loading cycles typically associated with fatigue damage. The Linear Amplitude Sweep (LAS) test (AASHTO TP 101) has been proposed as an improved specification test to characterize asphalt binder fatigue damage resistance. The LAS test uses systematically increasing strain amplitudes in the DSR to accelerate damage in asphalt binder specimens, enabling practical and efficient fatigue characterization.

Viscoelastic Continuum Damage (VECD) modeling has been applied extensively to asphalt mixtures and pavements to enable prediction of fatigue performance under variable conditions using limited test results (e.g., Underwood *et al.*, 2010; Lee and Kim, 2014). The VECD modeling approach has more recently been extended to asphalt binders tested using torsional loading in a DSR (Wen and Bahia, 2009; Johnson and Bahia, 2011; Hintz *et al.*, 2011; Safaei *et al.*, 2014; Wang *et al.*, 2015; Safaei and Castorena, 2015; Safaei *et al.*, 2016; Underwood, 2016). Consequently, LAS test results can be coupled with a Simplified Viscoelastic Continuum Damage (S-VECD) model for prediction of fatigue life at any strain amplitude and temperature of interest using limited test results. Varying strain amplitudes can be used to assess asphalt binder fatigue response to variable structure and traffic loading. Furthermore, it has been demonstrated that time-temperature superposition can be used to predict asphalt binder fatigue damage evolution under variable temperatures (Safaei and Castorena, 2016). The following provides a summary of the research that led to the development of the LAS test, provides an overview of the S-VECD modeling approach, and presents recent studies that validate the use of the procedure using binder and field

performance results. An overarching timeline of the LAS test development, the key elements, and literature are summarized in Figure 8.

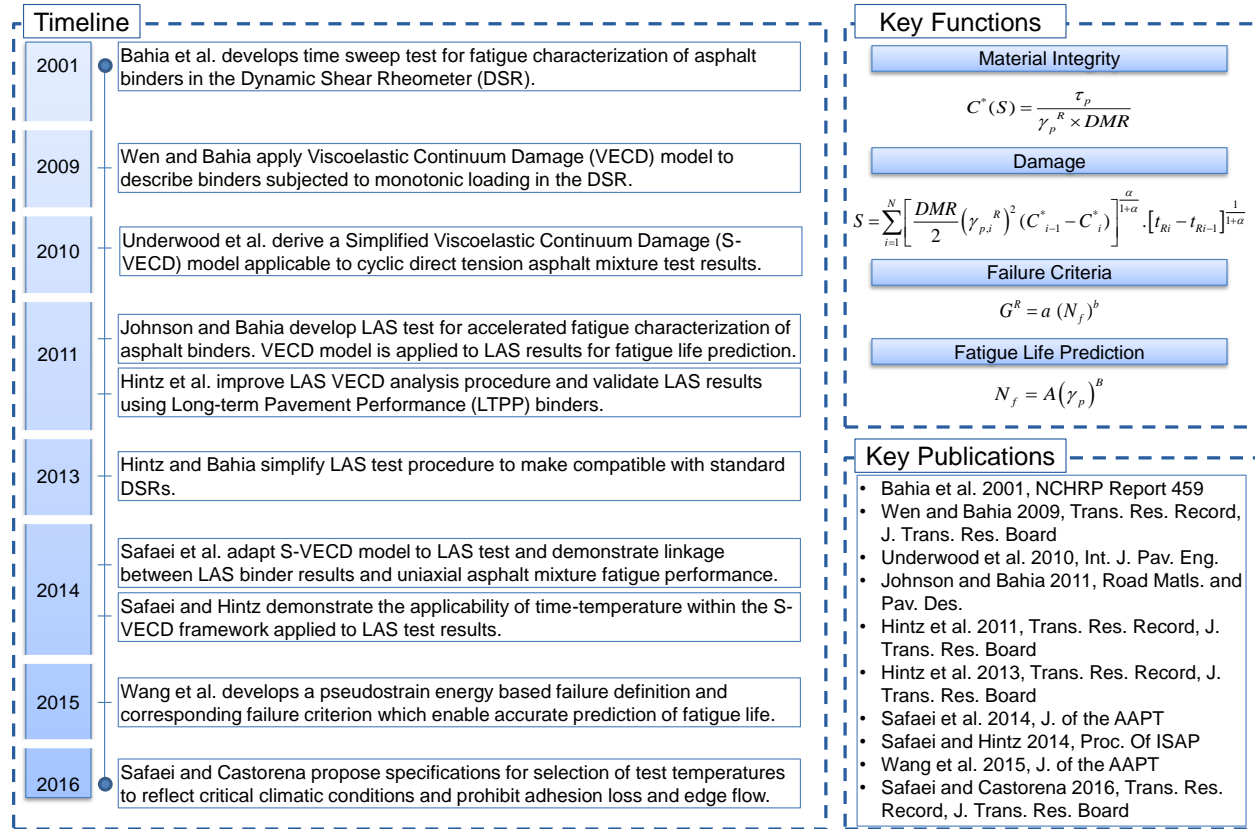


Figure 8. Summary of the LAS test.

Development of the LAS Test

Loading Scheme

Several damage-inducing tests can be implemented in a DSR. Bahia *et al.* (2001) initially introduced the time sweep test (see Section 2.1.1), as a means to characterize the fatigue resistance of asphalt binders in the DSR in an effort to overcome the deficiencies of the current specification. The time sweep test consists of repeated cyclic loading in the DSR in either stress- or strain-controlled mode, which is similar to many fatigue tests for characterizing asphalt mixture fatigue. However, the time sweep test poses some challenges for routine use because it is time-consuming and a strain or stress amplitude must be selected that will produce failure in a reasonable amount of time. Such selection is not possible without a priori knowledge of the binder's fatigue resistance.

Therefore, alternative procedures have been investigated under the assumption that their results can be input into a VECD model to derive fatigue responses under any loading history of interest with limited material characterization. Initially, Wen and Bahia (2009) investigated use of monotonic testing in the DSR for accelerated fatigue characterization. The monotonic test consists of subjecting asphalt binder to constant strain rate loading (i.e., noncyclic loading) in a DSR. Wen and Bahia (2009) applied VECD modeling to monotonic binder test results for the first time and found that the model to be applicable to unmodified asphalts. However, the model was found to be inapplicable for monotonic test results of polymer-modified binders that display two-phase behavior in monotonic tests (Johnson *et al.*, 2009). At a low strain level, the binder dominates the response to loading. However, at a high strain level, the binder yields and the polymer network is activated, leading to distinct changes in behavior that cannot be captured using a continuum damage approach (Johnson *et al.*, 2009). Furthermore, Safaei and Castorena (2016) demonstrated that significant normal stresses arise in monotonic binder tests, which will affect the resultant damage growth, which precludes their use in calibrating a VECD model.

Due to the problems encountered in monotonic tests, Johnson and Bahia (2011) proposed the application of a VECD-based model to an LAS test, which includes an oscillatory strain amplitude sweep that consists of linearly



increasing strain amplitudes from 0.1 percent to 30 percent over the course of just five minutes. The LAS test has been found to induce significant damage in all binders, irrespective of their fatigue resistance (e.g., modified versus unmodified). Hintz and Bahia (2013) later refined the LAS test amplitude sweep to be compatible with standard rheometers. Wang *et al.* (2015) incorporated a fatigue failure criterion into analysis of LAS test results for improved performance prediction. Deriving the fatigue failure criterion requires three tests with different loading histories. Therefore, three LAS tests are used to calibrate the S-VECD model. All three tests are conducted over the strain amplitude range of 0.1 percent to 30 percent but the times over which the strain amplitudes are incremented vary. Loading durations of 5, 10, and 15 minutes are used. The use of these three LAS tests with varying loading histories can be used in place of conducting replicate tests of the same conditions, which will be discussed in latter sections. The LAS test also includes a frequency sweep at the fatigue testing temperature which is used to obtain a fingerprint of the undamaged viscoelastic behavior of the asphalt binder. The frequency sweep does not induce damage and hence can be conducted directly prior to the LAS amplitude sweep on a single asphalt binder specimen.

Fatigue Damage Mechanism

In tests where the asphalt binder is subjected to damage-inducing cyclic loading in the DSR, fatigue failure will occur via the formation of radial cracks that start at the sample periphery (where strain levels are the highest) and grow inward, assuming that adhesion loss and plastic flow are avoided (Hintz and Bahia, 2013). Safaei and Castorena (2016) demonstrated that cohesive cracking failure occurs in cyclic DSR tests when the initial sample's dynamic shear modulus value is between 12 MPa and 60 MPa at the given test temperature and frequency based on visual observations of sample geometry and morphology following fatigue testing. Adhesion loss between the sample and the DSR plates is likely to occur when the modulus value of the sample exceeds 60 MPa, and edge flow impedes the results if the sample modulus value is lower than 12 MPa. When cohesive cracking is the failure mechanism, the formation of radial cracks within the sample will lead to a reduction in the effective area over which the stresses are distributed. This process results in a macroscale measure of loss in material stiffness, which can be used within the S-VECD model to quantify damage growth.

Test Temperature Selection

It is recommended that the LAS test temperature be selected as the average of the high and low temperature climatic performance grades of the binder minus 4°C. Based on extensive analysis of the Enhanced Integrated Climatic Model (EICM) for a representative set of locations in the United States complemented with binder testing, Safaei and Castorena (2016) found that the average the high and low climatic PGs, determined from the Long-term Pavement Performance (LTPP) Bind program minus 4°C represents a critical temperature in terms of frequency of occurrence and material fatigue resistance. Selection of the LAS test temperature as the average of the high and low climatic PGs minus 4°C also ensures that the binder modulus is within the range where cohesive cracking is dominant failure mechanism.

Fatigue Failure Definition

A clear means to define fatigue failure in fatigue tests is an important component of fatigue characterization. Wang *et al.* (2015) demonstrated that the peak in the stored pseudo strain energy versus number of loading cycles curve is a suitable definition of failure for LAS tests. Initially in LAS tests, the stored pseudo strain energy increases with each cycle, indicating that the material is able to store additional energy as the strain amplitude (and hence input energy) increases. However, once the material fails, the binder loses its ability to store additional energy with the increase in strain amplitude, and thus, the stored pseudo strain energy will decay.

S-VECD Model Applied to LAS Test Results: Wen and Bahia (2009) first investigated the applicability of the VECD model to asphalt binders under monotonic constant strain-rate shear loading in the DSR. However, monotonic loading resulted in several problems as discussed. Therefore, Johnson and Bahia (2011) proposed the application of a VECD-based model based on dissipated energy concepts to asphalt binders subjected to cyclic loading in a DSR whereby the excessively high strains associated with monotonic testing were avoided. Their model was derived following the work of Kim *et al.* (2006) on torsion cylinders. Quantification of damage was performed by substituting the cyclic dissipated energy function into Schapery's Work Potential Theory functions (Schapery, 1975) and numerically integrating as follows:

$$S(t) \cong \sum_{i=1}^N \left[\pi I_D \gamma_0^2 (|G^*| \sin \delta_{i-1} - |G^*| \sin \delta_i) \right]^{\frac{\alpha}{\alpha+1}} (t_i - t_{i-1})^{\frac{1}{\alpha+1}} \quad [13]$$

where; S is the damage parameter (note that in Johnson and Bahia's initial work they used the variable D , but S is used to be more consistent with other research cited herein), I_D is a normalization parameter for specimen-to-specimen variability, α is damage rate variable, t is the time, and the subscript i indicates the cycle indices used for calculation.

The parameter $|G^*| \cdot \sin(\delta)$ was used as an indicator of material integrity and was plotted against accumulated damage. In order to provide a closed-form parameter to compare fatigue performance, a failure criterion was selected and the level of damage was computed up until that threshold (S_f). This threshold value was combined with the previous formulation as well as Schapery's Work Potential Theory to ultimately yield number of cycles to failure:

$$N_f = \frac{f(S_f)^k}{k(\pi I_D C_1 C_2)^\alpha} (\gamma_{\max})^{-2\alpha} \quad [14]$$

where; $k = 1 + (1 - C_2)\alpha$; f is the loading frequency(Hz), and S_f is the damage accumulation at failure.

Later, Safaei *et al.* (2014) refined the VECD model approach to better reflect the underlying VECD theory and current S-VECD asphalt mixture model proposed by Underwood *et al.* (2010). Their results demonstrated promising agreement between the asphalt binder and mixture fatigue performance predictions. Wang *et al.* (2015) incorporated an energy-based failure criterion to improve the predictive capabilities of the binder VECD model. Safaei and Castorena (2016) demonstrated the applicability of the time-temperature superposition principle to the VECD modeling of asphalt binders subjected to cyclic loading in the DSR. Safaei *et al.* (2016) demonstrated the applicability of Schapery's extended elastic-viscoelastic correspondence principle, validating the applicability of S-VECD modeling to torsional binder loading. The following presents the S-VECD model developed for the LAS test based on the culmination of past efforts. As shown in Figure 8, key components of the S-VECD model for LAS tests include:

(1) Material integrity (pseudostiffness)

$$C^*(S) = \frac{\tau_p}{\gamma_p^R \cdot DMR} \quad [15]$$

(2) Damage

$$S(t) = \sum_{i=1}^N \left[\frac{DMR}{2} (\gamma_p^R)^2 (C^*_{i-1} - C^*_i) \right]^{\frac{\alpha}{1+\alpha}} \cdot [t_{Ri} - t_{Ri-1}]^{\frac{1}{1+\alpha}} \quad [16]$$

(3) Failure criteria

$$G^R = a (N_f)^b \quad [17]$$

(4) Fatigue life prediction

$$N_f = A (\gamma_p)^B \quad [18]$$

where; $C^*(S)$ is the pseudostiffness, τ_p is the peak stress, DMR = dynamic modulus ratio = $|G^*|_{\text{fingerprint}} / |G^*|_{\text{LVE}}$, where $|G^*|_{\text{fingerprint}}$ is determined based on the initial $|G^*|$ in the amplitude sweep and $|G^*|_{\text{LVE}}$ is the corresponding linear viscoelastic $|G^*|$ determined from the frequency sweep, and γ_p^R is peak pseudostrain, S is an internal state variable representing damage, i is the cycle number, t_R is reduced time, α is a material dependent constant defined as $1/m + 1$ where m is the steady-state slope of the storage modulus versus frequency curve in log space determined from the frequency sweep portion of the LAS test, G^R is the average rate of pseudostrain release up to the point of failure, a and b are experimentally determined fitting coefficients, N_f is fatigue life, and A and B are analytically derived parameters which are a function of Equations [15] - [18] and the linear viscoelastic properties of the binder.

The crux of the S-VECD model is the relationship between $C^*(S)$ and S that has been shown to be independent of loading history and temperature, which allows the prediction of the damage response to any given loading history of interest using limited test results (Safaei *et al.*, 2016). This also allows the use of the three LAS tests conducted with varying durations to be used in place of replicates. Agreement between the $C^*(S)$ versus S curves resulting from the different tests can be used to assess repeatability. Pseudo stiffness is an indicator of material integrity,

which accounts for the viscoelasticity effects on the measured stress response. Pseudo strain is equivalent to the linear viscoelastic stress response of the binder. Equation [15] implies that $C^*(S)$ will be one if the material is behaving in a linear viscoelastic manner and will decrease as the stress deviates from linear viscoelasticity as a result of damage. In the case of cyclic loading applied in the DSR with zero mean strain, the peak pseudo strain in a given cycle can be approximated Equation [19].

$$\gamma_p^R = \frac{1}{G_R} \left(\gamma_p \cdot |G^*|_{LVE}(\omega_R) \right) \quad [19]$$

where; γ_p is the peak strain in a given cycle, and $|G^*|_{LVE}(\omega_R)$ is the linear viscoelastic dynamic shear modulus at the reduced frequency (ω_R) of testing.

Underwood (2016) presents an almost identical version of the damage evolution function, but separate damage calculation depending on whether it is being calculated for the first cycle (in which case damage is calculated by time step, j) or all other cycles (damage is calculated for cycles, i), Equation [20]. In this approach the damage is explicitly assumed to grow under both forward and reverse torsion and so the peak-to-peak values of strain and pseudo strain are adopted (γ_{pp}). The time varying nature of pseudo strain is also included through the B_1 variable, which is derived in the same way as the time varying function is derived with the S-VECD model in tensile loading (K_1 in Section 6.3.1), and is shown in Equation [21]. This time varying function is not needed in order to collapse damage behaviors or to use the model to predict the material response under sinusoidal loading (since sinusoidal loading is used for characterization); however, it is needed to apply the resultant damage functions to other, non-sinusoidal inputs. In Equations [20] and [21] t'_r = the reduced time and t'_{rp} = reduced pulse time. These are the same as in standard linear viscoelastic reduced time, except the time is reduced for temperature, frequency, and load/strain level (Underwood, 2016).

$$\Delta S_{j+1 \text{ or } i+N} = \begin{cases} \left(-\frac{1}{2} (\gamma_{j+1}^R)^2 (C_{j+1} - C_j) \right)^{\frac{\alpha}{1+\alpha}} \left(t_r^{(j+1)} - t_r^{(j)} \right)^{\frac{1}{1+\alpha}} & t'_r \leq t'_{rp} \\ \left(-\frac{1}{2} (\gamma_{pp}^R)^2 (C_{i+N} - C_i) \right)^{\frac{\alpha}{1+\alpha}} \left(t'_{rp} \times N \right)^{\frac{1}{1+\alpha}} \times B_1 & t'_r > t'_{rp} \end{cases} \quad [20]$$

$$B_1 = \frac{1}{(t'_{r,final} - t'_{r,ini})} \int_{t'_{r,ini}}^{t'_{r,final}} (f(t'_r))^{2\alpha} dt'_r = f_r \int_{t'_{r,ini}}^{t'_{r,final}} (f(t'_r))^{2\alpha} dt'_r \quad [21]$$

Underwood also postulates that in the case of asphalt binder, that explicitly accounting for the nonlinear viscoelastic response is paramount to generally characterizing the damage function. The nonlinear viscoelasticity is accounted for using Schapery's single integral non-linear function (Schapery, 1966; 1969). Underwood and Kim show how this model is capable of describing the nonlinear response of asphalt binder and mastics across multiple temperatures (Underwood and Kim, 2015). The formulation is integrated into the damage model by adjusting the pseudo strain function as shown in Equation [22].

$$\gamma^R = \begin{cases} \gamma^R = \frac{h_1}{G_R} \int_0^{t'_r} G(t'_r - \xi) \frac{d(h_2 \gamma)}{d\xi} d\xi & t'_r \leq t'_{rp} \\ (\gamma_{pp}^R)_i = \frac{h_1}{G_R} [(\gamma_{pp})_i] |G^*|(\omega'_r) & t'_r > t'_{rp} \end{cases} \quad [22]$$

where h_1 and h_2 are the variables of the nonlinear model.

Other interpretations of nonlinear viscoelasticity also exist, but have not been integrated into damage based modeling. Rajagopal and Srinivasa (1998; 2004) developed a NLVE model for asphalt cement by postulating that there exists a natural configuration for a body and that this configuration evolves when that body is subjected to some thermodynamic process. Narayan *et al.* (2012) studied the torque response of asphalt cement at different temperatures and shear rates in the parallel-plate geometry and then modelled these data with a Gibbs-potential-based thermodynamic framework (Narayan *et al.*, 2013). Motamed *et al.* (2012; 2013) present an alternative view of nonlinear viscoelasticity based on stress interaction nonlinearity.

To enable performance prediction with this model, the so-called G^R -based failure criterion, defined in Equation [17], is necessary which allows for predicting when the fatigue failure will occur under loading conditions other than those used in model characterization testing. G^R is calculated using Equation [23].

$$G^R = \frac{\frac{1}{2} \int_0^{N_f} (\gamma_p^R)^2 (1 - C^*)}{N_f^2} \quad [23]$$

The relationship between fatigue life (N_f) and G^R has been shown to be loading history and temperature independent for asphalt binders (Safaei *et al.*, 2016). The damage characteristic curve and G^R -based failure criterion can be combined to derive an analytical solution for the relationship between fatigue life and strain amplitude in the form of Equation [18]. Equation [18] can be used to predict fatigue life at any strain amplitude at a given temperature of interest using LAS results at a single temperature. If prediction of fatigue life at temperatures other than those used in LAS test is desired, time-temperature shift factors must be determined for the specific binder of interest using temperature – frequency sweep testing.

Validation of the LAS Test with Binder Test Results. The comparison between the fatigue life data measured from the time sweep tests and those predicted using the S-VECD modeling of the LAS test results are shown in Figure 9(a) for four binders (Safaei *et al.*, 2016). These results indicate relatively good agreement between the measured and predicted fatigue life data. At conditions that correspond to long-term fatigue (i.e., low strain and high temperature), the LAS test results tend to under-predict the fatigue life somewhat. However, the rankings of the predicted fatigue life data amongst the various materials and test conditions remain in good agreement with the measured trends from the time sweep tests, indicating that the LAS test can still be used to assess the relative fatigue performance of binders under various loading and thermal conditions. It is speculated that the under-prediction is the result of the material nonlinearity that is associated with the high strain amplitudes used in the LAS test, which are neglected in the analyses for simplicity. Underwood (2016) recently presented an S-VECD model for asphalt binders and mastics subjected to torsional loading that considers nonlinear viscoelasticity. However, separating nonlinearity and damage is challenging and requires more extensive testing than the quick LAS test. Thus, given the relatively good agreement between the fatigue life data predicted by the LAS test and the measured fatigue life data, it is recommended that the LAS test protocol coupled with S-VECD modeling should still be considered as a practical and efficient tool for assessing the fatigue performance of asphalt binders.

Validation of the LAS Test with Accelerated Loading Facility Results. A past Federal Highway Administration Accelerated Loading Facility (FHWA-ALF) study evaluated the effect of asphalt binder on pavement fatigue performance using test lanes constructed using equivalent structures and mixture compositions with the exception of different binder types (Gibson *et al.*, 2012). This study presents an ideal case for validating a binder test with field results. A subset of these FHWA-ALF binders was subjected to LAS testing. Resultant S-VECD models were used to predict fatigue performance based on the strain amplitudes anticipated in the FHWA-ALF field experiment. The loading conditions in the FHWA-ALF experiment along with the known wheel speed, pavement structure, temperature, and mixture dynamic modulus values were input into a layered viscoelastic model in order to determine the strain kernel at the bottom of the asphalt mixture for each lane. The maximum tensile strain values obtained from the analysis were multiplied by 80 based on recommendations of Safaei *et al.*, (2014) and input into the S-VECD-based fatigue life prediction models derived for each binder. The binder fatigue life predictions were compared to the ALF-measured fatigue life data as shown in Figure 9(b). Results demonstrate a strong correlation between fatigue life predictions from LAS test results and measured pavement fatigue lives at the FHWA-ALF, thereby providing validation that binder LAS testing coupled with S-VECD modeling can be used effectively to predict the binder's effect on the pavement's fatigue performance.

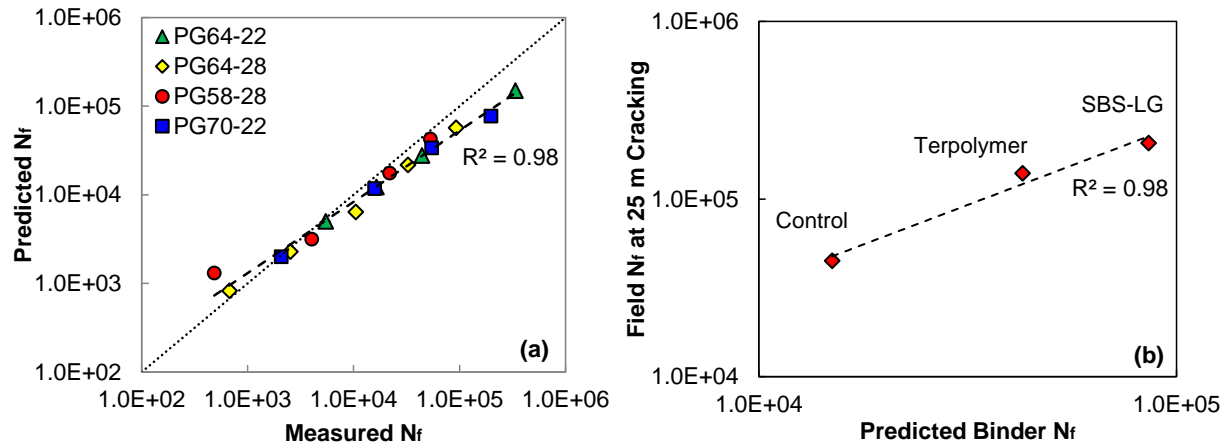


Figure 9. Validation of the LAS test with (a) binder test results and (b) FHWA ALF performance.

3. Crack Process, Damage Growth, and Macrocracking

The FHWA Distress Identification Manual (Miller and Bellinger, 2003), recognizes seven types of cracking of asphalt concrete pavements: fatigue, block, edge, longitudinal, reflection, and transverse (also known as thermal). This work focused on fatigue cracking, which is traditionally considered load related. In most instances, fatigue cracks are generated from repeated traffic loadings in the wheel paths. A common phrase that is associated with fatigue cracking is the “damage zone.” Damage zones form where distributed microstructural damage occurs, generally in the form of microcracks (Kim, 2009). This damage zone exists ahead of a macrocrack tip. Several factors of the microcracks influence the microcrack growth and healing, including propagation, coalescence, and rebonding.

Fatigue cracks either form at the interface of the aggregate and asphalt mastic (adhesive cracks) or within the asphalt mastic (cohesive cracks). The cracking mechanism is dependent on the temperature and rate of loading. Since asphalt concrete is a viscoelastic material, it behaves in a viscous manner at high temperatures (generally greater than 60°C) and an elastic manner at low temperatures (generally around the glass transition temperature). The glass transition temperature of a mixture determines when the binder has turned into a fully elastic material, which often occurs near the low temperature binder grade (Teymourpour and Bahia, 2014). However, the majority of fatigue cracking tends to occur at intermediate temperatures, which is represented in the fatigue testing of asphalt binders in the Superpave specifications. The intermediate temperature range is approximately 22-28°C, which is significantly higher than the low temperatures, implying that the material is not elastic in behavior.

While there is still healthy debate within the asphalt concrete community about the exact mechanisms of fatigue cracking, it is generally agreed on that macrocracks do not simply form after a single event (as they do in low-temperature cracking). Instead of a single event, there is a crack process that occurs. This document explores the concept of dissipated energy, dissipated creep strain energy, energy ratio, the Viscoelastic Continuum Damage Model, and several others. In short, all of these models predict some sort of damage accumulation in a region. The primary debate in the asphalt concrete community is the amount of damage and healing that occurs, and the mechanisms behind the damage and healing. As the loading continues, this damage increases over time, and the damage eventually turns into microcracking. Once a microcrack occurs, all of the energy input into the system targets these microcracks, which eventually lead to a single macrocrack. Macrocracks are commonly defined as being visible to the naked eye. Once the macrocrack is formed, if it is not properly maintained, it can quickly cause significant damage to the roadway.

4. Structural Influence on Cracking and Pavement Fatigue Analysis Techniques

One of the most common textbooks in asphalt materials, Pavement Analysis and Design (Huang, 1993), discusses that traditional fatigue cracking is “bottom-up” cracking, where the tensile stresses and strains at the bottom of the pavement layers were the area of the damage zone. This concept has driven the design of thicker structural cross sections with strongly bonded layers, which decreases the stresses and strains at the bottom of the layers. With the



significant increase in truck traffic over the past thirty years (from approximately 1,5 billion ton-miles of freight traffic in 1985 to 2,5 billion ton-miles of freight in 2010), this continues to be an area of importance. However, more recent research has indicated that top-down fatigue cracking may be just as detrimental (Molenaar, 2007; Roque *et al.*, 2010). Top-down fatigue cracking is caused by shearing forces between the tire and roadway, and the bending that is induced by surface tension away from the tire. As tire pressure increases, especially with innovations such as wide-based truck tires, top-down fatigue cracking warrants continued attention. There is not a consensus on which is more severe, or which mechanism is currently a great problem in the field.

Regardless of where fatigue cracks begin to form, the mode of cracking could also come into play. There are three modes of cracking: opening (Mode I), sliding in-plane (Mode II), and sliding out of plane (Mode III). A combination of these three modes is called mixed-mode cracking. The majority of fatigue cracking has only looked at opening cracks. While no sliding cracking or mixed mode cracking was found for fatigue cracking, there has been some work examining transverse (or thermal) cracking in sliding (Braham and Buttlar, 2009) and mixed-mode (Braham *et al.*, 2010). However, it is generally considered that mixed-mode fatigue cracking is an open area of research.

In addition to structural considerations and the mode of cracking, fatigue cracking is also considered in mixture design. The development research for Superpave recommended two mixture tests by ranking ten different fatigue cracking geometries and configurations (Tangella *et al.*, 1990). The two tests are repeated flexure and direct tension. Unfortunately, the standard mix design procedure could not require highly expensive or complicated equipment, as a large range of users perform mix designs. This balance between testing requirements for agencies and companies versus advanced characterizations of asphalt concrete prevented the implementation of either the repeated flexure or direct tension test, which has reduced the comprehension of fatigue cracking in the laboratory and how it relates to field performance.

5. Material Fatigue Assessment

5.1. Bulk

5.1.1. 4 Point Bending Test

Overview. This section details the development of the bending beam fatigue test and provides information on the strain life concepts developed. Methods, other than strain criteria of interpreting bending beam fatigue data, include the use of dissipated energy, which is discussed elsewhere in this document. The early development of bending beam fatigue tests used mechanical of relatively simple control systems that could be operated with the need for computer control. The initial fatigue development work for the four point beam used in the USA and standardized in the AASHTO and ASTM specifications was based upon work initially conducted by the University of California in Berkeley (UCB) Monismith, 1958; Monismith *et al.*, 1961; Deacon, 1965 and Santucci and Schmidt, 1969. This work is documented in early AAPT publications and other documents as shown in Figure 10.

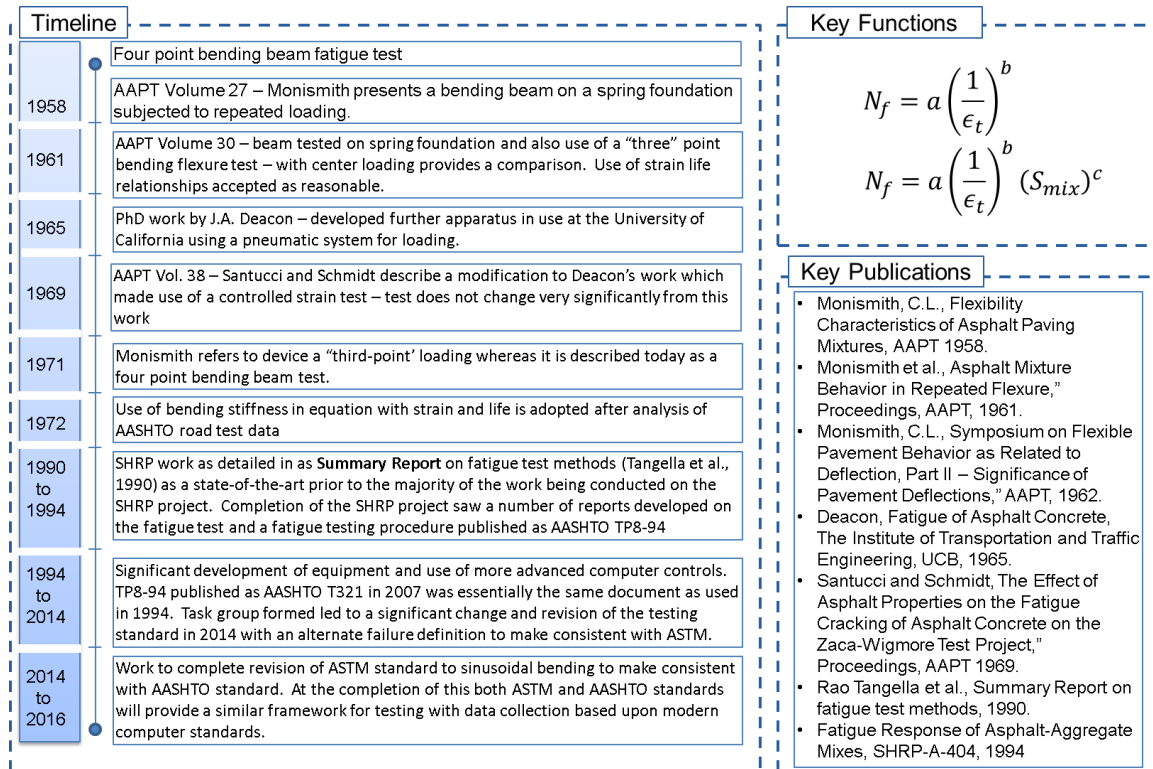


Figure 10. Development of the four point bending beam fatigue test

The device that was developed at this stage was essentially similar in all respects to that available during the beginning of the SHRP work as detailed in as summary report on fatigue test methods (Rao Tangella *et al.*, 1990). The device as time was described as “Third-Point” loading (Monismith *et al.*, 1971) whereas today it is typically described a 4-point bending beam fatigue. The use of the earlier wording represents that the beam is divided into three sections with loading applied at the “third” point distances from either end. Four-point loading is used to describe that four points are used to hold and load the beam – the two outer ones are held firm whereas load is applied at the two center locations. The loading in this version of the bending beam fatigue test consisted of an applied load pulse to the specimen for a specific duration after which a load was applied to return the specimen to the original position represented by the measurements on the specimen. The on specimen measurements on the device were located around a fixed target attached to the specimen at mid-height of the beam. These targets can be observed in the photographs of the apparatus dating to the mid 1960’s and ensures that no creep of the central point of the specimen is allowed (see Figure 11). It should be noted that the UCB device used specimens measuring 1.5 in. x 1.5 in. x 15 in. whereas the Asphalt Institute used specimens measuring 3 in. x 3 in. x 15 in. (Witczak, 1980), see Figure 12.

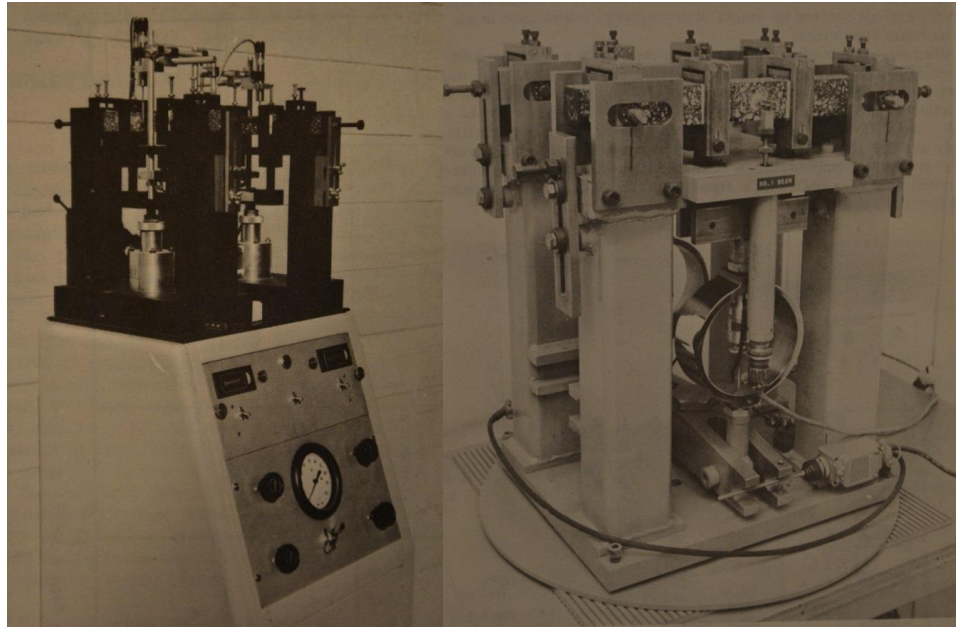


Figure 11. Constant stress fatigue equipment (left), after Vallerga et al., (1967) and Controlled Strain Fatigue test equipment (right), after Santucci and Schmidt (1969).

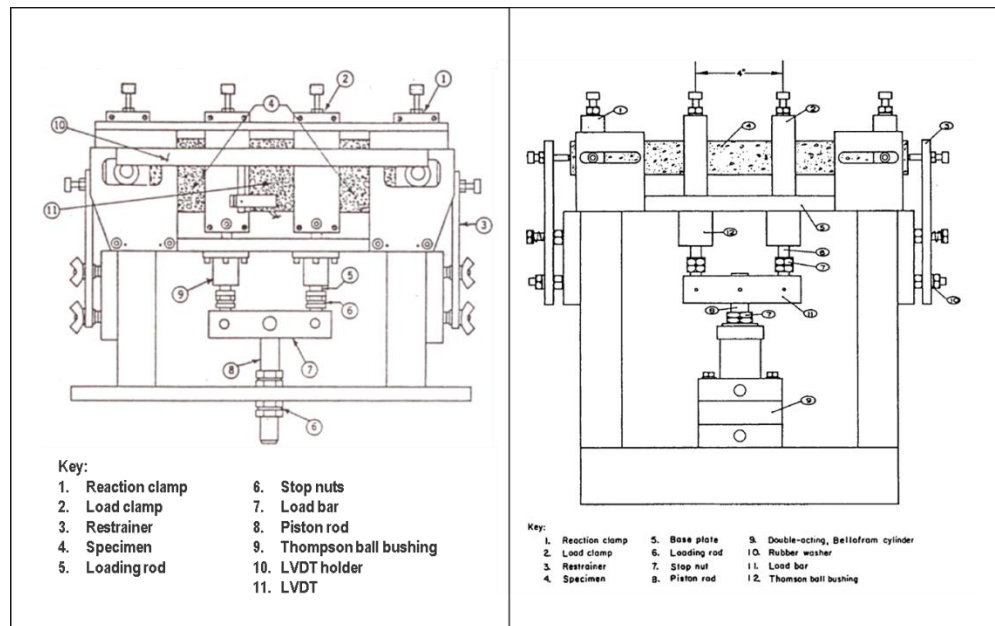


Figure 12. Asphalt Institute (left) and University of Berkley (right) fatigue four point bending beam fatigue test apparatus (after Monismith, et al., 1971 and Witczak, 1981.)

The test was further refined during the SHRP program with improvements to the data acquisition and control system and the use of sinusoidal loading. At the conclusion of the SHRP project a provisional ASSHTO standard was introduced (1994) which then became a full standard in 2003. The specification as developed contained the key wording “The loading device shall be capable of (1) providing repeated sinusoidal loading at a frequency of 5 to 10 Hz, (2) subjecting specimen to 4-point bending with free rotation and horizontal translation at all load and reaction points, (3) forcing the specimen back to its original position (i.e. zero deflection) at the end of each load pulse.”

The targets were used at the mid-specimen locations to ensure that the original position was maintained after each loading cycle. Subsequent implementation of this standard saw several pieces of equipment being marketed in



the USA and as additional equipment became available some differences in the results became apparent due to non-compliance with the requirements noted above and due to different data collection schemes being implemented. The original data collection schemes in the early 1990s involved the collection of about 10 to 25 data points to define a fatigue curve and then performing a regression analysis to fit a function form of $S=Ae^{bn}$, where S is the mix stiffness, n is the number of load cycles, e is the natural logarithm to the base e , and A and b are regression constants. The cycles to failure, taken as 50% stiffness reduction is taken from a manipulation of this expression.

Over the 20 years since the test specification was first developed a significant upgrade in computer technology has occurred that has resulted in significantly more data collected. Furthermore ASTM published a version of a similar standard. This prompted a review of the standards to ensure that both ASTM and AASHTO methods would produce similar results. One aspect that was observed to significantly affect the results in the AASHTO method was the amount of data that was fed into the regression analysis, Figure 13. After some consideration and detailed analysis the AASTHO standard has been revised in 2014 to incorporate the same failure definition as the ASTM standard while the ASTM standard (D7460 introduced in 2008, current revision 2010) is due to be revised to change the loading to sinusoidal (from the current haversine) which will bring these two standards to a compatible definition of the test method and analysis of the test data.

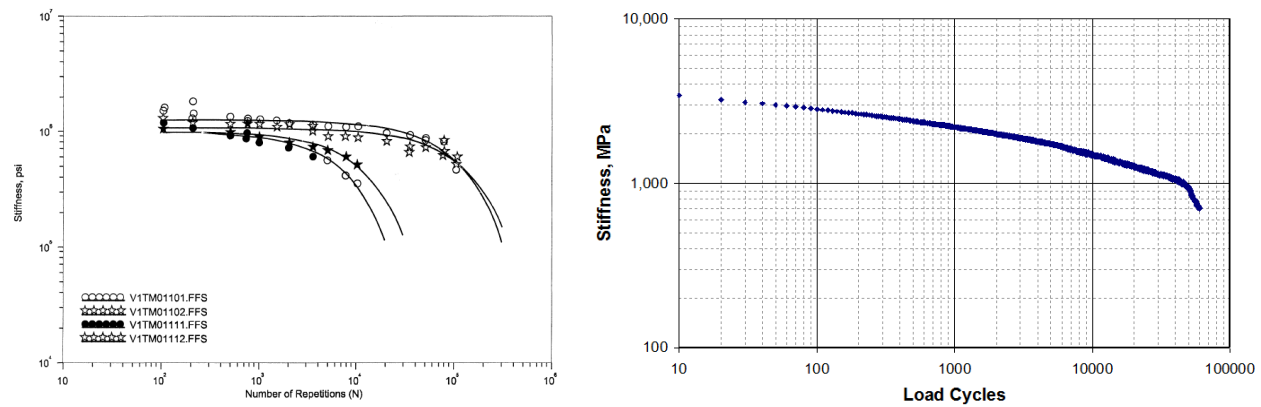


Figure 13. Original (left) and current (right) data collection scheme in the four point bending beam fatigue test (after Rowe, 2012).

In the beam tests, the calculation of the stiffness modulus from deflection measurements relies on the slender beam theory, in which deflection due to shear is ignored. Based on St. Venant's principle, far away from the source the stress distribution will not be influenced by the form of the source. Taking the shear force distribution calculated at the middle and used this distribution as the new input at the inner supports it can be found that the shear force distributions at the inner support and at the middle of the beam are not equal unless a correction value, α , is applied (Pronk and Huurman, 2009). In many textbooks and papers the value for α is taken equal to $2/3$. However, based on 1-D, 2-D, and 3-D finite element calculations, this value is found to be dependent upon Poisson's ratio and the geometry of the beam (specifically the ration of height to length and cross-sectional area to length). With typical values it is found that a value of 0.85 is more appropriate. It has been reported that the final correction is not large but in the order of 3-5% for ASTM conditions (Pronk and Huurman, 2009).

Strain life relationships. The tensile strain criterion was based on work performed by Professor Pell at the University of Nottingham in conjunction with the Shell Laboratories using a rotating cantilever beam wand was first reported in 1960 (Saal and Pell, 1960). This work paralleled a similar study by Professor Carl Monismith at UCB who published similar relationships the following year (Monismith et al, 1961). The work conducted with these devices led to relationships between tensile strain or stress and number of cycles to failure (typically taken as a 50% reduction in stiffness) being defined for asphalt materials. However, early fatigue work in the 1960s (for example Pell, 1962; Monismith, 1962; Epps and Monismith, 1969) found that fatigue life was better correlated with tensile strain than stress and consequently the basic fatigue relationship was characterized as:

$$N_f = a \left(\frac{1}{\epsilon_t} \right)^b \quad [24]$$

Often in recent publications the mix stiffness is added to this equation;



$$N_f = a \left(\frac{1}{\varepsilon_i} \right)^b (S_{mix})^c \quad [25]$$

In this case three parameters (a , b , and c) are determined by recession analysis.

The inclusion of stiffness was included based upon analysis of the AASHO road test conducted by as described by Kingham (1972). Witczak (1972) made use of this analysis in the development of criteria for the Asphalt Institute which was also included in the development of their subsequent design methods (Asphalt Institute, 1982). The addition of the asphalt stiffness was also justified by work developed by Claessen, *et al.* (1977).

It must be emphasized that the work with the AASHO road test made use of a direct correlation with the pavement performance and the mixture stiffness. The constants used in the design methods were not developed through laboratory testing but rather through field validation. Thus the inclusion of this parameter can be also considered as a “shift factor from the laboratory curves” to adjust to the conditions to field Finn *et al.* (1977). Finn *et al.* also includes a discussion of additional shift factors that relate to cracking for a 10% and 45% cracked performance. However, more recently various researchers have developed these factors through testing an individual mixes (Way *et al.*, 2012).

The factors developed by laboratory analysis will consider the sensitivity of the modulus to strain or stress level at which the test is being conducted but will not include the same factors that were considered in the original development of the equation with stiffness modulus by Kingham (1972) and Finn *et al.* (1977). Consequently, some care should be taken when reviewing analysis of data from bending beam fatigue when expressed with these equations and some consideration should be made to the actual field performance and the need for field verification as is performed with the MEPDG.

5.1.2. Cylindrical

Various laboratory testing methods have been developed to characterize the fatigue response of asphalt concrete (AC) mixtures. Among these laboratory tests, axial fatigue test on cylindrical specimens is a promising test method due to the constant stress state across the specimen section. Axial fatigue test results can be employed using two different approaches to assess fatigue behavior of AC. In the first approach, the stress or strain in the AC layer is related to the number of loading repetitions that causes failure. The second approach aims at measuring material fundamental stress-strain relationships to formulate rigorous constitutive models and predict the damage that can be then used as input for field performance prediction algorithms. This section overviews different uniaxial test protocols studies developed using specifically cylindrical specimens. For each test method, this section highlights the test objectives, sample preparation, specimen size and instrumentation, and test conditions. The time line of the fatigue test methods development using cylindrical specimens is shown in Figure 14. In the following section descriptions of several axial test methods are provided along with a summary of relevant information in Table 1.

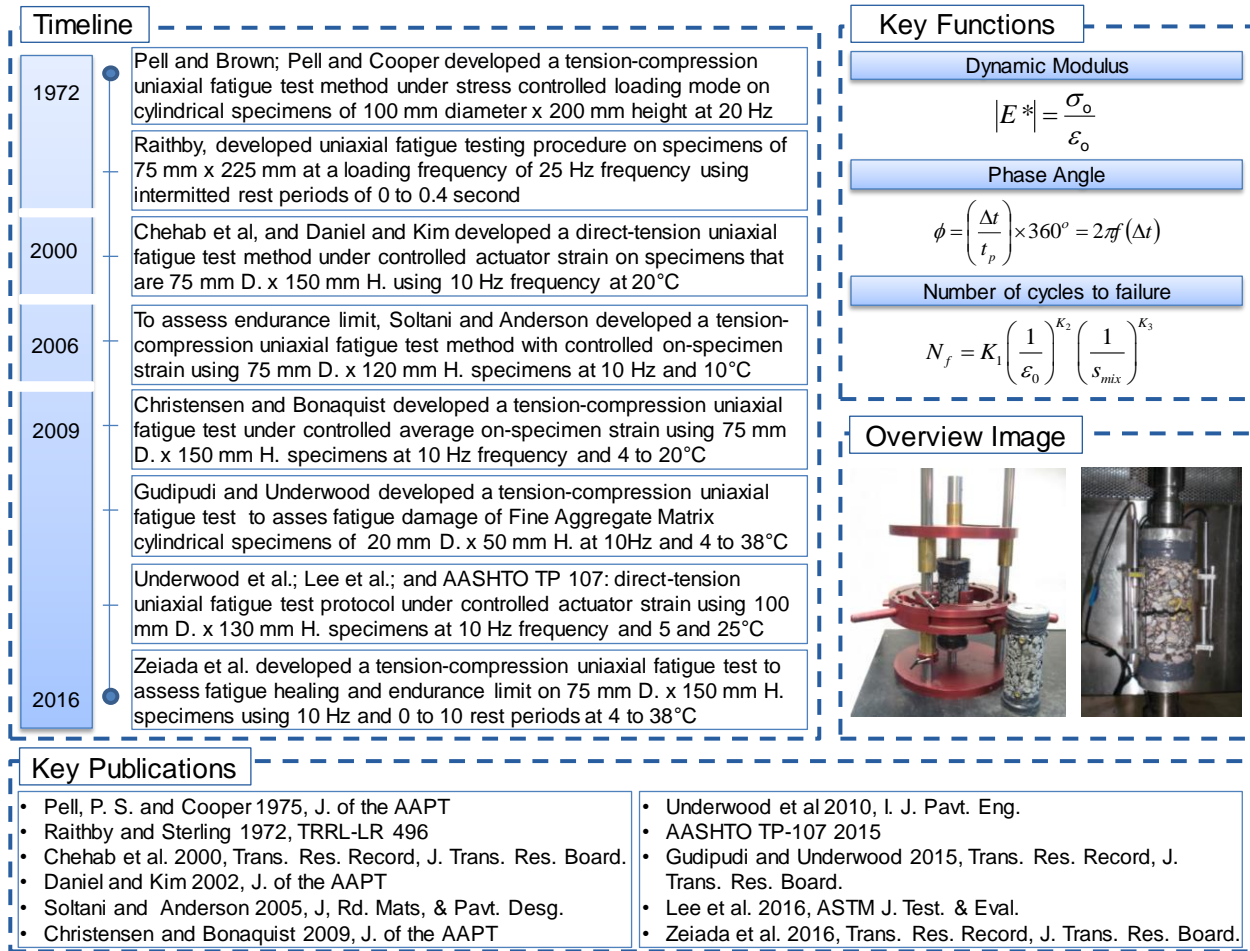


Figure 14. Overview of uniaxial fatigue test methods development.

Summary of Uniaxial Fatigue Test Methods

University of Nottingham. In the early 1970's researchers at the University of Nottingham devised testing equipment to conduct axial fatigue testing (Pell and Brown, 1972, and Pell and Cooper, 1975). For this particular equipment, cylindrical specimens with 100 mm diameter and 200 mm height were subjected to a sinusoidal loading (varying axial stress). This equipment has also been used for tension-compression testing with and without confining stress. End caps were glued to the specimens to accommodate for tension which provided an effective length for the measurement of vertical deformation of 150 mm.

The Transport and Road Research Laboratory (TRRL). The Transport and Road Research Laboratory (TRRL) of the United Kingdom developed a uniaxial fatigue test method to perform tensile tests without stress reversal at a loading frequency of 25 Hz. The uniaxial fatigue tests were conducted using a loading duration of 40 milliseconds and rest periods varying from 0 to 1 second (Raithby and Sterling 1972). The testing program was used to evaluate the effect of rest period, loading shape, and loading sequence.

Pennsylvania State University (PSU). Soltani and Anderson (2005) developed a new test protocol, testing machine, and software for the uniaxial fatigue test to estimate the fatigue endurance level of asphalt concrete. The uniaxial fatigue test protocol includes three stages of continuous loading without rest period. In stages I and III, strain level which is not exceeding the endurance limit of the HMA is applied. In Stage II, a strain with a magnitude exceeding the endurance limit and consequently causing fatigue damage is applied. The effects of non-fatigue phenomena such as self-heating and self-cooling are investigated by using eighteen thermocouples for the measurement of temperature at various locations in the specimen. Figure 15 shows the test setup including test specimen, fixtures, transducers and thermocouples.

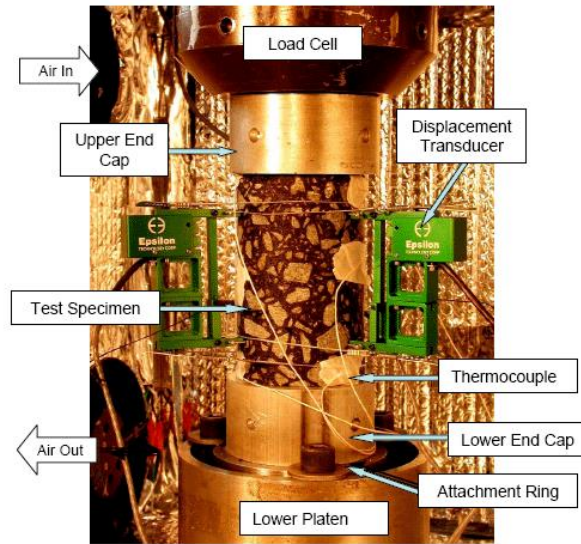


Figure 15. Detailed uniaxial fatigue test setup showing test specimen, fixtures, transducers, and thermocouples (Soltani et al., 2006).

Delft University of Technology (TU Delft). Uniaxial tension-compression test method to assess fatigue behavior of AC mixtures was developed at Delft University of Technology using a 25 kN Universal Testing Machine as shown in Figure 16 (Li, 2013). Cylindrical specimens were cored or sawn from blocks prepared with the PReSBOX compactor. The rectangular block prepared by the PReSBOX compactor has a fixed length and width of 450 mm × 150 mm. Specimens were glued to two steel plates at both ends using two-component fast curing adhesive glue. The thickness of the glue was around 3 mm. During the test, the load was applied to the top platen through the actuator.

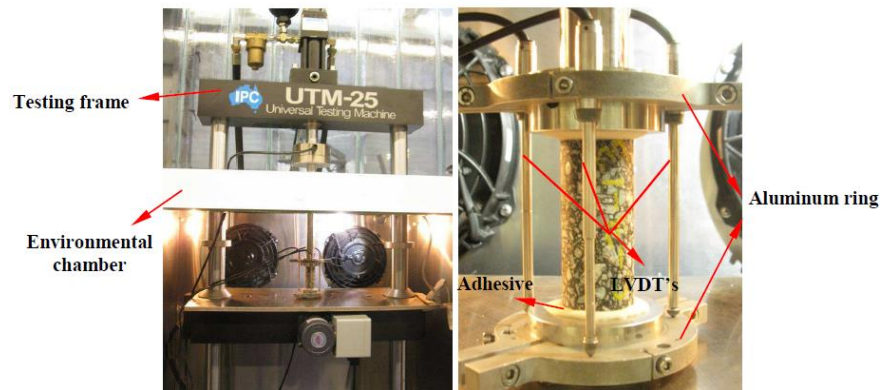


Figure 16. Uniaxial tension-compression test setup with the temperature chamber (left) and a close-up of a cylindrical specimen (right).

North Carolina State University (NCSU). North Carolina State University (NCSU) has utilized a uniaxial fatigue setup since the mid 1990's (Kim et al., 1997; Lee and Kim 1998a; 1998b). Through these initial studies and several follow-up experiments, a uniaxial fatigue test protocol (AASHTO TP 107) and analytical method has been developed (Chehab et al, 2000; Daniel and Kim, 2001; Underwood et al, 2010; AASHTO TP 107, 2014). The test method accompanies the Simplified Viscoelastic Continuum Damage Fatigue model (S-VECD), discussed at length in Section 6.3.1. However, the experiment can also be used to simply characterize the fatigue performance in a manner consistent with the other protocols listed herein.

Advanced Asphalt Technologies (AAT). Christensen and Bonaquist (2009) at Advanced Asphalt Technologies developed uniaxial fatigue test method and test software called Simplified Continuum Damage Uniaxial (SCDU) fatigue test. The reduced number of cycles concept is used to produce the damage characteristic curve which is a unique relationship for the same AC mixture at different strains and different temperatures, see Section 6.3.3. The



test itself is similar to the NCSU method with the exception that strains are controlled at a constant value throughout the testing by using feedback from the on-specimen LVDTs.

Arizona State University (ASU). As part of the NCHRP 9-44A study, a uniaxial fatigue and healing test method was developed at Arizona State University. Like many of the other methods, a servo hydraulic testing machine is used to load the specimens under an on-specimen strain-control mode of loading. Figure 17 shows specimen test setup for the fatigue test. To assess healing of fatigue damage, uniaxial fatigue tests are performed continuously and with intermittent rest periods applied after each loading cycle. As with the SCDU method the machine displacements are adjusted by the computer control software so that the on-specimen strains are constant throughout loading.

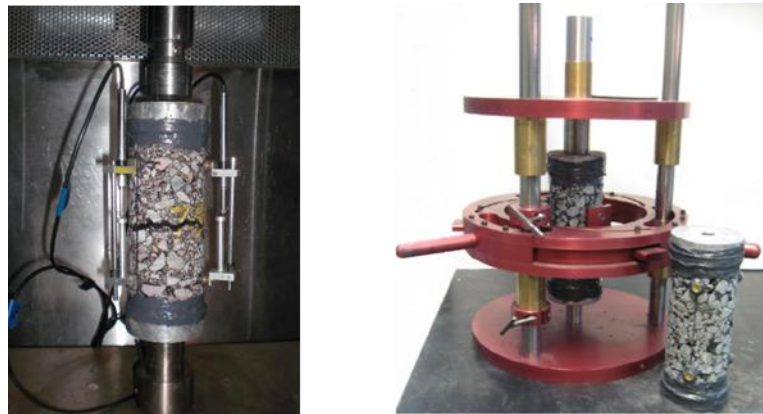


Figure 17. Uniaxial fatigue test specimen setup and gluing jig (Zeiada *et al.*, 2016)

Table 1. Summary of Relevant Details from Various Axial Fatigue Protocols.

Method	Loading ^{a,b}	Freq. [Hz]	Temp. [°C]	Geometry (d x h) [mm]	Meas. Gauge Length [mm]	On-Specimen Meas. Devices	Mode
Nottingham		20	0 to 40	100 x 200			Stress
TRRL	Push-Pull and Pull-Pull	25, 16.7	10, 25, 40	75 x 225	225	≥ 1	Stress
PSU	Push-Pull	10	10	75.5 x 120	75	3	On-specimen strain (one LVDT feedback)
TU Delft	Push-Pull	10	5, 20	25 to 75 x 62.5 to 178.5	Equal to Height	3	Stress and Machine actuator
NCSU	Pull-Pull	10	3 to 21	100 to 104 x 127.5 to 132.5	70	4	Machine actuator
AAT	Push-Pull	10	20	75 x 140 to 150	100	3	On-specimen strain (three LVDT feedback)
ASU	Push-Pull	10	4.4, 21.1, 37.8	75 x 150	100	3	On-specimen strain (three LVDT feedback)

^a Pull-Pull = Haversine loading with positive mean force/displacement

^b Push-Pull = Sinusoidal loading with zero mean force/displacement

Application to Small Sized Samples. Recently, the uniaxial fatigue test method has been adapted to smaller size specimens that can be extracted from in-service pavements. Several researchers (Kutay *et al.*, 2009; Li and Gibson, 2013; Park *et al.* 2014; Diefenderfer *et al.*, 2015) performed experimental studies on both full-size and small-scale cylindrical specimens for dynamic modulus and uniaxial tension-compression fatigue testing. In their study's the authors used different small size test sample geometries with AC mixtures having a nominal maximum aggregate size (NMAS) ranging from 4.75 to 19.0 mm. The results concluded that the modulus measured with the small size



diameter specimens is similar to that measured on full size specimens, but they are slightly softer at high temperature and low reduced frequencies. The fatigue test data on small scale samples showed that the modulus reduction at failure and endurance limit are comparable between full size and small scale specimens. Among several tested mixtures, fatigue resistance ranking was mostly similar with full size and small size samples. However, for the dynamic modulus test, studies concluded that for 9.5 and 12.5 mm NMAAC mixtures both small size diameter (38 and 50 mm) samples are showing similar results but for 19 and 25 mm NMAAC mixtures the 50 mm diameter is a better alternative to the full scale AC samples. Figure 18 shows the small size sample setup and instrumentation for testing procedure.

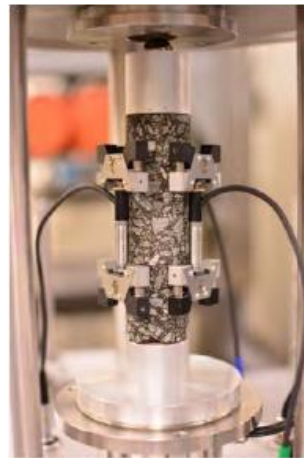


Figure 18. *Small size AC sample instrumentation and setup for dynamic modulus testing (Diefenderfer et al, 2015).*

North Carolina State University is currently developing a small specimen geometry for AC mixture performance testing. This project is focusing on development of small size geometry samples of 38mm x 100mm height and a small prismatic geometry 25 (T) mm x 50 (W) mm x 100 (H) mm. In this study the authors are performing both uniaxial cyclic, direct tension and monotonic direct tension testing for the purpose of AC fatigue characterization. The data will be used to characterize the AC material fatigue resistance using the S-VECD formulation similar to the approach taken by Park *et al.* (2014). In recent years the investigation on small size AC test sample is gaining importance as it helps to test the field cored samples for the AC performance in addition it also useful in improving the AC mixture testing efficiency as small size test samples enable for the coring of multiple test samples from single gyratory sample.

Application to Fine Aggregate Matrix. The uniaxial fatigue protocol has also been adapted for application to fine aggregate matrix (FAM) specimens (Gudipudi and Underwood, 2016) to predict AC damage behavior (Figure 19). This test procedure is developed at Arizona State University and uses a smaller scale uniaxial loading equipment (Electroforce 3330 load frame with 3kN capacity). The test method borrows substantially from the NCSU method and involves actuator controlled displacement loading. Figure 8 below shows the uniaxial fatigue test setup on FAM samples.

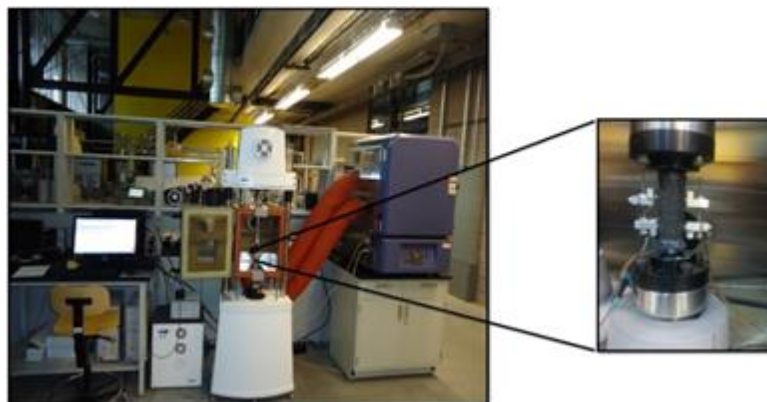




Figure 19. *Uniaxial fatigue test setup for FAM sample (Gudipudi and Underwood, 2016)*

5.1.3. Indirect Tension Test (IDT)

Overview. This section describes the Superpave Indirect Tension Test (IDT) and its current and potential applications in pavement cracking, with an emphasis herein on thermal and fatigue cracking in asphalt pavements. The IDT test includes the evaluation of mixture creep compliance and tensile strength. This test was developed under the Strategic Highway Research Program (SHRP) project A-357 at Penn State University in the early 1990's (Roque and Buttlar, 1992; Buttlar and Roque, 1994). It was originally developed as part of a comprehensive thermal cracking testing and software simulation suite, with a secondary goal of providing a parameter for the fatigue cracking model being developed at Texas A&M University (SHRP A-357). It has subsequently been used in various testing and analysis schemes, mainly, but not exclusively in research, to study and/or control various forms of asphalt pavement cracking. Specifically, the IDT test has been used to address low-temperature cracking, single-event thermal cracking and thermal fatigue cracking (Hiltunen and Roque, 1994; Roque *et al.*, 1995; Marasteanu *et al.*, 2012), traffic-induced fatigue cracking (Roque *et al.*, 2002; Dinegdae and Birgisson, 2016), reflective cracking (Wagoner *et al.*, 2006; Kim *et al.*, 2009; Dave *et al.*, 2010), and top-down cracking (Roque *et al.*, 2004; Roque *et al.*, 2010).

The IDT test can be conveniently summarized by reviewing its original development and application in the SHRP program. To calibrate both thermal and fatigue cracking models in the SHRP A-357 program, it was necessary to be able to test both gyratory-compacted specimens and field cores; hence the use of a circular indirect tension test geometry (150 mm standard, or 100 mm diameter optionally) with modest sample thickness (50 mm standard thickness and valid as low as 19 mm thickness). The original use of the indirect tension test geometry dates back to the Brazilian split tensile test used for rock and Portland cement concrete. This geometry was later adapted in the Canadian SHRP program with a horizontal surface-mounted gage and later in the SHRP program with bi-axial, surface mounted gages. The surface mounted gages were employed to increase test accuracy and to allow extraction of Poisson's ratio in the case of the SHRP program. In conjunction with the advent of 3D finite element analysis, the test was analyzed and correction factors obtained to allow users to determine accurate measures of mixture creep compliance and Poisson's ratio, which in turn could be used in material specifications and pavement simulation models.

The SHRP A-357 project featured the development of a mechanistic-empirical thermal cracking model named TC-MODEL. The model calculated thermal stress in a simulated asphalt pavement based on a creep compliance master curve and temperature shift factors combined with temperature profiles versus time, coefficient of thermal contraction, layer thicknesses, and a computational 2D viscoelastic stress model for the pavement. Next, the model used tensile strength and a slope parameter called 'm-value', which was obtained by fitting a power law function to the creep compliance master curve, along with a 2D stress intensity factor model ('CRACKTIP model' developed by Chang *et al.*, 1976), a Paris-law based crack propagation model, and a statistical crack distribution model. The 2D stress intensity factor and Paris-law based crack propagation models evaluated the depth of cracking generated by a single thermal discontinuity, and the statistical crack distribution model related the depth of cracking from the single thermal crack to a probabilistic amount (feet) of thermal cracking in a given 500 ft section. In simpler terms, a mechanistic-empirical thermal cracking model was developed, which primarily used material inputs obtained from a single test, the IDT, where the 'response' engine or numerical scheme to estimate pavement stress versus time was driven by creep compliance, and the 'distress' engine or cracking model was driven by mixture tensile strength. The IDT creep and strength tests were standardized in AASHTO T-322 in the late 1990's.

The IDT creep compliance, m-value, and tensile strength parameters have been used in numerous research and practical applications. The applications include: the NCHRP 1-37A thermal cracking prediction system used in ME-PDG/Darwin ME, the improved thermal cracking model developed at the University of Illinois (ILLI-TC Model), and the Florida top-down fatigue fracture mechanics model (HMA-FM-E (described in a later section)). The new thermal cracking model was developed in a low-temperature pooled fund study (FHWA Pooled Fund Study 776) leading to ILLI-TC Model. This model added disk-shaped compact tension (DC(T)) test (ASTM D7313) fracture energy to the IDT tensile strength and creep compliance to improve model accuracy. Numerous field and laboratory forensic studies have included IDT creep compliance and strength evaluation to determine thermal cracking potential. Two particular research studies focusing on reflective crack control and the magnitude of asphalt binder replacement are highlighted below in the Modern Uses of IDT section. However, before delving into sample data, the following section will take a look at how the test works and how data is interpreted.

IDT Creep Test. The two-part IDT test provides measures of time- and temperature-dependent creep response and strength. The creep response, if kept to relatively low levels of horizontal straining, can be used in the form of creep compliance to define the linear viscoelastic properties of the asphalt material. Creep compliance is defined as time-dependent strain over stress, which is often used to evaluate the viscoelastic behavior of asphalt mixtures at low-to-intermediate temperatures, particularly under slow loading pulses such as those associated with temperature cycling. Creep compliance of asphalt mixtures is influenced by many factors, such as performance grade of virgin binder (Wagoner *et al.*, 2006; Dave *et al.*, 2010), presence of asphalt modifiers (Hill *et al.*, 2012; Hill *et al.*, 2013a; Hill *et al.*, 2013b), asphalt binder content (Dave *et al.*, 2010), aggregate type (Buttlar and Wang, 2016), aging conditions (Braham *et al.*, 2009), and RAP/RAS or ABR content (Behnia *et al.*, 2011; Hill *et al.*, 2013a; Hill *et al.*, 2016). Creep compliance testing in asphalt mixtures is often conducted in the indirect tensile testing model according to AASHTO T-322, as shown in Figure 20. In this test, three replicates are generally tested using a quickly applied, step-type creep load at 0, -10, and -20°C for 1,000 seconds. In general, any test temperature can be used, but in order to stay in the linear viscoelastic range of most asphalt mixtures, test temperatures below 20°C are most widely used with the IDT test and its standard test equipment. The horizontal and vertical displacements at the center of each side of the specimen are measured with LVDT's or strain gage based extensometers with a 0.10 μm resolution (Epsilon 3910 extensometers are shown in Figure 20). These gauges span across a 38-mm gage length when 150 mm diameter specimens are tested (standard thickness is 50 mm).

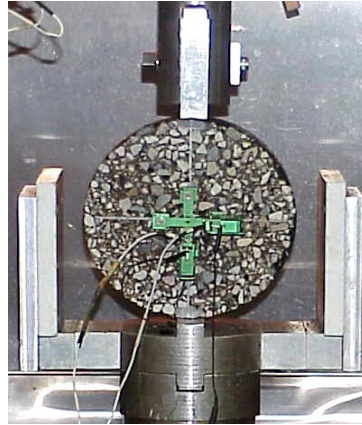


Figure 20. Indirect tension creep compliance test.

Creep compliance, $D(t)$, for an idealized biaxial stress state condition on the surface of the specimen is obtained through Hooke's law as follows:

$$D(t) = \frac{\varepsilon_x}{\sigma_x - \nu\sigma_y} \quad [26]$$

The 3D FEM correction factor developed by Buttlar and Roque (1994) to account for specimen bulging effects is given by:

$$D(t) = \frac{\varepsilon(t)}{\sigma} \frac{H_m(t) \times D \times t}{P \times GL} (C_{cmpl}) \quad [27]$$

where; $D(t)$ = creep compliance response at time t , $H_m(t)$ = measured horizontal deflection at time t , GL = gage length (= 25.4 mm for 101.6 mm diameter, = 38.1 mm for 152.4 mm diameter), P = Creep load, t = Specimen thickness, D = Specimen diameter, ν = Poisson's ratio, and C_{cmpl} , C_{SX} , C_{SY} , C_{BX} = Correction factors for non-dimensional creep compliance (Equations [28] through [31]); horizontal stress correction factor (Equation [32]); vertical stress correction factor (Equation [33]); and horizontal bulging factor (Equation [34]), respectively.

$$C_{cmpl} = \frac{1.071 \times \pi \times C_{BX}}{2(C_{SX} + 3\nu C_{SY})} \quad [28]$$



$$C_{cmpl} = 0.6354 \left(\frac{X}{Y} \right)^{-1} - 0.332 \quad [29]$$

with the factor restricted to the limits of $0.20 \leq t/D \leq 0.65$.

$$0.20 \leq \frac{t}{D} \leq 0.65 \quad [30]$$

$$\left[0.704 - 0.213 \frac{t}{D} \right] \leq C_{cmpl} \leq \left[1.566 - 0.195 \frac{t}{D} \right] \quad [31]$$

$$C_{sx} = 0.948 - 0.1114 \left(\frac{t}{D} \right) - 0.2693(\nu) + 1.436 \left(\frac{t}{D} \right)(\nu) \quad [32]$$

$$C_{sy} = 0.901 + 0.287 \left(\frac{t}{D} \right) + 0.138(\nu) - 0.251 \left(\frac{t}{D} \right)(\nu) - 0.264 \left(\frac{t}{D} \right)^2 \quad [33]$$

$$C_{bx} = 1.03 - 0.189 \left(\frac{t}{D} \right) - 0.081(\nu) + 0.089 \left(\frac{t}{D} \right)^2 \quad [34]$$

Again, the reason for the relatively cumbersome analysis equations is to increase test accuracy, and to obtain Poisson's ratio, which is needed for 2D and 3D pavement modeling. The value of (X/Y) represents the absolute value of the ratio of measured horizontal deflection to vertical deflection, taken by averaging data points around the middle of the test duration (between 460 and 540 seconds in a 1000-second creep test). The X/Y parameter is then used to compute an idealized average (loading-time-independent) Poisson's Ratio for the material at the given test temperature as follows:

$$\nu = -0.10 + 1.48 \left(\frac{X}{Y} \right)^2 - 0.778 \left(\frac{t}{D} \right)^2 \left(\frac{X}{Y} \right)^2 \quad [35]$$

where $0.05 \leq \nu \leq 0.50$.

In this analysis, a special data averaging technique, a trimmed mean, is used to provide a more stable estimate of creep compliance in light of the fact that the gage-length-to-aggregate size ratio can be small, leading to significant variability between replicate measurements for larger NMAS mixtures. If the standard of three specimen replicates is followed, each having biaxial displacement measurements on both faces, a total of 6 displacement versus time curves are obtained. The trimmed mean approach drops the high and low readings and averages the middle 4 creep curves.

The formation of a creep compliance master curve is not described in detail herein for brevity. Once creep curves at multiple temperatures are shifted horizontally in time to obtain a single 'master' curve, it is necessary to fit a rheological model to the resulting master curve for use in subsequent pavement simulation models, and to fit the Power law model to get at the 'm-value' parameter. A generalized Voight-Kelvin model is typically fit to the master creep compliance curve, and shift factors are obtained based on the amount of shifting in time needed to bring the creep compliance curves from various temperatures into alignment, using the following equations:

$$D(\xi) = D(0) + \frac{\xi}{\eta_v} + \sum_{i=1}^N D_i \left(1 - e^{-\xi/\tau_i} \right) \quad [36]$$

where; ξ = reduced time, Equation [37], t = real time, a_T = temperature shift factor, $D(\xi)$ = creep compliance at reduced time ξ , $D(\infty)$, $D(0)$, D_i , τ_i , η_v = Prony series parameters.

$$\xi = \frac{t}{a_T} \quad [37]$$

The results of the master creep compliance curve are also fit to a Power Model defined by:

$$D(\xi) = D_0 + D_1 \xi^m \quad [38]$$

The relaxation modulus function is often obtained for simplification of thermal stress calculations by numerically ‘inverting’ the creep compliance function. The relaxation modulus is represented by a Generalized Maxwell model or ‘Prony series’ relationship:

$$E(\xi) = \sum_{i=1}^{N+1} E_i e^{-\xi/\lambda_i} \quad [39]$$

where; $E(\xi)$ = relaxation modulus at reduced time ξ and E_i and λ_i = Prony series parameters for master relaxation modulus curve (spring constants or moduli and relaxation times for the Maxwell elements). Finally, knowledge of the relaxation modulus function allows for the computation of the thermal stresses in the pavement according to the following constitutive equation:

$$\sigma(\xi) = \int_0^{\xi} E(\xi - \xi') \frac{d\varepsilon}{d\xi'} d\xi' \quad [40]$$

where; $\sigma(\xi)$ = stress at reduced time ξ , $E(\xi - \xi')$ = relaxation modulus at reduced time $\xi - \xi'$, ε = strain at reduced time ξ ($= \alpha(T(\xi) - T_0)$), α = linear coefficient of thermal contraction, $T(\xi)$ = pavement temperature at reduced time ξ , T_0 = pavement temperature when $\sigma = 0$, ξ' = variable of integration.

IDT Strength Test. The IDT strength test evaluates the indirect tensile strength of the material at a rate of 12.7mm/min. Versions of AASHTO T-322 prior to 2007 outline a procedure to estimate a so-called first failure indirect tensile strength of the mixture, S_t , as follows:

$$S_t = \frac{2P_f C_{sx}}{\pi D t} \quad [41]$$

where; P_f = failure load, C_{sx} = correction factor as obtained from creep testing, t = specimen thickness, and D = specimen diameter. This definition of tensile strength considers the onset of crack growth which typically occurs prior to reaching the peak load capacity of the material. The post-2007 versions of AASHTO T-322 define the value of P_f as the maximum load measured during the IDT strength test.

IDT Fracture Test. The monotonic IDT fracture test has been proposed as a simple yet promising test method for evaluating the fatigue cracking and transverse cracking performance of asphalt mixtures. It not only can provide IDT strength data, which indicates the maximum load that asphalt mixtures can withstand, but also gives other fracture properties such as fracture energy, fracture work, and failure strain that takes into account the mixtures' flexibility and resistance to fracture. The fracture property (fracture energy) obtained from the monotonic IDT fracture test was found to correlate well with field fatigue performance of WesTrack pavements (Wen and Kim, 2002; Wen, 2013). The IDT tests were also applied in several studies to evaluate the fracture properties of WMA, SMA, RAP and RAS mixtures for Washington State (Bower *et al.*, 2015; Wu *et al.*, 2015; Wu *et al.*, 2016). Shen *et al.* (2016) studied the field performance of twenty-eight HMA and WMA projects and identified that material properties obtained from the IDT fracture test as promising significant determinants for field performance, which includes fracture work density at -10°C for transverse cracking (Zhang *et al.*, 2015), and vertical failure deformation at 20°C for top-down cracking (Wu *et al.*, 2016).

The monotonic IDT fracture test is conducted at 20°C for fatigue performance or at -10°C for thermal cracking performance. At 20°C, the constant displacement rate of 50.8 mm/min is applied until the specimen experiences fracture failure. At -10°C, the displacement rate is 2.54 mm/min. The test specimen can be either 100 mm or 150 mm in diameter. The test can be performed in two setups, with linear variable differential transformer (LVDT) (Figure 21), or without LVDT. The aid of LVDT is helpful to measure the vertical and horizontal deformation during the monotonic loading so that the corresponding strain can be determined. However, the LVDT could be damaged easily during a fracture test and additional protection to the LVDT must be provided. For example, rubber tubes can be used to wrap both ends of the LVDTs, and two blocks can be placed at each side of the test specimen to prevent over-stretching the LVDT after the specimen is fractured.

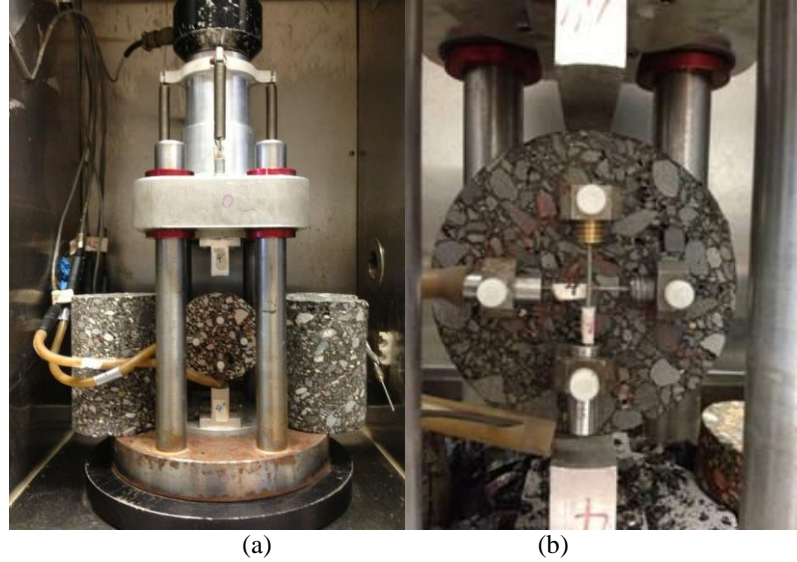


Figure 21. IDT test setup with LVDT mounted on specimen: (a) overview of the test setup; (b) close look of the LVDT mounted on specimen.

IDT fracture test without LVDT

Fracture work, defined as the area beneath the load versus vertical displacement curve, can be obtained from an IDT fracture test without the need of incorporating LVDT. It is based on the assumption that the external work done by the machine ram is ultimately dissipated by the specimen neglecting any thermal dissipation during the short period of testing. Wen (2013) evaluated the effect of machine compliance (i.e. the difference between the recorded ram movement and the displacement measured by the LVDTs) and concluded that the fracture work determined based on the ram movement and LVDTs shows no difference. Fracture work is further converted into fracture work density by dividing the fracture work by the volume of the specimen to eliminate the effect of geometry on test results.

Figure 22 shows a plot of the load versus vertical displacement from an IDT fracture test, with fracture work and vertical failure deformation illustrated. The total area can be approximated as the sum of the trapezoidal areas between each data point until the load decreases to zero. Thus, the fracture work value is calculated as shown in Equation [42].

$$W_f = \sum_{i=0}^f \frac{1}{2} (P_{i+1} + P_i) (\delta_{i+1} - \delta_i) \quad [42]$$

where; W_f = fracture work, N·mm, P_i = load observed at each point, N, and δ_i = ram (vertical) displacement corresponding to P_i , mm.

Vertical failure deformation is the critical deformation at the peak load, which can be used to characterize the flexibility of asphalt mixture under extreme loading. A higher vertical failure deformation is usually associated with a more flexible the material, and less cracking potential in the field.

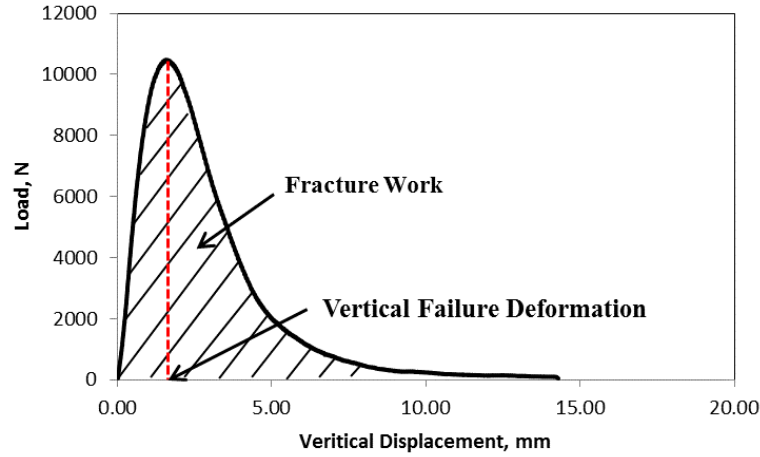


Figure 22. Load versus vertical displacement from IDT fracture test without LVDT mounted.

IDT fracture test with LVDT

IDT fracture test with LVDTs mounted on both sides of testing specimen allows one to obtain the strain information during the test. As shown in Figure 23, horizontal failure strain is the horizontal strain at the peak stress in the stress-strain curve, and the fracture energy is the area up to peak stress under the curve. Based on field investigation, researchers indicated that the horizontal failure strain, rather than the fracture energy, obtained from the IDT fracture test correlates with the field top-down cracking performance (Shen *et al.*, 2016; Wu *et al.*, 2016).

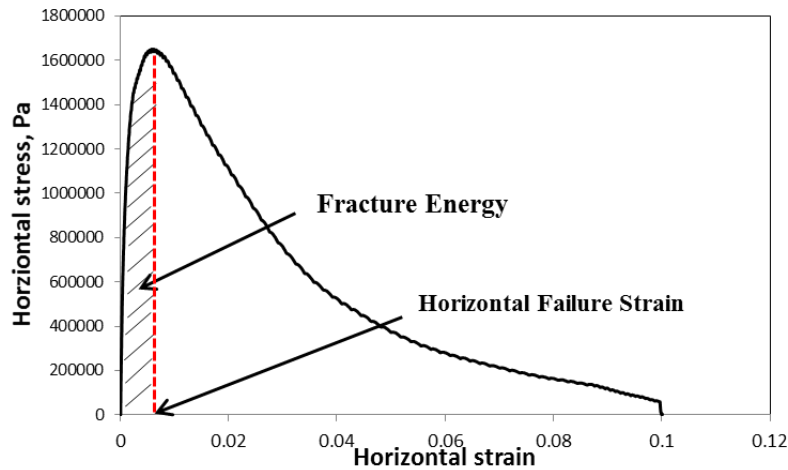


Figure 23. Horizontal stress versus horizontal strain from IDT fracture test with LVDT mounted.

Horizontal failure strain is time and loading rate dependent, which can also be expressed by Equation [43].

$$\log \varepsilon_f = a + \frac{b}{1 + \exp^{(c+d \log \dot{\gamma}_r)}} \quad [43]$$

where; ε_f = horizontal failure strain, a , b , c , d = coefficients determined by nonlinear optimization, and $\dot{\gamma}_r$ = reference loading rate.

Modern Applications of IDT. ABR, binder type, and binder content effects have been differentiated using creep compliance portion of the IDT test. Two particular projects which demonstrate these differentiation capabilities are the Illinois Tollway SMA (Buttlar and Wang, 2016) and NSF GOALI reflective crack control (Dave *et al.*, 2010) studies. The Illinois Tollway study creep compliance results are shown in Figure 24. The Illinois Tollway employs RAP and RAS in SMA mixtures in low to high (0-40%) ABR combinations. Typically, these SMA mixtures are



used in conjunction with virgin modified asphalt cements containing styrene-butadiene-styrene (SBS) or ground tire rubber (GTR) to increase cracking resistance. The mixtures tested and shown in Figure 24 were evaluated because they were placed between 2008 and 2012 before the onset of cracking test use in design. The results demonstrate the sensitivity of the Power Law model m -value to aggregate type and ABR. High ABR coupled with Quartzite aggregate led to the lowest creep compliance, and thus largest bulk mixture stiffness, across the reduced time domain and agreed with the findings of Behnia *et al.* (2011) and Hill *et al.* (2012; 2013a).

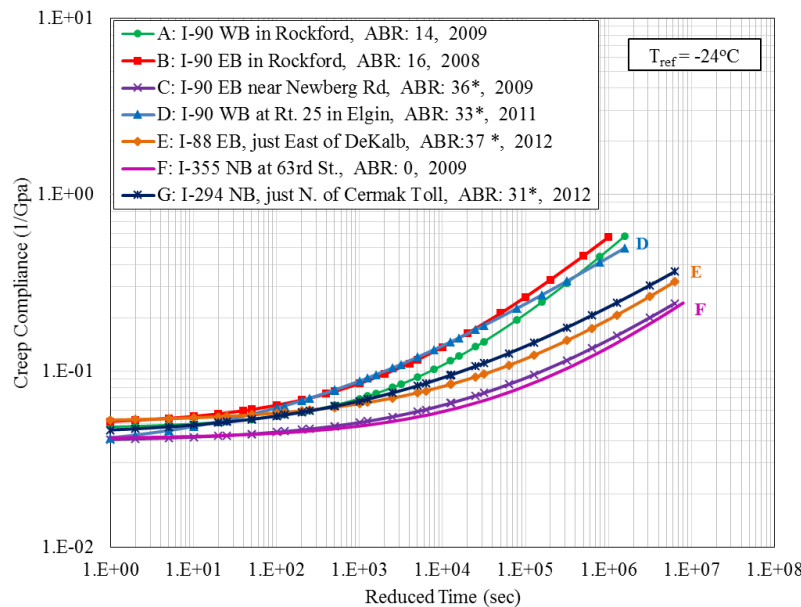


Figure 24. IDT Creep Compliance of Illinois Tollway Mixtures ($T_{ref} = -24^{\circ}\text{C}$).

The NSF GOALI reflective crack control study completed an investigation of strain tolerant asphalt systems and their respective abilities to resist reflective cracking. Analysis was completed using laboratory testing, numerical simulations, and accelerated load testing of four different test sections (Dave *et al.*, 2010). The materials in each of the four test sections are shown in Figure 25 and included a standard overlay mixture (PG-95 with PG64-22 asphalt binder), an interlayer mixture (RC-RI (Reflective Crack-Relief Interlayer) with a proprietary polymer-modified asphalt binder), and four transitional asphalt mixtures (2-4.75 mm NMA mixtures (B1-475 and B2-475) and 2-9.50 mm NMA mixtures (B1-95 and B2-95) where B1 and B2 contained 2/3 PG64-22 and 1/3 RC-RI binder and 1/3 PG64-22 and 2/3 RC-RI binder, respectively). The interconverted relaxation modulus results shown in Figure 25 demonstrate that asphalt binder grade and content affected bulk mixture response. The primary differences were evident at longer reduced times as the polymer modified and smaller NMA mixtures with higher asphalt contents had the lowest relaxation moduli.

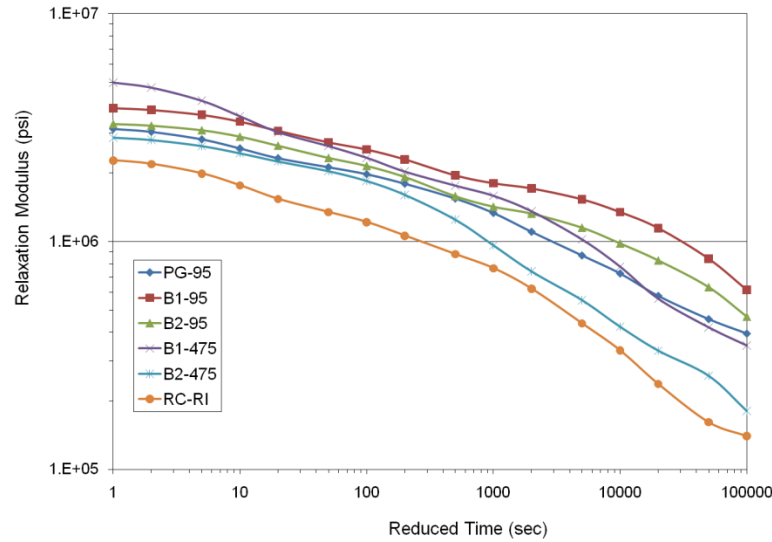
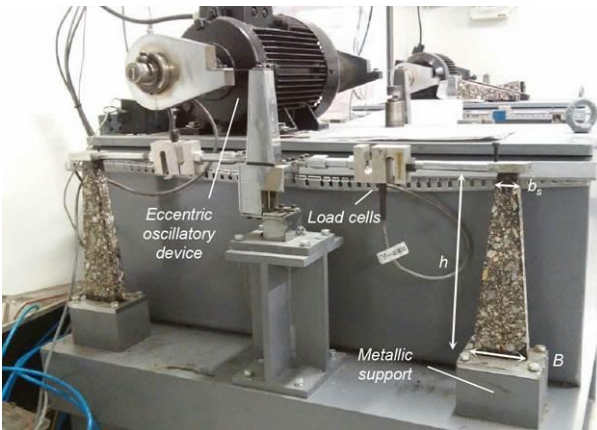


Figure 25. IDT Relaxation Modulus Converted from Creep Compliance for Dave *et al.* (2010) Study of Reflective Crack Relief Systems.

Finally, it should be noted that it is not always convenient for research or practitioner labs to possess creep, strength, and fracture/simple cracking performance test equipment. To address these issues, Kebede (2012) and colleagues (Behnia *et al.*, 2013) developed a procedure to obtain creep compliance using the ASTM D7313 DC(T) equipment. In this manner, creep compliance, mixture tensile strength (from fracture energy), and fracture energy can be obtained from a single piece of test equipment. These parameters can then be used in cracking simulation models, such as the ILLI-TC thermal/thermal fatigue cracking model and the Florida fracture mechanics model.

5.1.4. Trapezoidal Test

Overview. During the trapezoidal test an isosceles trapezoidal sample of asphalt concrete is subjected to repeated sinusoidal displacement of its narrow end (25 Hz), while the wide end is rigidly attached to a metal support. The force required to apply a consistent displacement is recorded and used to identify failure of the asphalt concrete mixture. The test is repeated at multiple displacement levels and the results are used to construct the *fatigue law* of the mixture, which corresponds to the linear regression on a bi-logarithmic space of amplitude strain level vs. number of cycles to failure. The set-up of the test and the dimensions of the specimens are presented in Figure 26 and Table 2. The overview diagram is shown in Figure 27.



(a)



(b)

Figure 26. (a) Experimental set-up of the fatigue test with trapezoidal specimen, and (b) detail of the trapezoidal specimen.



Table 2. Dimensions of the test specimens.

Dimension	Type of mixture*		
	$D \leq 14\text{mm}$	$14 < D \leq 20\text{mm}$	$20 < D \leq 40\text{mm}$
B (major base)	$56 \pm 1 \text{ mm}$	$70 \pm 1 \text{ mm}$	$70 \pm 1 \text{ mm}$
b_s (minor base)	$25 \pm 1 \text{ mm}$	$25 \pm 1 \text{ mm}$	$25 \pm 1 \text{ mm}$
e (thickness)	$25 \pm 1 \text{ mm}$	$25 \pm 1 \text{ mm}$	$50 \pm 1 \text{ mm}$
h (height)	$250 \pm 1 \text{ mm}$	$250 \pm 1 \text{ mm}$	$250 \pm 1 \text{ mm}$

* D is the maximum nominal aggregate size of the asphalt mixture

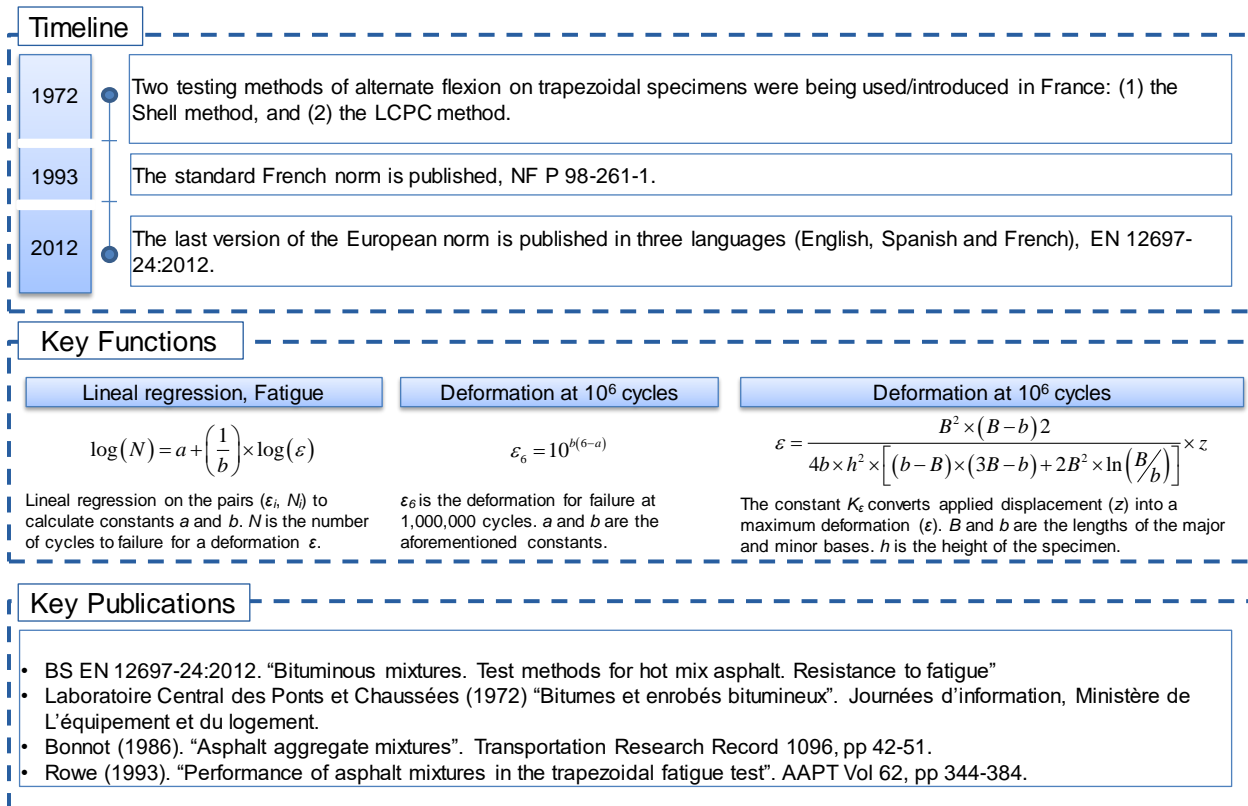


Figure 27. Summary of development of trapezoidal test.

Characteristics of the test. This loading scheme, which is sometimes also referred to as "two-point bending fatigue", is currently regulated by the European standard BS EN 12697-24:2012, "Bituminous mixtures – Test methods for hot mix asphalt. Part 24: Resistance to fatigue" (The British Standards Institution 2012). This norm describes in detail the requirements for the specimens, the characteristics of the experimental-set up, and the analysis of the associated results. The following is some of the most relevant information specified in this standard:

- Material:** the test can be conducted on any asphalt mixture. However, the geometry of the specimen changes as a function of the maximum nominal aggregate size of the gradation of the mixture, as specified in Table 2.
- Sample fabrication and preparation:** specimens can be obtained by sawing laboratory-manufactured slabs (thickness not less than 40 mm) as well as slabs taken from road layers or from field cores with a minimum diameter of 200 mm. After fabricating the testing specimens with the required geometry and prior to testing, the samples should be stored during 14 to 42 days at a temperature of no more than 20°C. During

this period, the specimens should be exposed to air at a relative humidity condition of less than 80% and a temperature lower than 20° C, with the objective of drying the sample. Afterwards, the specimens should be glued to the metal base with a thin gluing film. After assuring that the specimen is properly glued to the metal base (i.e. that the epoxy used has dried), the test can be initiated.

- **Replicates:** a minimum total of 18 specimens should be tested.
- **Failure criterion:** similar to other displacement-controlled fatigue tests, the conventional failure criterion for this trapezoidal fatigue test is the number of load applications when the complex stiffness modulus of the sample has diminished to half of its initial value (N).
- **Selected strain levels:** the precise values of the strain levels (ε_i) to be applied to the specimen are not specified in the standard. Instead, they should be selected using any of the following criteria: 1) the values are approximately regularly spaced on a logarithmic scale, or 2) there are at least three levels of deformation, with the same number of specimens (1 or 2) at each level. Additionally, it is required that at least one third of the selected deformations provide N values of less than 1,000,000 cycles, and one third provides N values greater than 1,000,000 cycles.
- **Main results:** as mentioned previously, the main result from the test is the fatigue law of the material, which correlates the applied strain to the number of cycles to failure (N).
- **Equipment restrictions:** the test requires a system able to apply a sinusoidal displacement with a fixed frequency of 25 ± 1 Hz. Also, a ventilated thermostatic chamber shall be used to control the temperature of the metal base of the specimens and the average temperature of the air close to the specimens. To measure the force, it is necessary to use a system with accuracy of $\pm 2\%$ for forces greater or equal than 200 N, and accuracy of ± 2 N for forces less than 200 N. To measure the horizontal displacement applied at the head of the specimens, the equipment requires the use of sensors with an accuracy of at least $1.5 \mu\text{m}$.

Calculations. The conversion from the horizontal displacement that is applied on top of the specimen (z) into the maximum horizontal deformation (ε), can be computed through the constant K_ε as follows:

$$\varepsilon = K_\varepsilon \times z \quad [44]$$

where K_ε is defined as:

$$K_\varepsilon = \frac{B^2 (B - b_s)^2}{4b_s \times h^2 \left[(b_s - B)(3B - b_s) + 2B^2 \ln\left(\frac{B}{b_s}\right) \right]} \quad [45]$$

In Equation [45], B and b_s = the lengths of the major and minor bases of the trapezoidal sample, respectively, and h = the height of the specimen. All dimensions are in meters, and they appear marked in Figure 26. This constant is used to calculate the desired head displacement for each specimen. As mentioned before, the final result from this test is the fatigue law of the material, or a lineal regression that correlates N and ε , in logarithmic scales. That linear regression is expressed as follows:

$$\log(N) = a + \left(\frac{1}{b}\right) \times \log(\varepsilon) \quad [46]$$

where; a and b = fitting constants, and $1/b$ = the slope of the regression curve. Equivalently, b is the slope of the $\log(\varepsilon)$ vs. $\log(N)$ curve, which is the usual way to present the results. Typically, the fatigue law of the material is represented through the slope of the linear regression of $\log(\varepsilon)$ vs. $\log(N)$, or b , and the strain that should be applied to the material to cause failure at one million of cycles ($N = 1 \times 10^6$), or ε_6 , which is computed as:

$$\varepsilon_6 = 10^{b(6-a)} \quad [47]$$

These two parameters are considered crucial properties in the French mechanistic-design pavement design method (LCPC, 1997), which has been also commonly used in other countries for more than 16 years. A summary of the experimental data obtained through this method at the Laboratory of Pavement Engineering at Universidad de los Andes (Bogotá, Colombia) for 80 surface mixtures with varying designs and specifications, yielded typical average values of b ranging from -0.28 to -0.23, and average values of ε_6 around 1×10^{-4} . Specifically, Figure 28 presents the fatigue results for 3 different hot dense-graded asphalt mixtures with different gradations (named MDC-



1, MDC-2, MDC-3), which satisfy the Colombian road specifications (INVIAS, 2013).

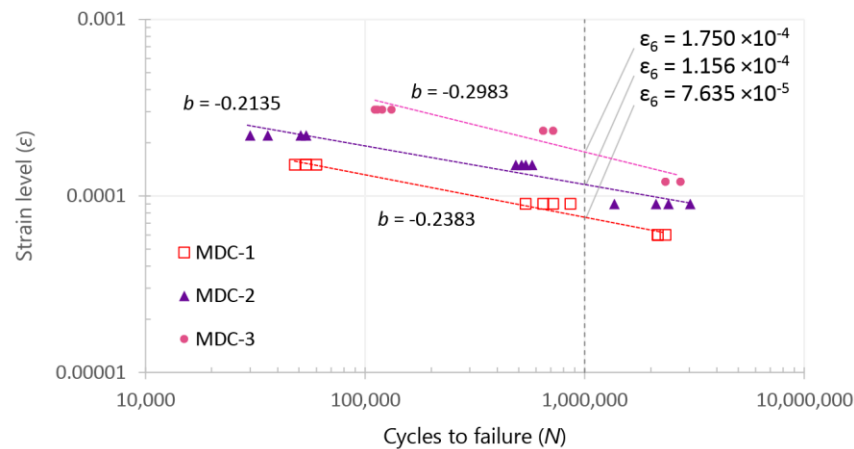


Figure 28. Experimental results for three Colombian hot mix dense-graded materials.

Timeline of the development of the test. In 1972, alternate flexure, traction-compression and rotative flexure tests were already in use in France for fatigue testing (Chompton *et al.*, 1972). According to these authors, at the time, there were also two fatigue flexural or bending testing methods on trapezoidal beam specimens: (1) the Shell method, and (2) the LCPC (*Laboratoire Central de Points et Chaussées*, currently IFFSTAR, *l'Institut Français des Sciences et Technologies des Transports, de l'Aménagement et des Réseaux*) method, both at strain and stress-controlled conditions. These two methods used the same principle of applying a horizontally sinusoidal load on top of a vertical cantilever trapezoidal beam of an asphalt mixture, to cause tension on its middle third. The methods used samples of similar geometry but they presented some differences in the conditions of the test (i.e. temperature, frequency range, and particular ranges of applied load or displacement). In particular, the LCPC test was performed under controlled stress or strain conditions with fixed or increasing amplitudes ('sweeping'), and sometimes it was also conducted using resting periods to study healing processes in the asphalt material. On the other hand, the Shell method could also be conducted over larger samples taken from base layers, using a more powerful equipment. As it can be observed, the method used today has preserved some of the main characteristics of the original experimental set-ups, especially those related to the geometry of the specimen and to some features of the load application procedure.

Francken and Verstraeten (1974) conducted a study in which trapezoidal specimens were subjected to stress-controlled sinusoidal bending, to identify variables that were useful to predict the fatigue life of the material. Through these results, the authors found that the fatigue law of an asphalt mixture could be predicted based on its volumetric composition and on the asphaltene content of the bitumen.

Bonnot (1986) presented a summary of some of the mechanical tests that were being used in France at the time for characterizing the performance of asphalt mixtures. This summary included the imposed-displacement alternating bending test on trapezoidal specimens with a restrained end. The authors then noted that the strain at 1×10^6 cycles, i.e. ϵ_6 , was one of the most useful parameters to control fatigue degradation in pavement design methodologies. At the same time, the authors pointed out that LCPC was moving towards shear fatigue testing instead of bending, due to the fact that the former presented less scattered results, and it considered loading types for thin surface courses and interlayers. By that time, the authors were mainly using the trapezoidal fatigue test to study healing in asphalt mixtures, and to develop fatigue damage accumulation laws.

In the context of the Strategic Highway Research Program (SHRP), Rowe (1993) tested several asphalt mixtures using the trapezoidal fatigue test. The authors performed an extensive and detailed analysis about the cumulative energy dissipated during the test to evaluate crack initiation, seeking to overcome differences related to the characteristics of the specimen and changes in temperature, and also with differences induced by the mode and frequency used for load application. Both the binder content and the viscoelastic properties of the mixture were found to be potential descriptors of fatigue performance. They also proposed and presented a physically-based method to predict failure initiation. The tests were conducted under both controlled stress and strain conditions.

It should be pointed out that, with the exception of this last study, it is generally agreed that the trapezoidal fatigue test has been more commonly used in Europe (Witczak *et al.*, 2013) and in some countries of Latin America



(e.g. Brazil and Colombia).

Strengths and shortcomings of the trapezoidal fatigue testing. As with any fatigue tests there are strengths and weaknesses. When compared to other fatigue procedures that use rectangular specimens, the fabrication of high quality and precise trapezoidal specimens constitutes an important challenge in this test. If overcome though the experimental set-up of the test is relatively simple, especially when compared to other fatigue tests. Also, depending on the specific experimental set-up configuration, it is usually possible to conduct several tests at the same time. The experimental set-up presented in Figure 26, for example, permits to test four replicates simultaneously (two on each side of the machine). This condition optimizes the overall testing time required to determine the fatigue law of a mixture. In the Laboratory of Pavement Engineering at Universidad de los Andes (Bogotá, Colombia), for example, there are a total of three devices as that shown in Figure 26, which permit testing 12 specimens simultaneously. As most fatigue tests, the data is somehow scattered and it is sometimes necessary to repeat some of the tests to acquire reliable data for the construction of the fatigue law. Also, as any bending-based test, the flexural load in the specimen does not generate a homogenous stress distribution within the specimen.

5.1.5. Overlay Tester

Overview. The Overlay Tester (OT) is a cyclic test originally designed by Lytton and his associate at the Texas A&M Transportation Institute (TTI). It consists of two steel plates, one fixed and the other movable horizontally to simulate the opening and closing of the cracks/joints. Since its development in late 1970s, it has been widely used in evaluating anti-reflective cracking measures, balanced mix design, and recently pavement design. The OT standard Tex-248-F is modified as a two-step test protocol, including a non-destructive step and a destructive step. In each load cycle, the specimen is subjected to a triangular shaped displacement load with a 5-second loading and 5-second unloading process. The non-destructive step includes 10 load cycles with an opening displacement of 0.05mm. The test rests for 15 minutes after the non-destructive step ends. The destructive step uses a maximum opening displacement of 0.32mm. In this step, the crack initiates from the bottom of the specimen, and then propagates to the top of the specimen. The destructive step stops when a 93% reduction of the maximum load occurs. An overarching timeline of the OT development and application history are summarized in Figure 29.

OT Development. Overall OT development can be divided into three stages: OT concept and original test machine, upgraded OT machine and standard test method, and OT-based cracking model. Brief description of each stage is provided in the following paragraphs.

Stage 1-OT concept and test machine: Lytton and his associate at TTI originally developed the OT concept and the original test machine (Germann and Lytton, 1979). The main focus was to evaluate the effectiveness of different types of anti-reflection cracking measures. The long beam specimens were often used. It was used extensively in the 1980s to study inter-layers and fabrics.

Stage 2-Upgrade OT machine and standard test method: TTI sponsored by the Texas Department of Transportation, started to evaluate the potential use of the OT as a mix design tool in 2001. After the promising results, the original OT machine was upgraded into a more practical and user friendly test system (Zhou and Scullion, 2004), and the first upgrade machine was delivered to TxDOT in 2004. The major upgrades include specimen size, specimen preparation procedure, gluing, and failure definition and determination. Zhou and Scullion (2004) also standardized the OT test procedure which was later adopted into Tex-248-F: Texas Overlay Test (TxDOT, 2009). Furthermore, both Walubita *et al.* (2012) and Ma *et al.* (2015) made efforts to improve OT repeatability. Additionally, both Bennert and Maher (2008) and Ma *et al.* (2015) confirmed that OT was a simple and effective cracking test for characterizing cracking resistance of asphalt mixes.

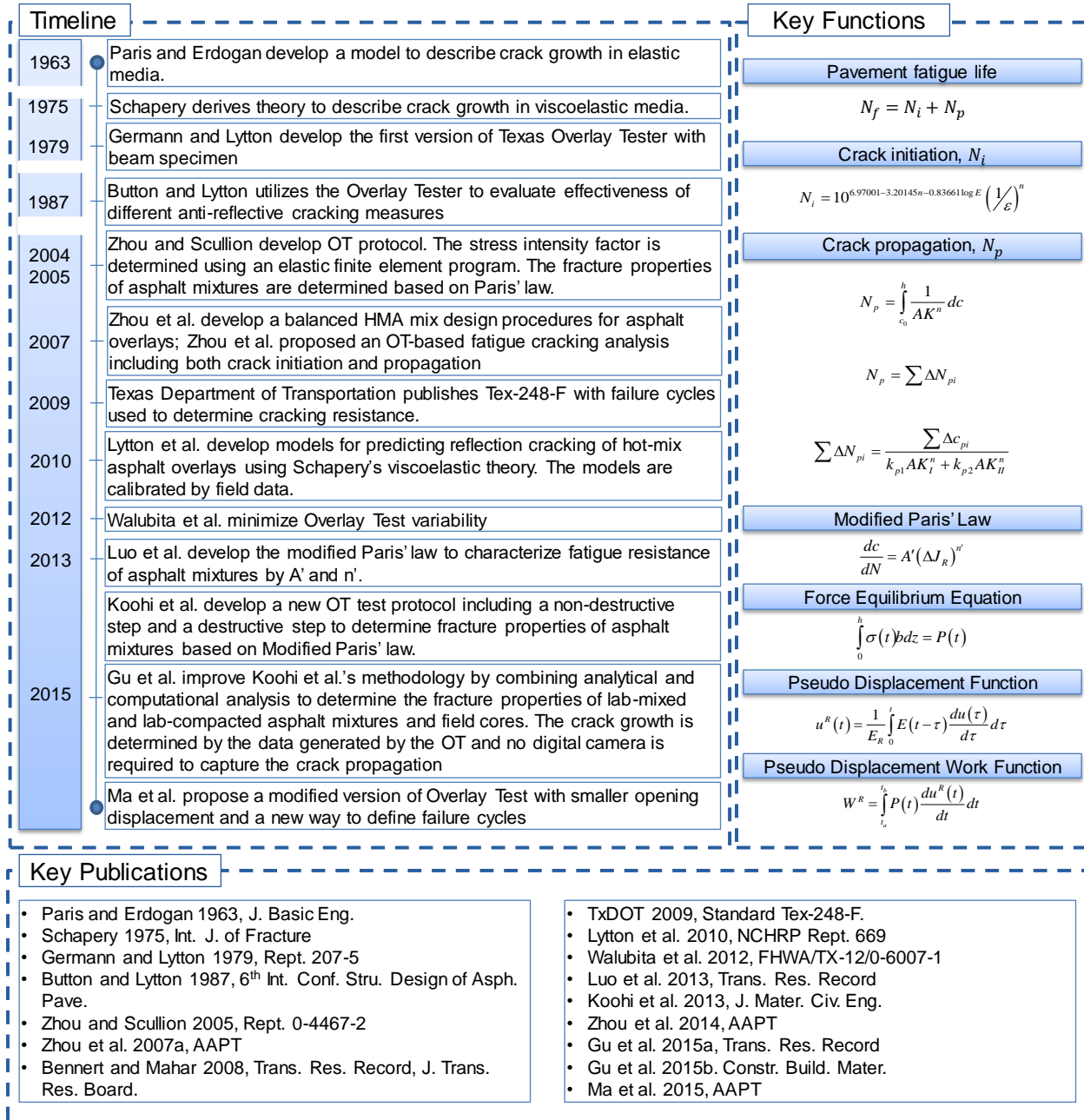


Figure 29. OT Test summary.

Stage 3-OT-based cracking model: Zhou *et al.* (2007a) developed an OT-based fatigue cracking model. It is believed that fatigue cracking is a combination of crack initiation and crack propagation process. The crack initiation is determined based on the tensile strain at the bottom of asphalt layer, and the crack propagation is determined by Paris' Law based on fracture mechanics. The key parameters of this model are fracture properties A and n determined by OT. The OT-based fatigue cracking model has three sub-models: (1) fatigue life model (see Equations [48]-[52]), (2) fatigue damage model (see Equation [53]), and (3) fatigue area model (see Equation [54]). These models and similar cracking propagation models have been adopted by Texas mechanistic-empirical (ME) pavement designs for both new flexible pavements and asphalt overlays (Zhou *et al.*, 2010a; 2010b).

$$N_f = k_i N_i + k_p N_p \quad [48]$$



$$N_i = k_1 \left(\frac{1}{\varepsilon} \right)^{k_2} \quad [49]$$

$$k_1 = 10^{6.97001 - 3.20145k_2 - 0.83661 \log E} \quad [50]$$

$$k_2 = n \quad [51]$$

$$N_p = \int_{c_o}^h \frac{1}{k_b AK_I^n + k_s AK_{II}^n} dc \quad [52]$$

$$D = \sum \frac{N}{N_f} \quad [53]$$

$$fatigued\ area(\%) = \frac{100}{1 + e^{C \log D}} \quad [54]$$

where; N_f = fatigue life, N_i = crack initiation life, N_p = crack propagation life, k_i , k_p , k_b , and k_s = calibration factors, ε = maximum tensile strain at the bottom of asphalt layer, E = dynamic modulus, A and n = fracture properties determined from OT testing, K_I and K_{II} = stress intensity factors (SIF) caused by bending and shearing stresses, c_o = initial crack length, h = asphalt layer thickness, D = accumulated fatigue damage, N = is applied load repetitions, and C is the field calibration factor.

OT Applications. The OT has been applied in three areas: (1) evaluation of anti-reflection cracking measures, (2) balanced mix designs, and (3) ME pavement designs. It has been widely used and approved that OT is an effective tool to compare and evaluate the effectiveness of different anti-reflection cracking measures (Button and Epps, 1982; Pickett *et al.*, 1983; Button and Lytton, 1987; Cleveland *et al.*, 2003). The OT has represents a critical component of the balanced mix design system proposed by Zhou *et al.* (2007b; 2014). Also, TxDOT specifications were updated in 2014 to require the OT cycles on SMA, fine porous friction course (PFC), and thin overlay mixes. Furthermore, the OT-based cracking models (fatigue, reflection cracking, and thermal cracking) were adopted into the Texas ME pavement designs. Beyond Texas, the OT has been employed to design high performance mixes in New Jersey and other DOTs (Bennert *et al.*, 2012; Bennert *et al.*, 2014).

Extracting Fracture Properties from Overlay Test Principles

As mentioned above, fracture analysis with the OT is based on the Paris' law (Paris and Erdogan, 1963), where the determined coefficients of Paris' Law are fracture properties, which can accurately and efficiently predict the crack growth within the pavement structure under repeated loading. The OT fracture analysis combines the mechanical analysis of viscoelastic force equilibrium in the OT specimen and finite element (FE) modeling simulations. Figure 2 presents a flowchart to illustrate the process of OT analysis, which consists of five steps.

- 1) FE modeling of the OT to provide the horizontal strain profiles for computing the undamaged tensile properties and estimating the crack growth function in both the non-destructive and destructive steps, respectively;
- 2) Computing the undamaged tensile properties (E_1 and m), which are described in more detail in the following paragraphs, based on the force equilibrium with the undamaged strain inputs from the FE model;
- 3) Estimating the crack growth function based on the force equilibrium with the damaged strain inputs from the FE model; and
- 4) Analyzing the evolution of the pseudo displacement work with load cycles to obtain the pseudo displacement work growth function; and
- 5) Using the crack growth function and the pseudo displacement work growth function to determine A' and n' .

Finite Element Model of OT. A two-dimensional (2D) finite element model is constructed to simulate the OT. The bottom left portion of the specimen is fully fixed and the bottom right portion can only move in the horizontal direction. A vertical seam is assigned along the center of specimen to determine the horizontal strain profile at various crack lengths. The determined horizontal strain profile is then integrated with respect the depth of specimen to obtain the integration area of the horizontal strain as it varies with crack length. Figure 30 shows the finite element models of lab compacted samples and field cores, and the corresponding horizontal strain profiles.

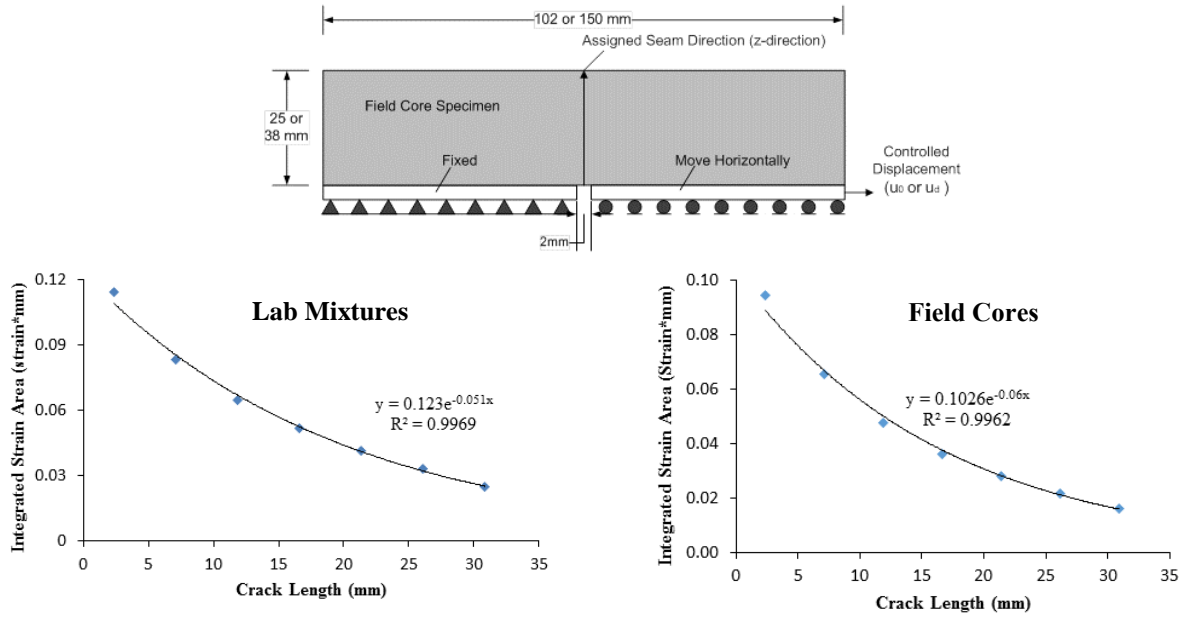


Figure 30. Finite element model of OT specimens and corresponding horizontal strain profiles.

Determination of Undamaged Tensile Properties. The force equilibrium equation of the OT specimen is expressed as,

$$\int_0^h \sigma(t, z) b dz = P_{VE}(t) \quad [55]$$

where; $\sigma(t, z)$ = viscoelastic stress within the specimen as a function of time, t , and depth, z , b = width of the specimen; h is the thickness of the intact specimen, and $P_{VE}(t)$ = measured viscoelastic force as a function of t . The viscoelastic stress, $\sigma(t, z)$, calculated using the constitutive model for the one-dimensional viscoelastic response, which is expressed as,

$$\sigma(t, z) = \int_0^t E(t - \tau) \frac{d\varepsilon(\tau, z)}{d\tau} d\tau \quad [56]$$

where; $\varepsilon(\tau, z)$ = linear viscoelastic strain at z , τ = time-integration variable, and $E(t - \tau)$ = relaxation modulus, which is approximately represented using a power model, which is shown in Equation [57].

$$E(t - \tau) = E_1 (t - \tau)^{-m} \quad [57]$$

where E_1 and m = undamaged tensile properties of asphalt mixtures. In the non-destructive step, the undamaged tensile properties of the asphalt mixture are calculated by Equation [58].

$$P_{VE}(t) = \frac{bE_1 t^{1-m}}{t_1(1-m)} s(u_0, c=0) \quad [58]$$

where $s(u_0, c=0)$ is the integration area of the horizontal strain profile over the depth at the maximum opening displacement in the non-destructive step.

Estimation of Crack Growth Function. Two steps are involved to estimate the crack growth function, dc/dN , including:

- 1) Calculating the integration area of the horizontal strain profile above the current length of the crack at each loading interval; and
- 2) Back-calculating the crack length corresponding to each obtained area of the horizontal strain profile.

Similar to the analysis in the non-destructive step, the measured force can be represented in terms of the undamaged tensile properties E_1 and m , loading time interval t_1 , specimen width, b , and the integration area of the horizontal strain profile of the specimen $S(u_d, c_i)$, which is expressed as,

$$P[(2i-1)t_1] = \frac{bE_1 S(u_d, c_i)}{t_1(1-m)} \sum_{n=1}^{2i-1} (-1)^{n-1} \left\{ -[(n-1)t_1]^{1-m} + (nt_1)^{1-m} \right\} \quad [59]$$

where $P[(2i-1)t_1]$ = measured force at the i^{th} loading peak. Equation [59] and the measured E_1 and m from the nondestructive characterization are used to determine the integration area of the horizontal strain profile $S(u_d, c_i)$ at each loading interval. According to the relationship between horizontal strain integration area and crack length shown in Figure 30, the crack length for each load cycle can be back-calculated. The crack growth function is fitted by a power function shown in Equation [60].

$$c(N) = d \times N^e \quad [60]$$

where c and d = regression parameters.

Analysis of Change of Dissipated Pseudo Displacement Work. The dissipated pseudo displacement work is used to quantify the crack propagation in the specimen during the destructive test. The pseudo displacement is calculated using Equation [61].

$$u^R(t) = \frac{1}{E_R} \int_0^t E(t-\tau) \frac{du(\tau)}{d\tau} d\tau \quad [61]$$

where; E_R = the reference modulus, $E(t-\tau)$ = relaxation modulus, $u(\tau)$ = displacement as a function of time, and τ = time-integrated variable. The enclosed area of the load-pseudo displacement hysteresis loop represents the dissipated pseudo displacement work, which is used to drive the propagation of the crack within the specimen. Equation [62] is used to calculate the dissipated pseudo displacement work by integrating the load and pseudo displacement.

$$W^R = \int_{t_a}^{t_b} P(t) \frac{du^R(t)}{dt} dt \quad [62]$$

where W^R = dissipated pseudo displacement work in a load cycle $[t_a, t_b]$. The evolution of the cumulative dissipated pseudo displacement work with the increasing number of load cycles is fitted by a power function, which is shown in Equation [63].

$$W^R(N) = a \times N^b \quad [63]$$

Determination of Fracture Properties of Asphalt Mixtures. The fracture properties of asphalt mixtures are determined using the modified Paris' law, as shown in Equation [64].

$$\frac{dc}{dN} = A' (\Delta J_R)^{n'} \quad [64]$$

where; c = crack length, N = number of load cycles, ΔJ_R = increment of the pseudo J-integral within one load cycle, and A' and n' = Paris' law parameters, or fracture properties. Because ΔJ_R represents the work dissipated to propagate cracks in the material, it can be represented by Equation [65].

$$\Delta J_R = \frac{\partial W^R}{\partial (c.s.a)} \quad [65]$$

where $c.s.a$ = total crack surface area. Equation [66] is used to calculate the $c.s.a$.

$$c.s.a(N) = d \times N^e \times w \times 2 \quad [66]$$



where w = width of the specimen. The fracture properties A' and n' are calculated by Equations [67] and [68], and Figure 31 presents the determined fracture properties of lab compacted asphalt mixtures and field cores using the OT fracture analysis methodology.

$$A' = \frac{(de)^{n+1}}{\left(\frac{ab}{2w}\right)^n} \quad [67]$$

$$n' = \frac{e-1}{b-e} \quad [68]$$

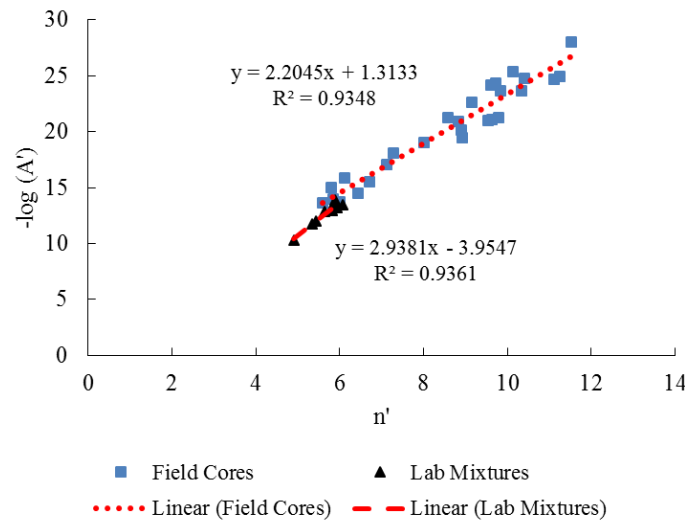


Figure 31. Determined fracture properties of lab compacted asphalt mixtures and field cores.

5.1.6. Dogbone Tester

Overview. Top down cracks appear to develop mostly as mode I fractures (Myers, 2000), indicating that tension is at least partially, if not predominantly responsible for the development of the cracks. There are currently several tests which are being used to measure the tensile properties of asphalt mixture in the laboratory: Superpave IDT (Roque & Buttlar, 1992; Roque *et al.*, 1997) (see Sections 5.1.3 and 6.2.2), semi-circular bend test (Li and Marastreanu, 2004; Huang & Shu, 2005) (see Section 5.2.1 and 0), hollow cylinder test (Buttlar *et al.*, 1999; Buttlar *et al.*, 2004), the uniaxial direct tension test (Bolzan & Huber, 1993, Kim *et al.*, 2002) (see Sections 5.1.2 and 6.3), and others. Each of these tests offers advantages and disadvantages from the standpoint of practicality as well as their ability to provide accurate damage and fracture properties.

In Florida, it is estimated that top-down cracking accounts for more than 90% of cracking in pavements and according to Florida specifications, a friction course is required on most state roads and highways; therefore, the effect of friction course mixtures and the interface condition between the layers may play a significant role in the development of the top-down cracking. Roque *et al.* (2009) studied this phenomenon in order to identify the effect of open graded friction course (OGFC) mixture and interface conditions on top-down cracking performance of asphalt pavement. In so doing, they questioned the reliability of the applicability of the aforementioned methods for OGFC materials. OGFC mixtures are distinctly different to dense graded asphalt mixtures. They are designed to contain about 15-25% air voids, preferably interconnected and use relatively uniform gradations with relatively low fine aggregate and filler. Asphalt contents for this mixture are slightly higher than that of dense graded asphalt mixtures (Cooley *et al.*, 2000). Furthermore, previous research by Varadhan (2004) had shown a region of high damage under the loading strips during Superpave IDT testing of open graded asphalt mixtures. A behavior that could be overcome by increasing specimen thickness and loading rate or decreasing temperature; however, by changing these variables, the correlation to in-service conditions could be questioned. In light of these concerns and

the researchers conceived, developed, and validated the dog-bone direct tension test (DBDT). They purport certain specific advantages of the method; the fact that the failure plane is known a priori so that failure limits can be measured directly on that plane, its potential for both laboratory gyratory compacted specimens and field cores, and finite element assisted corrections for non-uniform stress, strain, and rotation effects. Figure 32 below summarizes the key development and literature relevant to the DBDT test.

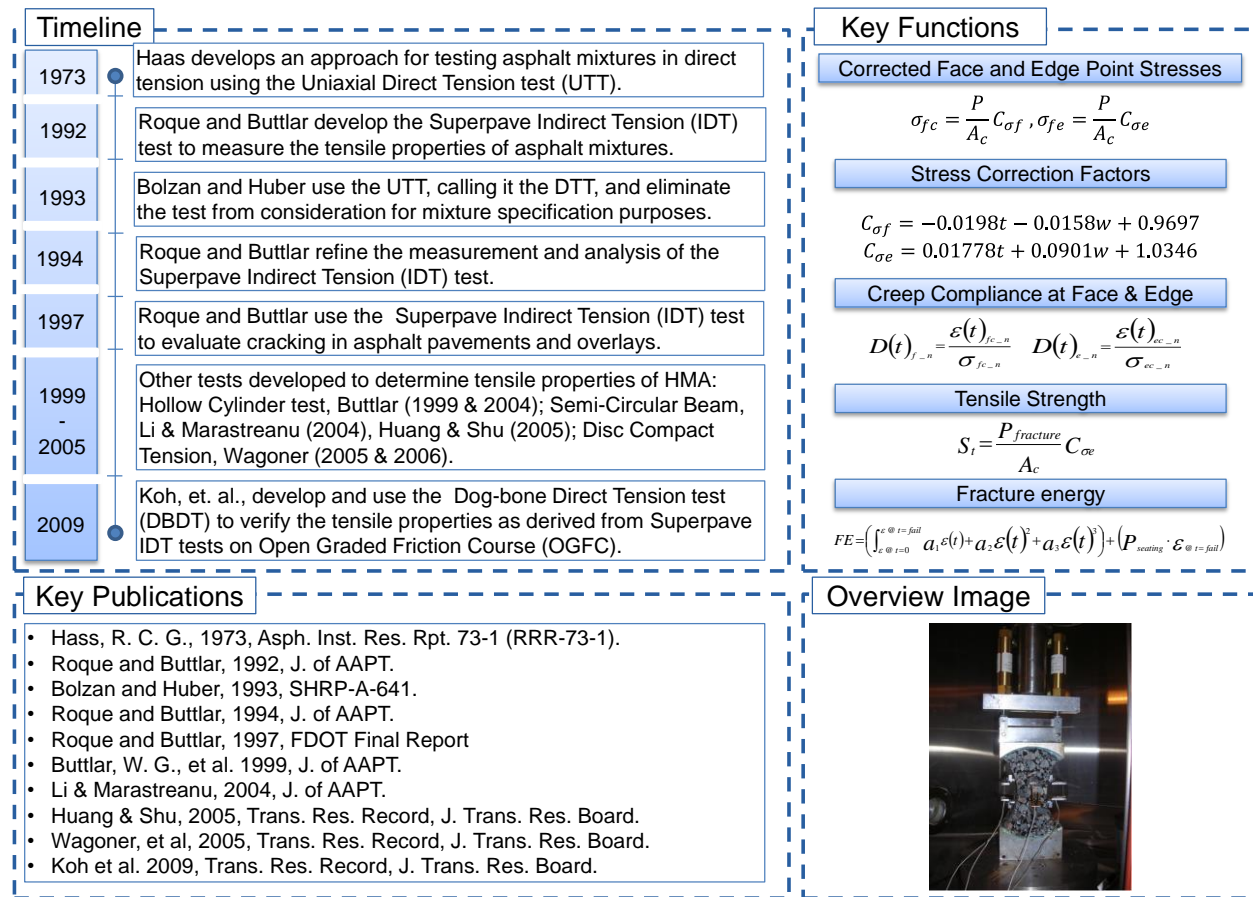


Figure 32. Summary of Dog-Bone Direct Tension test development.

The basis for the DBDT test lies in the work of Haas (1973), who articulated the need to obtain the stiffness of an asphalt mixture using a direct tension approach. The typical uniaxial tension test for asphalt mixtures uses a cylindrical specimen that is bonded to end caps of the same or slightly larger diameter (see Section 5.1.2). In theory, the uniaxial direct tension test benefits from the uniform stress and strain fields in the middle of the specimen. However, during the SHRP research project Bolzan and Huber (1993) noted some limitations:

- Stress concentration near the ends of the samples has been observed in many experiments.
- Sample failure can occur due to misalignment.
- Sample preparation requires a long time and a skilled operator/technician.
- The failure plane is presumed to occur at the center of the specimen perpendicular to the vertical axis, but in practice may occur at any location over the specimen length.
- This test has had some difficulty in obtaining repeatability

Furthermore, it might not be possible to do this test on field cores since in-service pavements may not exist in sufficiently thick layers. Thus, the motivation for DBDT lie in the lack of a test that mitigated the disadvantages of existing tests and at the same time met the following requirements:

- Should be a direct tension mode test
- The test can be performed on gyratory compacted specimens or field cores

- The test can be performed on samples of various thickness (thin or thick)
- The test can be used on all mixture types (dense-graded, open-graded).

Development of Test Method. The DBDT test was developed to provide accurate tensile properties of asphalt mixture. Due to DBDT specimen geometry, stress concentrations near the ends of specimen are less critical, and the location where failure is likely to occur is maximized. The intent behind the development of this direct tension test was to provide a comparison to the more easily performed Superpave IDT test. It should therefore be viewed as a research tool, rather than a production test.

Specimen Geometry. Two dimensional finite element method (FEM) analyses were conducted to determine optimum specimen dimensions. Stress distributions at the horizontal centerline and headline of the specimen were checked to ensure that failure would occur at the center of the specimen and not near the loading heads. The stress distributions across the middle centerline should also be as uniform as possible to guarantee stress concentration over a large enough area to capture a representative portion of the mixture.

Based on the predicted stress distributions for two-inch wide specimens, a coring radius of 75 mm and a coring overlap of 50 mm resulted in centerline stresses that were reasonably uniform and considerably greater than stresses near the loading heads (headline). This final specimen geometry results in a large enough cross section for testing without sacrificing the integrity of the mixture. The stress concentration at the centerline should cause the specimen to break in this region, thereby compensating for any density gradients in gyratory compacted specimens as previously exposed by researchers (Harvey *et al.*, 1991; Shashidhar, 1999; Chehab *et al.*, 2000). A key to necessarily developing this test successfully is to measure the strain directly on the planes of maximum stress. Therefore, measurements are obtained in the center of the edges of the specimen as well as on the specimen faces.

Three-dimensional finite element analysis was conducted to analyze stress and strain of a 150 mm diameter specimen. Asphalt modulus was set to 2,750 MPa, varying Poisson's ratio, the center width and thickness of the specimen. The 3-D FEM analysis indicated that corrections needed to be applied to accurately and reliably determine the properties with the proposed measurement system.

Stress Analysis and Correction. Tensile failure will initiate at the edge of the specimen and stress distributions do not depend significantly on the Poisson's ratio. Stress correction factors were developed to adjust the stress obtained with the proposed DBDT testing system. The corrected point stresses on the face and edge can be calculated using the following equations:

$$\sigma_{face_c} = \frac{P}{A_c} C_{\sigma_f} \quad [69]$$

$$C_{\sigma_f} = -0.0198t - 0.0158w + 0.9607 \quad [70]$$

$$\sigma_{edge_c} = \frac{P}{A_c} C_{\sigma_e} \quad [71]$$

$$C_{\sigma_e} = 0.0177t + 0.0901w + 1.0346 \quad [72]$$

where; σ_{face_c} = stress on face corrected, σ_{edge_c} = stress on edge corrected, P = applied load (kN), A_c = area at the center of a specimen (mm²), C_{σ_f} = stress correction factor on face, C_{σ_e} = stress correction factor on edge, t = thickness of a specimen (mm), and w = width at the center of a specimen (mm).

Strain Analysis and Correction. The strain values obtained from the DBDT test are based on the point-to-point displacements measured by the finite length extensometers and are better represented by the average of the strain distributions between gage points as expressed by the following equations:

$$\epsilon_{face_avg} = \frac{1}{GL} \int_{-GL/2}^{GL/2} f_1(x) dx \quad [73]$$

$$\epsilon_{edge_avg} = \frac{1}{GL} \int_{-GL/2}^{GL/2} f_2(x) dx \quad [74]$$

where; ε_{face_avg} = average strain between two gage points on face, ε_{edge_avg} = average strain between two gage points on edge, and GL = gage length (mm) = distance over which vertical deformations are obtained. The strain is corrected using following equations:

$$\varepsilon_{face_p} = \varepsilon_{face_c} = \varepsilon_{face_avg} C_{\varepsilon f} \quad [75]$$

$$C_{\varepsilon f} = -0.0028t - 0.0178w + 1.0545 \quad [76]$$

$$\varepsilon_{edge_p} = \varepsilon_{edge_avg} C_{\varepsilon e} \quad [77]$$

$$C_{\varepsilon e} = 0.0039t - 0.0015t^2 - 0.009w + 1.0770 \quad [78]$$

where; $\varepsilon_{face_p} = \varepsilon_{face_c}$ = corrected vertical point strain at the center of a specimen's face, ε_{edge_p} = corrected vertical point strain at the center of a specimen's edge, $C_{\varepsilon f}$ = strain correction factors on face, $C_{\varepsilon e}$ = strain correction factors on edge, and t and w were previously defined.

Strain Gage Mounting. Four extensometers are used to measure on-specimen deformations. Two of the sensors are placed at the center of the specimen's flat faces and the other two are placed at the center of curved edges. The extensometers placed on the faces are the most appropriate for determination of resilient modulus and creep compliance. Since the edge measures deformation in the immediate vicinity of maximum tensile stress, they can detect the instant when the material fractures and are most appropriate to determine failure limits (i.e., strength, failure strain, fracture energy etc.).

Edge Measurement Rotation and Correction. The edge gauge points rotate when tension is applied to the specimen and the rotational effect is significant. The following equations calculate the corrected strain, where, ε_{edge_d} = corrected strain for rotation effect on the edge, C_{de} is displacement correction factor for length of gauge = 0.81, ε_{edge_avg} as previously defined. Therefore, a corrected point strain on the edge, Equation [80], can be obtained using a combination of Equations [76] and [79], where, ε_{edge_c} = corrected strain for rotation effect on the edge, ε_{face_c} = corrected strain on the face and all other variables as previously defined.

$$\varepsilon_{edge_d} = \varepsilon_{edge_avg} C_{de} \quad [79]$$

$$\varepsilon_{edge_c} = \varepsilon_{edge_d} C_{\varepsilon e} = \varepsilon_{edge_avg} C_{\varepsilon e} C_{de} \quad [80]$$

$$\varepsilon_{face_c} = \varepsilon_{face_avg} C_{\varepsilon f} \quad [81]$$

System Verification and Testing. Preliminary tests were performed to investigate the feasibility and accuracy of the system for determining the tensile properties of asphalt mixtures and to validate the identified correction factors. In addition, the preliminary tests were used to evaluate all the sub-systems of the testing unit and determine whether there were any needs for modification. Preliminary testing of the prototype system was performed on a specimen made of Delrin, a material of known mechanical and physical properties. Published material specifications for Delrin report a modulus of 3.1 GPa (450 ksi). Verification was performed with resilient modulus, creep compliance and strength tests (Koh, 2009). With respect to cracking, the key failure properties from the DBDT test are the tensile strength and fracture energy.

Tensile Strength. The true tensile strength of the DBDT asphalt specimen can be calculated by determining the stress level at the edge of the specimen at the instant of failure. To accomplish this experimentally, a measurement system must be able to detect the instant when fracture occurs at the edge of the specimen. Accordingly, fracture should occur on either edge first, or on both edges simultaneously, in the DBDT testing system, since tensile stress is highest at the edges. Tensile strength of each specimen is calculated using the following equation:

$$S_t = \frac{P_{fracture}}{A_c} C_{\sigma e} \quad [82]$$

Stresses and strains are calculated from the start of the load to the instant of specimen failure. When calculating stress, the initial seating load is subtracted from the applied loads to simulate a zero stress state at the beginning of the loading cycle. Failure strain is determined strain on edge at failure.



$$\sigma(t) = \frac{P(t) - P_{seating}}{A_c} C_{\sigma e} \quad [83]$$

$$\varepsilon_{edge_c}(t) = \varepsilon_{avg}(t) C_{\varepsilon e} C_{de} \quad [84]$$

where; $\sigma(t)$ = corrected stress during loading time (t), $P(t)$ = tensile load during loading time (t), $P_{seating}$ = initial seating load applied to specimen, and $\varepsilon_{ec}(t)$ = corrected strain effect on the edge during loading time (t).

Fracture Energy and Tangent Modulus. To obtain fracture energy and tangent modulus, the stress-strain curve was fitted with a third-order polynomial function forcing the function to go through the origin. The area under the curve is the fracture energy. The fitted curve was obtained from stress-strain data that does not include the seating stress, but, when calculating fracture energy, the initial seating load must be included, as is shown in Equation [85]. The variable $\varepsilon@t=fail$ is the strain at failure.

$$FE = \left(\int_{\varepsilon@t=0}^{\varepsilon@t=fail} a_1 \varepsilon(t) + a_2 \varepsilon(t)^2 + a_3 \varepsilon(t)^3 \right) + (P_{seating} \varepsilon@t=fail) \quad [85]$$

In the test protocol, three replicate specimens are tested and evaluated to obtain the tensile properties. The trimmed mean approach of eliminating the highest and lowest values is also used for analyzing this data. The tensile strength (S_t), failure strain ($\varepsilon_{failure}$), fracture energy (FE), and tangent modulus (M_T) are obtained from strength test and the equations are presented below.

$$S_t = \frac{\left(\sum_{n=1}^6 S_{t_n} \right) - \text{Max}(S_{t_n}) - \text{Min}(S_{t_n})}{n - 2} \quad [86]$$

$$\varepsilon_{failure} = \frac{\left(\sum_{n=1}^6 \varepsilon_{failure_n} \right) - \text{Max}(\varepsilon_{failure_n}) - \text{Min}(\varepsilon_{failure_n})}{n - 2} \quad [87]$$

$$FE = \frac{\left(\sum_{n=1}^6 FE_n \right) - \text{Max}(FE_n) - \text{Min}(FE_n)}{n - 2} \quad [88]$$

$$M_T = \frac{\left(\sum_{n=1}^6 M_{T_n} \right) - \text{Max}(M_{T_n}) - \text{Min}(M_{T_n})}{n - 2} \quad [89]$$

Comparison Testing Between the DBDT and the Superpave IDT. Resilient modulus, creep, and strength tests were performed at multiple temperatures on dense graded and open graded asphalt mixtures with the newly developed DBDT and the existing Superpave IDT. From individual tests, on both dense-graded and OGFC asphalt mixtures, the tensile properties were successfully obtained with the DBDT, as well as with the Superpave IDT. Both tests provided reasonable and consistent test results with respect to specimen test temperature and mixture aging (Roque *et al.*, 2009; Koh, 2009).

5.1.7. Loaded Wheel Tester

Overview. A loaded wheel tester (LWT), also called wheel tracking tester, is device that has been widely used in the asphalt industry to evaluate the potential of asphalt mixture to rutting, fatigue cracking, and moisture susceptibility by applying moving wheel loads on asphalt mixture specimens. The LWTs commonly used across the world include the Asphalt Pavement Analyzer (APA), the Hamburg Wheel Tracking Device (HWTD), the French Rutting Tester (FRT), and the Third-Scale Model Mobile Load Simulator (MMLS3).

The APA, Figure 33(a), was modified from the Georgia Loaded Wheel Tester (GLWT) and first manufactured in 1996 by Pavement Technology, Inc. (Collins *et al.*, 1996; Cooley *et al.*, 2000). GLWT was developed in the mid-



1980s by a joint effort of the Georgia Department of Transportation (GDOT) and the Georgia Institute of Technology (GIT) to evaluate rutting susceptibility of asphalt mixture. In the initial APA, a loaded wheel moves on a pressurized linear hose resting on cylindrical or beam specimens and the load is transferred from the wheel through the hose to the specimens. Usually, rut depth is measured after 8,000 loading cycles to evaluate the rut potential of asphalt mixture in the field. Later, APA adopted steel wheels to apply the load and it is also used to evaluate the moisture susceptibility of asphalt mixtures (West *et al.*, 2004).

The Hamburg wheel-tracking device (HWTd), Figure 33(b), was developed in the mid-1970s and manufactured by Helmut-Wind, Inc. of Hamburg, Germany (Aschenbrener, 1995; Cooley *et al.*, 2000). It was initially used by the city of Hamburg to evaluate the rutting and stripping potential of asphalt mixtures (Cooley *et al.*, 2000). HWTd tests are typically performed on two slab specimens that are 260 mm wide, 320 mm long, and 40 mm high and submerged under water. Steel wheels 47 mm wide are used and test specimens are loaded for 20,000 passes or until 20 mm of deformation occurs (Aschenbrener, 1995).

The French Rut Tester (FRT), Figure 33 (c), was developed by the Laboratoire Central des Ponts et Chaussées (LCPC) of France in late 1980s to evaluate the rutting characteristics of asphalt mixtures and thus also called the LCPC wheel tracker (Aschenbrener 1994, Cooley *et al.* 2000). FRT tests are typically performed with a pneumatic tire for 30,000 cycles on two slab specimens that are 180 mm wide, 50 mm long, and 20 to 100 mm thick. Rut depth is expressed as a percentage of the original slab thickness (Cooley *et al.*, 2000).

The 1/3rd scale model Mobile Load Simulator (MMLS3), Figure 33 (d), was developed in the late 1990s in South Africa for asphalt mixture testing both in the laboratory and in the field. It is similar to the full-scale Texas Mobile Simulator (TxMLS), but scaled down in load and size. The pneumatic tires it uses are approximately one third the diameter of standard truck tires and the wheel load approximately one-ninth the load of a single tire on a standard single axle with dual tires. The MMLS3 device is 2.4 m long by 0.6 m wide by 1.2 m high and can test samples 1.2 m long by 240 mm wide in dry or wet conditions. In addition to rutting potential, MMLS3 can also be used to evaluate the damages caused by cracking and moisture (Cooley *et al.*, 2000).

The LWTs have been mainly used for evaluating the resistance of asphalt mixtures to rutting and moisture damage. So far, only a few researchers used LWT to evaluate the fatigue cracking potential of asphalt mixture. Bhattacharjee *et al.* (2004) and Bhattacharjee (2005) used MMLS3 to characterize the fatigue performance of asphalt pavement in the laboratory. Wu (2011) and Wu *et al.* (2013) modified APA by attaching a LVDT to the specimen bottom and used it to characterize the fatigue behavior and to test the viscoelastic properties of asphalt mixtures. Figure 34 summarizes the development of different LWTs.



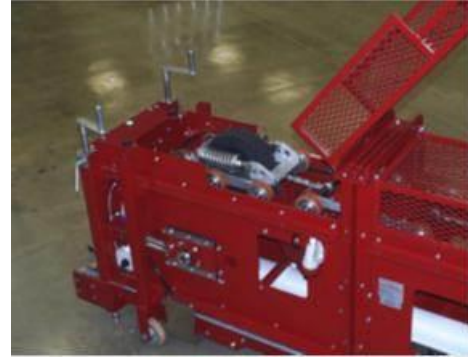
(a) Asphalt Pavement Analyzer (APA) (Courtesy of Pavement Interactive)



(b) Hamburg wheel-tracking device (HWTd) (Courtesy of FHWA)



(c) French Rutting Tester (FRT) (Courtesy of FHWA)



(d) One-Third Model Mobile Load Simulator (MMLS3) (Cooley *et al.* 2000)

Figure 33. Four types of LWT.

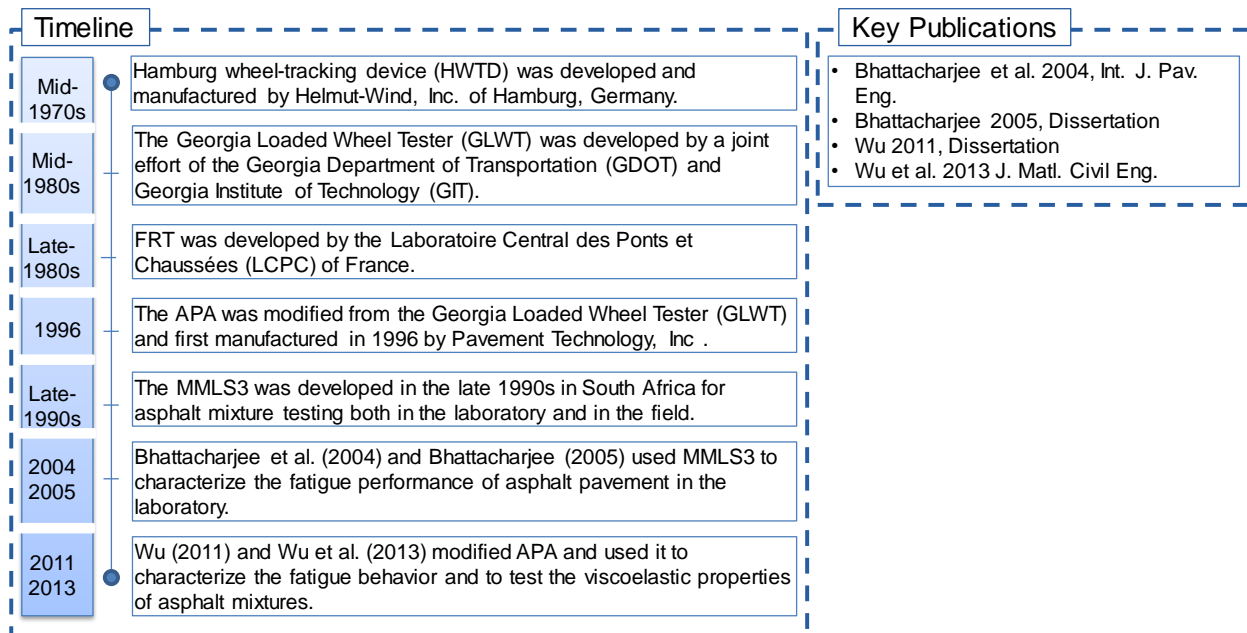
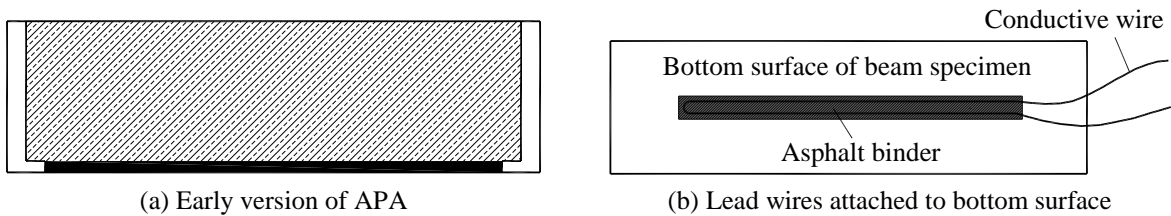


Figure 34. Summary of development of LWTs.

Issue of LWT for Fatigue Cracking Testing. Current LWTs have some issues when they are used for asphalt fatigue testing. Take APA as an example. APA does not have enough space below a specimen to allow for deflection till specimen break. In APA fatigue testing, conductive wires are used to attach to the bottom surface of beam specimen with molten asphalt to detect fatigue cracking of an asphalt specimen (Figure 35) (Huang *et al.*, 2016). Sometimes, the wires would not break or the break is not caused by fatigue cracking, which makes it difficult to detect cracking failure.



(a) Early version of APA

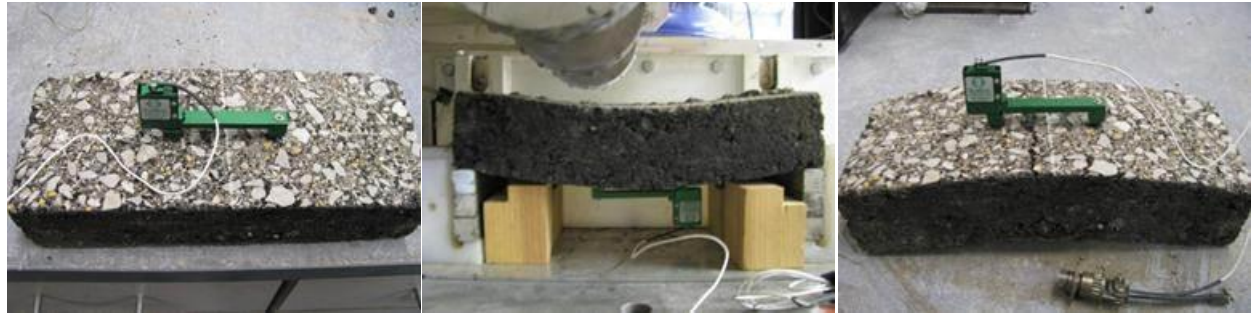
(b) Lead wires attached to bottom surface

Figure 35. Early version of APA for fatigue testing (from Huang *et al.* 2016)

Modified APA for Fatigue Testing. The APA was modified by Wu (2011) and Wu *et al.* (2013) to successfully perform asphalt mixture fatigue testing (Figure 36). A linear variable differential transformer (LVDT) was mounted at the middle of the bottom surface of beam specimen to accurately measure the tensile strain under the moving load. The tensile stress at the midpoint of the beam bottom under a moving load can be calculated using the 2-D beam theory:

$$\sigma_0 = \sigma_{amp} \sin^2 \left(\frac{2\pi}{T} t \right) \quad [90]$$

where σ_{amp} = amplitude of sinusoidal stress and T =the testing period (cycle/sec.). 3-D finite element analysis was performed to determine the error caused by the simplification from 3-D to 2-D and it was found that the error is about 3%, which is acceptable in engineering applications.



(a) A specimen with a LVDT (b) A specimen in testing position (c) A specimen after fatigue failure
Figure 36. Modified APA for fatigue testing.

Analysis Methods. Two methods can be used to analyze the fatigue behavior of asphalt mixtures: stiffness reduction method and dissipated energy method. In the stiffness reduction method, fatigue life is defined as the number of loading cycles when the stiffness decreases to 50% of its initial value measured at the 50th load cycle. In the dissipated energy method, a plateau value (PV) is obtained from the second phase of Ratio of Dissipated Energy Change (RDEC) vs. loading cycle and can be written as follows:

$$PV = \frac{1 - \left(1 + \frac{100}{N_{f50}} \right)^k}{100} \quad [91]$$

where k = coefficient and N_{f50} = number of loading cycles determined based on the 50% stiffness reduction.

Validation of Modified APA Fatigue Testing. The modified APA fatigue testing was validated through its comparison with flexural beam fatigue test and direct tension fatigue test (Wu, 2011; Wu *et al.*, 2013). Figure 37 shows the results of four asphalt mixtures from these three fatigue tests. The modified APA fatigue test gave the same ranking of the four mixtures in terms of fatigue life and PV as that from the other two fatigue tests, showing that the modified APA test was capable of differentiating between different asphalt mixtures in terms of their fatigue behavior.

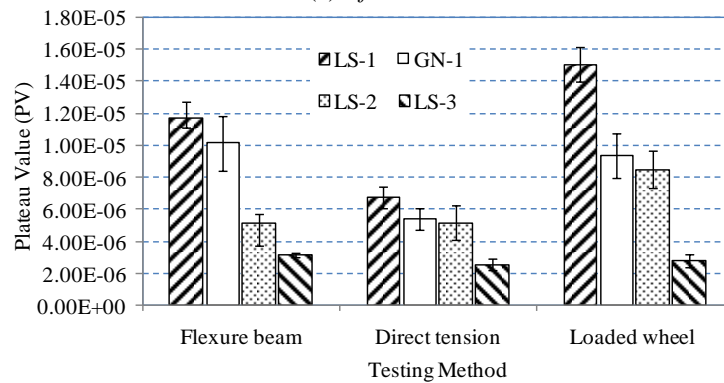
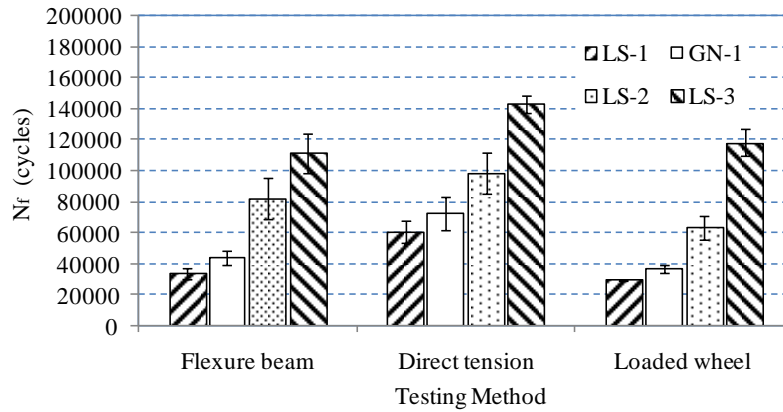


Figure 37. Comparison of modified APA with other fatigue tests.

5.2. Notch

5.2.1. Semi-Circular Beam (SC(B)) LTRC Method

Overview. The semi-circular bend (SCB) test and the resulting critical strain energy release rate, J_c , are based on fracture mechanics principles. An overarching timeline of development and application of the test, and key literature are summarized in Figure 38.

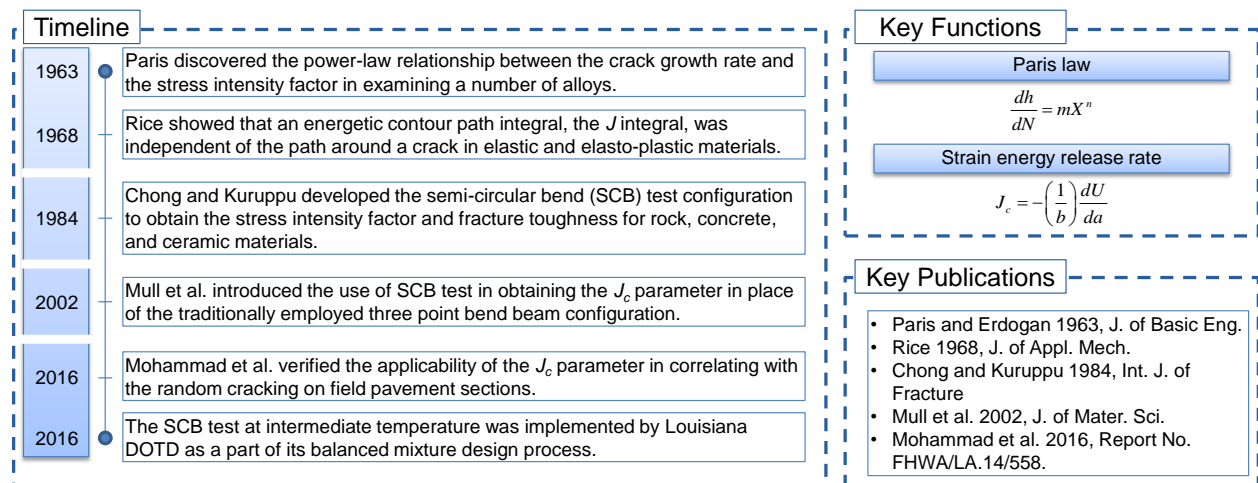


Figure 38. Summary of the SCB fatigue evaluation method.

As demonstrated in Figure 38, the SCB test has its root in fracture mechanics principles. The fracture mechanics approach correlates the crack driving force (X) with the rate of crack propagation (dh/dN) based on the Paris law (Paris and Erdogan 1963):

$$\frac{dh}{dN} = mX^n \quad [92]$$

where; m and n = regression constants, h = crack length, N = cycle number, X = crack driving force that can be the stress intensity factor for linear elastic materials or the energy release rate for elastoplastic materials. Even though the Paris law is not capable to describe the crack evolution behavior over the entire fatigue life, these regression constants or the crack driving force can be used to rank the materials' crack resistance (Mull *et al.*, 2005).

To represent the fracture resistance of asphalt concrete, which is essentially a nonlinear viscoelastic-plastic material, the J -integral approach (Rice 1968) has been used in place of the stress intensity factor. The critical strain energy release rate is determined by the following expression:

$$J_c = -\left(\frac{1}{b}\right) \frac{dU}{da} \quad [93]$$

where; J_c = critical strain energy release rate, b = specimen thickness, a = notch depth, and U = total strain energy up to failure, i.e., the area enclosed by the load-deflection curve up to the peak load. J_c represents the amount of strain energy that is consumed in order to form a unit area of fractured new surface in a material. Therefore, higher J_c values suggest tougher materials which have more resistance to crack initiation and propagation. Although according to Equation [93] the J_c value can be determined using only two different notch depths, having three depths would improve the accuracy in the calculation of J_c and help examine the data quality.

Related Applications. The SCB test at intermediate temperature and the resulting J_c parameter have been applied to evaluate the crack resistance of asphalt mixtures and their performance in pavement structures. Mull *et al.* (2002) validated the use of J_c as a performance indicator by evaluating a chemically modified crumb rubber (CMCR) asphalt mixture, crumb rubber modified (CRM) asphalt mixture, and a control mixture. It was found that the J_c -value of the CMCR mixture was twice that of the CRM mixture, and the CRM mixture exhibited a slightly higher fracture resistance than the control mixture. These observations on materials' fracture resistance based on the SCB test were further confirmed by examining the microstructure of the fracture surface via the scanning electron microscope. The SCB specimens used by Mull *et al.* were sliced from gyratory compacted cylinders. This allowed for reproducible specimens and the geometry of the SCB minimized the sagging of the specimen under its own weight during testing.

This test has been favored by many researchers due to the ease of sample preparation including cores removed from the field and the quick and simple testing procedure (Li and Marasteanu, 2010). Elseifi *et al.* (2012) utilized the SCB test at 25°C in the evaluation of a number of asphalt mixtures, including mixtures with a high content of reclaimed asphalt pavement (RAP), against cracking failure. Results of the experimental program were used to validate a three-dimensional finite element model, which was used to interpret and analyze the failure mechanisms in the SCB test. It was shown that the SCB test results successfully predicted the fracture performance of the evaluated mixes and were able to differentiate between them in terms of crack resistance.

By analyzing the components of asphalt binder, Cooper *et al.* (2015; 2016) found that the high asphaltene content in the binder, which rendered a relatively brittle mix, was well correlated with the observed low J_c values in the mixture ($J_c < 0.5$ kJ/m²). Studies have also shown that the J_c parameter is sensitive to asphalt stiffness and modifier, asphalt content, air void, and the dosage of recycled materials (Mohammad *et al.*, 2004; Elseifi *et al.*, 2012; Biligiri *et al.*, 2015).

By comparing the J_c results from laboratory SCB tests with the field cracking rates, which is defined as the crack length per mile of pavement per million applications of equivalent single axle load (ESAL), Kim *et al.* (2012) observed that approximately 58% of the variability in the field cracking rate can be explained by the sole factor J_c . Further, using the cracking index system developed by Louisiana Department of Transportation and Development (DOTD), Mohammad *et al.* (2016) compared the random cracking on existing pavement sections with the J_c values obtained for the corresponding field cores, and showed that the field random cracking was well correlated with the laboratory SCB results with an R^2 -value of 0.73. Considering the fact that there are also many other structural and environmental factors affecting the field performance of pavement, it can be concluded that these observations demonstrated the potential of using the SCB test and the J_c parameter to assess the mixtures' fatigue performance in field pavements.



Based on the above observations, in 2016, Louisiana DOTD implemented the use of SCB testing at intermediate temperature and the resulting critical strain energy release rate as a part of its balanced mixture design process for both wearing and binder courses on high- and low-volume roadways (LA DOTD, 2016).

Recently, Cao *et al.* (2016a) applied the SCB test to evaluate the fatigue resistance of mixtures from the FHWA ALF full-scale test pavements. In 2013, ten lanes were constructed using various HMA and WMA mixtures containing RAP and RAS. Accelerated fatigue loading was accomplished via a wide-base tire travelling at 4.9 m/s with a wheel load of 63.2 kN. The pavement temperature was maintained constant at 20°C during loading. The effect of RAP/RAS content, WMA technology, and use of soft binder on mixtures' crack resistance was assessed based on the obtained J_c data. As shown in Figure 39(a), mixtures' crack resistance indicated by J_c was reduced with increase in the asphalt binder replacement (ABR) ratio. In addition, the effect of 20% RAS lied in between those of 20% and 40% RAP. Use of soft binder seemed to be more compatible with RAP than with RAS, as demonstrated in Figure 39(b). Finally, implementation of WMA technologies appeared to benefit mixtures' cracking performance, and yet the two technologies, Evotherm versus water foaming, did not present discernible differences; see Figure 39(c). It is worth mentioning that, the same mixtures were also characterized by the S-VECD approach, and the ranking of the mixtures' fatigue resistance based on J_c and S-VECD analysis were quite consistent (Cao *et al.* 2016b).

Admitting that like parameters from most of the other laboratory testing methods, the J_c parameter obtained from SCB test is an indicator of mixture's intrinsic resistance to cracking, and thus is only a measure of material property. The fatigue performance of asphalt pavement as a composite structure, however, depends on additional factors such as traffic, temperature, structural layout, and material properties of base and subgrade layers. As such, a mechanistic-empirical fatigue predictive equation was proposed based on the existing model in the AASHTOWare Pavement ME Design™ program. This existing model involves only mixture's stiffness and strain responses at the bottom of asphalt layer, while not taking into account material's crack resistance. Motivated by this observation, the following model form was proposed by introducing the J_c parameter (Cao *et al.*, 2016a):

$$N_f = k_{f1} C C_H \beta_{f1} \left(\frac{1}{\varepsilon_t} \right)^{k_{f2} \beta_{f2}} \left(\frac{1}{|E^*|} \right)^{k_{f3} \beta_{f3}} (J_c)^{k_{f4} \beta_{f4}} \quad [94]$$

where; N_f = allowable number of load repetitions to fatigue cracking, ε_t = tensile strain at the bottom of asphalt layers beneath the wheel, $|E^*|$ = dynamic modulus of asphalt mixture, C_H = thickness correction term, J_c = critical strain energy release rate, k_{f1-3} = global field calibration coefficients, and β_{f1-3} = local calibration factors (set to 1.0). The above J_c -based fatigue model was then calibrated using the measured ALF fatigue data. As shown in Figure 40, the proposed model form was able to provide a reasonable correlation with the fatigue performance of field pavements.

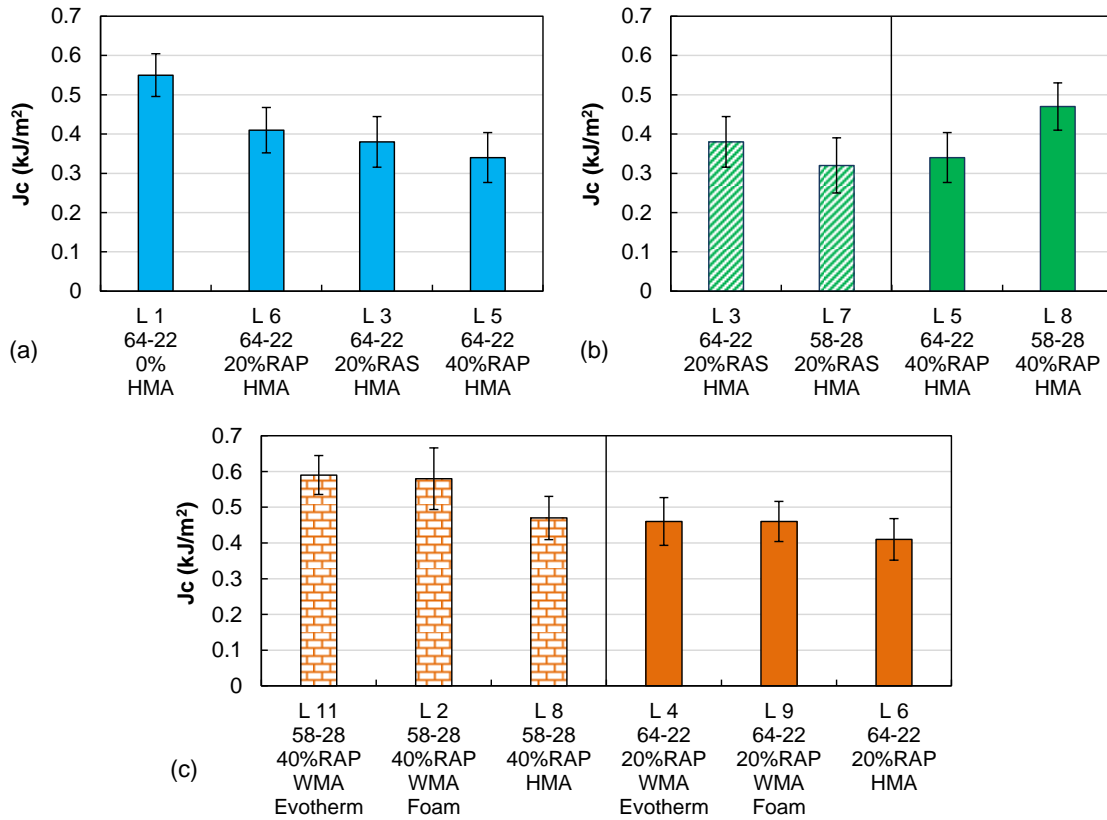


Figure 39. SCB test results: (a) effect of RAP/RAS content in terms of ABR percentage, (b) effect of use of soft binder with 20% RAS and 40% RAP, and (c) effect of WMA technologies with 20% RAS and 40% RAP.

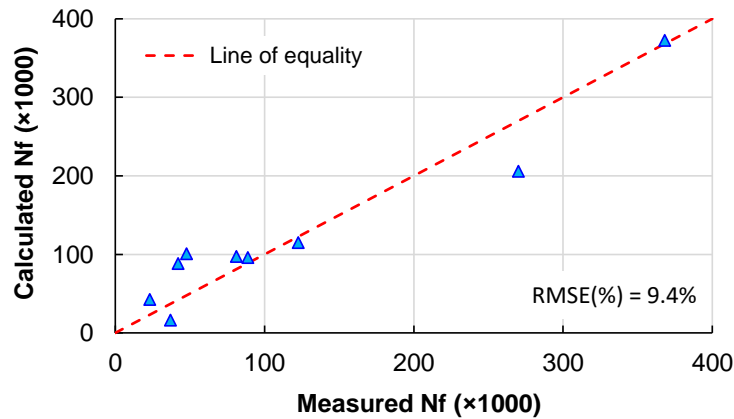


Figure 40. Performance of the J_c -based fatigue model.

5.2.2. Semi-Circular Beam (SC(B)) I-FIT Method

With the introduction a few years ago of a rutting performance test for AC acceptance, cracking of AC pavements is now driving the Illinois Department of Transportation's (IDOT) rehabilitation cycle. With existing pavement structures continuing to deteriorate and the occasional cold spikes in winter temperatures (-27°C in January 2014), fatigue, reflective, and thermal cracking resistance of AC are of paramount concern. Changing the material sources, especially stemming from the desire to be more sustainable, could increase the uncertainty in the value of historical performance, thereby hindering the accurate estimation of future pavement life cycles. Therefore, a distinct need existed for a comprehensive study to assess the impact of high RAP and/or RAS contents on critical AC performance criteria, such as thermal and fatigue cracking. In addition, a practical test suite and proven procedures

are needed for screening AC prepared with increased amounts of RAP and/or RAS to ensure that performance expectations are met.

The Illinois Center for Transportation (ICT) and IDOT partnered in a series of research projects beginning in 2012 with a specific objective of identifying, developing, and evaluating protocols, procedures, and specifications for testing engineering properties of AC mixtures with varying amounts of asphalt binder replacement (up to 60%) using RAP and RAS, as well as a number of other AC mixtures with various field performance and mixture volumetrics. One of the major outcomes of this study was development of the Illinois Flexibility Index Test (I-FIT) method and protocol that can rank AC mixtures based on their cracking resistance (Al-Qadi *et al.*, 2015). The overview of this method is summarized in Figure 41.

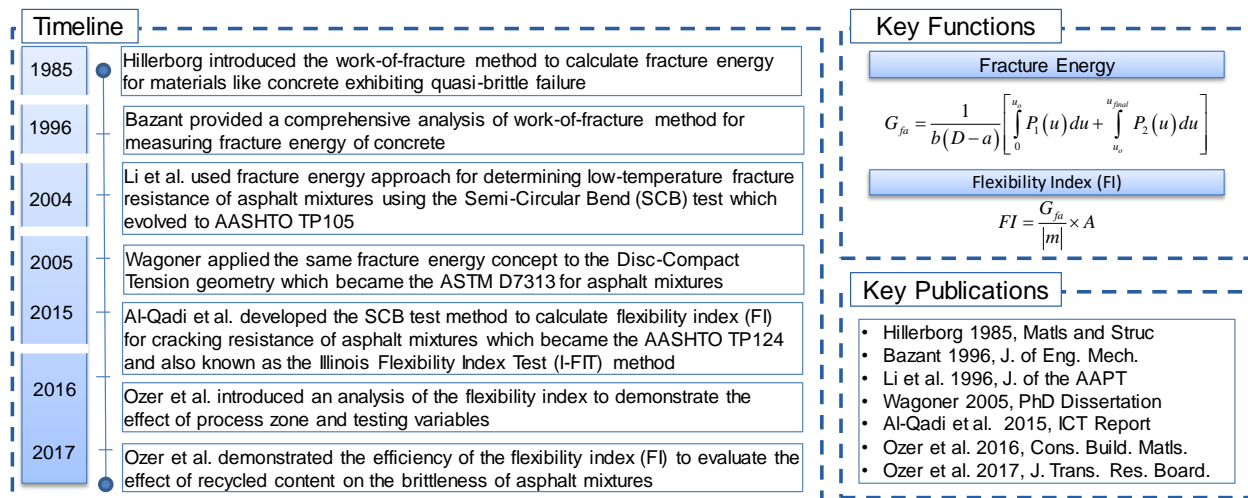


Figure 41. Summary of I-FIT method.

Development of the Illinois Flexibility Index Test (I-FIT) Protocol. The semi-circular bending (SCB) fracture testing protocol was developed to evaluate an asphalt mixture's overall resistance to cracking-related damage (Al-Qadi *et al.*, 2015; Ozer *et al.*, 2016a). The test was intended to be used at the mix design and production levels. In addition to the availability of off-the-shelf equipment, the following four criteria – along with simplicity, repeatability, efficiency, and cost effectiveness – were considered when selecting the test method: (1) a statistically significant and meaningful spread in test outcome, representing a mix's cracking resistance; (2) repeatability, practicality, low cost, and easy implementation by technicians; (3) correlation to other independent test methods and engineering intuition; and (4) correlation to field performance.

Test Method Description. The I-FIT protocol, also known as Illinois SCB (IL-SCB), is conducted at an intermediate temperature (25°C) using a custom-designed SCB fixture placed in a servo-hydraulic or pneumatic AC testing machine (AASHTO TP124). The test was conducted using load-line displacement control at a displacement rate of 50 mm/min (Al-Qadi *et al.*, 2015; Ozer *et al.*, 2016a; 2016b). The main outcome of the test procedure is a parameter called the flexibility index (FI), along with fracture energy. Figure 42 shows a typical SCB specimen during the fracture and specimen geometry.

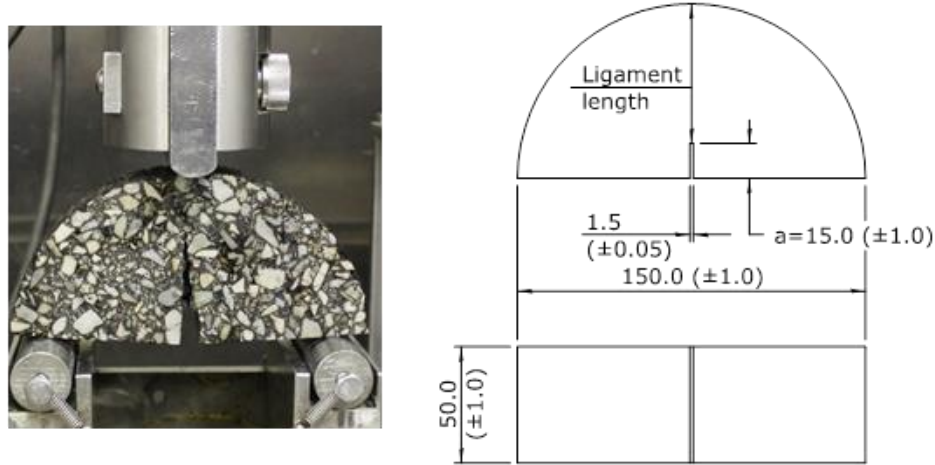


Figure 42. I-FIT test and specimen configuration (dimensions in millimeters).

According to the work-of-fracture method (Hillerborg, 1985; Bazant, 1996), fracture energy is the area under the load-displacement curve until the specimen is broken. The area corresponds to the work done by load (P) on the load-point deflection (u). Assuming that all of the work of load P is dissipated by crack formation and propagation, this work would correspond to fracture energy. The method determines fracture energy, or more accurately, apparent fracture energy, because not all energy may be dissipated at the crack tip, as follows:

$$G_{fa} = \frac{1}{b(D-a)} \left[\int_0^{u_o} P_1(u) du + \int_{u_o}^{u_{final}} P_2(u) du \right] \quad [95]$$

where; $P_1(u)$ and $P_2(u)$ = fitting equations before and after the peak, respectively; u_o = displacement at the peak; and u_{final} = final displacement that can be selected as the displacement at a cut-off load value where the test is considered at an end (usually taken as 0.1 kN). If desired, the load-displacement curve can also be extrapolated to calculate the remaining area under the tail part of the curve, which is generally less than 5% of the total area. The load-displacement curves for four mixes with varying degrees of recycled content (L3 to L6) are shown in Figure 43.

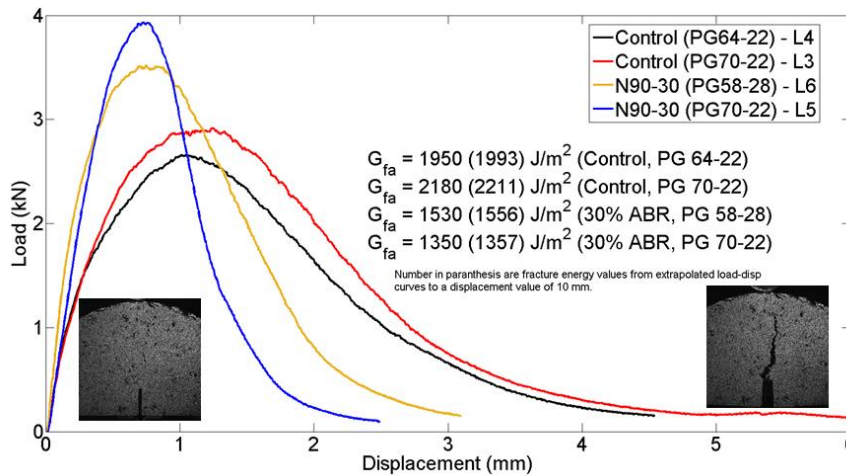


Figure 43. Typical load-displacement curves for AC mixes with varying ABR (L3 and L4: control; L5 and L6: 30% ABR) and corresponding fracture energy calculated at cut-off displacement (short) and extrapolated (long) from the I-FIT tests (Ozer et al., 2016a).

Flexibility Index Calculation. The flexibility index (FI) was introduced to capture the cracking resistance of AC mixes in a more robust and consistent way. Derived from the load-displacement curves obtained from the I-FIT



method with parameters of fracture energy and slope at the post-peak inflection point, the *FI* describes the fundamental fracture processes consistent with the size of the crack tip process zone. It was shown that the *FI* can capture the effects caused by various changes in the materials and volumetric design of AC mixes (Al-Qadi *et al.*, 2015; Ozer *et al.*, 2016a; 2016b). Plant-produced, laboratory-produced, and field core specimens were used in validating the potential of the IL-SCB test and the *FI* to predict cracking resistance in mixes. The effects of increasing the RAP and RAS content were shown, with a reduction in the *FI* indicating a more brittle behavior. The *FI* values varied from 15 to 1 for the best- and poorest-performing laboratory-produced AC mixtures, respectively. A typical load-displacement curve obtained from the SCB test is shown in Figure 44 with the parameters calculated from the test.

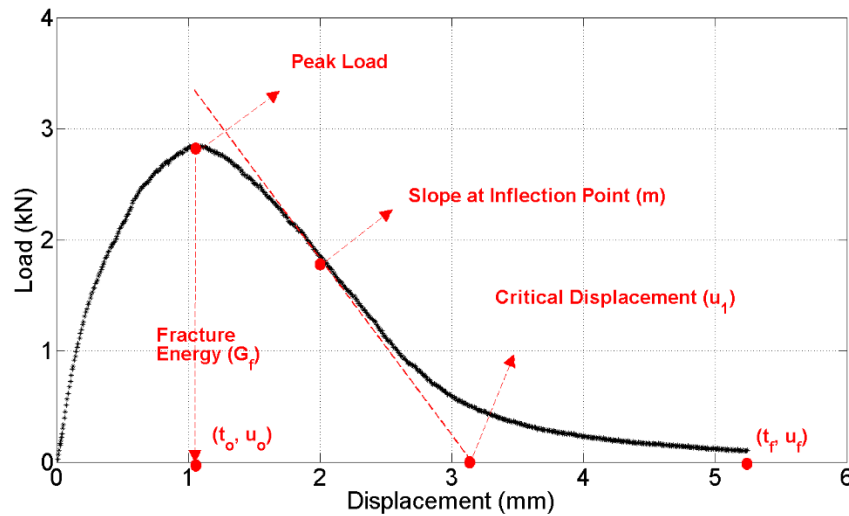


Figure 44. A typical outcome of the SCB test illustrating the parameters derived from the load-displacement curve including peak load (can be related to tensile strength), critical displacement, slope at inflection point, displacement at peak load, and fracture energy.

The *FI* is calculated using the overall fracture energy normalized by the slope at the inflection point of the post-peak part of the load displacement curve. The inflection point indicates that crack propagation is slowing down.

$$FI = \frac{G_{fa}}{|m|} \times A \quad [96]$$

where; $|m|$ = absolute value of the post-peak slope at the inflection point (reported as kN/mm); G_f = fracture energy reported in Joules/m² and represents the area under the load-displacement curve normalized by fractured area; and coefficient A = unit conversion factor and scaling coefficient (taken as 0.01 as the default).

Evaluation of Mixes with Varying Asphalt Binder Replacement. The effect of varying degrees of asphalt binder replacement (ABR) was assessed using the I-FIT protocol and *FI*. Various mixes were developed from a parent control mix design with the addition of RAP and RAS increasing up to 60%. The objective was to evaluate the flexibility of the AC mixes with increasing ABR with RAP and RAS together or RAS only, as well as to determine the effectiveness of binder grade bumping to compensate for the presence of recycled stiff binder. An N90 surface course dense-grade AC mix design was developed. The *FI* values and fracture energy are shown in Figure 45 for the AC mixes. The values were normalized with respect to the control AC mix with PG 70-22. The overall pattern with the *FI* was a consistent reduction with increasing ABR. The reduction was much more pronounced when it was compared with fracture energy values obtained at the same temperature.

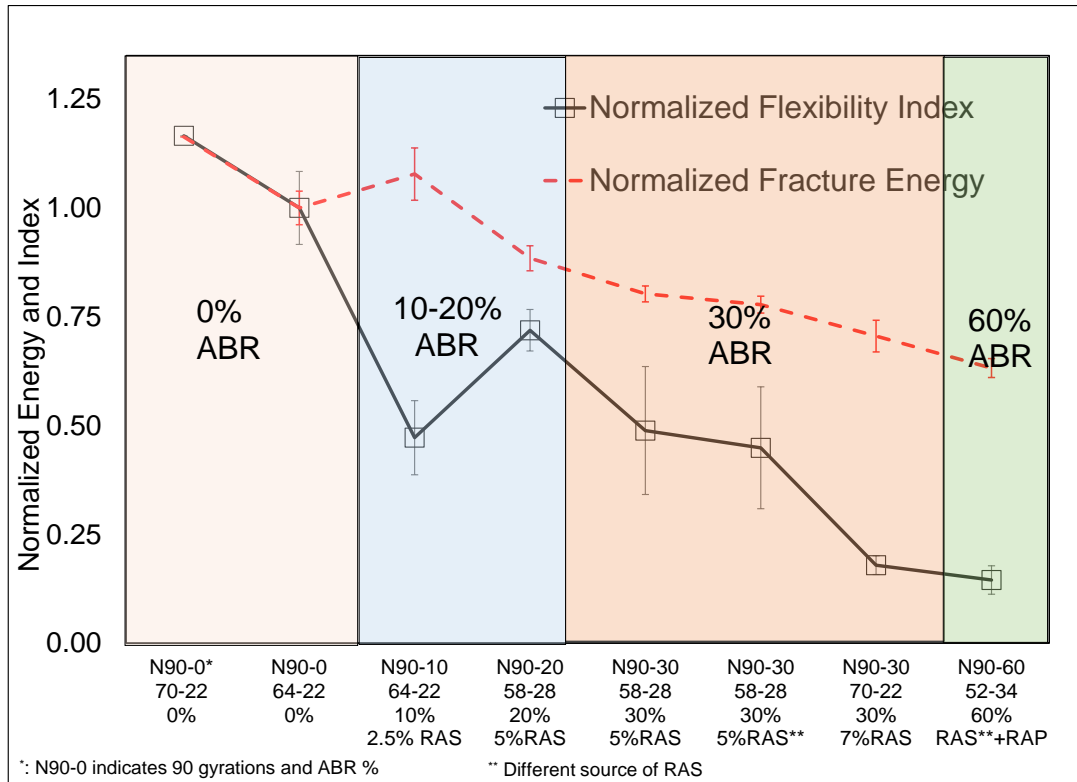


Figure 45. Comparison of normalized fracture energy with normalized FI for N90 design mixes with varying ABR (in %) obtained using various combinations of RAS and RAP (Ozer et al. 2016b).

Field Performance Validation. The accelerated test sections built in the Federal Highway Administration's (FHWA) Accelerated Loading Facility (ALF) were used to correlate with the results obtained from the I-FIT. Mixes used in the study contained various levels of RAP and RAS (up to 40% ABR), along with different binder grades commonly used to compensate for the presence of aged and stiff recycled binder. The test sections provided a unique opportunity to compare the performance of AC mixture tests because the accelerated test sections were intended to have identical pavement structures. ALF performance was grouped into three major categories (good, intermediate, and poor) for a distinct number of load repetitions to a threshold of fatigue cracking. The control AC mix with no recycled content (Lane 1) and AC mixes with low levels of RAP (Lanes 6 and 9) were among the good-performing group, whereas mixes with RAS (Lanes 3 and 7) and the highest recycled binder ratio without binder grade bumping to a softer grade (Lane 5) were in the poor-performing group. The I-FIT results with fracture energy and FI were evaluated, and the summary of FI results is shown in Figure 46. A clear reduction in flexibility of mixes with increasing recycled material content and presence of RAS was observed. A very good correlation exists between the number of cycles to failure during ALF experiments and the laboratory test FI values.

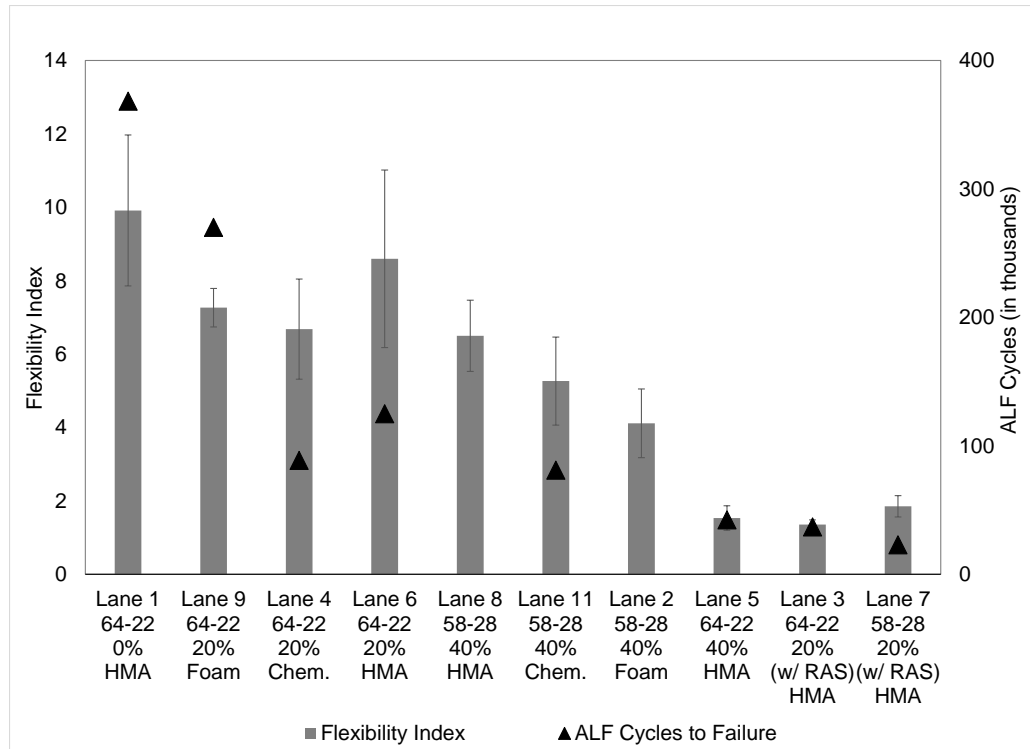


Figure 46. Summary of the I-FIT and its correlation to ALF cycles to failure performed on the plant-produced AC mixtures collected from the ALF experiment sections (Ozer *et al.*, 2017).

5.2.3. Disk Compact Tension (DC(T))

Overview. The disk-shaped compact tension, DC(T), test has become a standardized fracture test for cylindrical asphalt concrete specimens that have been either fabricated in the lab or obtained from cores in the field. Originally based on ASTM E399 “Standard Test Method for Linear-Elastic Plane-Strain Fracture Toughness of Metallic Materials”, the DC(T) test was modified for use on asphalt concrete materials, providing an alternative to the standard rectangular-shaped geometry that had been previously used (Wagoner *et al.*, 2005b). This test, which follows the procedure specified by ASTM D7313, can be used to determine fracture characteristics for different types of cracking in asphalt pavements, such as thermal, reflective, and block cracking. A summary of the timeline of the DC(T) test as it pertains to asphalt concrete, the key functions, and publications are presented in Figure 47.

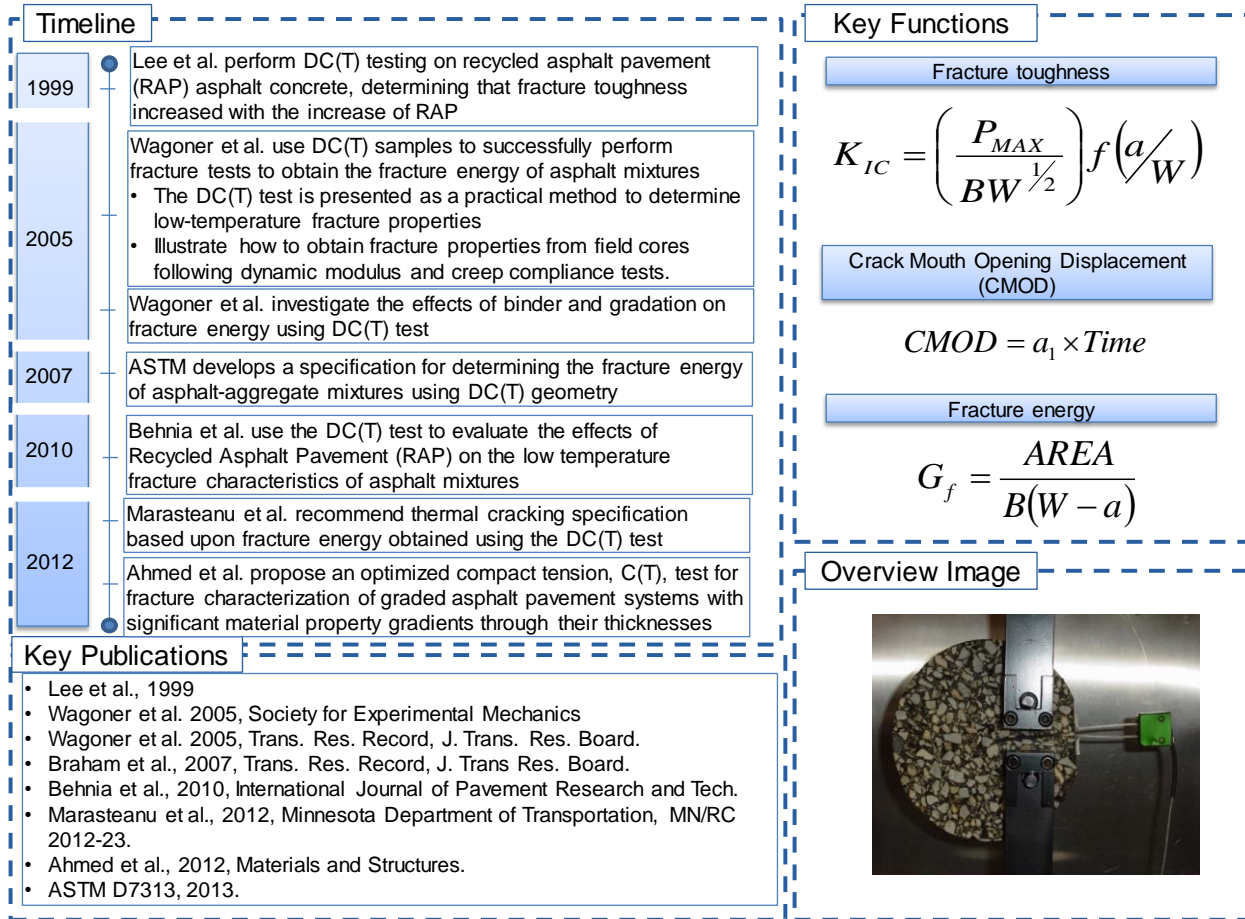


Figure 47. Summary of the DC(T) test.

By loading the single-edge notched disc specimen in tension, two fundamental material properties can be obtained from this test, as shown in Figure 74. These include 1) the fracture toughness, K_{IC} ,

$$K_{IC} = \left(\frac{P_{MAX}}{BW^{1/2}} \right) f(a/W) \quad [97]$$

and 2) the fracture energy, G_f ,

$$G_f = \frac{AREA}{B(W-a)} \quad [98]$$

which are based on the applied load and the crack mouth opening displacement (CMOD) data that is smoothed and fit to a linear regression of the form,

$$CMOD = a_1 \times t \quad [99]$$

where; P_{MAX} = the maximum applied load, B = specimen thickness, W = specimen width, $f(a/W)$ = geometry function based on crack size to specimen width ratio, $AREA$ = area under load-CMOD curve, $W-a$ = initial ligament length, a_1 = slope of the regression line, and t = test time.

Test Development. The DC(T) test was first applied to asphalt concrete by Lee *et al.* (1999), investigating the effects of different types and quantities of recycled asphalt pavement (RAP) in the mixture on the fracture toughness. In this research, brittle fracture occurred during testing performed at 0°C and the different levels of RAP had no significant effect; however, fracture toughness was shown to increase with an increase of RAP for tests performed at 22°C. At

this point, the geometry and procedure outlined by ASTM E399 were applied to asphalt concrete. It was not until six years later when Wagoner *et al.* (2005a) suggested modifications to the testing geometry that the test was evaluated for specific application to asphalt concrete.

In response to the need for a practical fracture test for asphalt concrete that has the capability of testing cylindrical specimens, Wagoner *et al.* (2005b) presented the DC(T) test as a viable option and illustrated how to obtain fracture properties from field cores of asphalt concrete following dynamic modulus and creep compliance tests by performing the DC(T) test on the same specimens. The DC(T) test configuration, as shown in Figure 48, was selected because it allows for the testing of cylindrical samples, similar to the SC(B) test; however, the DC(T) maximizes the potential fracture area, reducing the statistical variability of the fracture energy obtained from the test (Wagoner *et al.*, 2005a).

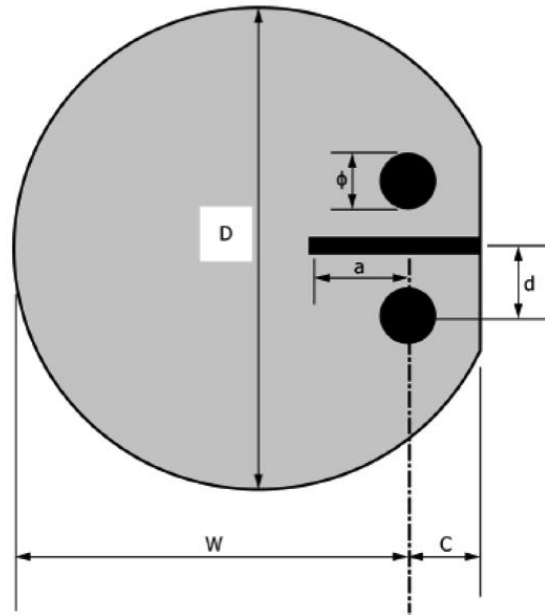


Figure 48. DC(T) specimen and dimensions (ASTM D7313 2013).

During the initial application of the DC(T) to asphalt concrete materials, localized failure was seen at the loading holes (Wagoner *et al.*, 2005a). However, after multiple iterations of laboratory testing, a geometry was developed that maximized ligament length but minimized specimen rupture at the loading holes. Table 3 displays these newly developed dimensions compared to those originally prescribed by ASTM E399.

Table 3. Comparison of DC(T) specimen dimensions.

	Dimensions in mm	
	ASTM E399	Recommended by Wagoner <i>et al.</i> , 2005a
D	150	150
W	111	110
B_{max}	56	50
C	28	35
ϕ	28	25
d	31	25
a_{max}	61	27.5

Three different temperatures, including -20°C, -10°C, and 0°C, and four different loading rates of 10, 5, 1, and 0.1 mm/min were investigated for use by the DC(T) on asphalt concrete. Computing fracture energy as the area



under the load-CMOD curve, Wagoner *et al.* found that temperature and fracture energy were directly proportional, whereas loading rate and fracture energy were inversely related. The variation seen in these fracture energy computations were comparable to those for the SE(B) and SC(B) tests, indicating that the DC(T) test is a reliable option for obtaining fracture properties of asphalt concrete (Wagoner *et al.* 2005a). To further evaluate the reliability of the DC(T) for use on asphalt concrete four different mixtures were evaluated to observe the effects of different binders, gradations, and sample thicknesses on fracture properties. The mixtures with the softer binders yielded higher fracture energies, with the polymer modified binder mixture having the highest fracture energy. Fracture energy was also shown to increase as the specimen thickness increased (Wagoner *et al.*, 2005b).

Two years later, in 2007, ASTM developed a specification for the determination of fracture energy of asphalt concrete mixtures using the DC(T) geometry based upon the recommendations and findings of Wagoner *et al.* (2013). Figure 48 above displays an image of the standardized testing configuration, with the clip gage and gage point placement along with the loading attachments. Sample fabrication requires both sawing and coring: Initially a water-cooled masonry saw is used to create a flat face. Then using a template, the locations of the loading holes are to be marked and drilled with a water-cooled drilling device. Finally, a smaller masonry table saw should be used to create the flattened face where the CMOD gage is placed and to make the notch (Marasteanu *et al.* 2007). According to the specification, ASTM D7313, it is suggested that the test be performed at 10°C greater than the lower temperature performance grade of the binder and with a constant CMOD rate of 0.017 mm/s (2013).

In the phase 2 report for the Investigation of Low Temperature Cracking in Asphalt Pavements National Pooled Fund Study, the DC(T) was recommended as the test method that should be used for fracture testing of asphalt mixtures, rather than the SC(B) test, due the existence of an ASTM standard and its history of acceptance for many years and for other materials as a reliable evaluation of fracture toughness (Marasteanu *et al.*, 2012). Low temperature cracking criteria were also developed based upon fracture energy obtained using the DC(T) test and presented in this report. These recommendations are presented below in Table 4.

Table 4. Recommended low-temperature cracking criteria based on DC(T) fracture energy.

Low-Temperature Cracking Criteria	Project Criticality/Traffic Level		
	High >30M ESALS	Moderate 10-30M ESALS	Low <10M ESALS
Fracture Energy, minimum (J/m ²), PGLT+10C	690	460	400

Related Testing Efforts and Applications. After the standardization of the procedure, further applications have been found and explored for the use of the DC(T) geometry on asphalt concrete. In 2010, Behnia *et al.* investigated the effects of RAP on the low temperature fracture characteristics of asphalt concrete by determining the fracture energy using the DC(T) test. This research indicated that adequate cracking resistance is possible in mixtures with 30% RAP if they are designed properly using an adjusted, softer virgin binder. It also demonstrated that the DC(T) test could be used for the design and cracking control of RAP mixtures (Behnia *et al.*, 2010).

Another application for the DC(T) test was investigated by Ahmed *et al.* (2012), considering the use of an optimized compact tension test for the fracture characterization of asphalt thin bonded overlays. This research acknowledged the need for a fracture test or modification of a fracture test that could consider thin bonded asphalt concrete overlay systems, which prove to have significant material property gradients throughout the thickness. Using ASTM E399, upon which the DC(T) test is based, and ASTM D7313, an optimized compact tension, C(T), test geometry and procedure were proposed for use on field cores and laboratory fabricated samples. This research concluded that the proposed C(T) test was capable of identifying fracture energy variation across a wide range of pavement systems with low variability, making it a viable option for fracture testing of these graded pavement systems (Ahmed *et al.*, 2012).

5.2.4. Single Edge Notched Beam (SENB)

Overview. The Single Edge Notched Beam, or SENB, is one of the less frequently used geometries to quantify cracking of asphalt materials with a notch. The main reason for the lower usage is the geometry of the specimen. Beams are not commonly fabricated in the laboratory (compared to cylindrical specimens), as they can't be formed in a Superpave Gyratory Compactor. In addition, beams are more difficult to extract from the field as they generally require a trench for extraction. However, beam geometry that has been tested in the lab has the advantage of having a very large ligament area, reducing the heterogeneous influence of asphalt materials on test results. The

development of using the SENB as a geometry is shown in Figure 49 and described briefly in the following pages.

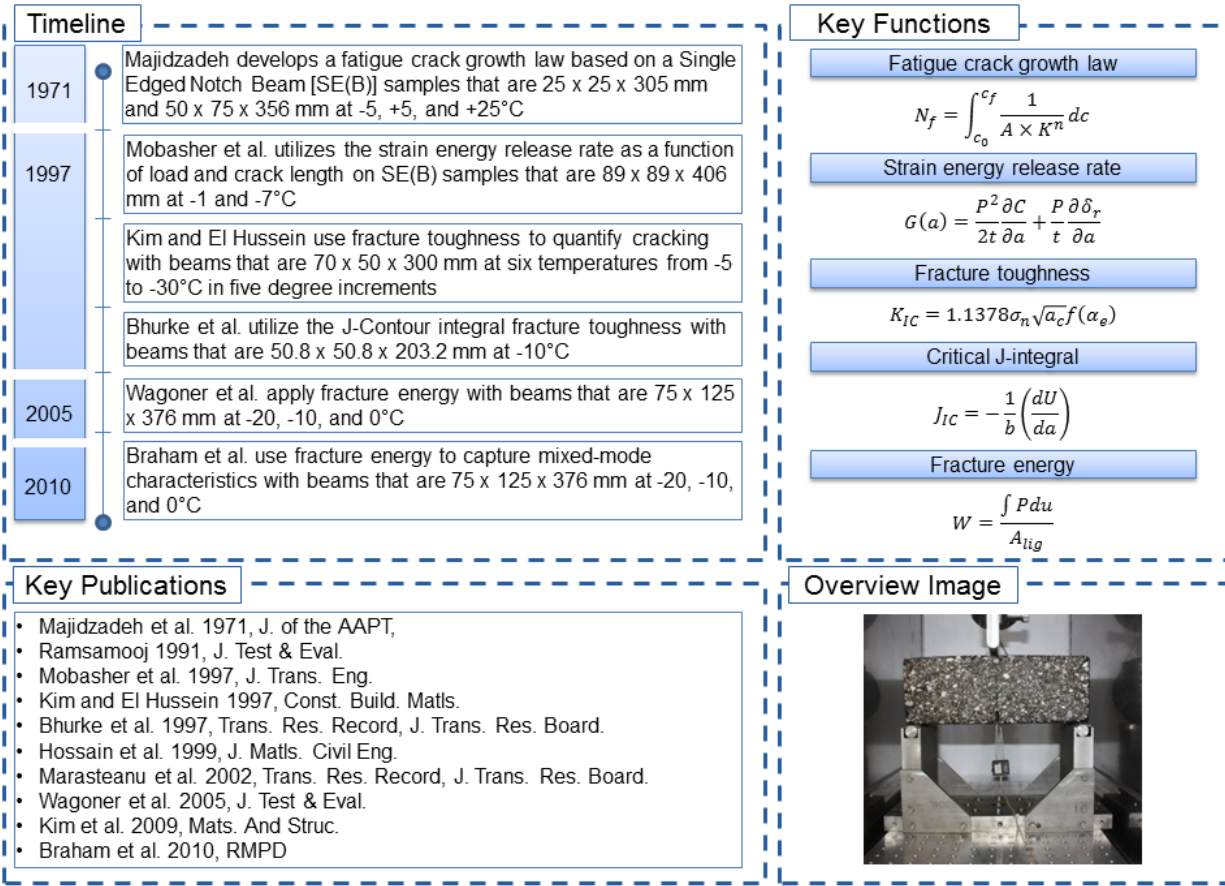


Figure 49. Summary of Single Edge Notch Beam (SENB).

Fatigue crack growth law. Majidzadeh *et al.* (1971) performed the first significant fracture work with the SENB configuration. Using simply-supported beam tests and beam on an elastic foundation, a cyclic loading was applied. Crack length was measured using the compliance method, which utilized the inverse of the slope on the load/deflection diagram. Using both the started flaw length (c_0), the final crack length (c_f), and the geometry of the beam, the fatigue life (N_f) was shown to be a function of A and n (material constants from Paris' Law) and the stress intensity factor (K). This fatigue crack growth law is shown in Equation [100]:

$$N_f = \int_{c_0}^{c_f} \frac{1}{A \times K^n} dc \quad [100]$$

Some key findings included the fact that creep was more influence on the simply supported beams versus the beams on an elastic foundation. This highlights a potential disadvantage of the geometry (50 x 75 x 356 mm) because of the high self-weight. Another finding of the research was the identification that at the lower testing temperatures (-5°C) the cracking is governed by the critical stress intensity factor, whereas at the higher testing temperatures (+25°C) the critical crack depth approaches the specimen thickness and the theories of elasticity no longer apply. Most importantly, this research established the potential of using this geometry for future testing. Ramsamooj (1991) continued work utilizing the fatigue crack growth law, using an equation similar to Equation [100], but incorporating a normalized stress intensity factor, the tensile strength, and the creep compliance, to make the concept applicable to viscoelastic materials.

Strain energy release rate. Mobasher *et al.* (1997) utilized an energy approach to quantify fatigue cracking. By using the load (P), compliance (C), thickness (t), and crack length (a), the energy release rate due to the incremental crack growth can be shown in Equation [101].



$$G(a) = \frac{P^2}{2t} \frac{\partial C}{\partial a} + \frac{P}{t} \frac{\partial \delta_r}{\partial a} \quad [101]$$

Mobasher *et al.* was able to differentiate energy values between -1 and -7°C on samples that were 89 x 89 x 406 mm in size. In addition, variation in energy values was found when changing asphalt content and when including asphalt rubber into the asphalt mixture.

Fracture toughness. Kim and El Hussein (1997) performed monotonic tests on the SENB configuration at -5, -10, -20, -25, and -30°C in order to quantify the fracture toughness (K_{IC}) of the material, as seen in Equation [102]:

$$K_{IC} = 1.1378 \sigma_n \sqrt{a_c} f(\alpha_c) \quad [102]$$

where; σ_n = the stress on the beam, a function of the load and geometry, a_c = effective crack length, and α_c = effective crack length to beam height ratio.

While this study did utilize the SENB configuration, it marks the deviation away from fatigue cracking, and toward monotonic cracking, which is more generally used in low-temperature or reflective cracking. This is demonstrated through additional research, where Bhurke *et al.* (1997) used the J-Contour integral fracture toughness, Hossain *et al.* (1999) used peak load and fracture energy, Marasteanu *et al.* (2002) used fracture toughness, Wagoner *et al.* (2005) used the fracture energy for Mode I failure, Kim *et al.* (2009) used discrete element modeling to simulate the SENB at low temperatures, and Braham *et al.* (2010) used the fracture energy for mixed-mode failure. The geometry recommended for use with the SENB test by Wagoner *et al.* (2005) and utilized by Braham *et al.* (2010) is shown in Figure 50.



Figure 50. Single Edge Notched Beam (SENB) testing configuration (Braham).

5.2.5. Double Edge Notched Prism (DENP)

One of the major tasks of NCHRP 9-19 project, *Superpave Support and Performance Models Management*, was to develop a cracking model that would be included in the overall material characterization scheme developed during the project. The behavior of asphalt concrete in tension was of primary concern to the prediction of cracking related distress. It was envisioned that the accurate simulation of cracking in asphalt concrete would require information from both continuum damage mechanics and fracture mechanics. Therefore, an experimental and analytical study was performed on a single asphalt mixture using both the continuum damage and fracture mechanics approaches. This section briefly summarizes the research efforts into the evaluation of crack formation and propagation in double edge notched asphalt concrete specimens. Figure 51 provides an overview of the development efforts, key publications, and key functions with the Double Edge Notched Prism (DENP) methodology.

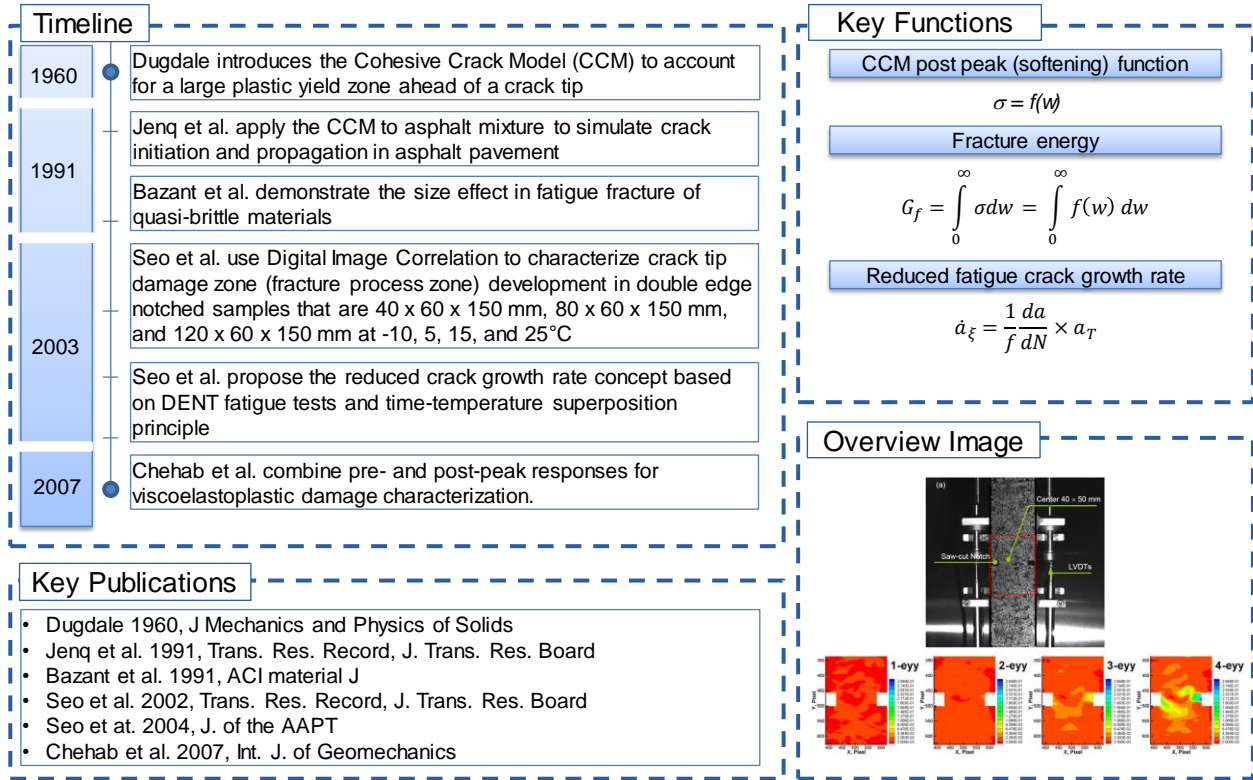


Figure 51. Summary of materials fracture and fatigue assessment with DENP.

Overview. Observations of crack initiation and propagation in asphalt concrete at low and moderate temperatures indicate that micro cracks ahead of the crack tip are growing and coalescing to form a macro crack that advances into the next weak (micro damage) zones. This behavior can be simulated using nonlinear models with an appropriate constitutive law for the damaged material in the Fracture Process Zone (FPZ). This section starts with concepts of the cohesive crack model, a nonlinear fracture model appropriate for quasi-brittle materials, such as concrete, asphalt concrete, ceramic, etc.

Experiment. Seo *et al.* (2003) used three specimen sizes (40, 80, and 120 mm) with double symmetric notches (3.5 × 7 mm) to model the development of fatigue cracking in asphalt concrete. Each specimen was cyclically loaded from a zero to a full tensile load at 2 Hz loading frequency with the selected stress levels being 50, 65, and 80% of the tensile strength. Fatigue cracks were monitored using a digital camera aimed at the front side of the test specimen. Then, the incremental increase of crack lengths was visually measured from the digital photographs taken at the tensile peak loads for every cycle to capture the moment the crack opening occurred

The concept of reduced crack growth rate is introduced to investigate whether crack growth rate prediction can be made from one temperature to another (i.e., crack growth rate master curve). Based on the time-temperature superposition principle, time, t , is divided by the shift factors determined from the complex modulus tests to obtain the reduced time, ξ , at the reference temperature of 25°C. The reduced crack growth rate, \dot{a}_ξ , is then determined by using this reduced time in the crack growth rate calculation:

$$\dot{a}_\xi = \frac{da}{d\xi} = \frac{da}{dt} \times a_T \quad [103]$$

with

$$\frac{da}{dt} = \frac{1}{f} \frac{da}{dN} \quad [104]$$

where f = loading frequency.



Analysis: Cohesive Crack Model. The cohesive crack model (CCM) is a simple model that can describe in full a nonlinear fracture process at the front of a pre-existing crack. Dugdale (1960) and Barenblatt (1962) introduced this model to account for a relatively large plastic yield zone ahead of a crack tip. Hillerborg *et al.* (1976) extended this model to concrete fracture and described a fairly large FPZ. The CCM represents the FPZ by employing a cohesive force (i.e., crack-closing stresses) at the near crack tip. It has also been applied to asphalt concrete materials to simulate crack initiation and propagation in asphalt concrete pavements (Jenq *et al.*, 1991).

The basic hypotheses of the CCM are as follows:

- A crack is assumed to form at a point when the maximum principal stress at that point reaches the tensile strength. The crack forms perpendicular to the maximum principal stress direction (i.e., crack initiation and propagation criteria).
- The properties of the materials outside the process zone are governed by the undamaged state.
- The stress transferred between the faces of the crack is described by a post-peak function (i.e., softening function). In the case of the opening mode, the function is:

$$\sigma = f(w) \quad [105]$$

where σ = tensile stress and w = crack opening displacement (i.e., the distance between the crack faces).

Analysis: Post-peak Function (softening curve). In a constant rate-of-displacement uniaxial tension test, the ability of the material to carry load decreases as deformation continues beyond the maximum loading-carry capacity. The shape of this softening curve for a given material is considered to be one of main components of the CCM. Although each material has its unique softening curve, determined only by experiments, Petersson (1981) first found that the softening curve is similar in shape for different mixtures of Portland cement concrete when the softening curves are plotted in a non-dimensional form.

Analysis: Fracture Energy (cohesive fracture energy). The fracture energy, G_f , is defined as the energy required to create a unit surface of crack, can be obtained from:

$$G_f = \int_0^{\infty} \sigma dw = \int_0^{\infty} f(w) dw \quad [106]$$

The CCM has been applied extensively to Portland cement concrete and has only recently been investigated for asphalt concrete (Jenq *et al.*, 1991). Jenq *et al.* used both indirect tensile tests and notched beams to assess the tensile strength and fracture energy of asphalt concrete. The shape of the function $f(w)$ was assumed and the parameters backcalculated using fracture energy and load-deflection curves from notched-beam tests. However, they admitted that a direct tensile test should be performed under different temperatures to adequately evaluate the effect of temperature on $f(w)$.

Analysis: Fatigue crack Propagation. It has been generally accepted that fatigue is a process of cumulative damage and one of the major causes of cracking in asphalt concrete pavement. In an effort to model fatigue crack growth, the Paris law (Paris and Erdogan, 1963) -- a logarithmic linear relationship between the incremental change in a crack length (da/dN) and the amplitude of the crack driving force (e.g., stress intensity factor) -- has been widely used. For elastic materials, this law can be presented as:

$$\frac{da}{dN} = C(\Delta K_I)^n \quad [107]$$

where C and n = empirical material parameters. It has been demonstrated that the Paris law based on a linear elastic stress intensity factor can successfully describe fatigue crack growth in a concrete beam (Bazant and Xu, 1993). Popelar *et al.* (1992) applied the Paris law to slow crack growth problems in polyimide films, which exhibit time and temperature dependent properties.

Image Characterization of FPZ. Since the advent of new state-of-the-art experimental techniques and numerical algorithms, several mechanisms that are responsible for the Fracture Process Zone (FPZ) formation in concrete have been investigated. Cedolin *et al.* (1983) measured high values of strains developed in the FPZ with the moiré interferometry method. These high strains suggested the need for new constitutive model for concrete. Krstulovic-

Opara (1993) visualized the distribution of micro cracks before the crack tip in mortar using high-magnification scanning electronic microscopy (SEM). Seo (2003) first investigated the characteristics of FPZ in asphalt concrete under fatigue and fracture loadings using a computer vision technology known as Digital Image Correlation (DIC). As shown in Figure 53, the heterogeneous characteristic of the asphalt-aggregate mixtures and the presence of aggregate with variable shapes and sizes always provoke a pronounced scatter of the process zone. The range of vertical strain is set between 0 and 0.05 to best match the strain localization patterns with the location of aggregates in the specimen. It is worth noting that the higher localized strain zones start forming from the notches and eventually become the FPZ. As expected, it is observed that the process zones coincide well with regions where small aggregates and asphalt binder are located between large aggregate particles.

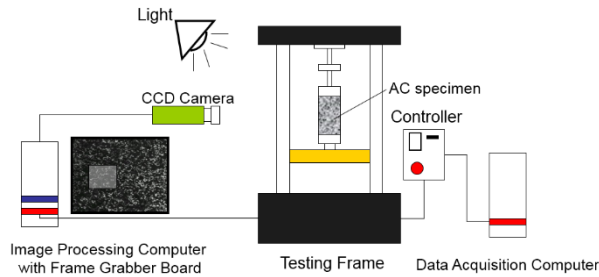


Figure 52. DIC test setup.

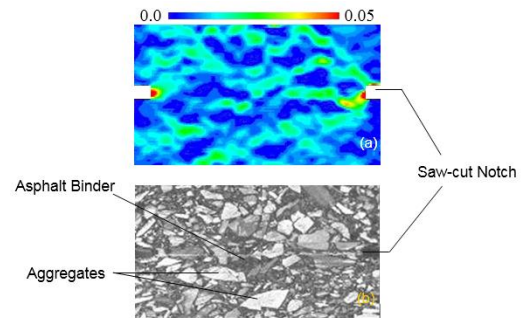


Figure 53. Image mapping between process zones and aggregate structure; center 80×40 mm area of an 80 mm wide specimen subjected to 2 Hz fatigue loading at 25°C : (a) DIC image for vertical strains; (b) aggregate structure.

Calibration of the VEPCD Model with FPZ Strains. Seo (2003) also demonstrated how fracture and continuum damage could be combined. With the FPZ strains measured by DIC, the VEPCD model (mentioned in Section 6.3.1) was calibrated for accurate strain predictions after localization because LVDT-based strains are not valid as macro cracks develop in the specimen. So, as such, there is a switch in the source of strain data at peak stress that consequently leads to a switch in the calculated values of normalized pseudo stiffness C and damage parameter S^* yielding a new characteristic relationship between C and S^* as shown in Figure 54. It is worth noting that the transition in the C versus S^* curve corresponding to the switch from LVDT to DIC-based data is smooth and continuous thus ensuring continuity in the model as DIC-based measurements are incorporated in the model. The FPZ based model predicts strains accurately even beyond localization up to the instance of macro crack development and propagation. Beyond that instance, fracture mechanics needs to be used to model the crack growth.

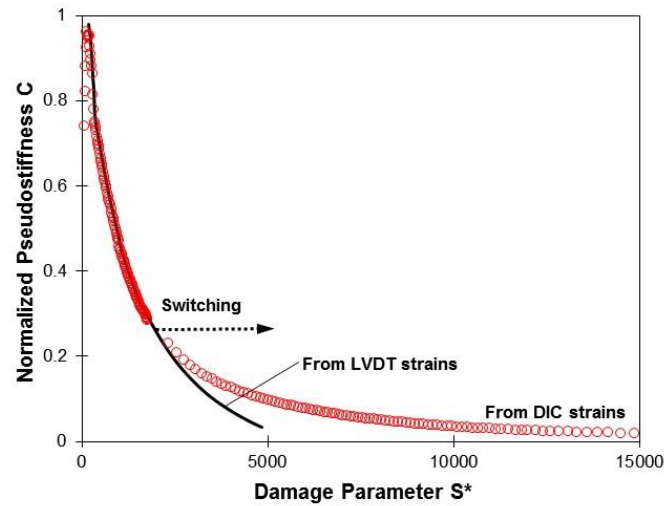


Figure 54. C - S characteristic curves (0.00003 strain/s at 5°C).

6. Asphalt Mixture Analysis Theory

6.1. General Fatigue Approach

Overview. While significant work was performed in the 1800s and early 1900s in general concepts of fatigue, the first instance of a design tool that could be practically used in engineering applications was produced in 1945 by Miner. This section will provide a summary of fatigue in engineering applications from Miner in 1945 to Paris in 1963, which is a common first reference point in fatigue cracking for asphalt material research. A summary of the content is shown in Figure 27.

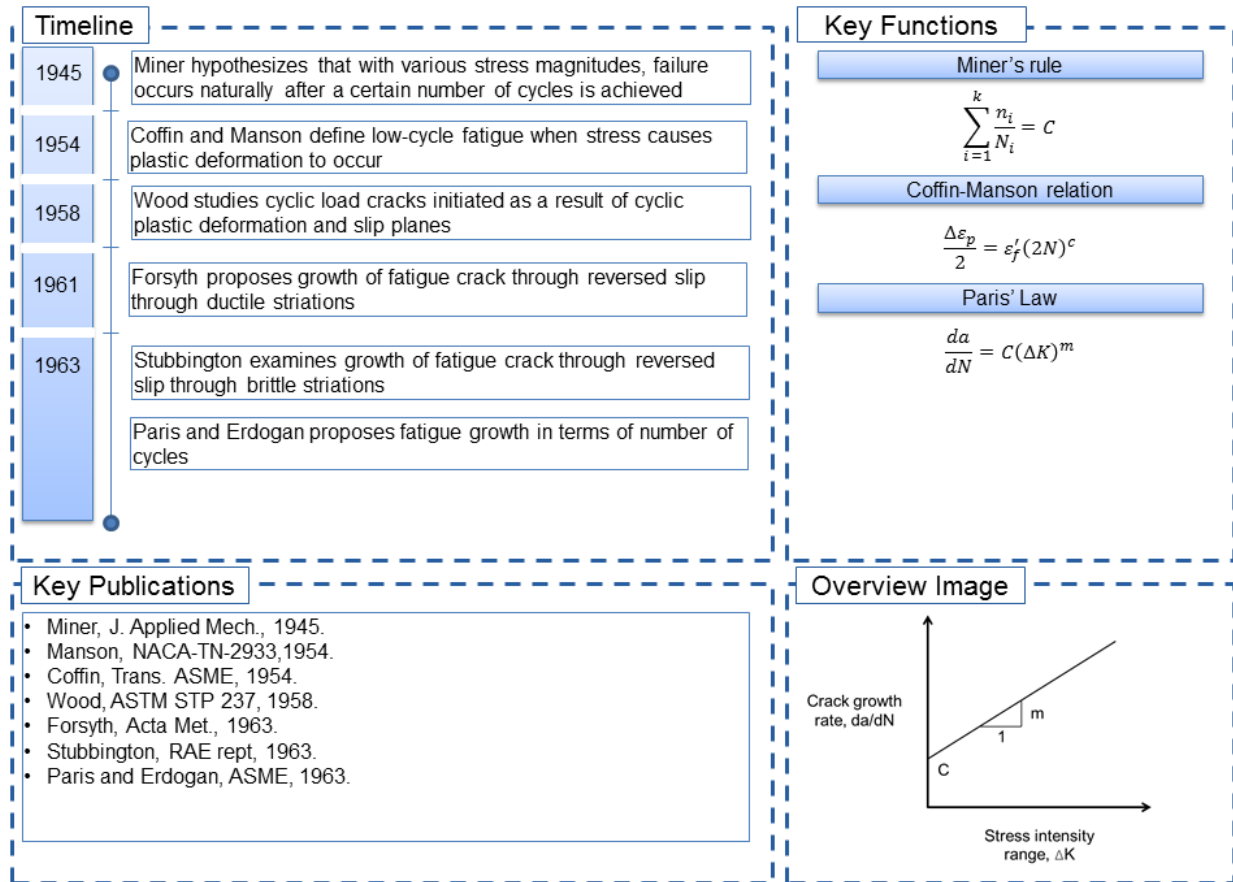


Figure 55. Summary of general fatigue research up to Paris' Law in 1963.

Miner's Rule. Miner's rule (Miner, 1945) revolves around the concept that a body or piece of material can tolerate a certain amount of damage. Fatigue cracking is the result of a high number of very small loads that in isolation do not cause significant damage. However, over time, with enough repetitions, these small loads lead to quantifiable damage. This concept is shown in Equation [108]:

$$\sum_{i=1}^k \frac{n_i}{N_i} = C \quad [108]$$

where; k = different stress levels, i = number of stress levels (σ), N_i = average number of cycles to failure at the i^{th} stress, n_i = number of cycles accumulated at stress σ_i , and C = fraction of life at different stress levels. Failure occurs in Miner's Rule when $C = 1$, as that is when the number of cycles reaches the failure limit. However, a limitation to this theory is that there is no account of the order of loading. Therefore, it does not matter if the larger stresses are applied at the beginning or at the end of the loading cycles, they will be accounted for in the same manner.

Coffin-Manson relation. Coffin (1954) and Manson (1953) independently developed a relationship between the plastic strain and the cycles to failure. This occurs when the loads applied on the material are high enough to introduce plastic behavior, which reduces the service life of the material, thus reducing the number of cycles compared to non-plastic materials. Another effect of these higher loads is that the strain of the material offers a simpler and more accurate description of behavior. This can occur for materials that are under relatively high pressures or heat sources that induce thermal expansion. The resulting relationship is shown in Equation [109]:

$$\frac{\Delta \epsilon_p}{2} = \epsilon'_f (2N)^c \quad [109]$$



where; $\Delta\epsilon_p/2$ = plastic strain amplitude, ϵ'_f = fatigue ductility coefficient (empirical constant), strain intercept at $2N = 1$, $2N$ = number of reversals to failure (N cycles), and c = fatigue ductility exponent (empirical constant), commonly -0.5 to -0.7 for metal materials. When testing steel, the result of this low-cycle fatigue is a straight line.

Around this time, Wood (1958) was also exploring an alternate model explaining the initiation of fatigue cracks by local plastic deformation. In this work, Wood theorized that when you apply tensile load, slip occurs on a “favorable oriented slip plane.” When the load moves to a compressive state, slip takes place in the reserve direction on a parallel slip plane. A second plane is formed because the first plane is restricted by strain hardening and oxidation of the newly created free surface. These two parallel planes, over multiple loading cycles, create extrusions and intrusions, and the intrusions eventually grow into a crack by continuing plastic flow.

A final model of fatigue cracking introduced around this time incorporates the concept of reversed slip. This model can be applied in either ductile striations (Forsyth, 1961) or brittle striations (Stubbington, 1963). In this model, a sharp crack in tension causes a stress concentration where slip can occur easily. On one side of the crack, the material may slip along a plane in the direction of maximum shear stress. This slip causes the crack to open and extend in length. This causes the slip to occur in a second plane, and the trend continues as work hardening and increasing stress will activate other parallel slip lanes, creating a blunt crack tip with a crack propagation length of Δa . At this stage a small plastic region has developed but is surrounded by elastic material, which causes compressive stresses on the plastic region as it grows, causing more yielding and reversed plastic deformation. This cause “ripples” in the material, also known as fatigue striations. The models and theories developed above led to Paris’ work in 1963.

Paris’ law. Paris and Erdogan, in the early 1960’s, found that plots of crack growth rate versus a range of stress intensity factors produced straight lines on log-log scales. Equation [110] shows the relationship:

$$\frac{da}{dN} = C(\Delta K)^m \quad [110]$$

where; da/dN = crack growth rate, C and m = material constants, and K = stress intensity factor. The relationship in Equation [110], which is usually simply called Paris’ Law, can be shown graphically in Figure 56.

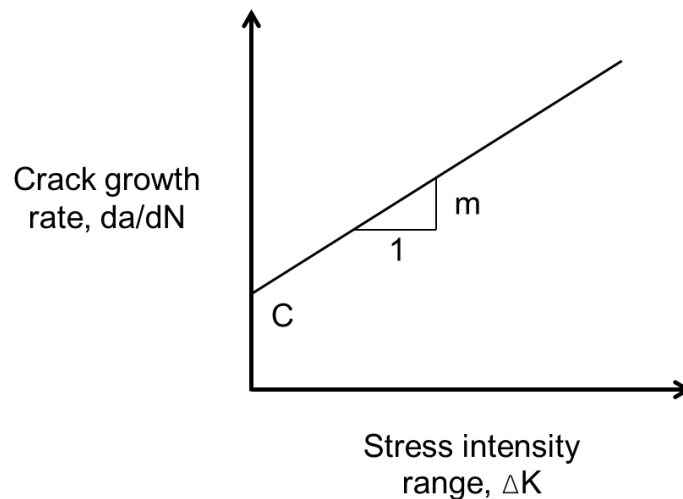



Figure 56. Graphical representation of Paris’ Law.

As mentioned before, a significant number of fatigue research lines in asphalt materials begin with Paris’ Law. These research lines will be discussed in detail in subsequent sections.

6.2. Energy and Energy Inspired Methods

6.2.1. Development of Dissipated Energy Concepts



Energy is dissipated in asphalt mixtures during loading and relaxation because the material behaves substantially in a viscoelastic manner at ambient temperatures. With an elastic material, the energy stored in the system (when loaded) is equal to the area under the load-deflection curve and, during unloading, all the energy is recovered. By contrast, a viscoelastic material, when unloaded, traces a different path to that when loaded resulting in hysteresis and the dissipation of energy. The concepts of dissipated energy as related to pavement design and materials testing were initially developed in the early 1970s and are included in pavement design methods. This section documents the early development that took place and the further development activities that took place during the Strategic Highway Research Program (SHRP), as illustrated in Figure 57. In addition, concepts applied to test data interpretation developed using methods developed during the SHRP contract discussed. Development of other methods after this period is documented in others sections of this document.

Tests used by researchers can be conducted in many different loading configurations such as trapezoidal, cylindrical push-pull, beam, indirect tension, etc. Each of these tests will use a slightly different notation to express the modulus – for example S or S^* (or $|S^*|$) can be used for the beam tests to represent a stiffness in bending whereas an E^* (or $|E^*|$) is often used in for the tests with a cylindrical push-pull (tension/compression) configuration. These moduli are similar and if linear conditions exist and deflections due to shear can be neglected, then for all practical purposes they can often be considered the same. In developing the discussion in this document the extensional notation is used (E^* to represent the complex extension modulus and D^* to represent the extensional complex compliance). Phase angle/lag has been represented by a ϕ whereas in shear it would be typically represented by δ . In some cases where a particular procedure has been referenced the units have been shown consistent with that procedure.

The earliest work using dissipated energy with asphaltic materials was reported by Chomton and Valayer (1972) and van Dijk *et al.* (1972). Chomton and Valayer (1972) presented a relationship in terms of "cumulative dissipated energy" versus number of loading cycles. This relationship and the cumulative dissipated energy are calculated by summing the dissipated energy throughout a fatigue test can be expressed as follows:

$$W = AN^z \quad [111]$$

$$W = \pi \sum_{i=0}^N \sigma_i \varepsilon_i \sin \phi_i \quad [112]$$

Chomton and Valayer presented the results for three materials (two wearing courses and one base course) and suggested that the parameters A and z could be "independent of the mix formulation". It should be noted that Chomton and Valayer used the terms absorbed energy, E , and k in place of W and A , and they gave a value for z of 0.66. However, subsequently W (cumulative dissipated energy), A and z have become the norm in the literature for the expression of the relationship and to avoid confusion they are used throughout this document. Van Dijk *et al.* (1972) reported results in a similar form to Equation [112] with an exponent of 0.625 but no allowance was made for change of stiffness and phase angle in these calculations. In addition, they observed that the percentage retained bending strength of an asphaltic specimen was related to the total energy dissipated. Van Dijk (1975) and van Dijk *et al.* (1977) reported further work which demonstrated several important aspects. It was clear that a single relationship could not be used for all materials (see Table 5 for mix details used), Figure 58.

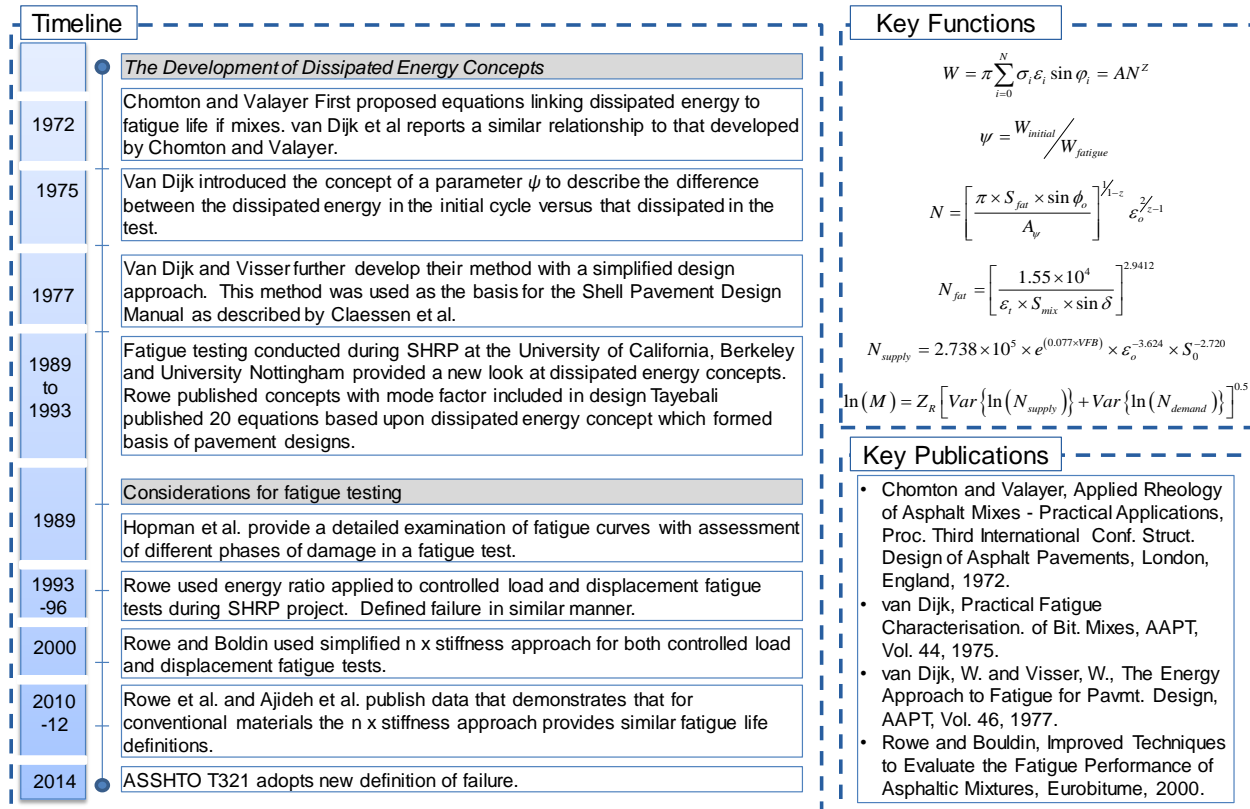


Figure 57. Summary of the development of the dissipated energy concept.

Table 5. Summary of mixture information from van Dijk and Visser (1977)

Mix Number	1	2	3	4	5	6	7	8	9	10	11	12	13
Mix Type	Asphaltic Concrete (California)	Lean Sand Asphalt	Dense Bitumen Macadam	Gravel Sand Asphalt (Dutch)	Lean Bitumen Macadam	Dense Asphaltic Concrete	Dense Bitumen Macadam	Rolled Asphalt Base Course	Grave Bitume (French)	Asphalt Base Course (German)	Rich Sand Asphalt	Gravel Sand Asphalt (Dutch)	Bitumen Sand Base Course
Mix Volumetrics													
Aggregate Volume, %	84.1	81.1	85.6	78.0	61.9	86.7	85.4	83.7	81.4	88.1	72.9	79.1	70.8
Binder Volume, %	14.2	10.5	11.0	11.0	4.9	11.4	11.0	14.1	9.3	9.3	19.3	13.3	8.9
Air Void Volume, %	1.7	8.4	3.4	11.0	33.2	1.9	3.6	2.2	9.3	2.6	7.8	6.6	20.3
Binder Properties													
Softening Point, °C	61	52	52	64	51	59	60.5	62.5	60	52	53.5	60	67
Penetration, mm/10	38	61	59	26	68	36	40	34	27	58	60	40	20

Note: For additional information see van Dijk and Visser, 1977

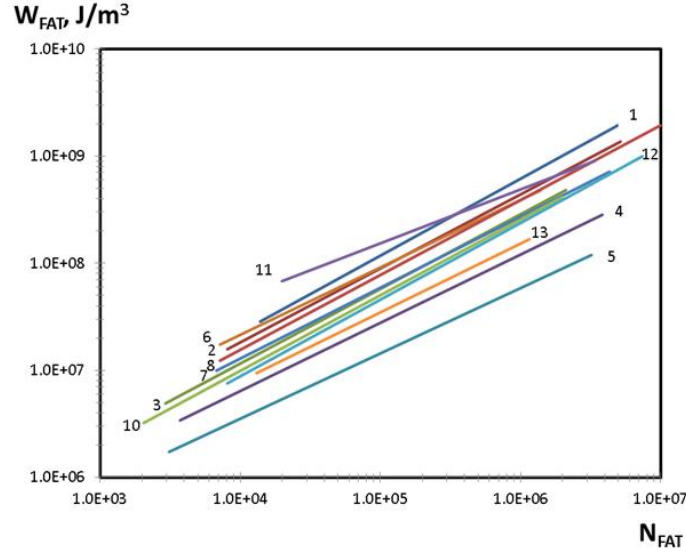


Figure 58. Relationships obtained by van Dijk and Visser (1977) for various mixtures as defined in Table 5 between dissipated energy and fatigue life.

Van Dijk and Visser also developed a ratio which takes values which are related to the mixture stiffness and the mode of loading. This ratio was found to be above unity for controlled displacement (controlled strain) tests and below unity for controlled load (controlled stress) tests. This is a result of decreasing dissipated energy per cycle in a controlled strain test compared to increasing dissipated energy per cycle in a controlled stress test. It can be seen from Figure 59 that as the materials get stiffer, the ratio tends to approach unity. Clearly, ψ is a function of the mode of testing and the mixture stiffness.

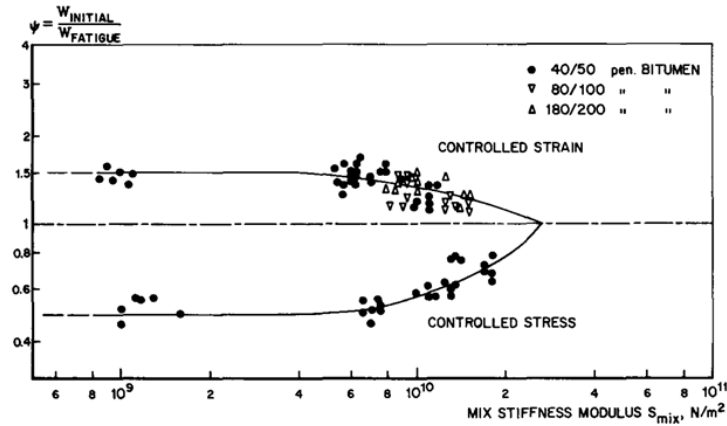


Figure 59. Relationship between total dissipated energy and dissipated energy in first cycle multiplied by number of cycles.

A simplified method developed by Van Dijk and Visser (1977). They gave constant values (the mean obtained from experiments) to the parameters ψ , Z and A of 1.22, 0.66 and $4.0 \times 10^4 \text{ J/m}^3$ respectively. The ψ factor of 1.22 resulted in the prediction method being more appropriate for controlled strain tests. This gave a relationship between the permissible tensile strain, ϵ_t , mixture stiffness, S_{mix} , phase lag and the fatigue life, N_{fat} , as follows:

$$N_{fat} = \left[\frac{1.55 \times 10^4}{\epsilon_t \times S_{mix} \times \sin \delta} \right]^{2.9412} \quad [113]$$



This approach was adopted in the Shell Pavement Design Manual (SPDM) (Claessen, *et al.*, 1977) and used to develop the fatigue criteria that appeared in this design method. In the SPDM the strain is calculated and the pavement life is expressed as strain but the curves developed are those based upon the dissipated energy approach. Rowe (1993) presented a method combining the mode factor with this approach taken by van Dijk and Visser (1977) which gave a correlation coefficient (R^2) for beam fatigue test results of 0.703 regardless of mode of loading. The critical aspect of this work was to develop an approach in which the stiffness and phase angle of a material changes during a test thus allowing an estimation of ratio proposed by van Dijk and Visser. The mode of loading is then considered by the change in stress and strain that results for a given stiffness drop which was taken as 40% rather than the more traditional 50%.

A similar approach was adopted by the University of California team during the SHRP project who conducted extensive work looking at the dissipated energy concept. In the work developed by UCB the concept of dissipated energy was effectively built into the developed fatigue equations. Tayebali *et al* (1993) presented 20 equations linking the fatigue life to a dissipated energy concept for controlled strain fatigue tests. In this work the reported regression coefficients (R^2) ranged between 0.84 and 0.87. Deacon *et al.*, 1994 a relationship which used the loss stiffness modulus. This parameter, as discussed earlier, is directly related to the energy dissipated in an asphaltic mixture. The relationship developed (with an R^2 of 0.79) is as follows:

$$N_{supply} = 2.738 \times 10^5 \times e^{(0.077 \times VFB)} \times \epsilon_o^{-3.624} \times S_o^{-2.720} \quad [114]$$

where; N_{supply} = the number of load repetitions to a 50% reduction in stiffness, e = base of the natural logarithm, ϵ_o = flexural strain, S_o = initial flexural loss stiffness modulus estimated from shear testing (psi), and VFB = voids in the mineral aggregate filled with binder. The predicted fatigue life (N_{supply}) is compared, in a probabilistic manner, to the fatigue life required. Thus for a mix to be satisfactory the N_{supply} must be greater than $M \times N_{demand}$. M is a reliability multiplier whose value depends on the design reliability and on the variability's of the estimates of N_{supply} and N_{demand} . N_{demand} is the design ESAL's (equivalent single axle loads) adjusted to a constant temperature of 20°C divided by an empirically determined shift factor which takes a value of 10 and 14 for 10% and 45% cracking allowed in the wheel paths respectively. The reliability multiplier is estimated from the following

$$\ln(M) = Z_R \left[\text{Var}\{\ln(N_{supply})\} + \text{Var}\{\ln(N_{demand})\} \right]^{0.5} \quad [115]$$

where; Z_R = function of the reliability level which assumes values of 0.253, 0.841, 1.280 and 1.640 for reliability levels of 60, 80, 90 and 95%, $\text{Var}\{\ln(N_{supply})\}$ = variance of the natural logarithm of N_{supply} , and $\text{Var}\{\ln(N_{demand})\}$ = variance of the natural logarithm of N_{demand} . From the mid-1990s onwards the methods developed by UCB has been used for the design of pavements in some regions in the USA and in particular California. The designs have generally been based upon the equations developed using the dissipated energy and reliability concepts (for example Martin *et al.*, 2001) but with the fatigue performance expressed by a strain criteria in a similar manner to that contained within other design methods based upon dissipated energy (Claessen, *et al.*, 1977).

Implications for Test Data Interpretation. The traditional approach as mentioned earlier was to consider a specimen to have fatigue failed when it reached a 50% stiffness value for controlled displacement tests or when the specimen had broken for a controlled load test. Further work was conducted in Europe in the 1980s which resulted in the definition of a fatigue life N_1 in a specimen which was defined on the basis of change in a dissipated energy ratio rather than the more traditional 50% stiffness reduction which has typically been used up to that time. Hopman *et al.* (1989) also used the same data analysis approach to confirm the linear miner law hypothesis for asphalt materials was valid to this condition although some modification may be needed for different definitions of life.

This concept was adopted by Rowe (1993; 1996) who made some important observations. First it was noted that the rate of change of properties in a fatigue test could be best understood by the construction of linear plots of stiffness, phase angle, dissipated energy, etc. versus the number of load cycles (see Figure 60). The condition described by Hopman *et al.* (1989) could be explained by examination of the data to be consistent with several observations. Other work conducted during SHRP at the University of Nottingham showed that the change in dissipated energy in a controlled stress and strain test can be regarded as increasing or reducing in an essentially linear manner to a point where as sharp crack consistent with the suggestions by Hopman *et al.* (1989) as shown by Rowe (1993). Using a simple mathematical approach to the analysis Rowe and Bouldin (2000) demonstrated that the simple product of cycles and a function of the stiffness (either a bending stiffness or complex modulus) could be used to define the location where the slope of the dissipated energy per cycle started to deviate from a straight line to either controlled load (stress) or deflection (strain) fatigue tests. These functions are shown in Equations [116] and [117]. This point is also approximately



consistent with the fatigue failure for conventional asphalt mixtures using the 50% stiffness reduction criteria (see Figure 60) but better captures less stiff modified materials which tend to reduce more in stiffness before a sharp crack initiates (Rowe *et al.*, 2012). The concept of using the reduced dissipated energy ($n.E^*$ or $n \times$ stiffness), which gives a clear defined peak for an easy definition of failure, was built into the ASTM standard for fatigue testing and has most recently been applied in the AASTHO T321 2014 version which significantly reduces the error associated with regression analysis thus producing a most robust test standard

$$\text{Controlled Strain: } R_n^e = \frac{n}{(E^*)_n} \quad [116]$$

$$\text{Controlled Stress: } R_n^e = n \times (E^*)_n \quad [117]$$

Work has been conducted with a scanning laser system to detect surface defects of specimens as they fatigue and this work confirms that the approach developed by dissipated energy techniques and a crack detected by laser scanning produce practically identical results (Ajideh *et al.*, 2010; Ajideh *et al.*, 2012). The significant advantage of this method is that no model fit is applied to the data and a simple peak in a curve is used to define the failure point. In addition, for conventional materials, the failure number of cycles is essentially the same as previously defined by the 50% criteria, thus resulting in previous calibrations of mechanistic design methods being equally applicable (Ajideh *et al.*, 2012; Rowe *et al.*, 2012). The improved definitions are significantly better in defining life of modified binder systems and problems in life estimation using regression analysis techniques are avoided.

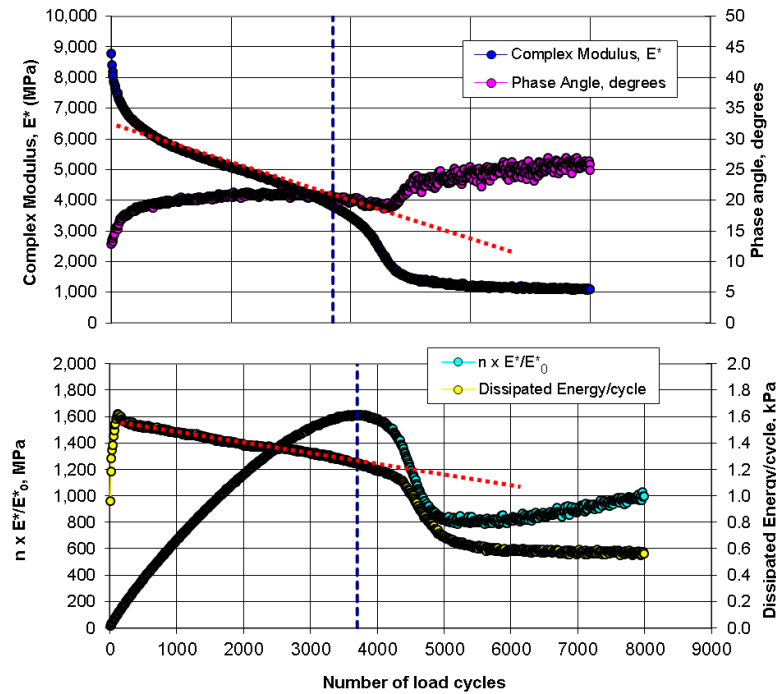


Figure 60. Change in modulus, phase angle, dissipated energy per cycle and energy ratio versus the number of load cycles for a specimen being tested in a four bending beam test.

6.2.2. HMA Fracture Mechanics and Energy Ratio

Overview. The hot mix asphalt-fracture mechanics (HMA-FM) is a viscoelastic fracture mechanics-based system developed to provide a comprehensive framework for practical implementation of mechanisms of pavement cracking into an evaluation and prediction model (Zhang *et al.*, 2001; Roque *et al.*, 2002). The system considers both fundamental failure limits and rate of damage for crack initiation and growth. Asphalt mixture is modeled as a viscoelastic material; damage is associated with its viscous response (creep). The threshold concept is at the core of the system: If the threshold (or the failure limit) is not exceeded, only healable microdamage develops; nonhealable macrodamage (crack initiation and growth) results once the threshold is exceeded. The energy ratio (*ER*) parameter

and associated criteria were developed based on a detailed analysis and evaluation of 22 field test sections throughout the state of Florida using the HMA-FM (Roque *et al.*, 2004). The *ER* was determined to accurately distinguish between pavements that exhibited cracking and those that did not. A timeline of the HMA-FM system, the principle, the key functions, and literature are summarized in Figure 74.

Model Development and Verification. Development of the HMA-FM involved determination of three key elements: failure limit, rate of damage, and crack growth law, which are centered on the threshold concept. This concept is based on the observation that micro-damage in asphalt mixtures appears to be fully healable, whereas macro-damage does not appear to be healable (Zhang *et al.*, 2001; Roque *et al.*, 2002). This implies that a damage threshold exists below which damage is fully healable. Once the threshold is exceeded, the developed macro-damage is no longer healable. Therefore, the threshold defines the development of macro-cracks (macro-damage), at any time during either crack initiation or propagation, at any point in the mixture.

As discussed by Zhang *et al.* (2001) and Roque *et al.* (2002), fracture (crack initiation or crack propagation) can develop in asphalt mixtures in two distinct ways: repeated load applications or a single load excursion. An energy threshold or failure limit has then been defined for each distinct fracture mode: dissipated creep strain energy limit and fracture energy limit, respectively. The Failure limits can be obtained from the stress-strain response of an asphalt mixture under a tensile strength test (see Figure 62). The fracture energy limit (FE_f) is determined as the area under the stress-strain curve, while the dissipated creep strain energy limit ($DCSE_f$) is the fracture energy limit minus the elastic energy (EE) at the time of fracture. Resilient modulus (M_R) and tensile strength (S_t) are used to define EE . It is important to point out that these two failure limits ($DCSE_f$ and FE_f) have been identified as fundamental material properties of asphalt mixtures, independent of mode of loading, rate of loading and specimen geometry (Birgisson *et al.*, 2007).

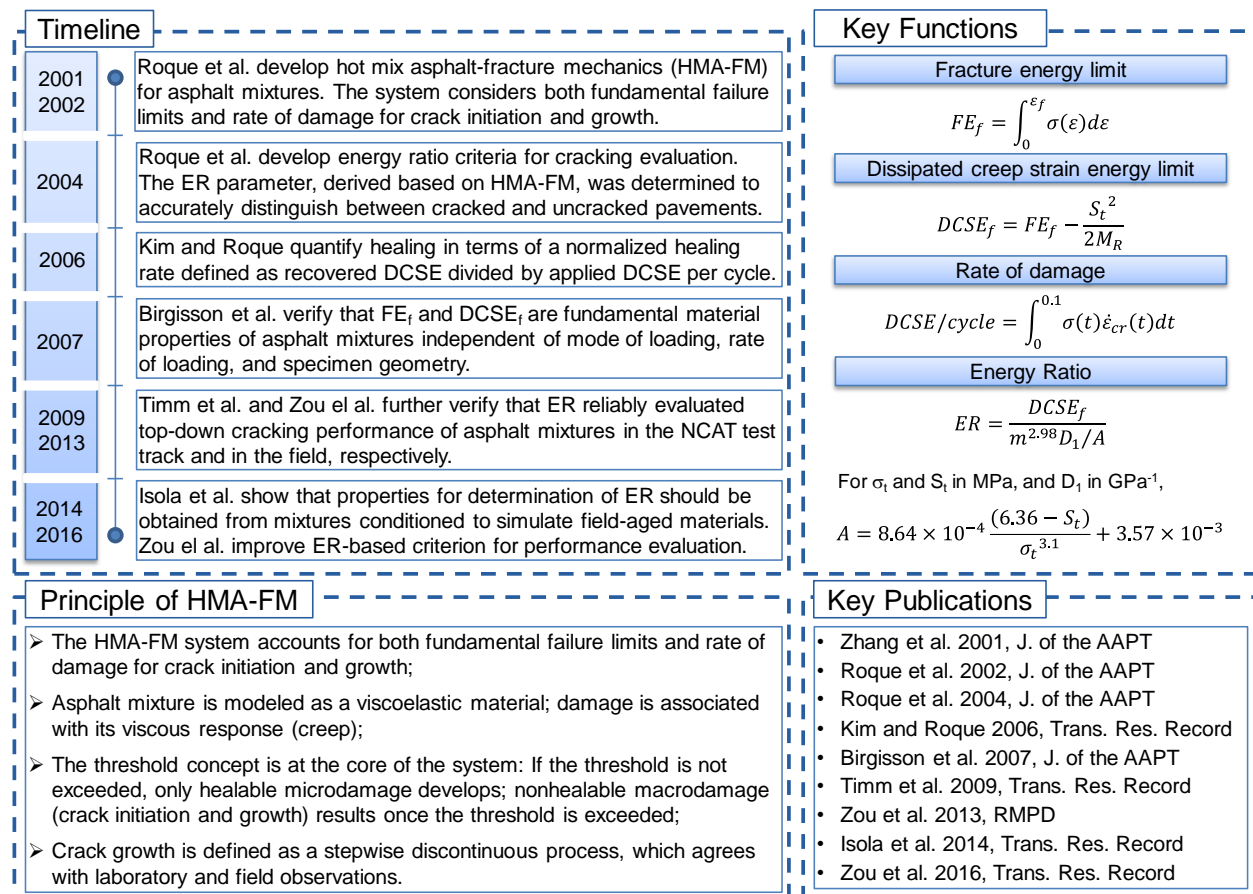


Figure 61. Summary of the HMA fracture mechanics and energy ratio.

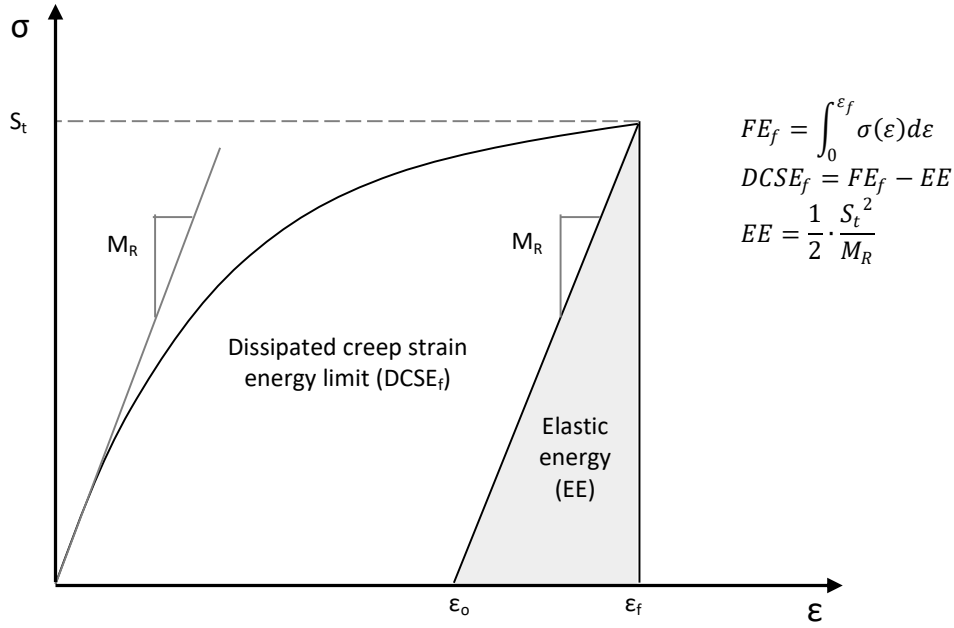


Figure 62. Determination of failure limits in asphalt mixtures.

The rate of damage of an asphalt mixture under repeated load applications is defined as the dissipated creep strain energy accumulated per load cycle ($DCSE/cycle$). Therefore, there is an inherent assumption that damage can be quantified in terms of the viscous response (creep) of asphalt mixture. For a haversine load consisting of a 0.1 second loading period followed by a 0.9 second rest period, which represents a moving wheel in the field, $DCSE/cycle$ is defined as the integral of the stress $\sigma(t)$ multiplied by the creep strain rate $\dot{\epsilon}_{cr}(t)$:

$$DCSE/cycle = \int_0^{0.1} [\sigma(t) \times \dot{\epsilon}_{cr}(t) dt] = \int_0^{0.1} [\sigma_{ave} \sin(10\pi t) \times \dot{\epsilon}_{cr,max} \sin(10\pi t) dt] \quad [118]$$

where σ_{ave} represents the average peak stress in the zone of interest and $\dot{\epsilon}_{cr,max}$ is the maximum creep strain rate, which occurs at the peak stress. The maximum creep strain rate for a haversine load can be estimated from a 1000-second creep test as shown below:

$$\dot{\epsilon}_{cr,max} = \sigma_{ave} \times m \times D_1 (1000)^{m-1} \quad [119]$$

where D_1 and m are the creep compliance power-law fitting parameters.

Substituting Equation [119] into Equation [118] and solving the integral in time for the sinusoidal function, the rate of damage ($DCSE/cycle$) is obtained:

$$DCSE/cycle = \frac{(\sigma_{ave})^2}{20} \times m \times D_1 (1000)^{m-1} \quad [120]$$

It is important to note that a healing parameter termed normalized healing rate and defined as recovered $DCSE/cycle$ over applied $DCSE/cycle$ has been developed to help consider the effect of healing on damage accumulation (Kim and Roque, 2006).

Crack growth in the HMA-FM system is defined as a stepwise discontinuous process (see Figure 63). After a damage accumulation phase, crack initiates when $DCSE$ accumulated in the zone with the highest average tensile stress equals the $DCSE_f$ of the mixture. Next, a potential path where crack growth may be of interest is selected and divided into contiguous zones. Previous analysis showed that zones of variable size had little effect on the predicted rate of crack growth (Sangpetngam, 2003), so zones of fixed size are considered to be appropriate. Typically, a zone size of 6 mm (about one-half of the 12.5 mm NMAS) is used, which is assumed to capture the effect of stress concentration near the contact points between aggregates within the asphalt mixture. After another damage accumulation phase, crack will propagate through the zone in front of the initial crack when the $DCSE$ accumulated



in that zone equals the $DCSE_f$ of the mixture, and so on. Note that the system keeps track of the $DCSE$ induced in all zones at every step of the process. Previous results showed that crack propagation predicted by the system agreed closely with laboratory measurement in terms of crack length versus number of load repetitions (Zhang *et al.*, 2001; Roque *et al.*, 2002).

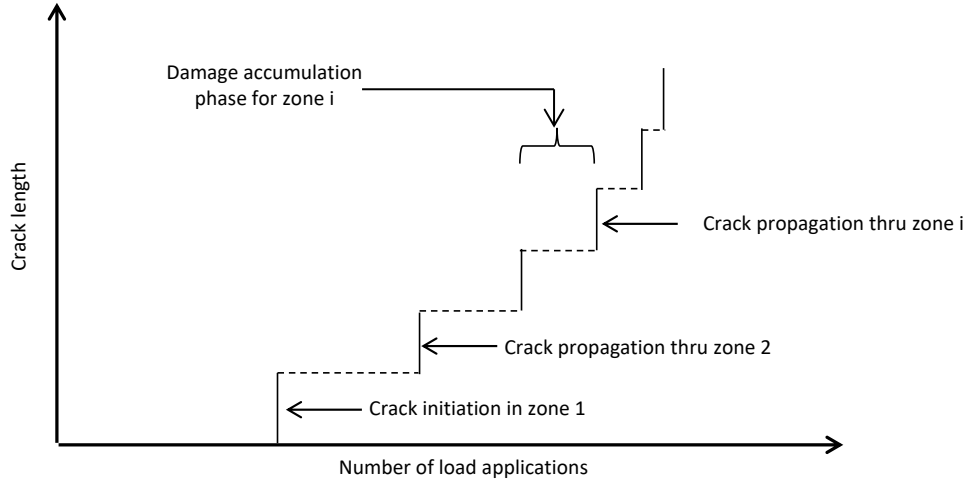


Figure 63. Stepwise discontinuous crack growth law.

The ER is defined as the dissipated creep strain energy limit of the mixture ($DCSE_f$) divided by a minimum dissipated creep strain energy ($DCSE_{min}$):

$$ER = \frac{DCSE_f}{DCSE_{min}} = \frac{DCSE_f}{m^{2.98} \times D_1 / A} \quad [121]$$


where m and D_1 were defined earlier and A is an empirical parameter that depends on the tensile stress in the pavement section (σ_t) and the tensile strength of the mixture (S_t). For σ_t and S_t expressed in MPa, and D_1 in GPa^{-1} , A can be calculated as:

$$A = 8.64 \times 10^{-4} \frac{6.36 - S_t}{\sigma_t^{3.1}} + 3.57 \times 10^{-3} \quad [122]$$

The ER accounts for the effects of material properties ($DCSE_f$, S_t , m , D_1) as well as pavement structural characteristics (σ_t) on cracking performance: the higher the value of the ER , the better the expected cracking performance of the section. All material properties can be accurately determined using Superpave IDT tests following the procedure described by Roque *et al.* (1997). Previously established minimum values of ER (ER_{min}) for adequate cracking performance are (i) 1.0 for ≤ 5 million ESALs, (ii) 1.3 for ≤ 10 million ESALs, and (iii) 1.95 for ≤ 20 million ESALs, which were determined by taking into account the change in pavement structure with varying traffic level (Roque *et al.*, 2004). The ER criteria were evaluated and calibrated using field-aged cores taken from pavements throughout Florida. Recently, Timm *et al.* (2009) and Zou *et al.* (2013) verified that ER reliably evaluated top-down cracking performance of asphalt mixtures in the NCAT test track and in the field, respectively. Therefore, ER can be used to integrate asphalt mixture properties in the pavement design process as well as to evaluate the performance of in-service pavement sections.

It is important to note that mixture properties for determination of ER should be obtained from mixtures conditioned to simulate field-aged materials. Isola *et al.* (2014) have determined that oxidative aging alone using the long-term oven aging (LTOA) procedure does not satisfactorily simulate long-term field aging as reflected by mixture failure limits. This work showed that cyclic pore pressure conditioning (CPPC) of mixture is required after LTOA to more properly simulate field aging. In addition, ER should not be used to evaluate brittle mixtures as reflected by a $DCSE_f$ lower than 0.75 kJ/m^3 (Roque *et al.*, 2004).

Related Modeling Efforts and Applications. Implementation of the HMA-FM was conducted along two main directions: (i) use of the ER parameter and associated criteria for performance evaluation of laboratory-compacted



mixtures and mixtures compacted and served in the field (i.e., field cores); and (ii) Development and integration of mixture property models and damage models into the HMA-FM framework to form a top-down cracking prediction model for use in pavement performance evaluation and in pavement design to mitigate top-down cracking.

Along the first direction, the *ER* has been employed to evaluate the effect of Reclaimed asphalt pavement (RAP) and the effect of lime-modification on mixture performance, respectively. Kim *et al.* (2009) conducted Superpave IDT tests on RAP mixtures with polymer-modified binder fabricated containing different RAP contents (0%, 15%, 25%, and 35%). Interestingly, *ER* results showed that 25% and 35% RAP mixtures exhibited slightly better performance due to lower creep compliance rates. Yan *et al.* (2016) evaluated cracking performance of RAP mixtures designed with polymer-modified binder, two RAP sources, and high RAP contents up to 40%. After being conditioned using the LTOA plus CPPC procedure to simulate long-term field aging, all RAP mixtures still exhibited *ER* values higher than the minimum *ER* requirement, indicating acceptable cracking performance. So, it was concluded that up to 40% RAP was acceptable for well-designed polymer-modified asphalt mixtures. In addition, Zou *et al.* (2016) improved equivalent performance (*ER*) criterion and assessed impact of hydrated lime (HL) on cracking performance of asphalt mixtures for a range of aggregate types including granites and limestones. Results showed that granite control mixtures known to be moisture-susceptible failed to meet the minimum *ER* requirement, while limestone control mixtures exhibited *ER* values higher than the minimum requirement. Introduction of HL appeared to mitigate detrimental effects of oxidation and moisture on damage and fracture-related properties of both granite and limestone mixtures. This effect resulted in better cracking performance for the same design AC layer thickness, or lower cost to achieve the same level of good performance.

While the *ER* is important for performance evaluation of field cores or laboratory-compacted specimens conditioned to simulate field aging, a performance prediction model capable of predicting the onset of cracking and crack growth rate is needed to better assist material and pavement engineers to optimize their designs. Therefore, significant efforts were used along the second direction. As part of the NCHRP Project 1-42A (Roque *et al.*, 2010; Zou and Roque, 2011), a top-down cracking prediction model was formed by integrating material property models developed to consider changes in properties with aging (including failure limits, rate of damage, and healing potential) and a damage model created to address the effect of transverse thermal stresses (in addition to the effect of load-induced stresses) on top-down cracking. A damage recovery and accumulation procedure was implemented in the model to address the combined effects of aging and healing on cracking performance, which was developed based on results of analysis and evaluation of full-scale tests conducted using HVS (Zou *et al.*, 2012). The model was calibrated and validated using data from 11 field sections in Florida (Roque *et al.*, 2010). Furthermore, the accuracy of the model was verified through long-term field evaluation and analysis of top-down cracking for 10 additional Florida field sections (Zou *et al.*, 2013).

6.2.3. Ratio of Dissipated Energy Change Method

Overview. The Ratio of Dissipated Energy Change (*RDEC*) approach is an energy based approach developed to characterize the fatigue performance of asphaltic materials. The *RDEC* approach and its former Dissipated Energy Ratio (*DER*) approach was developed and refined by Ghuzlan and Carpenter (2000) based on the work done by Carpenter and Jansen (1997) and built on the work done by other researchers (Hopman *et al.*, 1989; Pronk and Hopman, 1991; Rowe, 1993) on dissipated energy. An overarching timeline of the approach development, the key functions, and the key publications are summarized in Figure 64.

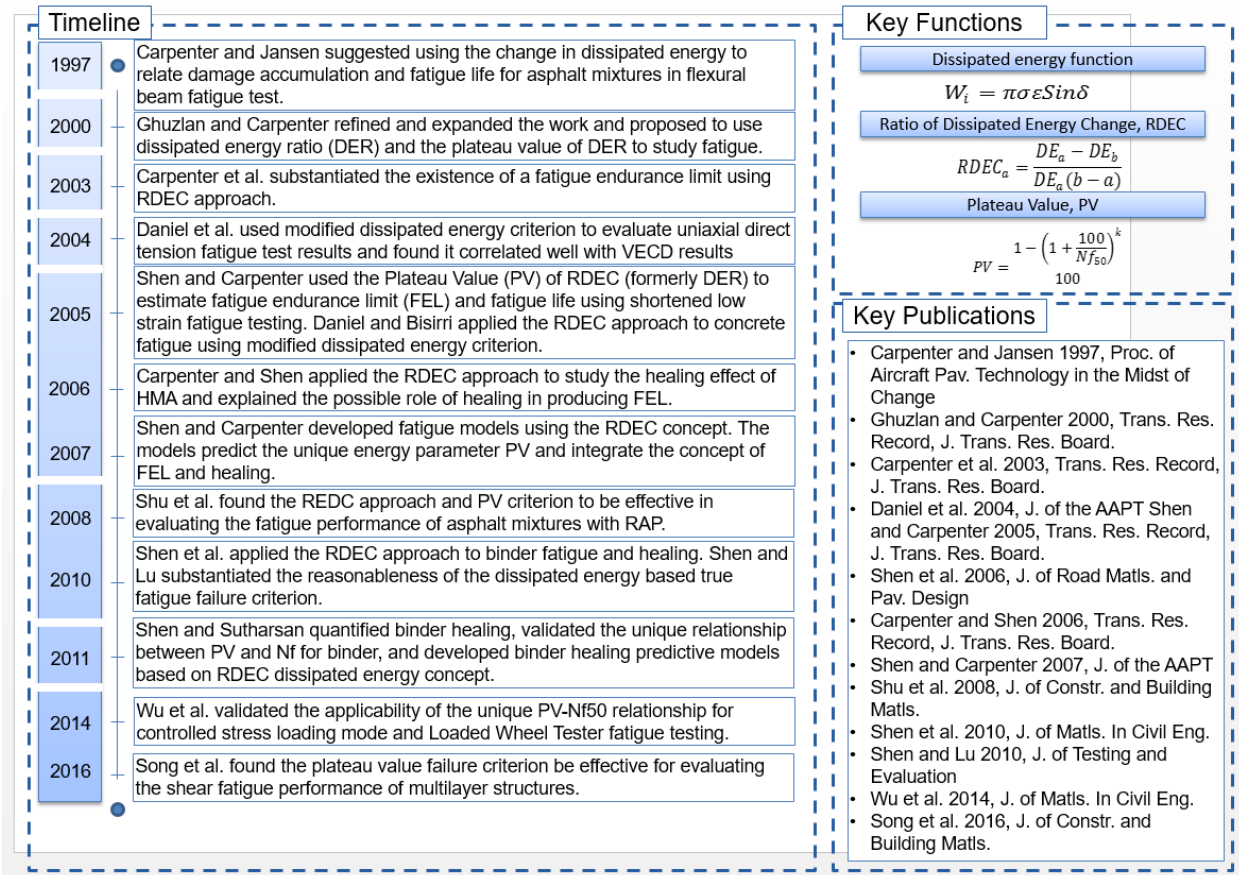


Figure 64. Summary of the RDEC approach development.

The RDEC approach acknowledges that during a cyclic fatigue test the stress-strain hysteresis loop of later load cycles do not overlap the previous ones and the area of the loops have changed, as shown in Figure 65. By investigating the change of the dissipated energy during cyclic fatigue tests, it confirms that not all the dissipated energy is responsible for material damage. For each cycle, the loss of energy due to material mechanical work and other environmental influence remains almost unchanged. If the dissipated energy starts to change dramatically, it indicates a sign of damage development. In other words, the RDEC approach believes it is the change of the dissipated energy, not the dissipated energy itself that should be used to relate to the fatigue damage of asphalt materials.

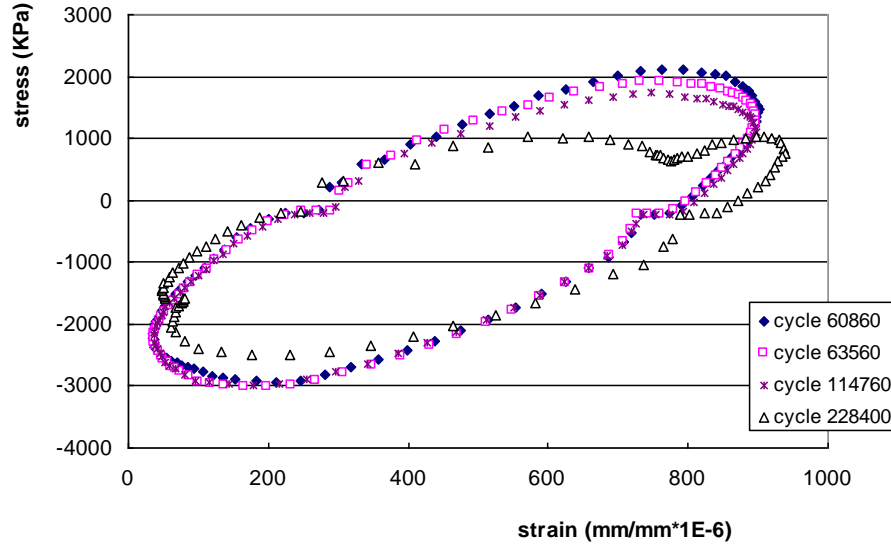


Figure 65. Different Stress-Strain Hysteresis Loops (Different Load Cycles) for the Same Mixture (Shen 2006).

The *RDEC* is defined as a ratio of the change in dissipated energy between two cycles divided by the dissipated energy of the first cycle:

$$RDEC_a = \frac{DE_a - DE_b}{DE_a (b - a)} \quad [123]$$

where; a, b = loading cycle a and b , respectively, $RDEC_a$ = the average ratio of dissipated energy change at cycle a , comparing to cycle b , DE_a and DE_b = dissipated energy at cycle a and b , respectively, which were calculated directly by fatigue testing program or be calculated using Equation [124], kPa.

$$W_i = \pi \sigma \varepsilon \sin \delta \quad [124]$$

where; W_i = dissipated energy at cycle i , σ_i = stress level at cycle i , ε_i = strain level at cycle i , and δ_i = phase angle at cycle i . A typical *RDEC* vs. loading cycle curve can be seen in Figure 66. The curve can be divided into three distinct stages. Of interest is Stage II, during which the *RDEC* data maintain at a relatively constant level, called Plateau Value (*PV*). The plateau stage represents a period during which there is a constant percentage of input energy being turned into damage. The plateau value (*PV*) appears to be related to mixture and load or strain input. For any one mixture the *PV* is a function of the load inputs, and for similar load inputs, the plateau value is different for different mixtures.

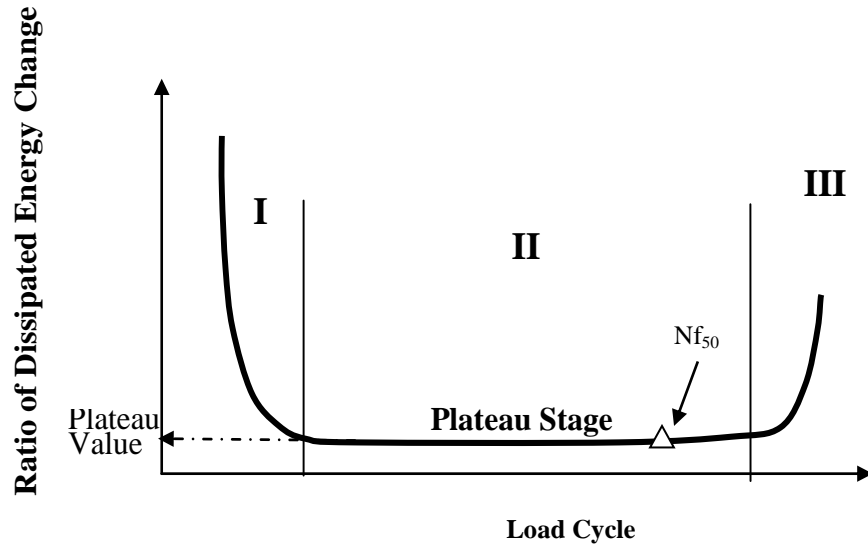


Figure 66. Typical RDEC Plot with Three Behavior Stages (Carpenter *et al.* 2003).

The benefit of this approach over alternatives such as cumulative dissipated energy approach is that it excludes other components of the energy that are dissipated throughout a cyclic fatigue test such as thermal energy, but only concentrates on the dissipated energy that is responsible for damage. The method also maintains the inherent simplicity of the other energy based methods making it arguably simpler to use than other sophisticated mechanical fatigue models. Since the plateau stage commences relatively quicker than the defined fatigue failure and the *PV* value is unique for specific mixture and loading level, it has been utilized to study the low load-level fatigue behavior such as fatigue endurance limit with shortened tests (Carpenter *et al.*, 2005). The *PV* value as a characteristic parameter that is influenced by the material type and load levels (stress or strain levels, with or without rest periods) can be fundamentally utilized to characterize the fatigue performance of an asphalt mixture or binder under various loading conditions.

Plateau Value Determination. The determination of the *PV* value from experimental fatigue data is sometimes difficult and cumbersome due to the large variation of the fatigue data, as shown in the Figure 67 example plot. Therefore, Carpenter and Shen (2006) proposed to practically use the *RDEC* value at the 50% stiffness reduction point as the *PV* value since (a) this value is always within the plateau stage, (b) a fixed definition will reduce the random error due to data processing.

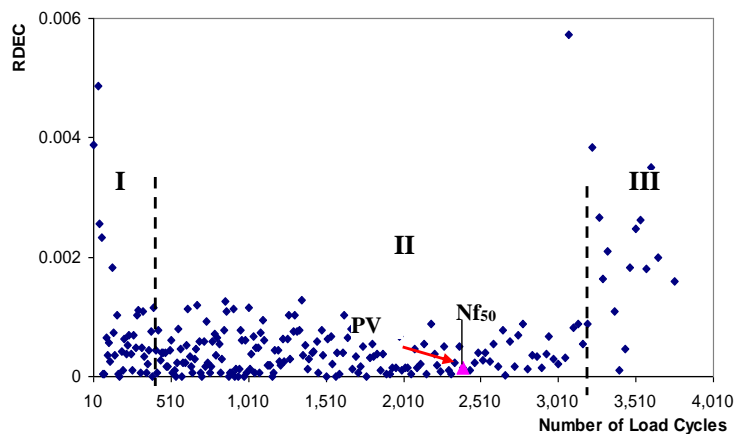


Figure 67. Example plot of the *RDEC* vs. loading cycles relation and the indication of *PV* from fatigue testing (Carpenter and Shen, 2006).



The general procedure to perform *RDEC* analysis and obtain the *PV* from the fatigue tests have been provided by Carpenter and Shen (2006). It involves obtaining the dissipated energy (*DE*) vs. loading cycle (*LC*) curve and determining the exponential slope *k* of the *DE*-*LC* curve during the plateau stage (the stage when the change of *DE* is relative constant) by fitting the curve using power law regression (Figure 68). Hence, the *PV* value defined as the *RDEC* value at the 50% stiffness reduction failure point (*Nf*₅₀) can be calculated using Equation [125].

$$PV = \frac{1 - \left(1 + \frac{100}{Nf_{50}}\right)^k}{100} \quad [125]$$

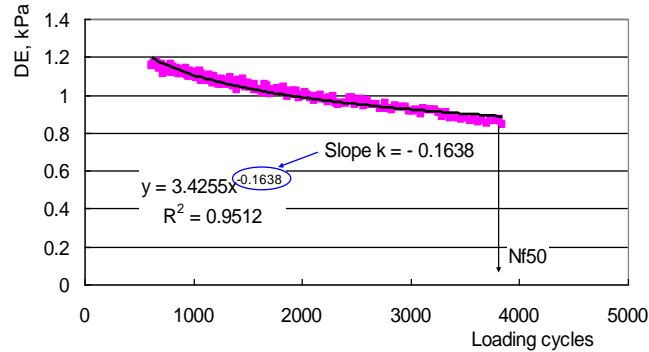


Figure 68. Example of determining the exponential slope of the fitted *DE*-loading cycle for *PV* calculation (Carpenter and Shen, 2006).

The *PV* is a comprehensive damage index that contains the effects of both material property and loading conditions and hence can be a fundamental energy parameter to represent HMA fatigue behavior (Carpenter and Shen, 2005). For a strain-controlled test, the lower the *PV*, the longer the fatigue life for a specific HMA mixture (Shen and Carpenter, 2005). A low *PV* value can be found either in high fatigue resistant materials, low external loading amplitude, or both.

Fatigue Failure Criteria. Carpenter *et al.* (2003) demonstrated that the *DER* (or *RDEC*) provides a true indication of the damage being done to the mixture from one cycle to another as a function of how much dissipated energy was involved in the previous cycle. Different loading conditions will produce different dissipated energy hysteresis curves. Because damage is the difference in dissipated energy, this ratio clearly illustrates the percentage of the input dissipated energy that goes into damage for a cycle. Ghuzlan and Carpenter (2000) proposed that when the *RDEC* starts to increase dramatically at the end of the plateau stage as shown in Figure 65, the corresponding load cycle at the transition between the second and the third stage is related to the initiation of unstable macrocrack propagation, defined as true fatigue failure. Such failure criterion is considered more fundamental than the arbitrary *Nf*₅₀ (i.e., the load cycle at 50% initial stiffness reduction) criterion (Carpenter *et al.*, 2003; Shen and Carpenter, 2005; Ghuzlan and Carpenter, 2006). In a later study of comparing the various fatigue failure criteria, by analyzing fatigue test data for both asphalt binder and mixtures, Shen and Lu (2010) demonstrated that the true failure defined by the *RDEC* approach has good correlation with other dissipated energy defined failure criteria such as *Np*₂₀ by Bonnetti *et al.* (2002) as well as the traditional *Nf*₅₀ definition.

Daniel *et al.* (2004) proposed a modified dissipated energy failure criterion, which defines failure at the point where the dissipated energy ratio just starts to increase above the plateau value. They further presented a comparison of the viscoelastic continuum damage (VECD) and dissipated energy (*DE*) approaches using uniaxial direct tension fatigue tests performed on eight WesTrack mixtures. The two approaches were also compared to the traditional phenomenological approach using the number of cycles to 50% initial stiffness reduction as failure criterion. Their work indicated that the number of cycles to failure calculated using the VECD and *DE* failure criterion are highly correlated and are very similar if a modified *DE* failure criterion is applied. It also showed that the *DE* approach had promise for ranking the field performance of the mixtures; however limited data at different strain amplitudes made it difficult to state any conclusions with confidence.



PV-Nf relationship. Shen and Carpenter (2005) further substantiated that the relationship between PV and Nf_{50} to be fundamental in that it is independent of loading levels (normal or low damage level), loading modes (controlled stress or controlled strain), mixture types, and testing conditions (frequency, rest periods, etc.). The established $PV-Nf_{50}$ relationship is presented in Equation [126]. Later many literatures (Shen *et al.*, 2010; 2011; Wu *et al.*, 2014; Nejad *et al.*, 2015) confirmed the reasonableness of such unique $PV-Nf$ relationship, and found the equation to be similar.

$$PV = 0.4428Nf_{50}^{-1.1102} \quad [126]$$

Application of RDEC Approach in Fatigue Analysis.

The *RDEC* approach was further applied to study the fatigue, fatigue endurance limit, and healing of asphalt binder and mixtures. It was also demonstrated as a fundamental and effective approach for fatigue analysis by later researchers through extending it to various materials and different fatigue test methods.

Fatigue Endurance Limit (FEL). The study of fatigue endurance limit for asphalt mixtures usually rely on low damage level fatigue tests. The fatigue lives of the tested samples at those low damage levels can be extremely long and the traditional 50% initial stiffness reduction failure points are not reached within testing time as long as 48 million repetition. Based on the *RDEC* analysis, Shen and Carpenter (2005) validated the existence of a fatigue endurance limit in asphalt mixtures below which the asphalt mixture can have an extremely long fatigue life. Depending on the mix type, the fatigue endurance limit can vary from 70-350 microstrain based on traditional fatigue analysis. However, the *RDEC* analysis suggests there is a unique energy level, defined as the energy based fatigue endurance limit PV_L , which is the onset of the fundamental change in HMA fatigue behavior at a breakpoint fatigue life of around 1.1×10^7 . If the energy level of a HMA mixture is below the PV_L due to the combination effect of material resistance and external load, the mixture is expected to have extended long fatigue life. According to the study by Shen and Carpenter (2005), this critical PV_L value is 6.74×10^{-9} . By comparing the fatigue endurance limits obtained from several methods, Prowell *et al.* (2010) found that the *RDEC* approach may overestimate fatigue life and shift factors may be required in this case.

Fatigue and Healing. Carpenter *et al.* (2003; 2006) used the *RDEC* approach to study and examine the role of healing in HMA fatigue behavior and its significance for the existence of a FEL. By introducing rest periods into cyclic loading, the PV value is reduced, indicating an extended fatigue life and an improved fatigue performance. Results show that the *RDEC* approach is effective for evaluating the healing effect of HMA material and its role in perhaps producing the FEL. Based on dissipated energy concept, Shen and Carpenter (2007) established a fatigue model for PV , which also integrated the effect of rest periods on fatigue. Such energy based fatigue model has the ability to utilize existing pavement response values with mixture properties to generate the $PV-Nf$ relationship validated in the *RDEC* analysis, and the future capability of directly utilizing viscoelastic pavement responses when these structural models are integrated into a pavement analysis procedure (Shen 2006). The *RDEC* approach is further extended to study the fatigue and healing behavior of asphalt binder (Shen *et al.* 2006, 2010; Shen and Sutharsan, 2011) and found the $PV-Nf_{50}$ relationship is still valid for asphalt binder, with and without rest periods.

Asphalt Mixtures Containing RAP. The plateau value failure criterion was applied to evaluate the fatigue performance of HMA mixtures containing different percentages of RAP, along with a number of other popular fatigue evaluation approaches such as IDT test, SCB test, and the $DCSE_f$ from the IDT test (Shu *et al.*, 2008; Huang *et al.*, 2011). The studies noted that the PV and the $DCSE_f$ from the IDT test are more reasonable in evaluating the fatigue performance of HMA mixtures containing RAP. Generally, the inclusion of RAP and long-term aging increased the PV , and thus decreased the fatigue life. Both IDT and SCB tests gave highly consistent ranking for the mixtures but showed difficulty in determining the overall effect of RAP on the fatigue resistance of the mixture.

Fatigue Test Methods. The *RDEC* approach was originally developed based on the four-point bending flexural fatigue test for asphalt mixtures following AASHTO T321 or ASTM D7460. It was later applied to a number of testing methods including two-point bending fatigue test (Maggiore *et al.* 2014), loaded wheel tracking (LWT) fatigue test (Wu *et al.*, 2014), and dynamic shear rheometer (DSR) test for asphalt binder (Shen *et al.*, 2006; 2010; Shen and Sutharsan, 2011). The $PV-Nf_{50}$ relationship was found to be still valid. In other words, the $PV-Nf_{50}$ relationship is fundamental and unique also for different testing methods.



Other Applications. Daniel and Bisirri (2005) applied the DER (a former version of RDEC) to evaluate the fatigue performance of both asphalt concrete and Portland cement concrete mixtures. It was found that the number of cycles to failure determined from the dissipated energy approach using a modified failure criterion agreed well with the values determined from a fundamental viscoelastic VECD approach for asphalt concrete, and agreed well with those predicted using three different fatigue models for Portland cement concrete. The study suggested that DER approach is a promising method for characterizing the fatigue behavior of concrete materials. Song *et al.* (2016) used *RDEC* concept to evaluate fatigue resistance of composite pavement (open-graded friction course and underlying layers). It was concluded that the plateau value failure criterion appeared effective for evaluating the shear fatigue performance of multilayer structures.

6.2.4. Asphalt Concrete Pavement-Fatigue Model

Overview. An overall summary of the ACP-F model is shown in Figure 69. The ACP-F model is based on the assumption that fatigue crack initiation damage processes are strongly related to the dissipated energy during a load cycle. The existence of such a relationship between dissipated energy and fatigue damage was already presented by Van Dijk and Visser at the AAPT conference in 1977. Hopman, Kunst and Pronk introduced the dissipated energy ratio (the accumulated dissipated energy up to cycle N divided by the dissipated energy in cycle N) at the 4th Eurobitume Symposium in 1989 as a tool for the determination of the fatigue life N1 in both deflection and force controlled fatigue tests. A follow up was a paper by Pronk and Hopman at the ICAP conference in 1990 in London using composed sinusoidal loadings. During the ninety's, several reports were published based on the dissipated energy concept (Pronk, 1995). However, the problem remains that a homogenous stiffness distribution was assumed during the whole deflection controlled fatigue test.

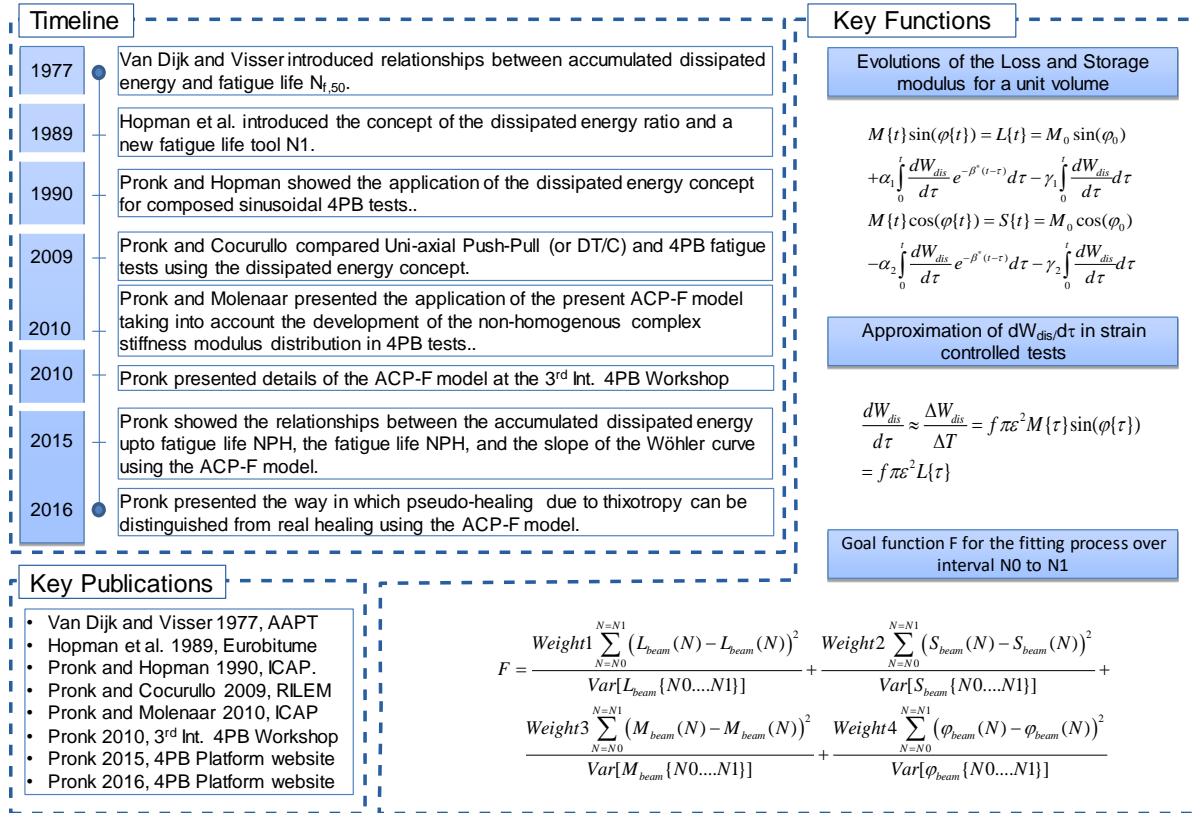


Figure 69. Summary of the ACP-F model.

Thus the influence of the non homogenous strain distribution as in a Four Point Bending (4PB) test was ignored. Nevertheless excellent fittings were obtained for the evolutions of both the beam stiffness modulus and beam phase lag (Di Benedetto *et al.*, 2001). Later on the linear decrease of the strain amplitude from the maximum value at the surface of the beam to nil at the centre line was taken into account (Pronk and Cocurullo, 2009). At that time it was still assumed that the complex stiffness modulus distribution in the outer sections of a 4PB test did not

have a big influence on the weighted complex stiffness modulus response for the whole beam. At the ICAP Conference in 2010 Pronk and Molenaar compared the Uni-axial Push-Pull (UPP) or Dynamic Tension/Compression (DT/C) fatigue tests and 4PB tests using an Excel program in which the correct weighting of the complex stiffness modulus over the whole 4PB specimen was applied (Pronk, and Molenaar, 2010). A new fatigue life definition N_{PH} was also introduced. The ACP-F model explains very well the findings of Van Dijk for the relationship between the accumulated dissipated energy and the fatigue life. In addition this fatigue life agrees strongly with the definition proposed by Rowe (see Section 6.2.1) with the exception that the cycles should be raised to a power of 0.6 before multiplying by the loss modulus. At the 3rd 4PB international workshop in 2010, details were presented on how to integrate the complex stiffness modulus distribution in a 4PB specimen for the determination of the measured response in practice. A quarter of the beam was divided in $10 \times 10 + 1 \times 10$ elements (Figure 70). Each element was considered as a unit volume with a certain strain value and complex stiffness modulus.

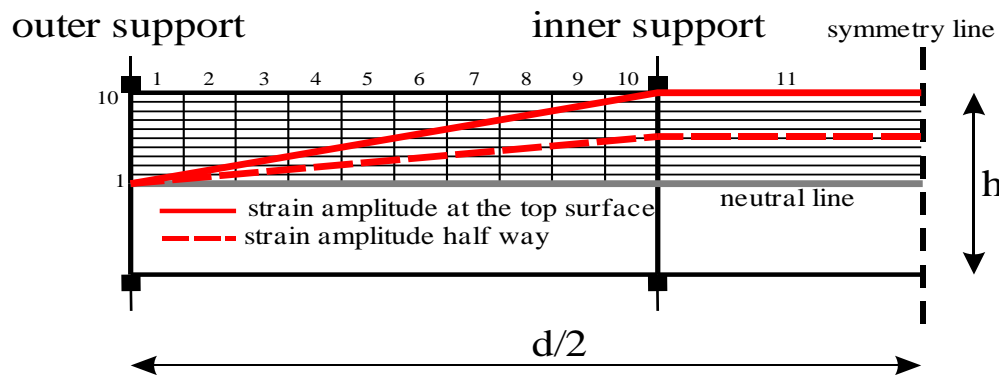


Figure 70. Localization of integration elements for analysed 4PB beam for calculation of the summary answer.

It should be noted that the ACP-F model describes the evolutions of the complex stiffness modulus (modulus and phase lag) in a strain controlled single sinusoidal fatigue test taken into account the reversible thixotropic behaviour of bitumen and (irreversible) fatigue damage. Restoration of the complex stiffness modulus during a rest period (or periods with a lower strain amplitude) can be calculated. However, this is a recovery process due to the thixotropic behaviour (Partial Healing) and not healing of the fatigue damage during real rest periods and is not incorporated in the present model. At the other hand the model takes into account the possible existence of an endurance strain level. When the strain amplitude in a location of the 4PB specimen is below this level, no fatigue damage occurs at that location.

Model Development. In case of a strain controlled sinusoidal fatigue test the two evolutions for the loss and storage modulus can be solved analytically, Equations [127] and [128]. These functions are used for a fit of the measured response on the interval of $N_0 = 300$ and N_1 cycles. N_1 is defined as the number of cycles at which the dissipated energy ratio starts to deviate from a straight line.

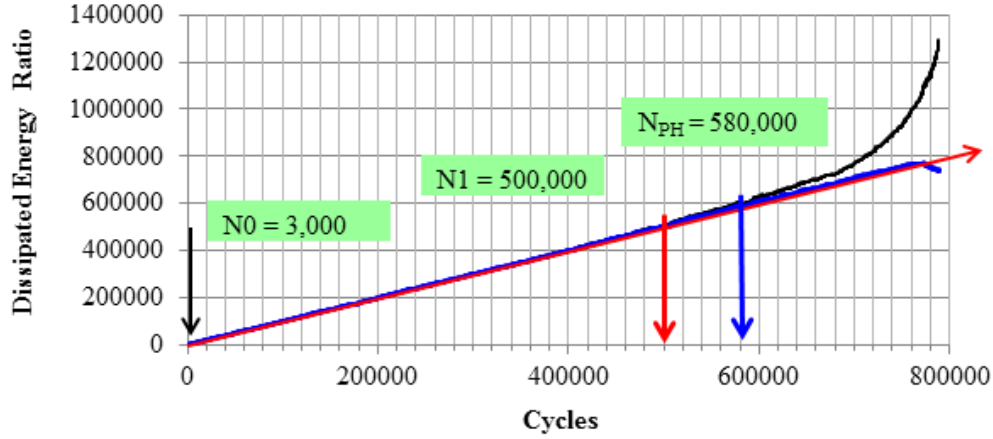


Figure 71. The dissipated energy ratio as a function of the cycle number N .

$$L\{t\} = M\{t\} \sin(\varphi\{t\}) = M_0 \sin(\varphi_0) e^{-Bt} (\cosh(Ct) + D \sinh(Ct)) \quad [127]$$

$$S\{t\} = M\{t\} \cos(\varphi\{t\}) = M_0 \cos(\varphi_0) - M_0 \sin(\varphi_0) \left[\frac{\alpha_2^*}{C} e^{-Bt} \sinh(Ct) + \frac{\gamma_2^*}{\gamma_1^*} (1 - e^{-Bt} [\cosh(Ct) + E \sinh(Ct)]) \right] \quad [128]$$

$$\text{In which } B = \frac{\beta^* - \alpha_1^* + \gamma_1^*}{2}, C = \sqrt{B^2 - \beta^* \gamma_1^*}, D = \frac{\beta^* + \alpha_1^* - \gamma_1^*}{2C}, E = \frac{\beta^* - \alpha_1^* - \gamma_1^*}{2C}. \quad [129]$$

$$\begin{aligned} \alpha_1^* &= \pi f \alpha_1 \varepsilon^2 = \pi f Tg \alpha_1 \varepsilon^3; \alpha_2^* = \pi f \alpha_2 \varepsilon^2 = \pi f Tg \alpha_2 \varepsilon^3; \beta^* = \beta \varepsilon^2; \\ \gamma_1^* &= \pi f \gamma_1 \varepsilon^2 = \pi f Tg \gamma_1 \varepsilon^{2+p} (\varepsilon - \varepsilon_{endurance}); \gamma_2^* = \pi f \gamma_2 \varepsilon^2 = \pi f Tg \gamma_2 \varepsilon^{2+p} (\varepsilon - \varepsilon_{endurance}) \end{aligned} \quad [130]$$

The coefficient p is defined as the (lower) integer value of the slope for the Wöhler curve $N=k_1 \varepsilon^{k_2}$ obtained by plotting $N1$ (or $N_{f,50}$) values as a function of the strain amplitudes on a log-log scale. It should also be mentioned that there exists a relation with the Plateau Value (PV) definition (see Section 6.2.3). The PV value is equal to the difference in the quantities B and C ($B-C$). This difference is in return strongly related to the parameter γ_1^* . The final (fitted) parameters in the ACP-F model are given by:

- The initial values for the modulus (M_0) and the phase lag (φ_0).
- The parameters $Tg \alpha_1$, $Tg \alpha_2$ and β for the thixotropic phenomenon.
- The parameters $Tg \gamma_1$, $Tg \gamma_2$ and the endurance limit $\varepsilon_{endurance}$ for the fatigue.

The predecessor to the ACP-F model was the Partial Healing (PH) model, which was only used to fit the measured responses (loss and storage modulus) for the tested specimen as a whole ignoring a possible non homogenous stress-strain distribution within the specimen. This approach is only correct for UPP (or DT/C) tests for which in principle a homogenous strain distribution exists. Unfortunately a homogenous strain distribution in UPP tests is hard to keep constant. Measuring at three locations with e.g. LVDT's the mean value can be kept constant easily but the three individual values may differ more than a factor of two. Many fatigue tests are carried out using the Four Point Bending (4PB) device. When using a strain controlled sinusoidal 4PB fatigue test at low frequencies (≤ 10 Hz), the strain amplitude distribution within the beam is quite simple (see Figure 70) and mass inertia effects can be neglected in the calculations for the response of the beam. An Excel program is made in which a quarter of the beam is simulated by 110 elements each having its own complex stiffness modulus. The section between the outer support and the inner support is divided into $10 \times 10 = 100$ elements. The section between the inner support and the centre of the beam is divided into $10 \times 1 = 10$ elements. Each element gets its characteristic strain amplitude. Starting with seed values for the parameters involved, the evolution for each element of the (material) loss and storage modulus can be calculated for each cycle. Then the weighted mean stiffness modulus is calculated for the 10 elements above each other (column). Using the general static solution for a bent beam, the response for the whole

beam can be determined for each cycle. This simulation is validated using known loss and storage modulus distributions for which an analytical solution could be determined.

Remarks. Some specific remarks with respect to the ACP-F model.

- In practice 4PB tests are carried out in controlled deflection mode. This is not equal to a strain controlled mode. The induced error is in the order of a few percent. A real strain controlled 4PB fatigue test can only be achieved by using the deflection difference between the centre and one of the inner supports as the control parameter. However, this value is around 7 times lower than the centre deflection. From this point of view the deflection measure using a “bridge” with supports at $x = L/6$ and $5L/6$ has some advantages while it takes already into account a lower decrease in stiffness modulus of the material in the two outer sections.
- In general all the weight factors in the goal function are set to one. However, when problems arise with the phase lag determination it is advised to use more weight for the stiffness modulus values. The positive sign for the first integral in the equation for the evolution of the loss modulus seem odd, but in practice it can occur that at the start of a fatigue test the increase in phase lag has more impact than the decrease in stiffness modulus (see Figure 72).
- The starting point N_0 of the fit interval is taken equal to 5 minutes. In this way the changes in the stiffness modulus due to temperature increase are partially eliminated.
- The value N_1 for the end of the fit interval is always lower than the traditional fatigue life definition $N_{f,50}$.
- In general the fatigue life N_{PH} , which is defined as the number of cycles at which the dissipated energy ratio according to the fitted ACP-F model starts to deviate from the measured value, is also lower than $N_{f,50}$. However, recently a mix was evaluate in which the initial drop in stiffness due to thixotropy was so high that N_{PH} was much bigger than $N_{f,50}$.

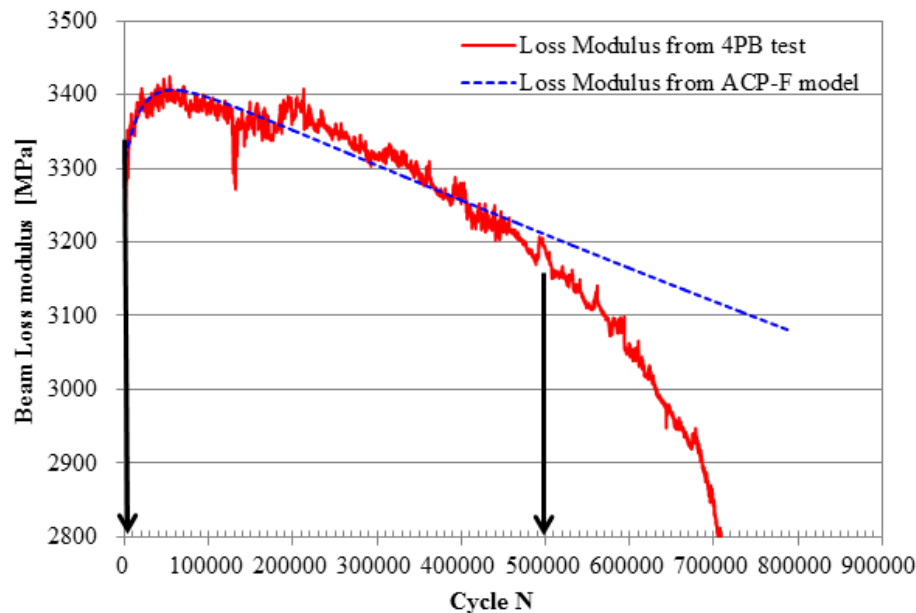


Figure 72. Comparison of the evolutions for the beam loss modulus L_{beam} according to the model (dashed yellow line) and the measured values (red line).

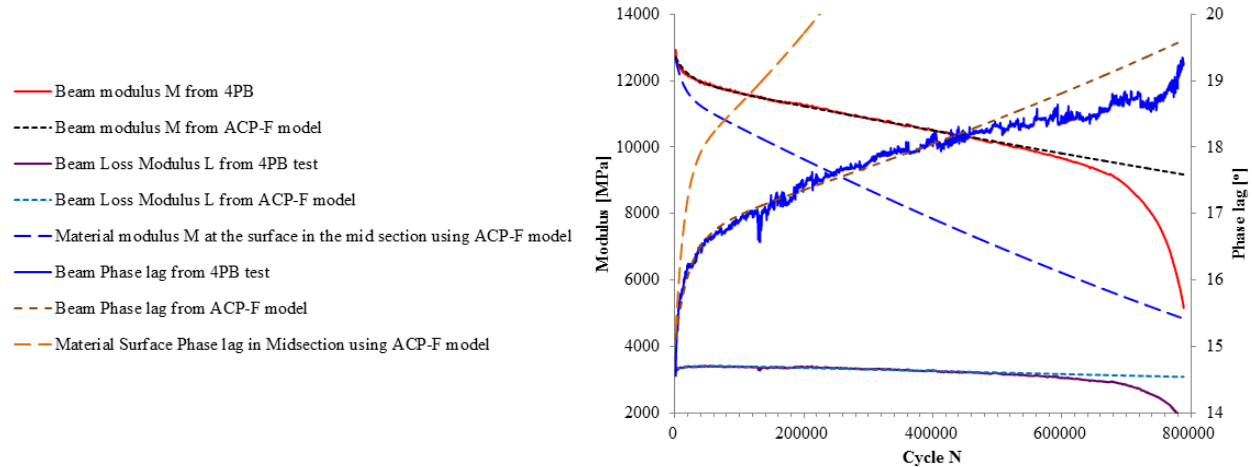


Figure 73. Comparison of measured and fitted values. Notice that at $N = 580,000$ cycles also the deviations between measured values fitted values start for the beam phase lag ϕ_{beam} and the beam stiffness modulus M_{beam} .

6.3. Continuum Damage Methods

Continuum damage mechanics is a branch of mechanics arising from the need to describe the change in continuum properties of materials under load levels less than the ultimate strength of that material. The initial development of the theory is largely attributed to a series of papers in the late 1950's, first by Murzewski (1957) who used the method to describe the probabilistic degradation of cohesion in a mechanical body and soon after by Kachanov (1958) and Rabotnov (1959) which used a similar approach to study material degradation under uniaxial creep loads. These latter two papers also proposed the concept of a damage parameter that would describe the underlying structural causes of the degradation in properties. The theory was further developed and improved upon during the 1960's, but gained real popularity in the 1970's and 1980's due to numerous and parallel international efforts (Lemaitre and Chaboce, 1978; Murakami, 1983; Krajcinovic, 1984). The essential concepts of this branch of mechanics are that a material initially exists as a whole and continuous body, but that under loading this body undergoes "damage" in the form of first initiation of microcracks or other disruptions in the undamaged body and then the nucleation and propagation of these defects until a point when the deformation of the body is dominated by one or more of these damage areas, known as localization. At this point the body is no longer continuous and the rigorous application (rigor here refers to mathematical rigor) of this theory begins to break down.

The benefits of this approach over alternatives such as fracture mechanics or micromechanics is that many of the complications associated with describing and then considering the probabilistic behaviors of local defects and flaws can be ignored. Instead these individual sub-macro scale damage behaviors are smeared into state variable terms that reflect the influence of these flaws on the macroscale behaviors. Since this smearing often permits adherence to other continuum concepts, the approach can often provide an accurate and general representation of the material properties for structural analysis. As a result they are quite useful in efficiently predicting how asphalt concrete behaves in a pavement structure. This benefit is also one of the limitations of this approach since oftentimes it is necessary to understand the sub-macro scale behaviors in detail order to gain insights that help the engineering of the macroscale. Since continuum damage approaches incorporate the net effect of all of these flaws into state variables the influence of material factors (asphalt content and type, air void content, gradation, etc.) must be empirically determined. There are several different continuum damage approaches that have been developed for asphalt concrete. These approaches share many similarities, but some important differences.

6.3.1. Viscoelastic Continuum Damage Model

Overview. The viscoelastic continuum damage (VECD) model and the closely related simplified viscoelastic continuum damage (S-VECD) model are based on Schapery's theoretical work – first his work on viscoelastic fracture and later his work on distributed damage (Schapery, 1981; 1997; 1999). Figure 74 presents an overarching timeline of the development of the model, its key elements, and its associated literature.

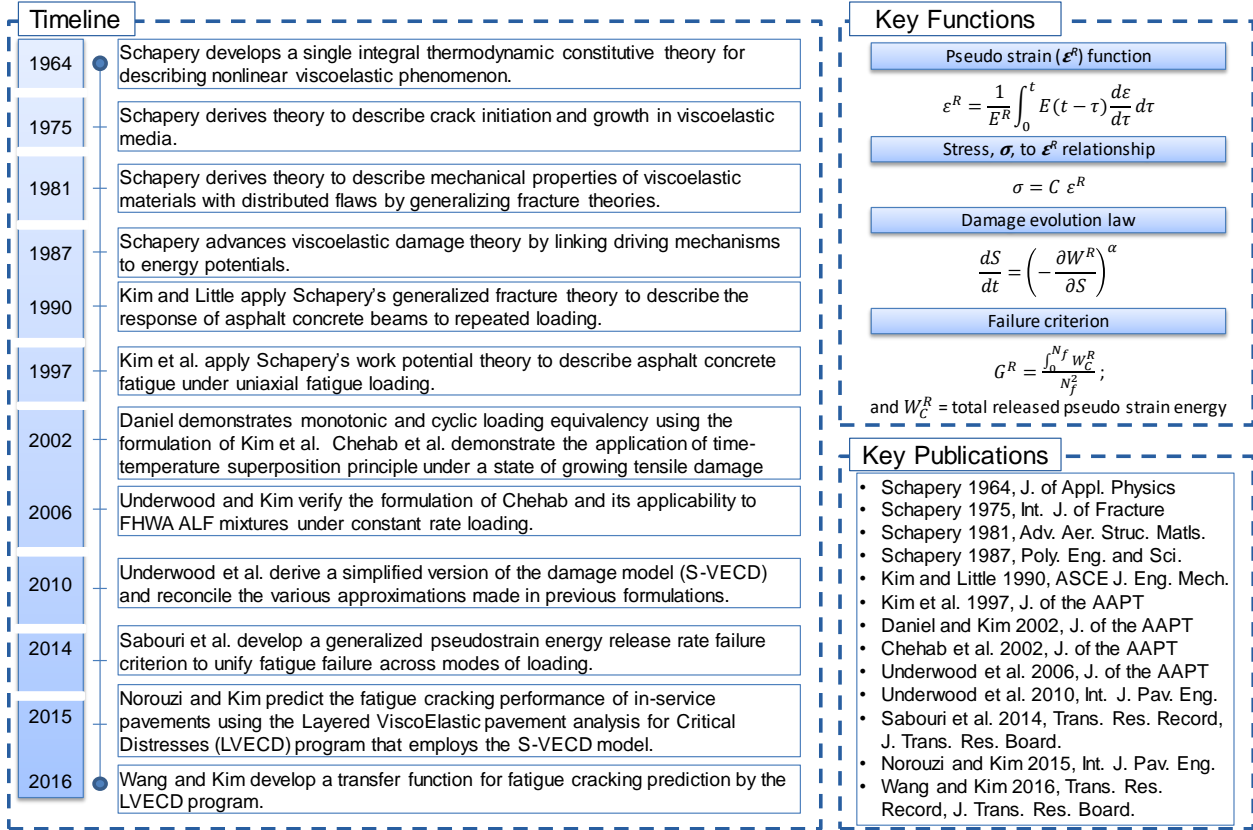


Figure 74. Summary of the VECD model.

As demonstrated in Figure 74, the main parts of the VECD model include: 1) the pseudo strain (ε^R) function, which accounts for linear viscoelastic and time-temperature effects,

$$\varepsilon^R = \frac{1}{E_R} \int_0^t E(\xi - \tau) \frac{d\varepsilon}{d\tau} d\tau \quad [131]$$

2) the pseudo strain energy density function, W^R ,

$$W^R = \frac{1}{2} (\varepsilon^R)^2 C, \quad [132]$$

3) the stress, σ , to ε^R relationship, and

$$\sigma = \frac{dW^R}{d\varepsilon^R} = C \times \varepsilon^R, \text{ and} \quad [133]$$

4) the damage evolution law

$$\frac{dS}{d\xi} = \left(-\frac{\partial W^R}{\partial S} \right)^\alpha \quad [134]$$

where $E(\xi)$ = the linear viscoelastic relaxation modulus, τ = the integration term, ξ = reduced time, E_R = the reference modulus (taken as 1), C = the pseudo secant stiffness (material integrity), and S = damage.

Model Development. Although the foundational theory that underlies the VECD model has been in place for many years, the precise solution to each of its components has evolved over time. In all these cases, the key function in the VECD model is the damage characteristic curve. This function relates the amount of damage, S , in a specimen to the pseudo secant modulus, or material integrity, which is denoted as C . The initial work with this model was carried

out by Kim and Little (1990) who applied the theory to describe the behavior of sand asphalt under controlled strain cyclic loading. In their work, the damage evolution law was solved using a Lebesgue norm approach (Schapery, 1981), as shown in Equation [135], which is based on the maximum value of pseudo strain in a loading cycle. Kim and Little verified this formulation using random loading histories.

$$S = \left(\int_0^t |\varepsilon^R|^\alpha dt \right)^{1/\alpha} \quad [135]$$

Lee and Kim (1998a; 1998b) continued to develop the model to describe the behavior of asphalt concrete under both controlled stress and controlled strain cyclic loading. In their formulation, they normalized the damage parameter with respect to its maximum value, but in doing so showed that tests at multiple strain levels could be described using a single damage function.

Daniel and Kim (2002) also applied this approach to describe the cyclic behavior of asphalt concrete, but they adhered to Schapery's original theory in a more mathematically rigorous way by eliminating the damage parameter normalization approach that Lee and Kim had used. Daniel and Kim (2002) proposed the VECD model as a key component of a simplified fatigue test procedure, which they then verified by characterizing WesTrack mixtures. Chehab et al. (2002) also applied the theory and focused on describing the material response under constant rate loading, as the ultimate goal was to develop both viscoelastic damage and viscoplastic models. The advantage of the constant rate loading tests was the ability to follow Schapery's derivation more precisely without the need for cycle-wise approximations. Using this model and other tests, Chehab et al. demonstrated that the same time-temperature superposition principle that applies when considering linear viscoelastic behavior could also apply when damage is growing. This finding has since been verified by several researchers (Zhao, 2003; Gibson, 2006; Underwood et al., 2006; Yun, 2010). The two key outcomes from the efforts by Daniel and Kim (2002) and Chehab et al. (2002) are that the damage characteristics of the material are independent of the mode of loading and that the time-temperature superposition principle that typically is used to analyze low-strain dynamic modulus tests also can be applied at high levels of damage. These two findings led to a significant reduction of the required testing protocol while simultaneously extending the realm of application for the model. Equation [136] presents the discrete solution to the damage evolution law suggested by these outcomes. Note that the division of time by a factor of four in the case of cyclic loading is a semi-empirical factor that is based on the assumption that only one-fourth of the loading in a cycle contributes to damage. Also note that the subscript i refers to the cycle or time step of interest.

$$\Delta S_i = \begin{cases} \left[\frac{1}{2} (\varepsilon_0^R)_i^2 \Delta C_i \right]^{\frac{\alpha}{1+\alpha}} \left(\frac{\Delta \xi_i}{4} \right)^{\frac{1}{1+\alpha}} & \text{cyclic loading} \\ \left[\frac{1}{2} (\varepsilon^R)_i^2 \Delta C_i \right]^{\frac{\alpha}{1+\alpha}} (\Delta \xi_i)^{\frac{1}{1+\alpha}} & \text{monotonic loading} \end{cases} \quad [136]$$

Underwood et al. (2010) refined the work of Daniel and Kim (2002) and Chehab et al. (2002) to develop a formulation that could model the fatigue and constant rate results under the umbrella of a single, mathematically rigorous function. This model is described as the simplified viscoelastic continuum damage (S-VECD) model to differentiate it from other earlier formulations and avoid the confusion that exists when multiple formulations carry the same name. This model distinguishes the damage calculation according to whether it is calculated in the first loading cycle or in later cycles, as shown in Equation [137], where f_r is the reduced frequency of loading, K_1 is the loading shape factor, and $\varepsilon_{0,ta}^R$ is the pseudo strain amplitude used for the damage calculation.

$$\left(\frac{dS}{d\xi} \right)_i = \begin{cases} \left(-\frac{1}{2} (\varepsilon^R)^2 \frac{dC}{dS} \right)^\alpha & \text{loading path of first cycle} \\ \left(-\frac{1}{2} (\varepsilon_{0,ta}^R)^2 \frac{dC}{dS} \right)^\alpha \frac{1}{f_r} K_1 & \text{all other cycles} \end{cases} \quad [137]$$

Another important component in the development of the VECD-related models is the failure criterion that is used in the model. In the early efforts by Lee and Kim (1998a and b), model failure was indicated based on a pseudo stiffness value of 0.5, which also was used in the work of Daniel et al. (2002) and Kutay et al. (2008). However,



Chehab et al. (2002) used a pseudo stiffness value of 0.25. Also, Hou et al. (2010) found that a pseudo stiffness value of approximately 0.5 matched experimental data at 5°C, but that a value close to 0.25 was more representative at approximately 19°C and above. Hou et al. (2010) also proposed a function to predict C at failure as a function of temperature and frequency. Efforts to develop a more fundamentally-based failure criterion have resulted in pseudo energy-based failure criteria. For example, Zhang et al. (2013) developed a dissipated pseudo energy criterion. Sabouri and Kim (2014) found that this criterion worked well with controlled strain testing, but that it could not explain results from both controlled strain and controlled actuator experiments. Sabouri and Kim (2014) thus proposed an average dissipated pseudo energy rate criterion, Equation [138], which rectified this shortcoming. They found a power relationship between the pseudo strain energy release rate, referred to as G^R , and the number of cycles to failure, N_f , in arithmetic scale (Equation [139]). Moreover, this relationship is unique for a given mixture, regardless of test temperature, strain level, and mode of loading, as shown in Figure 75(a) in log-log scale.

$$G^R = \frac{\overline{W_C^R}}{N_f} = \frac{\int_0^{N_f} W_C^R}{N_f^2} = \frac{\frac{1}{2} \int_0^{N_f} (\varepsilon_{0,fa}^R)^2 (1-C)}{N_f^2} \quad [138]$$

$$G^R = \gamma N_f^\delta \quad [139]$$

Further analysis of the relationship between the G^R and N_f resulted in a simpler failure criterion, shown in Equation [139].

$$C_{Total} = \int_1^{N_f} C dN = k \times N_f \quad [140]$$

where; C_{Total} = cumulative pseudo stiffness until failure and k = material property. The same data that were used to plot Figure 75(a) are used in Figure 75(b) to describe the relationship between C_{Total} and N_f . The C_{Total} and N_f relationship also is shown to be unique for a given mixture, regardless of test temperature, strain level, and mode of loading. The advantages of the C_{Total} -based failure criterion over the G^R -based failure criterion are that (1) the C_{Total} -based failure criterion is in arithmetic scale and therefore reduces the sensitivity involved in the G^R -based failure criterion in log-log scale and (2), theoretically, only one test is necessary to define the linear relationship between C_{Total} and N_f because this relationship passes through the origin, although in practice two to three tests are necessary to account for the test-to-test variability.

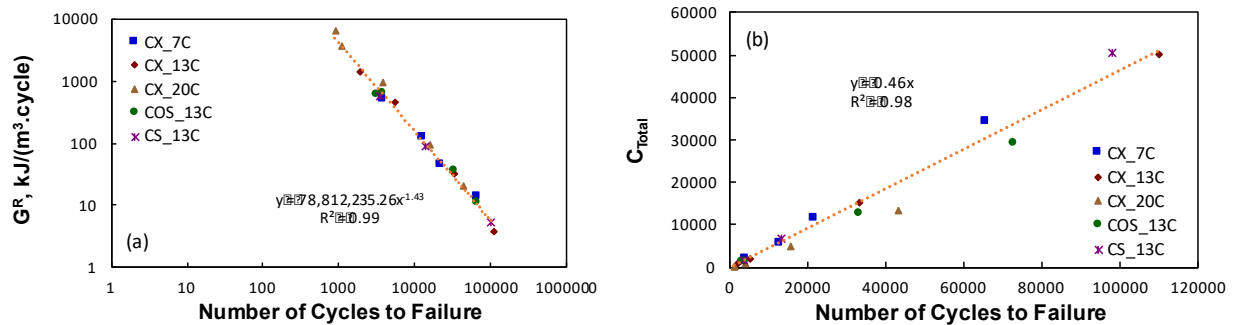


Figure 75. Energy-based failure criteria: (a) G^R -based and (b) C_{Total} -based.

In brief, the major strength of the S-VECD model is that the temperature-independent, stress/strain level-independent, and mode-of-loading-independent nature of the damage characteristic curve and energy-based failure criterion allows cracking to be characterized comprehensively under a wide range of loading and climatic conditions using only two to three cyclic fatigue tests and linear viscoelastic dynamic modulus tests.

Related Modeling Efforts and Applications. The VECD and S-VECD models have been applied in various ways to study and compare asphalt mixture performance. As aforementioned, Daniel et al. evaluated WesTrack mixtures using the earlier formulation. Lundstrom and Isaacson (2004) applied the VECD model form that was developed by Daniel et al. to evaluate modified and unmodified asphalt concrete mixtures in Sweden and concluded that the damage curves do not always provide a unique function. They postulated that the cause is related to self-heating of the sample and proposed a methodology to correct for this effect. Underwood et al. (2006) applied the VECD model



to mixtures from the Federal Highway Administration Accelerated Load Facility (FHWA-ALF) and developed rankings that could reflect the laboratory performance of the mixtures. Follow-up studies used the S-VECD model with layered elastic, layered viscoelastic, and finite element-based pavement response models to predict pavement fatigue performance. The resultant rankings matched those observed in the ALF experiments.

Other researchers have undertaken similar efforts. Kim et al. (2006) applied a similar simplification methodology to study asphalt concrete. Kutay et al. (2008) developed an algorithm that was similar to that of the S-VECD model after evaluating asphalt concrete mixtures from the FHWA-ALF. This work led to the successful ranking of the mixtures tested at the facility. The principal difference between this formulation and the S-VECD model is that the latter explicitly assumes that the damage described by S grows only under tension loading, whereas the former assumes growth under both tension and compression.

Hou et al. (2010) used the S-VECD model to examine the behavior of 15 different reclaimed asphalt pavement (RAP) and non-RAP modified asphalt mixtures from North Carolina. The model indicated that, for the mixtures studied, the inclusion of RAP reduced the fatigue resistance of the mixtures. Similarly, Sabouri et al. (2015) applied different fatigue testing and evaluation methods, including the S-VECD model, to evaluate mixtures with high RAP contents and found that the S-VECD model could distinguish between the different materials. Xie et al. (2015) evaluated different polymer- and rubber-modified stone matrix asphalt concrete mixtures using the S-VECD model and ranked the performance of the mixtures.

One of the major strengths of the VECD and S-VECD models is that they can be implemented into pavement structural models in a seamless manner due to their mechanistic nature. Kim et al. (2016) developed a three-dimensional layered viscoelastic finite element code, the Layered ViscoElastic pavement analysis for Critical Distresses (LVECD) program, to calculate the pavement response and performance under moving loads and realistic climatic conditions and implemented the S-VECD model into the program. Kim et al. (2016) used the S-VECD model and the LVECD program to evaluate the fatigue cracking performance of 59 asphalt mixtures from 55 different pavement structures in the FHWA project DTFH61-08-H-00005. The study asphalt mixtures included conventional Superpave mixes, polymer-modified mixes, warm-mix asphalt (WMA) mixtures, and mixtures with different RAP contents. The field projects included FHWA-ALF test sections, the National Center for Asphalt Technology (NCAT) test track (Lacroix 2013), Korea Expressway Corporation (KEC) test roads, Manitoba Infrastructure and Transportation test roads for RAP and WMA studies, as well as roadways under the purview of the New York State Department of Transportation, the Louisiana Department of Transportation and Development, the city of Binzhou in China, and various pavement sections in Brazil (Nascimento, 2015). The laboratory-measured material properties of these mixes were input to the LVECD program with section-specific structure, traffic, and climatic conditions to predict the performance of the asphalt pavements (Norouzi and Kim, 2015). The study found that the LVECD program can predict field performance with reasonable accuracy. Figure 76 presents some example prediction results. In addition, a transfer function for fatigue cracking was developed based on the limited data available in the FHWA project to translate model predictions to field distresses. Figure 77 shows the prediction of percent cracking area in 18 full-depth asphalt pavements with different asphalt mixtures and structural designs in the KEC test road project using the LVECD program with the transfer function.

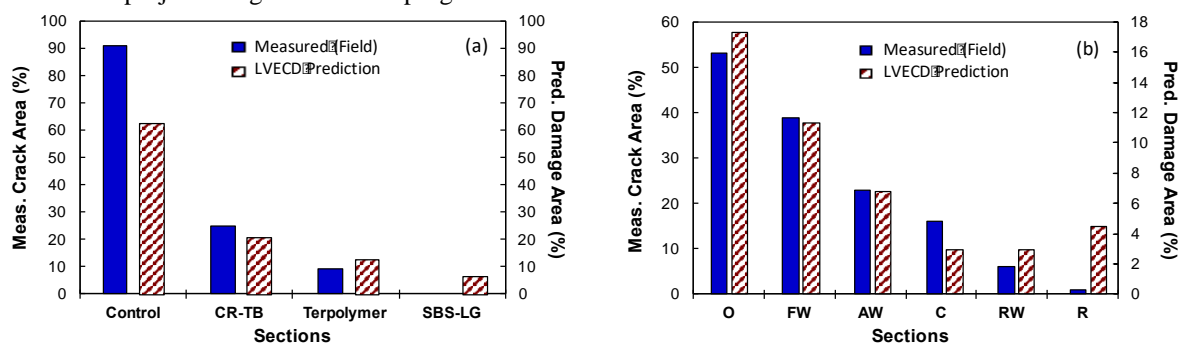


Figure 76. Prediction of percent cracking area using the LVECD program without transfer function: (a) FHWA-ALF pavements and (b) pavements in the NCAT Test Track.

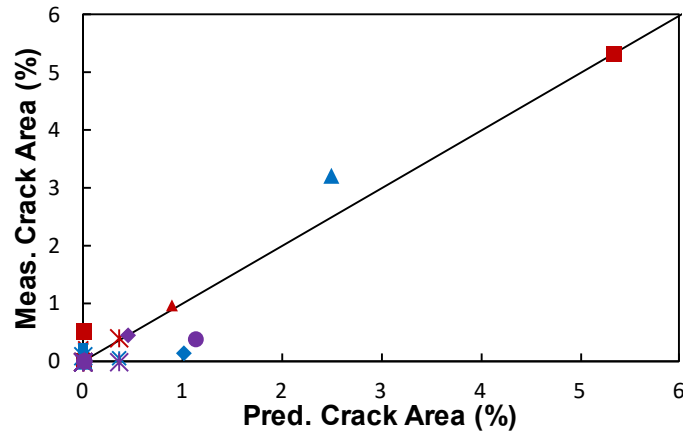


Figure 77. Prediction of percent cracking area in 18 full-depth asphalt pavements in KEC test road project after applying the transfer function.

6.3.2. French Method

Overview. The overall development and background of the French method of continuum fatigue analysis is given in Figure 78. The adopted fatigue resistance law is based on the Wöhler curve. This kind of curve presents the loading amplitude as a function of the fatigue life (number of cycles to failure - N_f). For bituminous mixtures, cyclic strain amplitude (ε) is used to define loading amplitude. Wöhler curve is characterized by the following equation:

$$\varepsilon = AN_f^{-b} \quad [141]$$

This equation corresponds to a straight line in logarithmic axes plot. Tests are required to determine the parameters (A and b) of this equation.

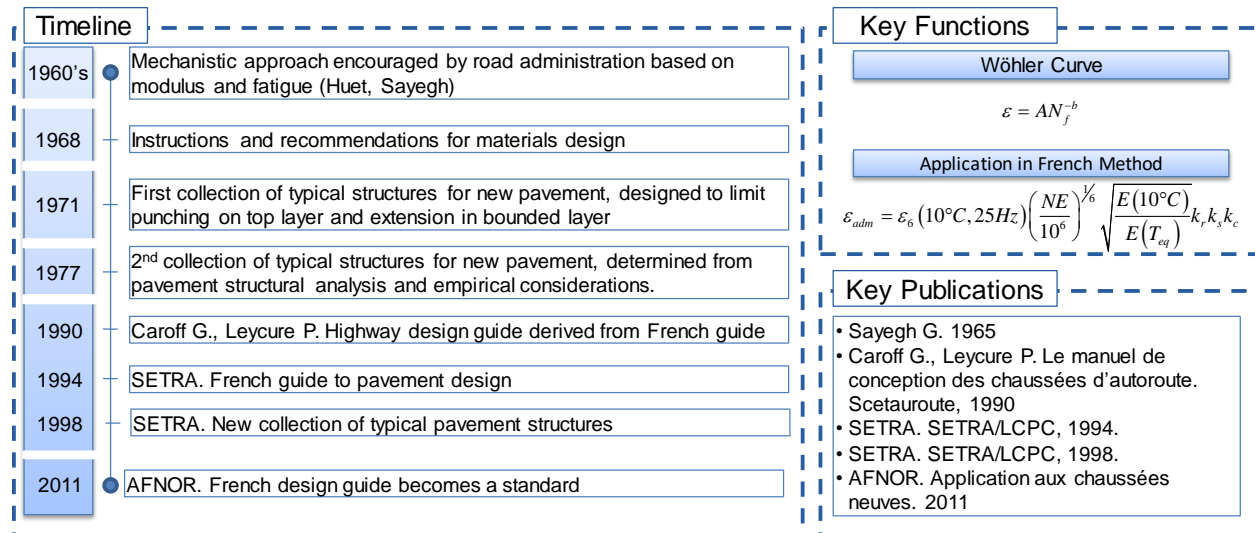


Figure 78. Development history of the French fatigue method.

Different methods exist to characterize fatigue of bituminous mixtures in laboratory. In France, the two-point bending test on trapezoidal specimen was chosen in the middle of 60s. During the test, the load and displacement at the top of the specimen is measured in order to determine the stiffness of the specimen. The relative stiffness is defined as the stiffness divided by the initial stiffness. Change in the material behavior is directly linked to the evolution of the relative stiffness as a function of the number of cycles. Failure is then defined when the relative stiffness reaches 50%. The number of cycles required to reach that relative stiffness is considered as the number of cycles to failure (N_f).

Several tests need to be performed at different strain amplitude levels to obtain the Wöhler curve parameters. As scattering is also high for fatigue results, standard imposes at least six repetitions for each level, and three levels of strain amplitude. Francken et al. (1996) reports great dispersion for the fatigue life obtained that way, results for (N_f) being sometimes 10 times higher with respect to another one at identical testing conditions.

Method Development. The fatigue resistance law (fitted Wöhler curve) is then used to determine an admissible strain in the bituminous mixture layer of the pavement. The comparison between this admissible strain and the calculated one using pavement structural analysis (modelling) allows determining thickness of layers. It is necessary to evaluate an equivalent number of axles (NE) that loads the bituminous mixture layer during its service life. This number depends on several parameters such as: the number of trucks at the beginning of the service life, type of traffic (more or less damaging for the pavement), the traffic growth, and the expected pavement life duration.

Once the value of NE is known, the equation giving the admissible strain ε_{adm} at a reference temperature is as follows:

$$\varepsilon_{adm} = \varepsilon_6(10^\circ C, 25Hz) \left(\frac{NE}{10^6} \right)^{1/b} \sqrt{\frac{E(10^\circ C)}{E(T_{eq})}} k_r k_s k_c \quad [142]$$

where; ε_6 = cyclic strain amplitude corresponding to a failure reached after 10^6 cycles, b = slope of the fatigue resistance law (Wöhler curve in logarithmic axes), $E(10^\circ C)$ = norm of complex modulus of the mixture at $10^\circ C$ and 10Hz, $E(T_{eq})$ = norm of complex modulus of the mixture at 10Hz and the equivalent temperature T_{eq} (fixed at $15^\circ C$ in France), and k_r , k_s , k_c = fitting parameters, explained in the following.

The calculation of the admissible strain takes into account not only the fatigue resistance law but also: the temperature of the standard fatigue test, which is not performed at the equivalent temperature; a fitting parameter k_r accounting for scattering of fatigue tests results and eventual error of the pavement layer thickness; a fitting parameter k_s accounting for an eventual bearing capacity default of the subbase; a fitting parameter k_c accounting for the observed behaviour in-situ and empirically determined.

The determination of the equivalent temperature uses Miner's law (Miner, 1945) to calculate the cumulated damage induced in a material under repetitive loading, with different cyclic strain amplitudes, at possibly different temperatures. The idea is to consider that the damage cumulated throughout one year at the equivalent temperature (d_{eq}) is equal to the calculated accumulation of damage associated to load repetitions at temperatures varying throughout the same year. For one cycle with strain amplitude $\varepsilon(T_i)$ occurring at temperature T_i , the corresponding damage may be calculated as:

$$d_i = \frac{1}{N_{fi}} = \left(\frac{\varepsilon(T_i)}{\varepsilon_6(T_i)} \right)^{1/b} \quad [143]$$

If n_i is the number of cycles occurring at temperature T_i , the cumulated damage is calculated as:

$$D = \sum_i n_i d_i = d_{eq} \sum_i n_i \quad [144]$$

With the equivalent damage, corresponding to the damage at the equivalent temperature T_{eq} :

$$d_{eq} = \left(\frac{\varepsilon(T_{eq})}{\varepsilon_6(T_{eq})} \right)^{1/b} \quad [145]$$

Regarding the three fitting parameters (k_r , k_s , k_c), values of the two last parameters may be found in the French pavement design guide (SETRA, 1994). The presence of parameter k_r gives the French method a probabilistic feature. In order to explain the parameter k_r , it is possible to consider:

the random error due to fatigue tests is represented by the variable e , which is supposed to follow a normal distribution with a null average and a standard deviation S_e . This error will affect the fatigue law $\varepsilon = A(N_f)^{-b}$ and the number of cycles as:

$$\log(N_f) = \log\left(A^{1/b}\right) - \frac{1}{b} \log(\varepsilon_0) + e \quad [146]$$

the random error of the layer thickness Δh , which is supposed to follow a normal distribution, with a null average and a standard deviation S_h . This thickness error will affect the strain as:

$$\log(\varepsilon) = \log(\varepsilon_0) - B\Delta h \quad [147]$$

Combining both errors, it comes:

$$\log(N_f) = \log\left(A^{1/b}\right) - \frac{1}{b}\log(\varepsilon_0) + \frac{B}{b}\Delta h + e \quad [148]$$

From the previous statistical assumptions, $\log(N_f)$ parameter follows a normal law, with an average $av(\log(N_f))$ equal to:

$\log\left(A^{1/b}\right) - \frac{1}{b}\log(\varepsilon_0)$ and a standard deviation

$$S = \sqrt{S_e^2 + \left(\frac{B}{b}S_h\right)^2}$$

Once a failure risk is chosen (a decision of the designer), the strain value ε_0 may be calculated so that $\log(NE)$ corresponds to the lower limit of the confidence interval:

$$\log(NE) = av\log(N_f) - zS \quad [149]$$

with z obtained by the normal distribution for the chosen failure risk. From this consideration, it comes:

$$\varepsilon_0 = \varepsilon_6 \left(\frac{NE}{10^6}\right)^b 10^{-zbS} \quad [150]$$

and then, the fitting parameter k_r may be expressed as 10^{-zbS} . Experiments carried out on the fatigue carrousel at Nantes and in laboratory have shown the necessity to use the fitting parameter k_c . Experience and results are detailed in de la Roche *et al.* (1994; 1997) and Odeon *et al.* (1997). Despite all effects taken into account (scattering of laboratory testing, variability of layer thickness, temperature influence and subbase layer quality), some difference remains between the life duration measured in the laboratory from fatigue tests and the life duration observed in-situ. That justifies the use of such fitting parameter, whose values vary according to the type of bituminous mixture used in the pavement.

Improvement needed. Some points have been discussed by different authors concerning the French method and, more generally, fatigue resistance of bituminous mixtures, such as: the type of test, the loading control mode, the testing temperature, the absence of rest periods, the failure criterion and the volumetric behaviour.

Nowadays, even if the two-point bending test is still the most used in France, several types of test are available in the standard NF EN 12697-24 (AFNOR 2012). Different results may be obtained according to the used test, as shown by the comparison made between five different types of test by Di Benedetto *et al.* (2004). Different types of loading control mode are also used to characterize fatigue, namely strain- or stress-controlled tests. Di Benedetto *et al.* (1996) and Bodin (2002) developed models for fatigue. They showed that with correct analysis of the tests and adapted models, both loading control modes allow defining intrinsic properties of the materials.

Another important aspect of the French method is the arbitrary choice of 50% modulus decrease to define fatigue failure. Many authors underline that at the beginning of fatigue tests, several phenomena inducing reversible stiffness changes occur and should not be considered as damage (irreversible phenomenon).

Among such phenomena, temperature increase in the specimen during cyclic test has been observed in different studies (de la Roche 2001; Bodin, 2002; Di Benedetto *et al.*, 2011; Nguyen *et al.*, 2012). Dissipated viscous energy in bituminous material under loading generates heat. Other recent studies (Di Benedetto *et al.*, 2011; Mangiafico *et al.*, 2015) investigated the beginning of fatigue tests and showed that other reversible phenomena occur and a very small part of complex modulus change may be attributed to real damage.

It should be underlined that such phenomena, described as biasing effects for fatigue tests, observed in laboratory under cyclic loading are less likely to be observed in a real pavement, due to the applied traffic loading which is not continuous (Moutier, 1991). Another aspect raised by some studies is the lack of knowledge on the behaviour of a damaged material, since only one “integrity” parameter is measured during the fatigue test, i.e. the complex modulus at one temperature and one frequency. Nguyen *et al.* (2015) performed a more complete viscoelastic characterization (different temperatures and frequencies) of a bituminous mixture before and after a

partial fatigue test (about 30% of damage was reached before rest was applied). Tapsoba *et al.* (2013, 2015) followed the volumetric deformation of cylindrical specimens during tension/compression fatigue test.

6.3.3. Reduced Cycles Approach

Overview. The reduced cycles approach to fatigue analysis is loosely based on continuum damage principles, but diverges in some important ways. The primary purpose of this approach is to provide a simplified approach to the calculation of a damage parameter—reduced loading cycles—that can then be related to the ratio of the damaged to the undamaged modulus (pseudo-stiffness, C). The model grew out of an approach to continuum damage analysis originally developed by Yong-Rak Kim and others at Texas A & M University (Kim *et al.*, 2002). This model was a somewhat simplified approach to continuum damage analysis applicable only to sinusoidal loading. Christensen and Bonaquist later further simplified the model by assuming a convenient mathematical form for the pseudo-stiffness C as a function of the damage parameter S (Christensen and Bonaquist, 2006). This allowed the resulting equation to be solved in a closed form. The reduced cycles approach is a logical extension of this work, in which the somewhat nebulous damage parameter S is replaced by the reduced cycles function (Christensen and Bonaquist, 2009). Although supported indirectly by continuum damage concepts, the use of reduced cycles in place of S cannot be supported by a direct derivation or proof. It however does seem to provide an equivalent means of tracking fatigue damage in asphalt concrete mixtures. Furthermore, the reduced cycles approach is much simpler to apply in practice and has the additional advantage of making the relationships among strain, modulus, loading cycles and damage much easier to visualize and evaluate. An overview and summary of the reduced cycles approach is given in Figure 74.

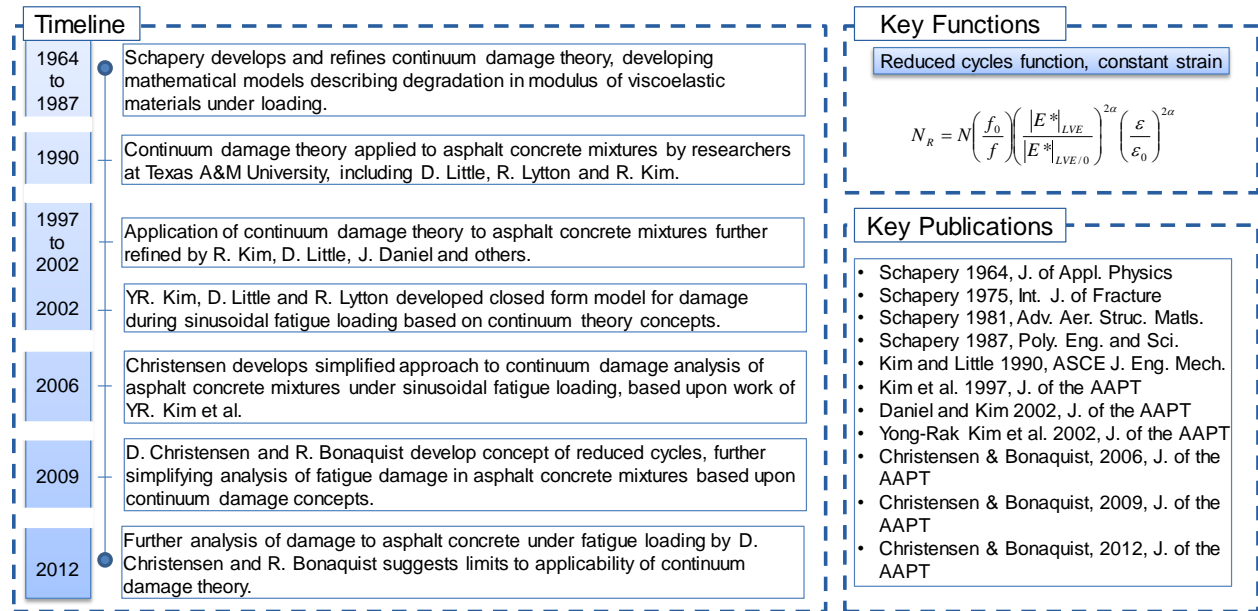


Figure 79. Summary of the Reduced Cycles approach.

Model Development. The two key relationships developed by Kim *et al.* that eventually led to the reduced cycles concept relates first the rate of damage growth to pseudo-strain energy, Equation [151], and the pseudo-strain energy density function W^R to the pseudo-stiffness C and the pseud-strain ϵ^R , Equation [2] (Kim *et al.*, 2002).

$$\frac{dS}{dt} = \left(\frac{\partial W^R}{\partial S} \right)^\alpha \quad [151]$$

$$W^R = 0.5C \left(\epsilon_{\max}^R \right)^2 \quad [152]$$



Kim *et al.* suggested that the relationship between pseudo-stiffness C and the damage parameter S can be characterized using a generalized power law (Kim *et al.*, 2002). However, this would predict that at some value of S , the pseudo-stiffness would become negative. This would mean that the damaged modulus would also become negative, and an applied tensile strain would result in a compressive stress—an obvious impossibility. A better function for relating pseudo-stiffness to the damage parameter is a simple exponential (Christensen and Bonaquist, 2006):

$$C = e^{C_2 S} \quad [153]$$

where C_2 = a constant indicative of the rate of damage accumulation in a specimen under cyclical loading, called here the continuum damage fatigue constant. Now, if Equation [153] is substituted into Equation [2] and differentiated with respect to S , the following relationship results:

$$\frac{\partial W^R}{\partial S} = 0.5 C_2 e^{C_2 S} (\epsilon_{\max}^R)^2 \quad [154]$$

Following the derivation by Kim *et al.* (with the exception of the different functions for pseudo-stiffness C), Equation [154] can be substituted into Equation [151], and integrated to solve for t :

$$t = \frac{2^\alpha e^{-\alpha C_2 S}}{\alpha (-C_2)^{1+\alpha} (\epsilon_{\max}^R)^{2\alpha}} \bigg|_{S=0}^{S=t} \quad [155]$$

Now, if the reference modulus $E^R = 1$, then $\epsilon^R(t) = \sigma(t)$. Also, for sinusoidal loading, the maximum tensile stress is equal to $|\sigma_{\max} - \sigma_{\min}|/2 = \sigma_0 = \sigma_0 |E^*|_{LVE}$, where $|E^*|_{LVE}$ is the LVE complex modulus. Keeping in mind that the number of loading cycles N is loading time t times frequency f (in Hz), Equation [155] can then be solved over the given integration limits and reduced to the following form:

$$N = \frac{2^\alpha f (e^{-\alpha C_2 S} - 1)}{\alpha (-C_2)^{1+\alpha} (\epsilon_0 |E^*|_{LVE})^{2\alpha}} \quad [156]$$

Substituting Equation [153] into Equation [156]:

$$N = \frac{2^\alpha f (C^{-\alpha} - 1)}{\alpha (-C_2)^{1+\alpha} (\epsilon_0 |E^*|_{LVE})^{2\alpha}} \quad [157]$$

Equation [157] is an extremely useful tool for applying continuum damage to cyclical testing and other fatigue phenomenon. It can be used to calculate the number of loading cycles N required to reach a given level of pseudo stiffness C , given the value of the continuum damage fatigue constant C_2 . Since the pseudo stiffness is simply the ratio of the damaged to initial (LVE) modulus, Equation [157] can be used to predict the decrease in modulus as fatigue progresses if C_2 is known. To calculate C_2 , a plot of pseudo stiffness versus the damage parameter S must be prepared, using a number of strains and test temperatures, and using reduced frequency in the calculation of S . The value of α is varied until the damage plots converge (more or less) to a single line. The value of C_2 is then calculated as the slope of a plot of $\ln C$ versus S . In order to do this, an equation for S is needed in terms of pseudo stiffness, strain, and LVE modulus. Equations [153] and [156] can be combined, and solved for S to provide such a relationship:

$$S = \left[\frac{\alpha N (-\ln C)^{1+\alpha} (\epsilon_0 |E^*|_{LVE})^{2\alpha}}{2^\alpha f (C^{-\alpha} - 1)} \right]^{\frac{1}{1+\alpha}} \quad [158]$$

The approach described above is simpler than a traditional continuum damage approach, but still has its limitations and its complexities. Based in part upon the appearance of Equation [158], Christensen and Bonaquist hypothesized that the pseudo-stiffness could be characterized as a function of reduced cycles, calculated using the following relationship (Christensen and Bonaquist, 2009):



$$N_R = N_{R-ini} + N \left(\frac{f_0}{f} \right) \left(\frac{|E^*|_{LVE}}{|E^*|_{LVE/0}} \right)^{2\alpha} \left(\frac{\varepsilon}{\varepsilon_0} \right)^{2\alpha} \left[\frac{1}{a(T/T_0)} \right] \quad [159]$$

Where; N_R = reduced cycles, N_{R-ini} = initial value of reduced cycles, prior to the selected loading period, N = actual loading cycles, f_0 = reference frequency (10 Hz suggested), f = actual test frequency, $|E^*|_{LVE}$ = initial (linear viscoelastic or LVE) dynamic modulus under given conditions, lb/in², $|E^*|_{LVE/0}$ = reference initial (LVE) dynamic modulus, lb/in² (the LVE modulus at 20°C is suggested), α = continuum damage material constant with values typically ranging from about 1.5 to 2.5, ε = applied strain level, ε_0 = reference effective strain level (0.0002 suggested), and $a(T/T_0)$ = shift factor at test temperature T relative to reference temperature T_0 .

In its original formulation, the effective applied strain level was used, meaning the applied strain minus the endurance limit. For the sake of simplification the concept of endurance limit has been left out of this derivation. It should also be noted that the researchers who developed this analysis (also the authors of this section of this document) have promoted various versions of this analysis, one of the important questions being whether or not the damage curves over a wide range of conditions truly converge to a single function, or if they tend to form instead of family of curves. The approach presented here assumes that convergence can be obtained, at least at moderate to high modulus levels. It is possible, as noted by other researchers, that the lack of convergence sometimes observed in continuum damage testing and analysis is primarily caused by large amounts of plastic deformation occurring on specimens tested at high temperatures and/or low frequencies.

Application of Method. The use of the reduced cycles approach can be illustrated by applying Equation 8 to the analysis fatigue data on an asphalt concrete mixture gathered over a wide range of temperatures and two different frequencies (Christensen and Bonaquist, 2014). The mixture that was used in this experiment was a 9.5 mm mixture produced from limestone aggregate and PG 64-22 binder. Table 6 summarizes pertinent properties of the mixture that was used. Specimens for fatigue testing were 100 mm diameter by 150 mm tall. These specimens were prepared to a target air void content of 7.0 percent in accordance with AASHTO TP 60. The specimens were tested in fatigue using uniaxial tension-compression. Fully reversed, stress-control loading was used, which typically results in strain levels that gradually increase with time, until localization occurs, at which point the strains increase rapidly with rupture sometimes occurring. Test temperatures included -5, 4, 10, 20, and 30°C. All specimens were tested at both 1 and 10 Hz. However, data at 1 Hz was somewhat noisier than the 10 Hz data, and also generally exhibited slightly lower damage ratios. The reason for this discrepancy is not clear, but it might be due to differences in the amount of plastic deformation occurring at the two different frequencies. Initial applied strains typically ranged from 150 to 200 × 10⁻⁶ for low strain tests, and from 300 to 500 × 10⁻⁶ for high strain tests. For every test, an initial modulus reading was taken at low strain so that an initial, undamaged modulus reading was available for calculation of the damage function.

Table 6. *Composition of mixture used in expanded range damage experiment (Christensen and Bonaquist, 2014).*

Properties		Value
Design Gyration Level		75
Gradation	Sieve Size, mm	% Passing
	12	100
	9.5	98
	4.75	72
	2.36	46
	1.18	26
	0.6	17
	0.3	11
	0.15	8
	0.075	5.0
Binder Content, wt %		5.9
Effective Binder Content, wt %		5.3
Fine Aggregate Angularity, vol %		45.2
Crushed Aggregate Fractured Faces, %		100/100



Sand Equivalent, %	78.0
Flat and Elongated Particles, %	0.2
Aggregate Bulk Specific Gravity	2.671
Design VTM, vol %	4.0
Design VMA, vol %	16.3
Design VFA, %	76

Figure 80 shows typical results of the fatigue tests, for data collected at 10°C and 1 Hz for the high strain condition. The first step in analyzing the data was to generate damage curves for each test. This simply involves calculating the ratio of the instantaneous modulus to the initial modulus as a function of loading cycles. Figure 81 below shows the damage function $|E^*|/|E^*|_{\text{initial}}$ for the 10°C, 1 Hz, high strain test—the test represented in Figure 80 above. Figure 82 shows the results of the analysis, as a plot of damage ratio as a function of reduced cycles; only 10 Hz data is shown in this figure. The initial modulus for this analysis was in most cases based on measurements made at low strain immediately before the fatigue tests, but in three cases the initial modulus was adjusted slightly (2 to 8 %) to provide a better fit to the damage curve. Also for three cases the specimens appeared to undergo macro-cracking prior to complete failure, so that the damage curves rapidly dropped towards the end of the test. Data points after this localization were removed. The fit to the data is quite good, although as mentioned above the plot becomes somewhat more scattered when the 1 Hz data is used. The data at 30°C data at 1 Hz could not be fit at all to the damage curve, supporting the idea that at higher temperatures and/or low frequencies plastic deformation can become excessive making a simplified continuum damage analysis impossible.

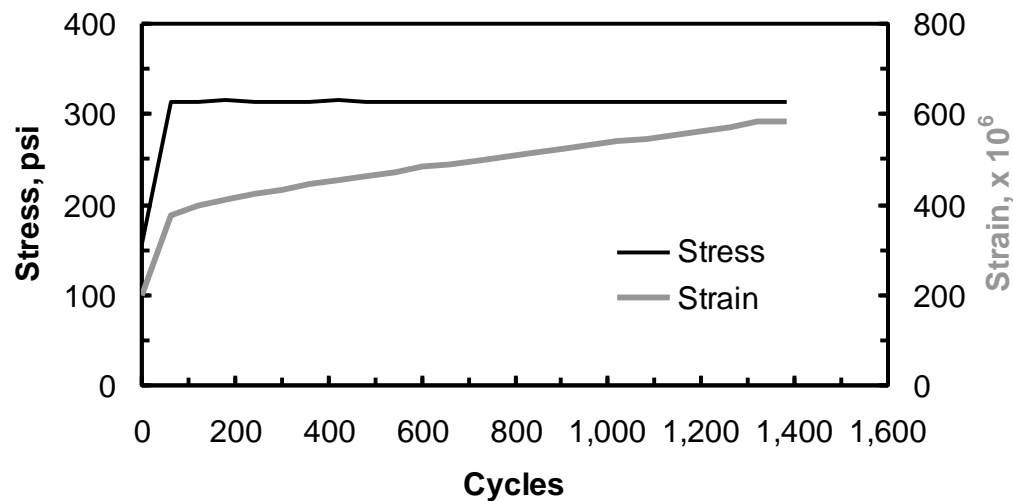


Figure 80. Stress and strain at 10 °C and 1 Hz during uniaxial fatigue loading, high strain (Christensen and Bonaquist, 2014).

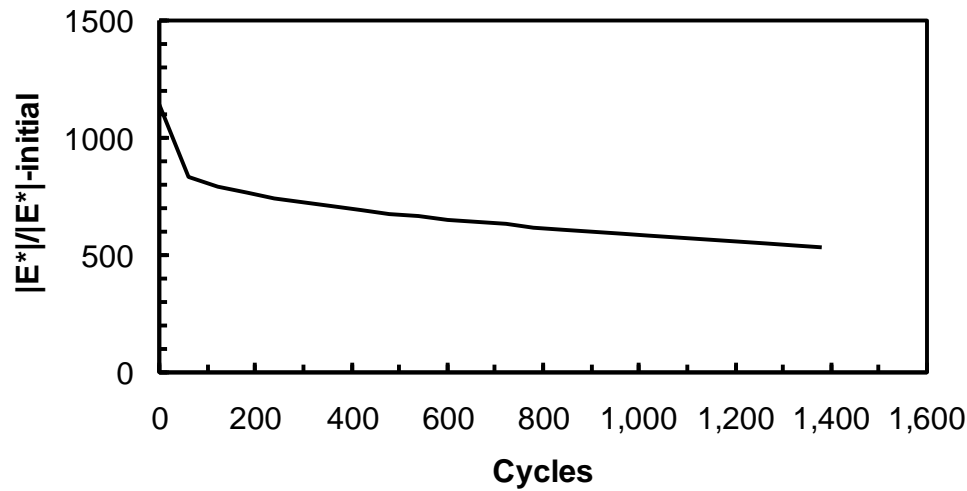


Figure 81. Damage function $|E^*|/|E^*|_{\text{initial}}$ for 10 °C and 1 Hz, high strain (Christensen and Bonaquist, 2014).

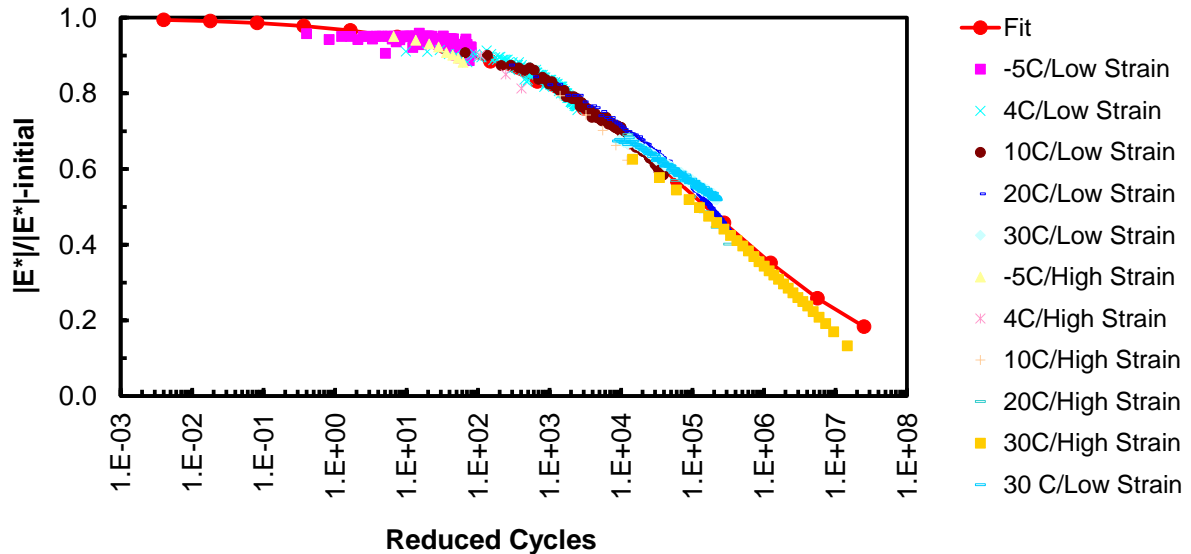


Figure 82. Damage Ratio as a Function of Reduced Cycle for an Asphalt Concrete Mixture at 10 Hz and Various Temperatures and Strain Levels (Christensen and Bonaquist, 2014).

In summary, the reduced cycles approach is a relatively simple means of analyzing fatigue data to produce damage curves. From such damage curves, the damaged modulus can be predicted for a variety of loading conditions which is potentially useful in advanced pavement analysis and design. It should however be pointed out that damage as measured by the decrease in modulus does not necessarily correlate closely to damage as it relates to cracking and overall pavement performance. There is as a result significant recent activity among pavement researchers to develop failure theories that can be combined with continuum damage analysis or even applied independently of such analyses to predict actual pavement cracking.

6.3.4. Texas A&M University Approach

Overview: the continuum-damage and micro-damage healing constitutive relationships were developed at Texas A&M University as part of the Asphalt Research Consortium (ARC) and were implemented in the FE package PANDA: Pavement Analysis using Nonlinear Damage Approach. PANDA's damage and micro-damage healing constitutive relationships are based on the extended continuum damage mechanics (CDM) framework. These

constitutive relationships were coupled to the Schapery's viscoelasticity (1969), Perzyna's viscoplasticity (1971), and Darabi et al. (2012a) hardening-relaxation constitutive relationships to predict the complex response of asphalt concrete pavements subjected to general loading conditions and multi-axial state of stresses. An overarching timeline of the model, the key elements, and literature are summarized in Figure 83.

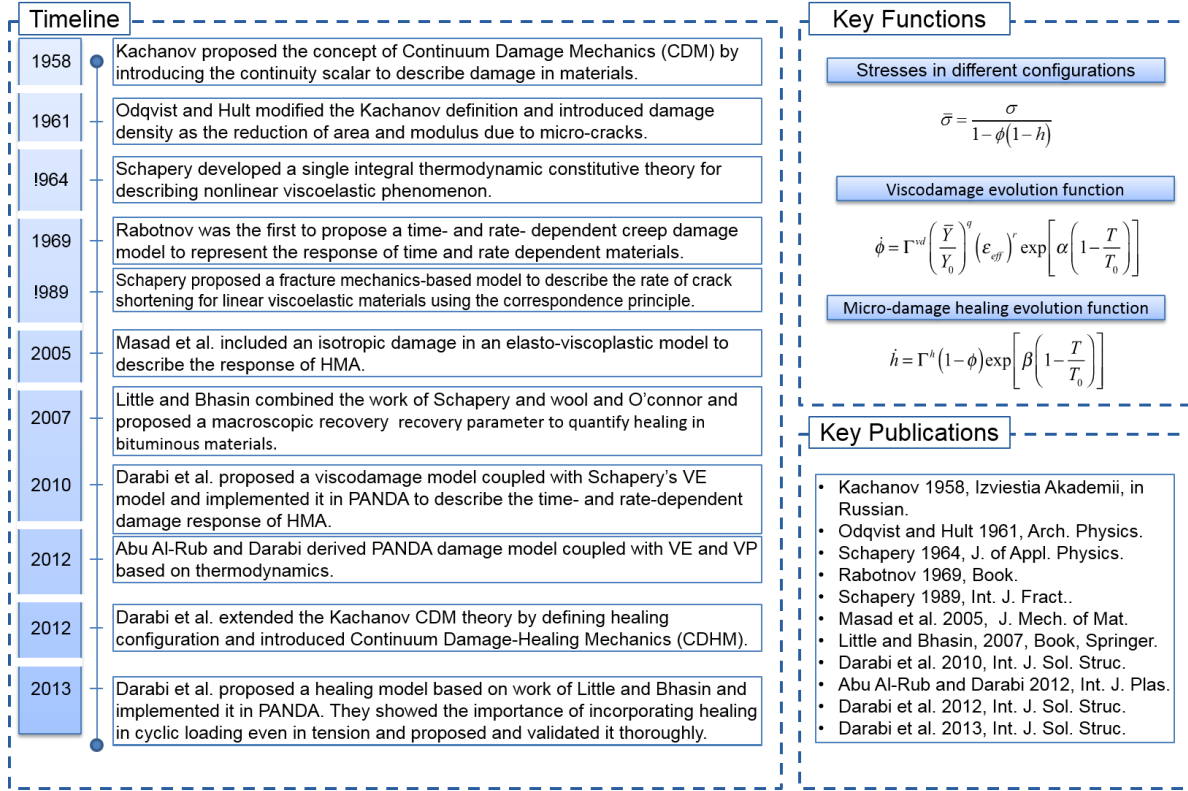


Figure 83. Summary of PANDA damage approach.

Model development: PANDA damage and micro-damage healing constitutive relationships are based on the concept of the continuum damage mechanics pioneered by Kachanov (1958) and later enhanced by Rabotnov (1969). They introduced a state variable referred to as the damage density, ϕ , to relate stress tensors in the nominal and effective configuration. To incorporate the effect of micro-damage healing, researchers at Texas A&M University extended the well-known effective (undamaged) configuration of CDM to incorporate both damage and micro-damage healing effects (Abu Al-Rub and Darabi, 2012; Darabi *et al.*, 2012b; 2013), such that one can write:

$$\bar{\sigma} = \frac{\sigma}{1 - \phi(1 - h)} \quad [160]$$

where $\bar{\sigma}$ = stress in the modified undamaged configuration, σ = stress tensor in the nominal configuration, ϕ = damage state variable, and h = micro-damage healing state variable. The implicit argument supporting Equation [101], is that once the material degrades, further loading only affects the intact portion of the material. This simple equation suggests that one can express the constitutive relationships in terms of the effective stress which facilitate accounting for damage and healing. The damage and healing variables evolve according to evolution functions. The nominal stress can then be obtained using Equation [101], which shows how nominal stress, damage, and micro-damage healing are coupled. This approach facilitates the coupling of damage and other components of the constitutive relationship, such as viscoelasticity and viscoplasticity.

Masad et al. (2005) included an isotropic damage in an elasto-viscoplastic model to describe the response of asphalt concrete pavements. Based on the damage model proposed by Masad et al. (2005) and after analyzing extensive set of experiments on asphalt concrete materials, a time- and temperature-dependent damage evolution function was proposed by Darabi *et al.* (2011; 2013) and implemented in PANDA, such that:



$$\dot{\phi} = \Gamma^{vd} (T) \left\langle \frac{\bar{Y}}{Y_0} \right\rangle^q (\epsilon_{eff})^k f(T) \quad [161]$$

where; Γ^{vd} = viscodamage fluidity parameter, Y_0 = reference damage force which can be assumed to be unity, k = material parameter; and ϵ_{eff} = effective total strain defined as shown in Equatino [162].

$$\epsilon_{eff} = \sqrt{\epsilon_{ij} \epsilon_{ij}} \quad [162]$$

A modified Drucker-Prager function is assumed for the damage force \bar{Y} :

$$\bar{Y} = \bar{\tau}^{vd} - \alpha \bar{I}_1; \quad \bar{\tau}^{vd} = \frac{\sqrt{3\bar{J}_2}}{2} \left[1 + \frac{1}{d^{vd}} + \left(1 - \frac{1}{d^{vd}} \right) \frac{3\bar{J}_3}{\sqrt{3\bar{J}_2^3}} \right] \quad [163]$$

The terms \bar{I}_1 , \bar{J}_2 , and \bar{J}_3 are the stress invariants; α and d^{vd} being the material parameters associated with the damage model. [163] converts the multi-axial stress states to a damage force, which is a scalar considering the general applied multi-axial stress levels that drive damage evolution. It has been shown that the damage evolution function is sensitive to the confinement level, combined effects of deviatoric stress level, and distinguishes between extension and contraction loading modes (Dessouky, 2005; Tashman *et al.*, 2005; Darabi *et al.*, 2013).

As it will be illustrated in the next sub-section, accurate prediction of fatigue damage of asphalt concrete requires the incorporation of both damage and micro-damage healing mechanisms. Once the material is damaged, healing can occur either during the rest period when the applied load is negligible or under compressive load. As shown by several researchers (e.g., Little and Bhasin, 2007) the micro-damage healing in asphalt concrete is due to two processes at the micro-scale, i.e. wetting and interdiffusion of molecular species between the crack faces. The micro-damage healing constitutive relationship implemented in PANDA is postulated to reflect these two processes (Abu Al-Rub *et al.*, 2010):

$$\dot{h} = \Gamma^h (T) (1 - \phi_{eff})^{b_1} (1 - h)^{b_2} \quad [164]$$

where $\dot{h} = dh/dt$ is the rate of the healing variable and $\Gamma^h(T)$ is the healing fluidity parameter that determines how fast the material heals which is a function of temperature T .

Importance of incorporating micro-damage healing: It is commonly believed that micro-damage healing of asphalt binder and asphalt concrete occurs only during the rest period between the loading cycles at intermediate and high temperatures. While this could be true for elastic media with healing potential, the existence of a rest period between the loading cycles is not the only condition under which micro-damage healing occurs in time-dependent materials (e.g., viscoelastic materials) with healing potential such as asphalt concrete and asphalt binder. Residual (internal) compressive stresses can also aid in the micro-damage healing of asphalt concrete. To show the importance of incorporating micro-damage healing mechanism even during a cyclic test in tension, Figure 84 illustrates part of strain and stress responses during the cyclic displacement controlled test (CDC). In the CDC test, the stress remains tensile during a large portion of the loading history. During the unloading (i.e. when the strain rate is negative), however, compressive stresses are induced in the specimen. These compressive stresses cause the micro-crack free surfaces to wet (i.e., get close to each other) and undergo healing and crack closure.

This effect can be explained based on the fading memory of viscoelastic materials and the lag between stress and strain responses, the term δ as shown in Figure 84. This is due to the fading memory effect (Coleman, 1964) and viscoelastic nature of asphalt concrete. In order to illustrate the effect of the fading memory, assume that the viscoelastic medium contains a single micro-crack of length a_0 at point “A” and the damage growth occurs when the tensile strain exceeds a threshold value (i.e. ϵ_{th}^{Damage}). Moving from point “A” to point “B” in Figure 84, the strain remains larger than ϵ_{th}^{Damage} and the induced stresses in the viscoelastic media are also tensile. Therefore, the micro-crack length increases by Δa^L , such that the crack length at point “B” reaches $a_0 + \Delta a^L$. However, fading memory causes the stresses induced in the material to relax and fade away with time. The increase in the strain level during the preceding loading stage has less effect on the stress level than the decrease in the strain level during the current unloading stage. Obviously, the negative increment in the stress due to the decrease in the strain level during the unloading stage is more than the positive increment in the stress due to the increase in the strain level during the preceding loading stage. Therefore, the viscoelastic medium feels compressive stresses at some point during the



unloading stage although the total strain is still tensile. Therefore, the crack length decreases when moving from point “B” to point “C” by the increment of Δa^{UL} .

The induced stresses are compressive during a small portion of the loading and deformation history for the tensile CDC test, such that Δa^L is always greater than Δa^{UL} (i.e. $\Delta a^L > \Delta a^{UL}$). Therefore, micro-cracks still propagate and increase in length when moving from point “A” to point “C”. However, accurate estimation of the damage density requires the incorporation of both Δa^L and Δa^{UL} components. It has been shown that it is necessary to incorporate the micro-damage healing constitutive relationship along with the damage model implemented in PANDA to accurately predict the fatigue response of asphalt concrete materials under general loading conditions (Darabi *et al.*, 2013).

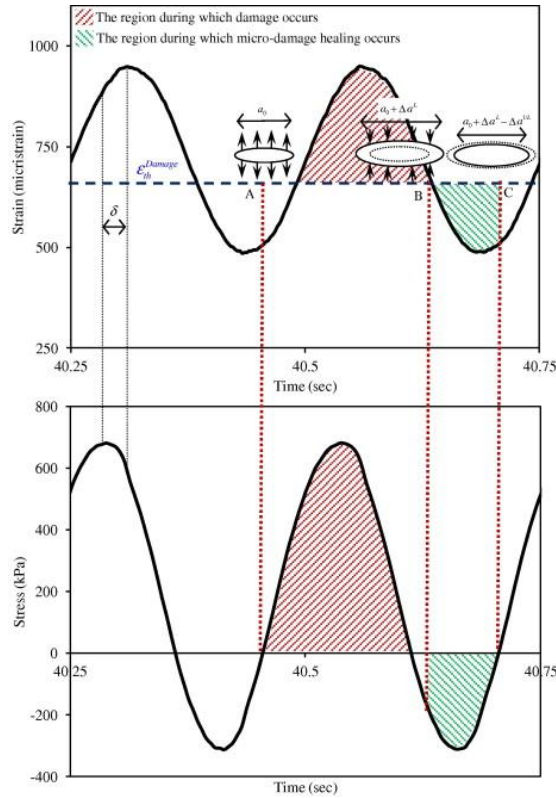


Figure 84. Illustration of the healing mechanism induced during a cyclic strain-controlled test.

Calibration and validation of PANDA damage and micro-damage healing models: One of the main issues that prevents the use of sophisticated mechanistic based constitutive relationships is the lack of a robust procedure to identify the parameters associated with such constitutive relationships. The main issue in this case is that most mechanisms occur simultaneously which makes it very difficult to assign unique values to each parameter. Developers of PANDA and their collaborators have thoroughly investigated this issue and proposed a systematic procedure to identify the parameters associated with PANDA damage model. The key in systematic calibration of such sophisticated constitutive relationships is to carefully design/select lab tests that show one or at the most two mechanisms at the same time. The damage parameters are extracted from laboratory tests that are conducted at relatively low temperatures (e.g., 5°C) to ensure that the induced viscoplastic strain is minimum and negligible. By analyzing the results of constant strain rate tests at relatively low temperatures but at different strain rates and having the nonlinear viscoelastic parameters in hand, the viscodamage parameters can be extracted. Figure 3 shows the analysis results of constant strain rate tests in tension at 5°C. Guided by the evolution function in Equation [161], a general form is assumed for the damage evolution function as a function of the damage force \bar{Y} and effective strain ϵ_{eff} , such that:

$$\dot{\phi} = \Gamma^{vd} f_1 \left\langle \frac{\bar{Y}}{Y_0} \right\rangle^q f_2(\epsilon_{eff}) \quad [165]$$



Figure 85 clearly shows that f_1 and f_2 follow a power-law form and the where the powers k and q are the slope of the lines extracted from constant strain rate tests.

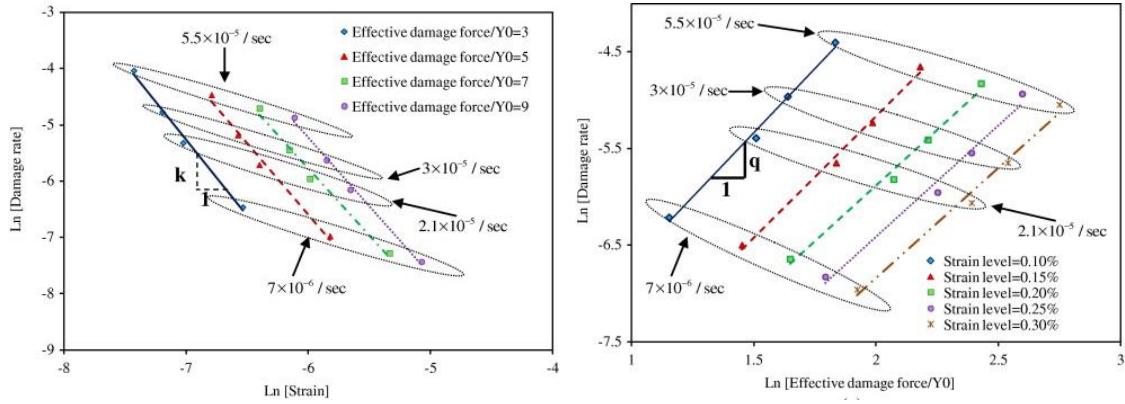


Figure 85. Illustration of the procedure for calibration of PANDA damage model.

Figure 86 illustrates few samples of prediction of PANDA damage and healing constitutive relationships as compared to the cyclic stress-controlled and strain controlled experiments.

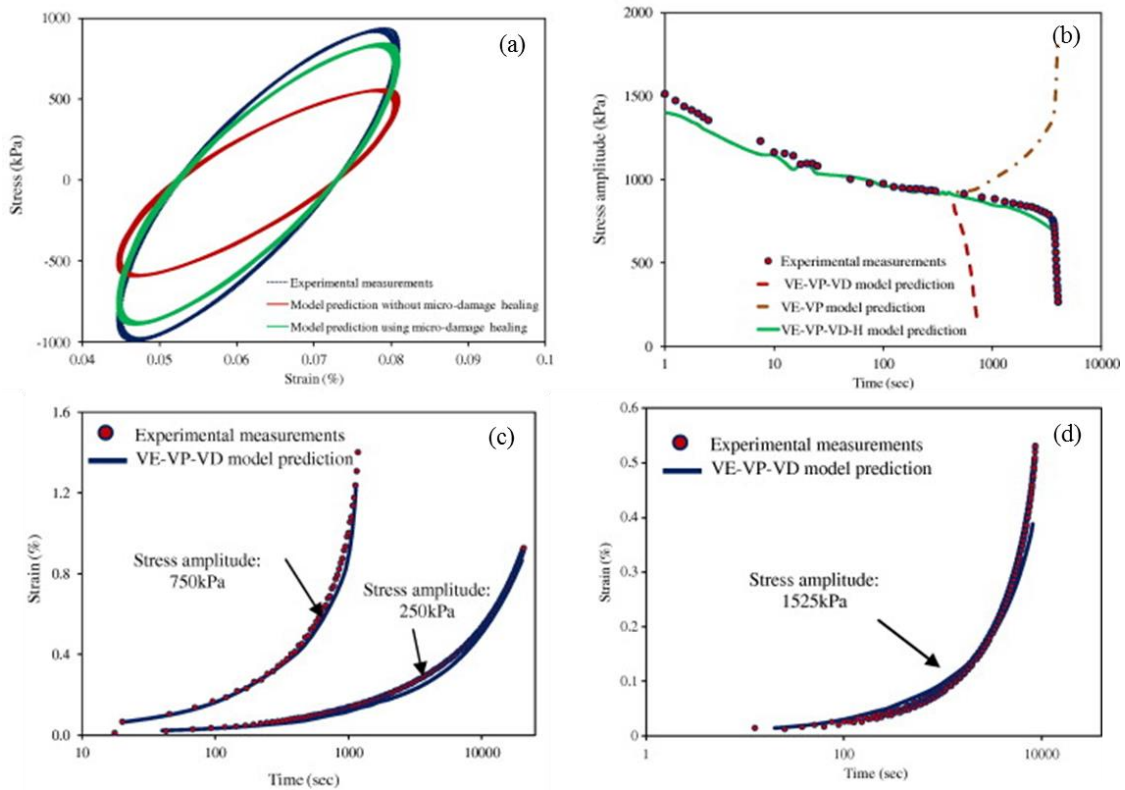


Figure 86. PANDA prediction of cyclic stress and strain controlled tests. (a) Stress-strain response in the CDC test (strain amplitude of 1200 $\mu\epsilon$); (b) stress amplitude in the CDC test (strain amplitude of 1200 $\mu\epsilon$); (c) strain amplitude in cyclic stress-controlled test at 19°C; (d) strain amplitude in cyclic stress-controlled test at 5°C.

The PANDA damage and healing models have been validated extensively against several lab databases. Recently, several researchers have successfully used the PANDA damage model to investigate effects of damage on response of asphalt concrete materials (e.g., Rushing *et al.*, 2015; Caro *et al.*, 2016; Castillo *et al.*, 2016).

6.4. Fracture Methods

6.4.1. Elastic Fracture Mechanics

Overview. The first work to quantify fracture characteristics of materials was performed on materials that obey Hooke's law ($F=kX$); all of the materials were linear elastic. 1960 is considered a tipping point, when significant research began on fracture theory outside of linear elastic materials, but work done to date is simply an extension of linear elastic fracture mechanics, or LEFM. Fracture mechanics is different from the traditional strength approach. In the traditional strength approach, some sort of applied stress produces a yield or tensile strength. However, in fracture mechanics, the applied stress produces fracture toughness, which is dependent of the existing flaw size. Whether the flaw is a notch or neck, the reduced area forces the stress to concentrate at the flaw location, and thus a crack is forced to begin at the flaw location.

This section will give a broad overview of the fundamental principles of elastic fracture mechanics, with approximately 2/3 of the content covering general development, and about 1/3 covering asphalt materials related development. A summary of the content is shown in Figure 87.

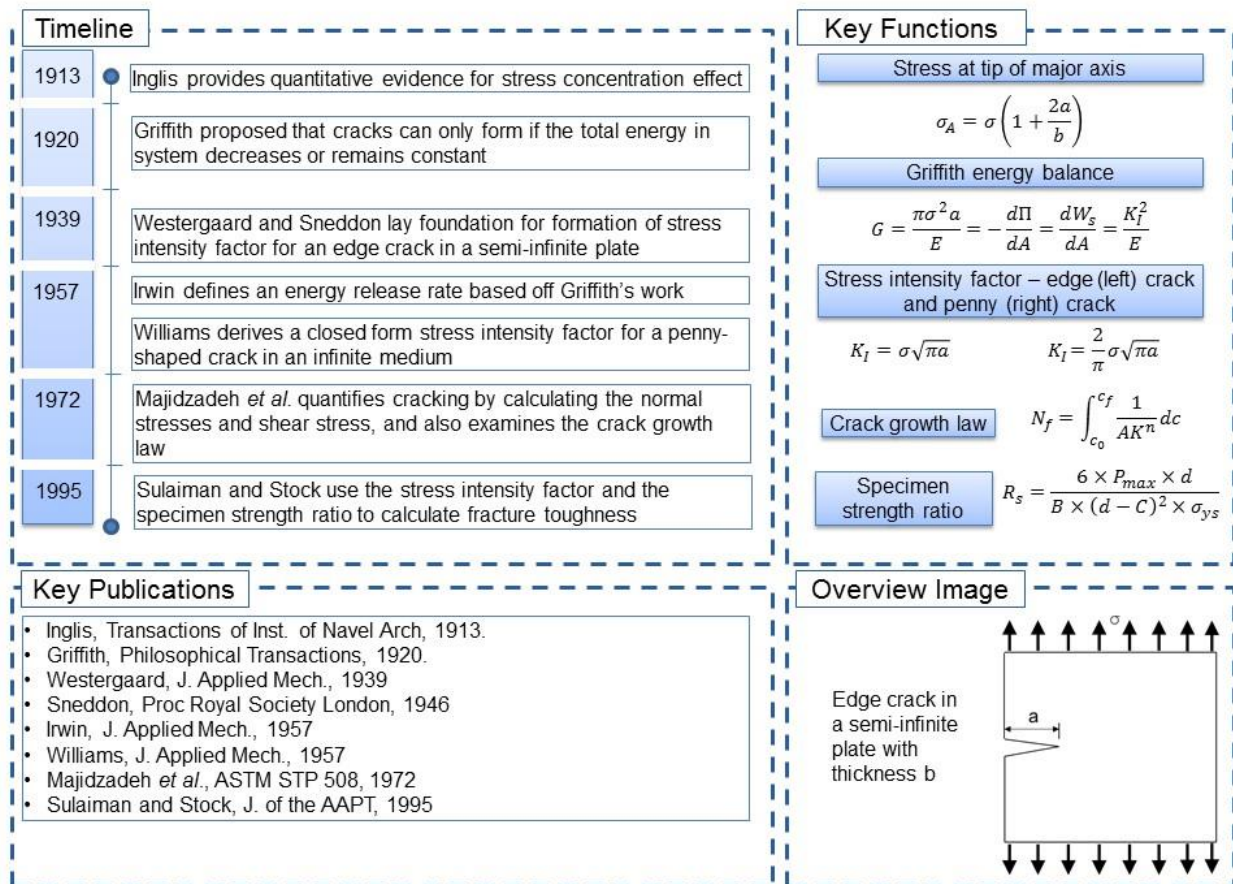


Figure 87. Summary of elastic fracture mechanics.

Stress at tip of major axis. The first indication of quantitative assessment of stress at a flaw location was put forth by Inglis in 1913. This work examined elliptical holes in flat plates. Assumptions include that the whole was not influenced by the plate boundary, so the plate width was much greater than $2a$, and the plate height was much greater than $2b$. Figure 88 shows a schematic of the setup and the stress at the tip of the major axis (Point A).

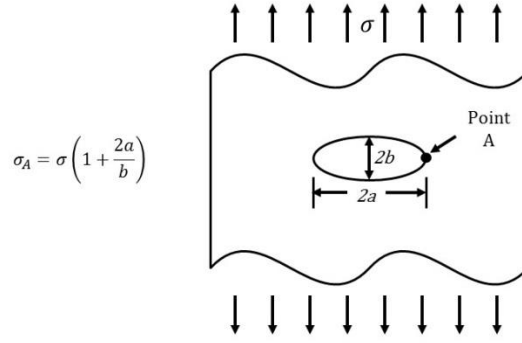


Figure 88. Stress at the tip of the major axis.

This work continued to investigate how a increases relative to b , the elliptical hole becomes a sharp crack. However, a material that contains an infinitely sharp crack, should in theory fail with the application of an infinitely small load. This issue motivated Griffith to develop fracture theory based on energy versus stress.

Griffith energy balance. The Griffith energy balanced (Griffith, 1920) is founded on the first law of thermodynamics. Griffith postulated that when a system goes from a non-equilibrium state to an equilibrium state, there is a net decrease in energy. Therefore, a crack can only form, or an existing crack can grow, if the process causes the total energy to decrease or remain constant. This is shown in Equation [10].

$$\frac{dE}{dA} = \frac{d\Pi}{dA} + \frac{dW_s}{dA} = 0 \quad [166]$$

where; E = total energy, dA = incremental increase in crack area, Π = potential energy supplied by internal strain energy and external forces, and W_s = work required to create new surfaces.

From a different perspective, the crack will propagate if the energy available to extend the crack equals the energy required to propagate the crack. A similar schematic can be used for Griffith energy balance that was used for Inglis (Figure 2), but the analysis revolves around the total energy, potential energy, work created to form new surfaces, and the surface energy of the material. In addition, it is assumed that the plate width is much greater than $2a$, and that plane stress condition prevail. These relationship are shown in Equation [167].

$$\frac{\pi\sigma^2 a}{E} = -\frac{d\Pi}{dA} = \frac{dW_s}{dA} = 2\gamma_s \quad [167]$$

where; σ = stress applied to sample, a = half-length of elliptical hole, E = Young's modulus, and γ_s = surface energy of material.

Stress intensity factor. Assuming isotropic linear elastic material behavior, closed-formed solutions can be derived for specific crack configurations. Westergaard (1939) and Sneddon (1946) provided much of the foundational work in this area, specifically focusing on edge cracking and penny shaped cracking. Since the loading of a crack essentially creates a singularity at the crack tip (the stress continues to increase as the distance to the crack tip decreases), so it is convenient to replace the stresses in Equations [10] and [167] with a stress intensity factor K . The stress intensity can be shown in either opening (Mode I), shear in plane (Mode II), or shear out of plane (Mode III). This synthesis will only focus on Mode I, which is represented by K_I . When examining an edge crack in a semi-infinite plate with thickness b (Figure 88 cut in half), the stress intensity factor (K_I) is simply a function of the applied stress (σ) and the notch length (a) as shown in Figure 89.

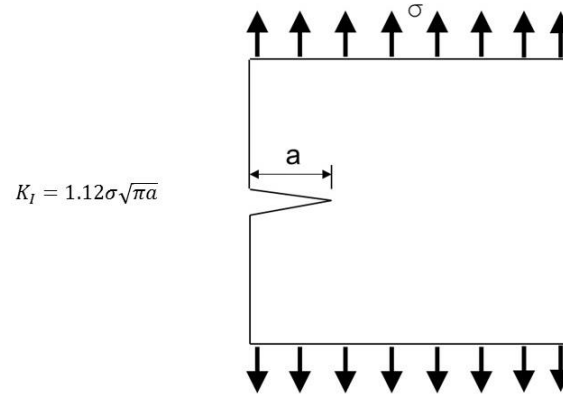


Figure 89. Stress intensity factor for edge crack.

A relationship can also be developed (Williams, 1957) for a penny shaped crack in the middle of a sample (a circle with radius a), as seen in Equation [168].

$$K_I = \frac{2}{\pi} \sigma \sqrt{\pi a} \quad [168]$$

Irwin energy release. The final fundamental principle of elastic fracture mechanics that will be discussed, before moving onto asphalt materials related development, is the Irwin energy release (1956). While the theory is very similar to Griffith's work, the form is much easier to solve for in engineering applications. Here, Irwin defined an energy release rate, G , that is dependent on the strain energy (U) and the work done by external forces (F), as seen in Equation [169].

$$G = -\frac{d\Pi}{dA} = -\frac{d(U - F)}{dA} \quad [169]$$

For an elastic body, the strain energy is simply the load multiplied by the displacement divided by two, while the external force is the load multiplied by the displacement. This allows for the area under the load/displacement curve to be divided by the area of the formed crack in order to find the energy. For an elastic material, a relationship between the energy release rate and stress intensity factor can be established with Young's modulus, as seen in Equation [170].

$$G = \frac{K_I^2}{E} \quad [170]$$

Elastic fracture in asphalt materials. With these fundamental principles of elastic fracture mechanics established, some examples of the principles applied to asphalt materials can be examined. These relatively early studies assume that asphalt concrete is a linear elastic material, which only occurs when the temperature is near or below the glass transition temperature of the asphalt binder. However, the concepts are still of interest to show how the field of cracking of asphalt materials has developed over the years.

In order to develop a crack growth law, Majidzadeh *et al.* (1972) began with Paris' law ($dc/dN = AK^n$). Next, they utilized the stress fields ahead of a crack tip to develop the fatigue life in Equation [171].

$$N_f = \int_{c_o}^{c_f} \frac{1}{A \times K^n} dc \quad [171]$$

where; N_f = number of cycles to failure, c = crack depth (initial and at failure), A and n = material constants, and K = stress intensity factor

This preliminary work demonstrated that Paris' law and the crack growth law showed promise in predicting fatigue life of asphalt materials, and was able to show the effect of asphalt content, mixture density, and asphalt penetration values. A second study that utilized linear elastic fracture (Sulaiman and Stock, 1995), compared LEFM to elastic-plastic data using the J-integral. Among other findings, the research found the relationship between K_I and RAP content, as seen in Figure 90.

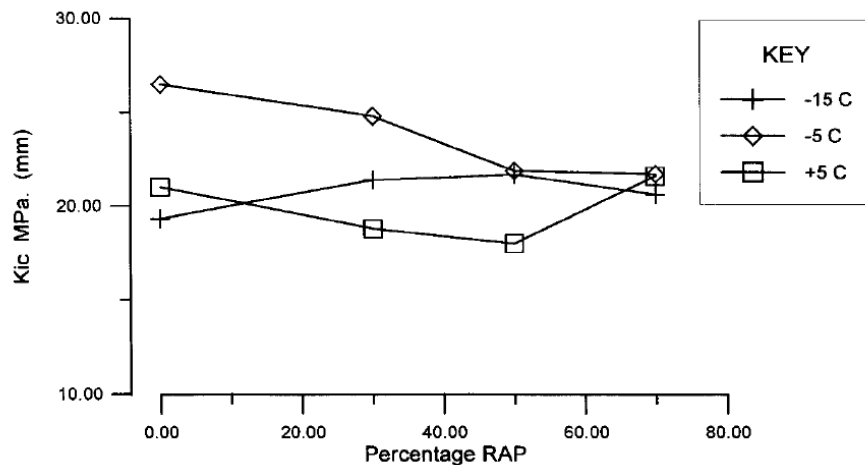


Figure 90. Stress intensity factor versus RAP content and temperature (from Sulaiman and Stock, 1995).

The conclusion from Figure 90 was that the quantity of RAP does not have an effect on the stress intensity factor, regardless of the testing temperature. In addition, they were not able to collect stress intensity factor data at temperatures greater than +5°C, as they postulated that the plastic zone at the crack tip became too large to apply the linear elastic theory. A key conclusion from this study, however, was that the stress intensity factor is not constant, which implies that it is improper to model asphalt materials using elastic fracture theory.

6.4.2. Distributed Continuum Fracture (DCF)

Overview. Cracking in a material that is loaded repeatedly is the net result of fracture and healing. Distributed Continuum Fracture (DCF) uses the fact that asphalt mixtures are built with a distribution of air voids of various sizes. It then develops criteria for the growth and coalescence of these air voids into increasingly larger distributed cracks. The mechanics rule for the growth of these cracks has the same form as Paris' Law and demonstrates the importance for mixture performance of initial air voids and the surface free bond energy and its sensitivity to moisture and aging. Figure 91 summarizes the timeline of the development of the DCF, the key elements, and relevant literature.

Table 8 summarizes the testing equipment and the brief times required to measure the DCF properties. They are complemented by the DCF healing properties which are the counter-fracture material properties of an asphalt mixture. The viscoplastic properties of an asphalt mixture are used to predict the permanent deformation and are determined using the same testing equipment and mechanics approach.

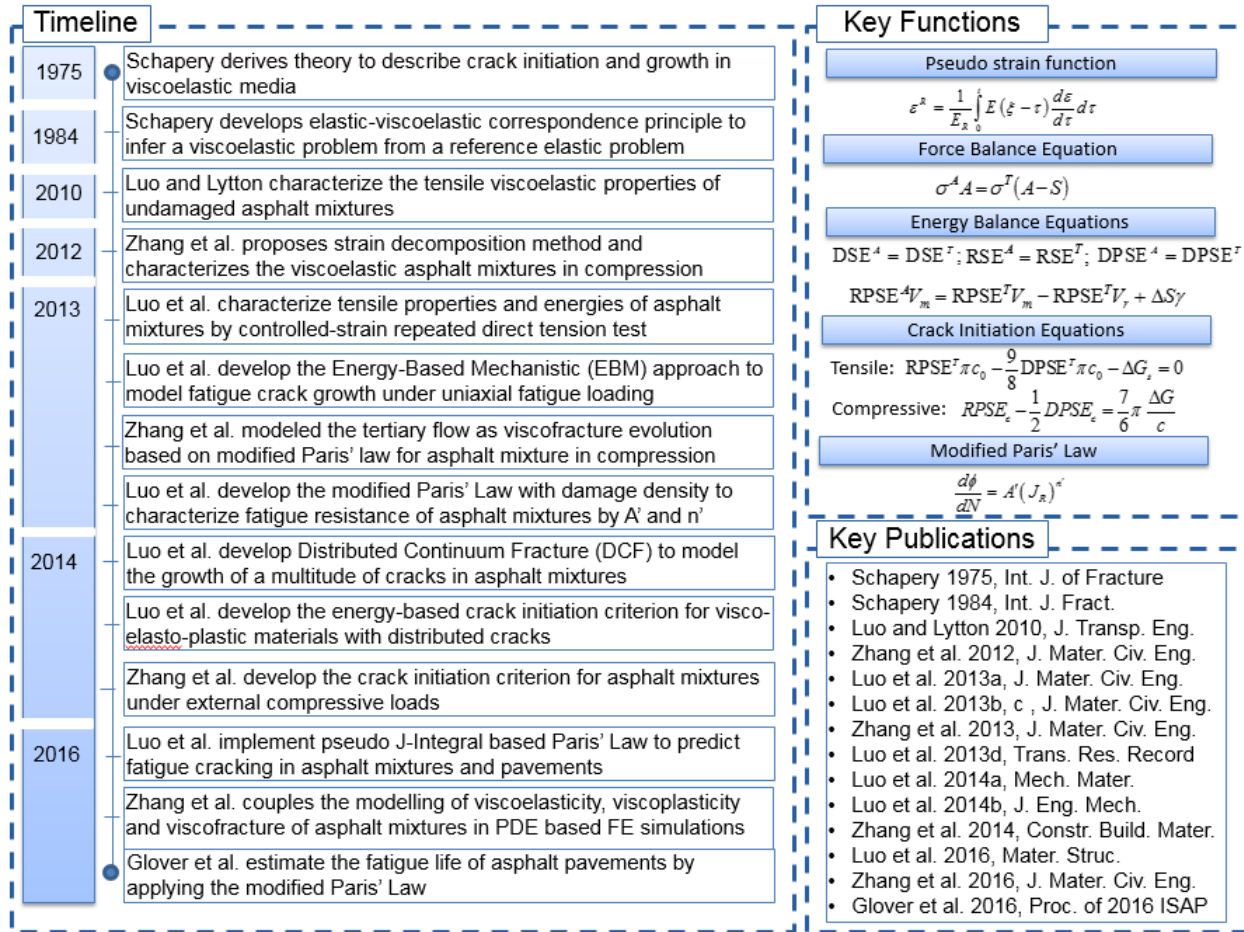


Figure 91. Summary of the Distributed Continuum Fracture (DCF).

Distributed Continuum Fracture Principles

The core principles governing the DCF approach include the balance equations, crack initiation criteria, crack growth criteria, and the need for related material properties.

Balance Equations (Force Balance). The force equilibrium principle states that the apparent force assumed to be carried by the entire cross section of the specimen equals the true force carried by the intact material (Luo *et al.*, 2013b; 2013c; 2014a; 2014b):

$$\sigma^A A = \sigma^T (A - S) \quad [172]$$

where; σ^A = apparent stress measured from the test, A = cross sectional area of the specimen, σ^T = true stress in the intact material, and S = total area of cracks on the cross section of the specimen.

Balance Equations (Energy Balance). The energy balance principle states that any kind of true energy within the intact material equates to its counterpart from the apparent measurement. This is because only the intact material can store, release and dissipate energy while cracks cannot. The energy balance is established for four types of energy (Luo *et al.*, 2013b; 2013c; 2014a; 2014b):

- dissipated strain energy (DSE), which represents the energy dissipated in a loading cycle due to the viscoelastic effects of the material and possible cracking and permanent deformation;
- recoverable strain energy (RSE), which represents the stored energy that can be recovered after removing the load;
- dissipated pseudo strain energy (DPSE), which represents the energy dissipated only for developing cracking and permanent deformation with removal of all of the viscoelastic effects; and

- recoverable pseudo strain energy (RPSE), which represents the stored and recovered energy corresponding to the elastic effect of the material after removing all of the viscoelastic effects.

The balance equations established for the above four types of energy are listed as follows:

$$1) \text{ DSE balance equation: } DSE^A = DSE^T \quad [173]$$

$$2) \text{ RSE balance equation: } RSE^A = RSE^T \quad [174]$$

$$3) \text{ DPSE balance equation: } DPSE^A = DPSE^T \quad [175]$$

$$4) \text{ RPSE balance equation: } RPSE^A V_m = RPSE^T V_m - RPSE^T V_r + \Delta S \gamma \quad [176]$$

where; V_m = volume of the asphalt mastic in one layer of the asphalt mixture specimen, whose thickness equals the mean film thickness; V_r = volume of the asphalt mastic that is subjected to a relaxation process and releases RPSE during the crack growth, which is calculated by:

$$V_r = \frac{2}{3} M_N \pi^2 \bar{c}_N^3 - \frac{2}{3} M_I \pi^2 \bar{c}_I^3 \quad [177]$$

where; \bar{c}_I and \bar{c}_N are average initial crack size before crack growth and average new crack size after crack growth, respectively; M_I and M_N are the number of initial cracks and number of new cracks, respectively; γ is the surface energy density; and ΔS is the area of all newly created cracks, which is expressed as:

$$\Delta S = 2 M_N \pi \bar{c}_N^2 - 2 M_I \pi \bar{c}_I^2 \quad [178]$$

Crack Initiation Criteria (Tensile Loading). A general form of energy-based crack initiation criterion for visco-elasto-plastic materials is (Luo *et al.*, 2014b):

$$\frac{d \left[w_r^R V_r - (w_n^R V_n + \gamma A_s) \right]}{dA_s} = 0 \quad [179]$$

where; w_r^R = released pseudo strain energy in the local energy release zones, V_r = total volume of the local energy release zones, w_n^R = consumed or dissipated pseudo strain energy in the local nonlinear zones, V_n = total volume of the local nonlinear zone; γ = surface energy per unit area, and A_s = crack surface area. In a tensile repeated load test, the general form becomes:

$$RPSE^T \pi c_0 - \frac{9}{8} DPSE^T \pi c_0 - \Delta G_s = 0 \quad [180]$$

where ΔG_s = bond energy, which equals 2γ and very sensitive to moisture and aging.

Crack Initiation Criteria (Compressive Loading). The same principle of Equation [179] was used to derive the crack initiation in compression. The only difference under compressive loading lies in the different V_r and V_n from that in tension. The crack initiation criterion in compression is defined by (Zhang *et al.*, 2014)

$$RPSE - \frac{1}{2} DPSE = \frac{7}{6} \pi \frac{\Delta G}{c} \quad [181]$$

where; $RPSE = (\sigma_{11}^2 + \sigma_{22}^2 + \sigma_{33}^2)/(2E_R) + 2(1+\nu_R)(\sigma_{12}^2 + \sigma_{23}^2 + \sigma_{13}^2)/E_R$ = recoverable pseudo-strain energy (density), E_R , and ν_R = reference modulus and Poisson's ratio which are derived to be Young's modulus and elastic Poisson's ratio. $DPSE$ = dissipated pseudo-strain energy (density) due to the accumulation of the VP deformation, and $DPSE = \int_0^t \sigma_{ij} \dot{\epsilon}_{ij}^{vp} dt$, and c = average air void radius that is also the critical crack size at which crack starts to grow, and one has (Zhang *et al.* 2014):

$$c = 0.0037(\%AV)^2 + 0.0071(\%AV) + 0.5583 \quad R^2 = 0.7431 \quad [182]$$

where; $\%AV$ = air void content of asphalt mixture in percentage. ΔG = bond energy of the asphalt mixture, which represents a combined bond energy for cohesive fracture and adhesive fracture. A higher temperature induces more percentage of cohesive fracture and therefore leads to a lower bond energy for the mixture.



Crack Growth Criteria (*Repeated Tensile Loading and Creep Tensile Loading*). Damage density is the ratio of the total area of cracks on a cross section to the cross sectional area. The total area of cracks consists of the pre-existing flaws and the newly created crack surface due to crack growth. Based on the characteristics of the number of cracks as they vary with the increasing number of repeated loads, the cracking history of a multitude of distributed cracks is divided into three phases (Luo *et al.* 2014a):

- I. Formative phase: more and more microcracks are generated and the size of microcracks increases;
- II. Coalescent phase: the microcracks start to merge and coalesce when the size increases to a specific value, and the number of cracks reaches its peak value. After that, the number of cracks keeps decreasing while the microcracks continue coalescing.
- III. Unitary phase: at the end of the coalescent phase, microcracks have formed a few macrocracks, which dominate the failure of the material and structure.

The modified Paris' law is formulated based on the damage density to simulate the growth of a multitude of cracks in asphalt mixtures. The formulation is given by the following relationship (Luo *et al.*, 2013d):

$$\frac{d\phi}{dN} = A' (J_R)^{n'} \quad [183]$$

where; ϕ = damage density; A' and n' = modified Paris' law parameters associated with the evolution of the damage density; and J_R = pseudo J integral

Crack Growth Criteria (*Repeated Compressive Loading and Creep Tensile Loading*). The same concept for damage density in tension is used to quantify the crack evolution of asphalt mixtures in compression. The modified Paris' law in Equation [183] is also employed to model the crack growth in compression (Zhang *et al.*, 2013). However different damage processes are identified in compression than that in tension due to significant viscoplastic deformation introduced before cracking. Three phases were also identified:

- I. Densification phase: air voids and flaws are compressed and tend to vanish due to the external compressive load. This corresponds to the primary stage in a repeated load test and the initial transition period in a monotonic load test. During this period, dynamic modulus increases and phase angle decreases.
- II. Viscoplastic phase: asphalt mixtures accumulate significant viscoplastic deformation during this period and become strain/work hardened. This corresponds to the secondary stage in the repeated load test and the before-peak yielding period in the monotonic load test. Dynamic modulus declines due to nonlinear viscoelastic and viscoplastic deformation, however phase angle remains unchanged.
- III. Viscoplastic phase: asphalt mixtures experience a saturated viscoplastic hardening at the end of phase II, thus the energy introduced by the external compressive load cannot be dissipated for plastic deformation, but has to be consumed for creating new cracks. This corresponds to the tertiary flow stage in the repeated load test and the after-peak softening period in the monotonic load test. Dynamic modulus declines in a much quicker rate and phase angle starts to increase.

Material Properties. There are several key undamaged and damaged material properties that need to be determined within the DCF. These properties are summarized in Table 7.

Table 7. Relevant Material Properties for the DCF.

Classification	Description
<i>Undamaged Material Properties</i>	
Tensile	Tensile complex modulus (magnitude and phase angle); Quasi-compressive complex modulus (magnitude and phase angle); Endurance limit
Compressive	Compressive complex modulus (magnitude and phase angle); Time-temperature shift factors
Surface Energy	Surface energy of cohesion; Surface energy of Adhesion
<i>Damaged Fracture Properties</i>	
Tensile	Damage density; Average crack size; Number of cracks; Modified Paris' Law coefficient A' and n' ; Cracking energy dissipation rate; Percentage of cohesive cracking; Percentage of adhesive cracking

Compressive	Internal friction angle; Cohesion; Strain hardening magnitude and rate; Activation energy for cohesion; Perzyna's viscosity and rate coefficients; Average crack size; Activation energy for mixture bond energy; Modified Paris' Law coefficients
-------------	--

Testing Equipment and Implementation.

The DCF parameters are characterized using material properties determined by experimentation. Table 8 summarizes the properties, test methods, required time (independent of any conditioning time), and test equipment for the DCF model.

Table 8. Testing Equipment and Time.

Material Properties	Test Methods	Time Required	Testing Equipment
Viscoelasticity	Nondestructive Repeated Direct Tensile Test	~ 5 min	Material Testing System (MTS)
	Compressive/Tensile Creep Test	~ 3 min	Universal Testing Machine (UTM) or MTS
	Dynamic Modulus Tests	~ 30 min	
Endurance Limit	Nondestructive Repeated Direct Tensile Test	~ 30 min	MTS
Viscoplasticity and Viscofracture	Uniaxial/Triaxial Strength Test	~ 5 min	UTM or MTS
	Destructive Repeated Compressive Load Test	< 2 hrs.	
	Destructive Repeated Direct Tensile Test	~ 16 min	MTS
Healing	Creep and Step-loading Recovery Test	~ 3 min	
Stiffness Gradient	Nondestructive Direct Tensile Test	~ 16 min	

Computer Prediction of Cracking. Cracking is the net result of fracture and subsequent healing. In the field, the stress state is neither pure tension nor pure compression, but a complex three dimensional stress. Furthermore, cracks and rutting can occur simultaneously and both contribute to permanent (irrecoverable) deformation. Modelling crack tip stress/strain field and simulating single crack growth make nonsense to asphalt pavement performance prediction as multiple and distributed cracks can be initiated under moving and repeated traffic loading. For a realistic computational prediction of asphalt pavements, the cracking damage (viscofracture) has to be coupled with viscoelastic and viscoplastic deformation via using the effective (true) stresses in constitutive relations, as presented in Zhang *et al.* (2016).

The coupling of multiple physics (viscoelasticity, viscoplasticity, viscofracture, healing, aging, etc.) in a computer program (e.g. Abaqus) has been achieved to an extent via coding user-defined material subroutine. However the issues caused by non-convergence, low-efficient iteration, and circular dependency have never been completely resolved, which has limited the practical applications of the advanced mechanics models. The weak form partial differential equation (PDE) based finite element technology has demonstrated a powerful capacity for multi-physics coupling (Zhang *et al.*, 2016). The viscoelastic-plastic-fracture (VDPF) models have been implemented in FE program to accurately predict mixtures' behaviors without a need of programming material subroutines.

Approximate Fatigue Equations. From a theoretical perspective, fracture mechanics can be used to predict N_f . One approach begins with the modified Paris' Law. Applying this law to the growth of the air voids with repeated loads, the number of load repetitions to reach failure is (Glover *et al.*, 2016):

$$N_f = \frac{(1-\phi_0)^{1-qn}}{A(r\sigma d)^n(1-qn)} \quad [184]$$

where; ϕ_0 = initial air voids content, r and q are calibration coefficients relating the J_{RI} to the damage density, σ = stress applied by the traffic, and d = thickness of the layer in which the cracks grow. If the changes of A and n with age are known, the effect of aging on N_f can be determined. Because A^{-1} in this equation is proportional to $(E\Delta G)^{1+n}\phi_0^{-0.5}$, the bond energy, ΔG , and initial air voids are important factors in fatigue fracture.

Summary

The objectives of the DCF model are as follows:

- By using measurable material properties in predicting fracture, not only rank mixture but predict how mixture will perform in different climates (e.g. solar radiation, relative humidity) by traffic loads.
- To determine, measure, and catalog mixture properties that can be used for specification limits.
- To make the prediction of the remaining life of pavements a reliable tool in pavement management and pavement design.

Within this model the important material properties are:

- Modified Paris' Law coefficients
- Bond energy and how moisture and aging change it
- Air voids
- Original undamaged tensile and compressive properties
- Endurance limit, crack growth criteria will set design and prediction criteria (healing criteria will permit the selection of the best of binder for heavy traffic pavements)

6.4.3. C* Fracture Test

The C* Fracture Test (CFT) was identified as a promising test to evaluate crack propagation and obtain the fracture mechanics based C* parameter, which considers the time-dependent creep behavior of the materials. This section describes the development and adaptation of this test for asphalt concrete. Figure 92 provides an overview and summary of this development effort.

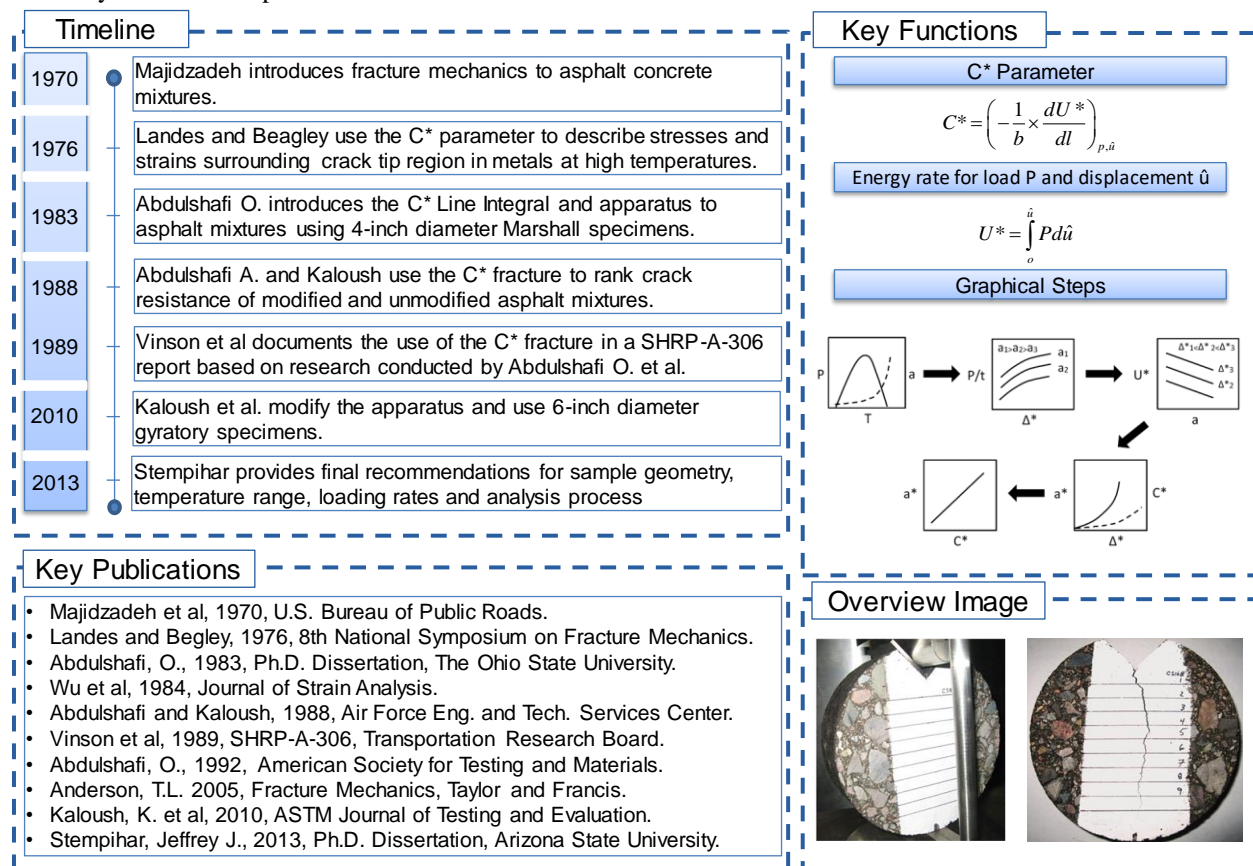


Figure 92. Summary of development of C* Line Integral test.

The C Line Integral.* The CFT has been used to a limited extent in asphalt concrete cracking evaluation and was identified as a promising test method (Vinson *et al.*, 1989). The test provides a fracture mechanics parameter (C*) and also the crack growth rate (a*). The C* parameter obtained from this test considers the time-dependent

behavior of asphalt and can be converted to the stress intensity factor (K) when elastic behavior of asphalt concrete prevails at low temperatures. Since its application to asphalt mixtures by Abdulshafi (1983), the C^* Line Integral has been used to successfully rank crack resistance of asphalt pavements with modified and unmodified asphalt [Abdulshafi, 1983; Abdulshafi and Kaloush, 1988; Kaloush *et al.*, 2010). Recently, a standard test procedure was documented along with a refined data analysis process (Stempihar, 2013).

C^* Parameter. The C^* parameter was first applied to fracture mechanics by Landes and Begley (1976) to describe the stresses and strains surrounding the crack tip region in metals at high temperatures. C^* can be described as an energy rate line integral that describes the stress and strain rate field surrounding the crack tip in a viscous material. This parameter was developed based on the J -integral which describes the crack tip conditions in elastic or elastic-plastic materials (Landes and Begley, 1976; Wu *et al.* 1984; Anderson, 2005). However, the C^* parameter can provide a more general case for materials that exhibit brittle and creep fracture (Abdulshafi, 1992). For stationary steady-state creep conditions, C^* is a parameter which relates the creep power dissipation rate to crack propagation (Wu *et al.*, 1984). It is important to note that this parameter assumes a nonlinear and steady-state creep law, which means that C^* is only applicable to long-term behavior. In addition, the authors note that C^* is not applicable to characterize creep crack growth in all ranges of cracking behavior.

Experimental measurement of C^* can be accomplished due to the relationship between the J -integral and C^* parameter. J is defined as the energy difference between two specimens that have incrementally differing crack lengths for the same applied load. In comparison, C^* can be calculated as power or energy rate difference between two specimens, loaded the same, with incrementally differing crack lengths (Landes and Begley, 1976). Given two identical specimens with different crack lengths, C^* is a measure of the change in power necessary to propagate each crack a distance of “ dl ” within the material. Mathematically, C^* can be expressed by Equation [185]. Since potential energy is a function of crack length, load and displacement, the partial derivative must be taken for a fixed load (P) and displacement (\dot{u}). The potential energy can be found as the area under the load-displacement rate curve for any given specimen (Landes and Begley, 1976). Equation [185] presents the calculation of the C^* parameter (Abdulshafi 1983).

$$C^* = \left(-\frac{1}{b} \times \frac{dU^*}{dl} \right)_{p, \dot{u}} \quad [185]$$

where; U^* = power or energy rate for a given load, P and displacement \dot{u} , given by, Equation [186] and b = specimen thickness.

$$U^* = \int_0^{\dot{u}} P d\dot{u} \quad [186]$$

Experimental evaluation of the C^* method can be accomplished using the graphical method proposed by Landes and Beagley (1976) and summarized in the following steps which are shown graphically in Figure 93.

1. For static loading, plot load (P) and crack length (a) as a function of time.
2. Use Step 1 data to plot load divided by specimen thickness (P/t) versus displacement rate (Δ^*) for each incremental crack length (a). The area under each P - Δ^* curve per incremental crack length represents the power or energy rate (U^*).
3. Plot U^* versus crack length for each displacement rate. C^* is taken as the slope of a linear fit of these data.
4. Plot C^* and a^* versus displacement rate, and
5. Plot the crack growth rate (a^*) as a function of C^* on a log-log plot.

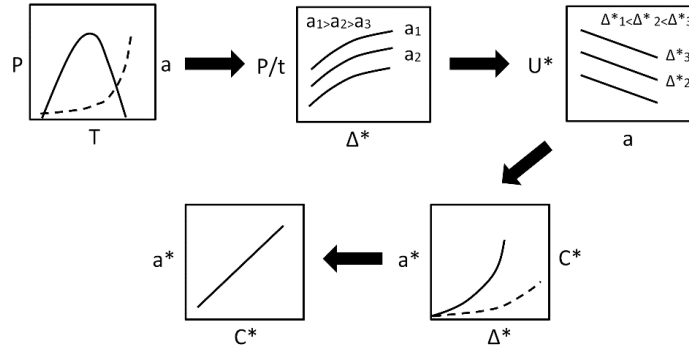
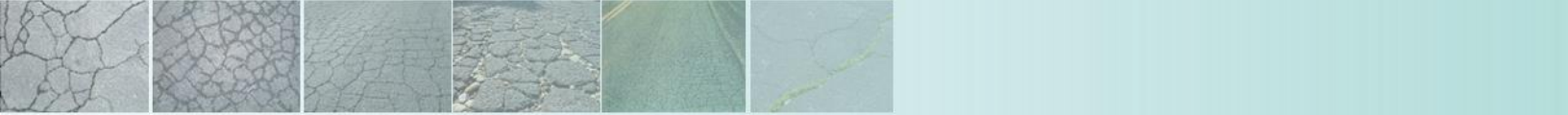


Figure 93. Graphical steps to determine C^* parameter.

C^* Fracture Test Setup. The CFT apparatus is based partially on the setup developed by Abdulshafi (1983) and modified by Kaloush *et al.* (2010). Two stainless steel loading plates (3 mm thick) with right-angled edges are used to form the loading plates placed in the right angle, notched cut. Loading is transferred to the specimen using a modified Lottman Breaking Head that applies a point load at a distance halfway along each notch face. Figure 94 presents a schematic of the CFT apparatus and photo of an actual specimen loaded into the apparatus. Frictionless lubricant is applied to the faces of the plates which contact the loading head. The dimensions of the modified loading head which mounts to the top plate of the Lottman Breaking Head are presented in Figure 95.

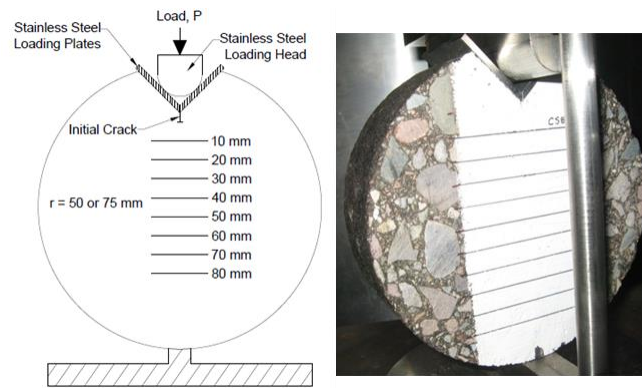


Figure 94. C^* Fracture Test setup.

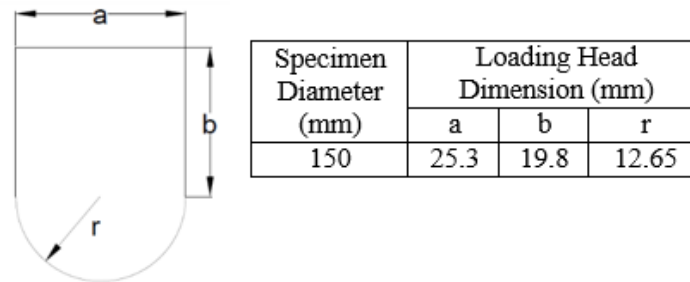


Figure 95. CFT loading head dimensions.

Specimen Preparation and Testing. Stempihar (2013) evaluated the specimen geometry for the CFT. CFT specimens are produced by cutting two 50 mm thick specimens from the center of a 150 mm diameter by 170 mm tall gyratory compacted sample. A right-angle notch (25 mm deep) was carefully cut into the specimen using a water-cooled diamond blade and a jig to hold the specimen. The specimen was rotated 45° in each direction from the vertical centerline to facilitate cutting the notch edges vertically. Next, a diamond coated scroll saw blade was used to introduce a 3 mm deep by 1.6 mm wide initial crack into the specimen. Finally, the specimen face was painted



white using acrylic paint and 10 mm incremental lines were marked on the specimen face to monitor crack progression during the test. Figure 96 presents the sequence of specimen preparation.

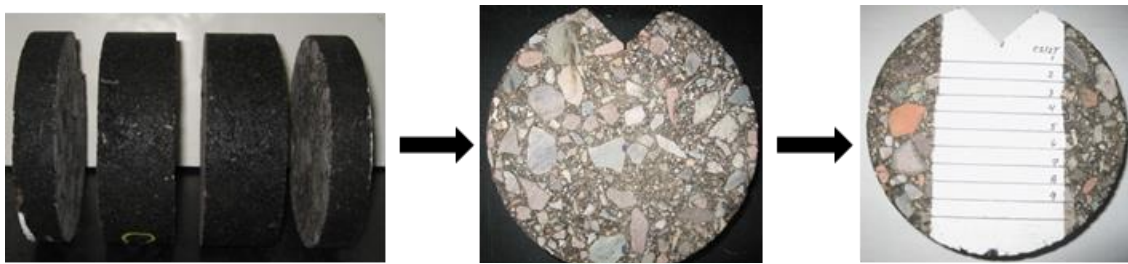


Figure 96. Specimen preparation sequence.

The CFT is conducted using a servo-hydraulic, Universal Testing Machine with 100 kN load capacity and environmental control chamber. Tests are conducted in the range of 4.4 - 10°C, with initial displacement rates of 0.15 and 0.30 mm/min, respectively. For each mixture, testing is carried out at a minimum of four loading rates with two replicates at each rate. Crack propagation rate is captured using a high definition digital video camera and crack length versus time measurements are extracted visually from video playback. Figure 97 presents an example of a cracked specimen at the completion of a test.

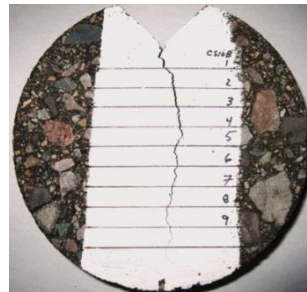


Figure 97. Example of crack specimen at the completion of CFT.

Test Results Demonstration. Stempihar (2013) conducted CFT on a control and rubber modified mixtures with warm mix additives using a UTM-100 test equipment at 4.4°C and test data are presented in Table 9. Crack growth rate was plotted as a function of C^* for each mixture and is presented in Figure 98 and modeled using a power function. The author concluded that the PG64-22AR mixture exhibits better resistance to crack propagation compared to the PG76-22 unmodified mixture at 4.4°C. For a C^* value of 0.05 MJ/m²-hr, the crack propagation rates are 5.0 m/hr and 1.1 m/hr for the unmodified and asphalt-rubber mixtures, respectively. The CFT results, tested at 4.4°C, indicate that the test is able to capture differences in crack propagation between an unmodified and asphalt-rubber mixture.

Table 9. C^* and crack growth data for control and asphalt rubber mixtures.

Temp. (°C)	Mixture	Displacement Rate (mm/min)	Crack Growth Rate (m/hr)	C^* MJ/m ² -hr
4.4	PG76-22 WMA	0.150	1.13	2.207E-02
		0.228	1.41	3.705E-02
		0.264	4.46	4.420E-02
		0.300	5.62	4.981E-02
		0.378	8.17	5.861E-02
	PG64-22 AR WMA	0.300	0.81	3.282E-02
		0.450	1.18	5.215E-02
		0.600	1.30	7.301E-02
		0.750	1.86	9.537E-02
		0.900	3.62	1.179E-01

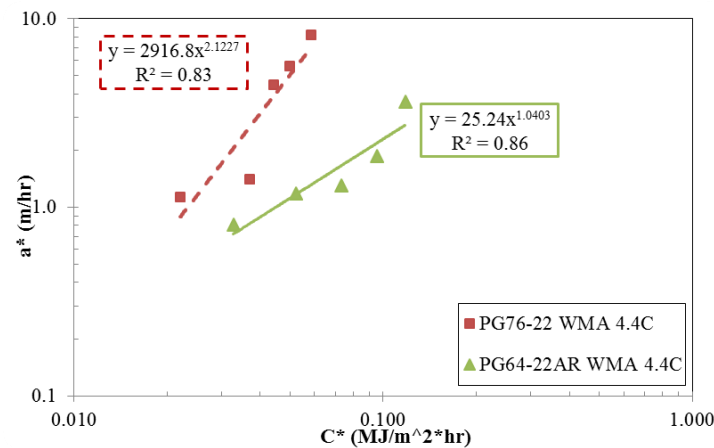


Figure 98. a^* - C^* relationship for the control and asphalt rubber mixtures.

7. Healing

While the majority of interest in cracking focuses on the development and propagation of cracks, an equally important component of fatigue is the ability of asphalt cement to self-heal, i.e., to erase the effects of micro-damage. The term healing can also be applied to indicate the recovery of mechanical properties after allowing a sample to rest for a period of time. However, this definition is imprecise as the viscoelastic nature of asphalt means that apparent recovery of mechanical properties can occur simply due to viscoelastic relaxation processes. Thus, in reviewing the literature one must be keenly aware of this fact in order to differentiate between true healing (according to the definition in the first sentence) and what can only be properly described as apparent healing.

The true healing phenomenon has been recognized to affect asphalt concrete behavior since at least the 1960's (Bazin and Saunier, 1967), and has been attributed as a key factor underlying the inability of laboratory experiments to match field fatigue cracking observations (Finn *et al.* 1977, Lytton *et al.* 1993). The phenomenon with respect to asphalt concrete mixtures has been studied extensively in the literature (Raithby, 1972; Witczak, 1976; Babissi, 1983; Kim *et al.*, 1990; Little *et al.*, 1997; Lee and Kim, 1998; Carpenter and Shen, 2006; Kim and Roque, 2006). A physical basis for the phenomenon generally centers around the process suggested by Wool and O'Connor (DATE), wherein healing manifests in a series of five steps; (a) surface rearrangement, (b) surface approach, (c) wetting, (d) diffusion, and (e) randomization. Little *et al.* (1997) and Little and Bhasin (2007) provide a detailed overview of the Wool and O'Connor approach, but even without the details it is clear based on the fact that diffusion takes place that healing is a time and temperature dependent process. Ayer *et al.* (2016) also provide an overview of the key factors that affect this phenomenon.

The specific nature of this process is asphalt binder dependent, but Kim *et al.* (1990) found correlations between a healing index and the presence of longer and less branched aliphatic hydrocarbons. Bhasin *et al.* (2011) used molecular dynamics simulations to investigate the effect of binder molecule characteristics and also found correlations between self-diffusion and chain length and branching. Little *et al.* (2001) reports on healing from a surface energy viewpoint and reports strong correlations between the rate of healing and the nonpolar components of the surface energy (long-term healing rate) and the acid-base component of the surface energy (short-term healing rate). Bommavaram *et al.* (2009) attempted to characterize these rates by measuring the change in deformation resistance with a dynamic shear rheometer over time between two initially separated asphalt binder surfaces and was able to detect differences in fast and slow healing rates for five different asphalts.

7.1. Continuum Damage Healing

Overview. Most healing theories are inherently limited to conditions where continuum theories apply. When cracks localize the faces of the resulting macrocrack are often too far apart to facilitate the wetting and diffusion process. This behavior does not mean that healing is irrelevant in macrocracked bodies, in fact the zone at the tip of the crack may contain defects that are small enough that healing can take place. However, a majority of the approaches focus on this, pre-localization area (Kim *et al.*, 1990; Carpenter and Shen, 2006; Kim and Roque, 2006). The application

to bodies wherein the damage process is described using a continuum damage model began in the work of Kim (1988) who used the pseudo strain concept to calculate the magnitude of pseudo strain energy recovered during a rest period. The pseudo strain approach was used to eliminate the time-dependent relaxation (what they referred to as mechanical healing) and isolate only the true healing (they referred to as chemical healing).

Lee and Kim (1998) were the first to incorporate healing into the then current version of the VECD model. The authors performed experiments wherein a rest period was introduced after the application of several cycles of load (referred to herein as group-rest experiments). The key experimental observation was that during the rest periods the pseudo-stiffness, C , would increase, and upon reloading it would continue to decrease. The decreasing pattern was found to occur at a faster rate until the pseudo-stiffness that existed before the rest period was reached. At this point the pseudo-stiffness would continue to decrease in the same pattern as the unhealed material. They postulated that the re-damage of healed material constituted a second type of damage and therefore introduced a second damage parameter into the VECD formulation. This second damage parameter, S_2 , carried the same form as the primary damage parameter, e.g., Equation [134]. They also hypothesized that the increase in pseudo-stiffness during the rest period would constitute a third type of material state, and formulated a healing function based on the change in the pseudo-stiffness with respect to this third state variable, S_3 . To verify their model random load tests where rest periods were introduced at random intermittent periods were conducted.

The inclusion of multiple state variables and pseudo stiffness terms complicates the use of Lee and Kim's formulation, and a simplification involving only a single damage function was proposed in Roque *et al.* (2010). The approach devised first consolidated the general patterns of healing that others recognized (Daniel and Kim, 2001; Kim *et al.*, 2002; Kim *et al.*, 2003) and are demonstrated in Figure 99. These patterns essentially suggest that healing results in an increase in the pseudo-stiffness of the material and that this increase is dependent upon the temperature and time (expressed as reduced time), the level of damage that existed at the time when the rest period began, S_k , and the amount of damage that had occurred since the previous rest period was introduced, ΔS_k .

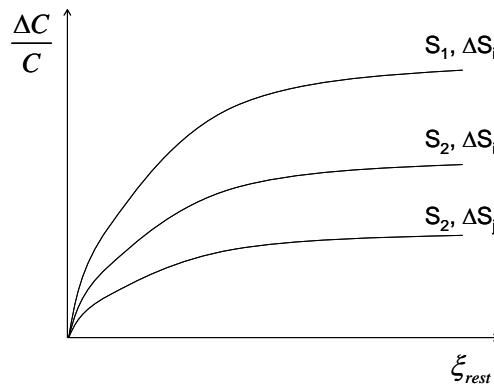


Figure 99. Effect of rest period on material healing.

The authors then formulate a single damage parameter version of Lee and Kim's model by devising a ratcheting scheme where damage increases during loading, but recovers during unloading according to the single damage characteristic function derived from non-rest period experiments (as in Section 6.3.1). The basic concept of the simplified model is schematically diagrammed in Figure 100. In this diagram the damage characteristic curve is shown for the first three cycles of loading. The points evenly labeled (0, 2, 4) represent the pseudo stiffness values at the beginning of load pulses 1, 2 and 3. The points labeled with the odd numbers 1, 3, and 5 represent the pseudo stiffness values at the end of load pulses 1, 2 and 3. The single damage parameter model will predict that during the first cycle damage will grow from point 0 to point 1. The simplified model would then suggest that during some rest period that the material would heal back to point number 2. Then when loading began for the 2nd cycle the damage would grow to point number 3. Upon resting after the end of the 2nd cycle healing would increase the pseudo stiffness to point number 4. Finally, after the 3rd loading cycle the damage would grow to point number 5. In total there are then three different segments where damage is assumed to occur in the virgin material; 1) from point 0 to point 1, 2) from point 1 to point 3 (2nd cycle), and finally from point 3 to point 5 (3rd cycle). Similarly there are only two different segments where damage is assumed to occur in the healed material; from point 2 to point 1 (2nd cycle) and from point 4 to point 3 (3rd cycle). Between all of these points though a single damage function, $C_1(S_1)$, is used to compute the damage.

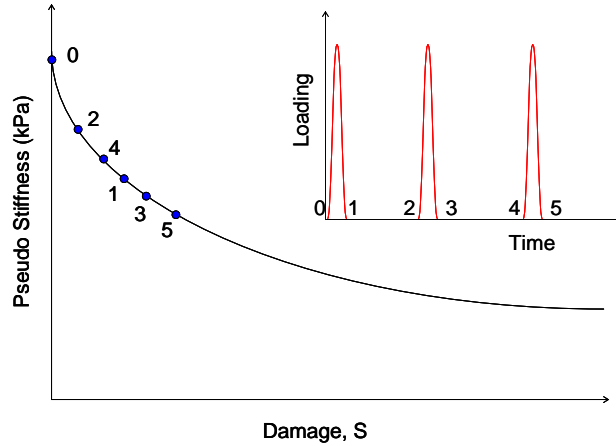


Figure 100. Simplified model conceptual schematic.

The model itself was characterized by first simulating a matrix of rest periods, damage levels, and damage increments using Lee and Kim's model and then regressing a function, Equation [187], to describe the change in pseudo stiffness during rest. During reloading the model would continue to grow damage according to the same damage function as before.

$$\frac{\Delta C_{Heal}}{C} = \frac{\kappa}{\left(1 + \left(\frac{\beta}{\xi_{rest}}\right)^{\gamma}\right)^{\frac{\delta}{\gamma}}} \quad [187]$$

where; $\kappa, \beta, \gamma, \delta$ = coefficients characterized from regression of Lee and Kim's model (see Roque *et al.*, 2010 for the details) and ξ_{rest} = duration of rest period in reduced time.

The Lee and Kim model and the resulting simplification described above have one key limitation in that the formulas are not bound and the model can mathematically predict pseudo stiffness increases beyond the initial, undamaged pseudo-stiffness of the material. When testing consists of groups of cycles followed by a rest period the shortcoming is not evident since each loading block will introduce a larger change in the total damage. However, Roque *et al.* (2010) demonstrated how a loading pattern with a single load pulse followed by a rest period (pulse-rest loading) could result in illogical predictions. As a result, they devised an empirical factor (referred to as a healing potential factor) that supposed the healing potential of asphalt diminished as it was damaged and re-damaged multiple times.

Karki (2014) presents a very similar ratcheting approach to healing, but in his case the healing of the material is tracked through a change in damage, S , instead of a change in pseudo-stiffness. Patterns of material recovery (e.g., increase of modulus after a rest period) are experimentally observed and used to characterize the proposed healing functions. This model successfully predicted the damage-healing response of asphalt fine aggregate matrix. The loading was applied in a group-rest pattern, and no verification was presented with respect to pulse-rest loading.

While the issue of single loading pulse followed by a single rest period was evaluated extensively in the 1960's and 1970's, it has recently reemerged in two highly related studies. During NCHRP 9-44A, healing was a primary mechanism supporting the existence of an endurance limit. Zeiada (2012) proposed that the endurance limit was defined as the strain level for which the healing (in his case healing was defined as the combination of time-dependent relaxation and true healing) that took place during the rest period completely reversed the effect of damage during the pulse. Experiments were conducted using three mixtures and multiple rest periods in order to characterize a regression model to predict the strain value at which this balance took place.

Underwood and Zeiada (2014) used this same data to propose a so-called smeared healing model where the effect of rest period was implicitly included in the damage function. In this approach, fatigue experiments with rest periods were used to establish the damage characteristic function (C vs. S function) of the S-VECD model. Mathematically the process involved modifying the pseudostrain function to account for the pulse-rest nature of loading. The authors demonstrate expected trends with respect to the effect of healing (e.g., greater impact from longer rest periods and high temperatures).

Ashouri (2014) investigated both pulse-rest loading and group-rest loading. With respect to group-rest loading a mechanistic-phenomenological approach consisting of a horizontal shifting scheme to develop healing mastercurves as a function of pseudo stiffness recovery, rest period, and increment of damage were devised. For pulse-rest loading, Ashouri combined the smeared damage approach with a phenomenological observation of similarities between the resultant smeared damage functions. A shift factor was introduced into the damage rate function, see Equation [188], in order to provide a complete damage function inclusive of any specified rest period, RP_R .

$$\frac{dS}{d\xi} = h(C, RP_R) \left(-\frac{\partial W^R}{\partial S} \right)^\alpha \quad [188]$$

7.2. Distributed Continuum Healing

Overview. Cracking in a material is the net result of fracture under repeated loading and healing between load applications. Distributed Continuum Healing (DCH) uses the fact that asphalt mixtures are constructed with numerous air voids of various sizes which grow in size with repeated loading and which close and heal during the rest period between load applications. Designing asphalt mixtures to resist cracking requires the selection of a combination of binder and aggregate that not only resists fracture but also heals quickly during rest periods. Much of the well-known lab-to-field fatigue life shift factor is due to healing. Using the healing tests and analysis described here it is possible to select the best binder to heal quickly under heavy traffic conditions and thus achieve the maximum extension of the fatigue cracking life of that pavement. The tests that measure the healing properties are rapid (a matter of minutes) using commercial standard equipment. Healing rate predictions use the undamaged properties of a mixture in tension. Figure 101 summarizes the timeline of the development of the DCH, the key elements, and relevant literature.

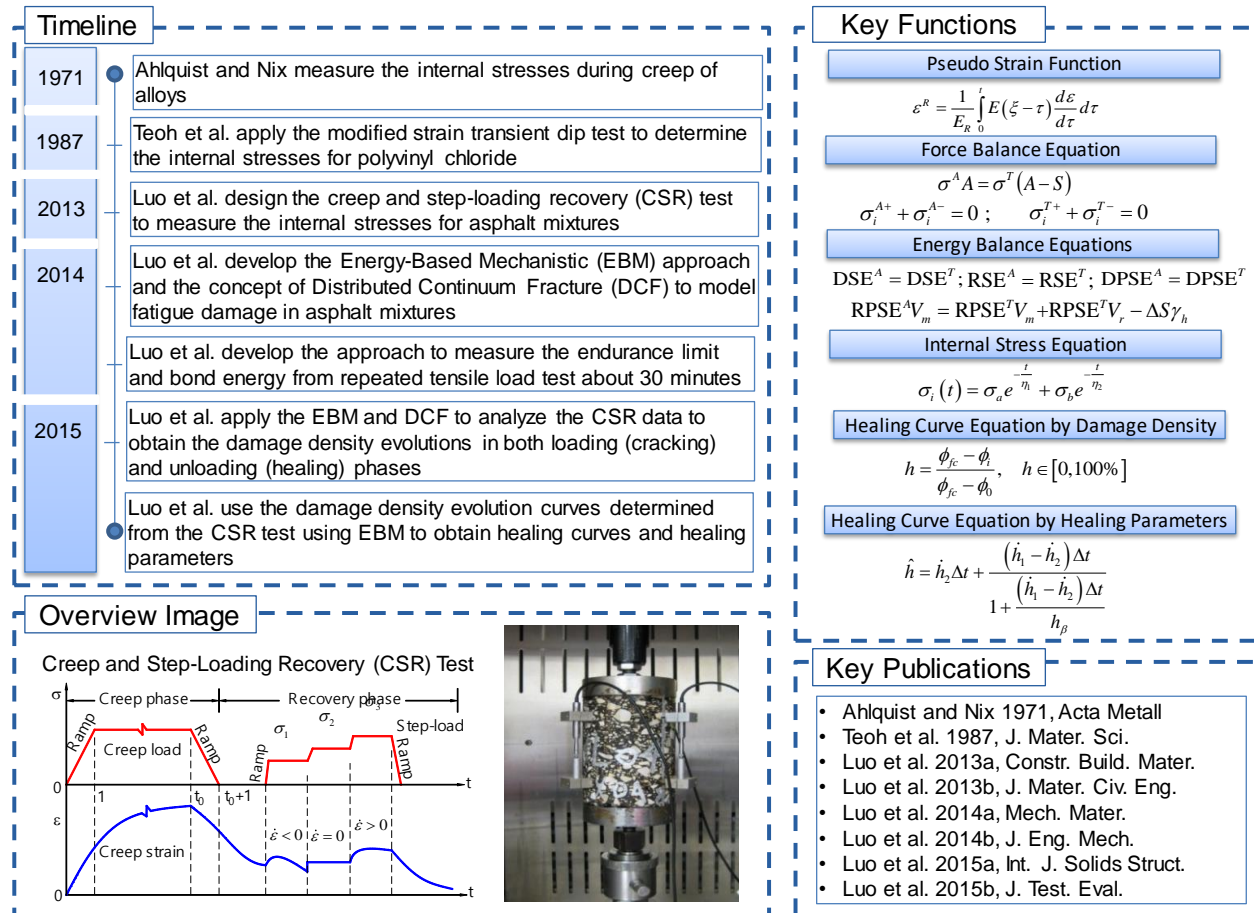


Figure 101. Summary of the DCH.

Distributed Continuum Healing Principles

The key principles governing the DCH model are the physical mechanisms responsible for the healing, the balance equations,

Healing under Internal Stress and Intermolecular Forces (Relationship between Healing and Recovery). Healing occurs after removing the external load on a damaged material so it usually accompanies the recovery of the material. To better distinguish healing and recovery, a composite material like an asphalt mixture is divided into the intact material (asphalt binder plus aggregates) and air voids or cracks. The recovery of the intact material is defined as “true recovery”. The recovery of a damaged bulk material is defined as “apparent recovery”, which is comprised of the true recovery and healing (Luo *et al.*, 2015a).

Healing under Internal Stress and Intermolecular Forces (Recovery and Internal Stress). Recovery of both undamaged and damaged asphalt mixtures has been studied using creep and step-loading recovery (CSR) tests (Luo *et al.*, 2013). The CSR test is designed especially to measure the internal stress that drives the recovery of an asphalt mixture after unloading. The internal stress that drives the apparent recovery of a bulk damaged asphalt mixture is defined as “apparent internal stress”. The internal stress that drives the true recovery of the intact material is defined as “true internal stress”.

Healing under Internal Stress and Intermolecular Forces (Driving Forces of Healing). During the process of healing, the energy redistribution is (Luo *et al.*, 2015a):

- The energy is restored in the intact material above and below the crack; and
- The energy is released from the closed crack surfaces.

The energy restored is the work done by the true internal stress in the intact material. The energy released equals the surface energy. In other words, it is the work done by the interfacial force of attraction. Therefore, there are two forces involved in the healing process: the true internal stress and the interfacial force of attraction. Both of them contribute to the energy interchange and drive the increase of the contact area between the crack surfaces.

Balance Equations (Force Balance). In the loading phase, the force equilibrium principle states that the apparent force assumed to be carried by the entire cross section of the specimen equals the true force carried by the intact material:

$$\sigma^A A = \sigma^T (A - S) \quad [189]$$

where; σ^A = apparent stress measured from the test, A = cross sectional area of the specimen, σ^T = true stress in the intact material, and S = total area of cracks on the cross section of the specimen. Note that this is the same force balance function used in the DCF model.

In the unloading phase, the apparent internal stress and true internal stress are self-balanced (Luo *et al.* 2015a):

$$\sigma_i^{A+} + \sigma_i^{A-} = 0 \quad [190]$$

$$\sigma_i^{T+} + \sigma_i^{T-} = 0 \quad [191]$$

where; σ_i^A = apparent internal stress, σ_i^T = true internal stress, and the superscripts “+” and “-” denote the stress above a plane and below a plane, respectively.

Balance Equations (Energy Balance). The energy balance principle states that any kind of true energy within the intact material equates to its counterpart from the apparent measurement. This is because only the intact material can store, release and dissipate energy while cracks cannot. In the loading phase, energy is dissipated due to the viscoelastic effect of the asphalt mixture and the damage generated in the material, called dissipated strain energy (DSE). By replacing the strain with the pseudo strain to eliminate the viscoelastic effect from the DSE, the remaining energy represents the energy expended for the damage generated in the mixture, called dissipated pseudo strain energy (DPSE). The balance equations established in the loading phase are:

1) DSE balance equation: $DSE^A = DSE^T$ [192]

2) DPSE balance equation: $DPSE^A = DPSE^T$ [193]

In the unloading phase, the strain energy originally stored in the material recovers with time. This part of strain energy is called recoverable strain energy (RSE). After removing the viscoelastic effect from the RSE using the pseudo strain, the remaining energy, called recoverable pseudo strain energy (RPSE), is the stored and recovered energy corresponding to the elastic effect of the material. The balance equations established in the unloading phase are (Luo *et al.*, 2015a):

$$1) \text{ RSE balance equation: } RSE^A = RSE^T \quad [194]$$

$$2) \text{ RPSE balance equation}$$

$$RPSE^A V_m = RPSE^T V_m + RPSE^T \left(\frac{2M_{lh}\pi^2 c_{lh}^3}{3} - \frac{2M_{Nh}\pi^2 c_{Nh}^3}{3} \right) - \gamma_h (2M_{lh}\pi c_{lh}^2 - 2M_{Nh}\pi c_{Nh}^2) \quad [195]$$

where; V_m = volume of the asphalt mastic in one layer of the asphalt mixture specimen, c_{lk} = initial average crack size before healing, M_{lh} = number of initial cracks before healing, c_{Nh} = new average crack size after healing, M_{Nh} = number of new cracks after healing, and γ_k is the surface energy density for healing.

Measurement of Healing (Creep and Step-Loading Recovery Test). The CSR test is especially designed to measure the internal stress in an asphalt mixture (Luo *et al.*, 2013). It is the creep recovery test incorporated with several step-loads in the recovery phase. The internal stresses are measured by several step-loads in the recovery phase. There are three steps in each step-load, which cause the change of the strains at the corresponding point in time. The strain rate may be in one of the following three conditions, which indicates the relationship between the step-load and the internal stress:

- $\dot{\varepsilon}_r < 0$ at σ_1 : $\sigma_1 < \sigma_i$;
- $\dot{\varepsilon}_r = 0$ at σ_2 : $\sigma_2 = \sigma_i$;
- $\dot{\varepsilon}_r > 0$ at σ_3 : $\sigma_3 > \sigma_i$;

where; $\dot{\varepsilon}_r$ is the residual strain rate in the recovery phase; σ_1 , σ_2 , and σ_3 are the three steps in an increased order in any of the seven step-loads; and σ_i is the internal stress. According to the second condition, the internal stress is measured by the second step σ_2 . The measured internal stresses are fitted by an exponential model to produce a continuous curve:

$$\sigma_i(t) = \sigma_a e^{-\frac{t}{\eta_1}} + \sigma_b e^{-\frac{t}{\eta_2}} \quad [196]$$

where; t = recovery time (any time in the recovery phase), and σ_a , σ_b , η_1 , and η_2 = fitting parameters for the internal stress.

Measurement of Healing (Characteristics of Recovery Properties). The internal stress is used to define a new type of modulus: recovery modulus as follows (Luo *et al.*, 2013):

$$R(t) = \frac{\sigma_i(t)}{\varepsilon_r(t)} \quad [197]$$

where; $R(t)$ = recovery modulus, $\sigma_i(t)$ = internal stress, $\varepsilon_r(t)$ = strain in the recovery phase, called the residual strain, and t = recovery time. The recovery modulus of undamaged asphalt mixtures remains the same at different loading levels as long as the load is nondestructive. However, the recovery modulus becomes different when the asphalt mixture is damaged. This is because the apparent recovery measured from the test reflects the net effect of the true recovery and healing inside the tested specimen.

Measurement of Healing (Healing Curves and Healing Parameters). The healing curve is defined as the normalized extent of healing versus the rest time during which healing occurs. The normalized extent of healing is defined as (Luo *et al.*, 2015b):

$$h = \frac{\phi_{jc} - \phi_t}{\phi_{jc} - \phi_0}, \quad h \in [0, 100\%] \quad [198]$$

where; h = normalized extent of healing, ϕ_c is the initial damage density before healing starts, or equivalently the final damage density at the end of the creep phase, ϕ_i is the damage density at any data point i during the recovery phase, and ϕ_0 is the initial damage density, which equals the air void content. The healing curve shows that: the healing rate is very large at the beginning and then it gradually decreases and the change of the measured healing reduces as the rest time increases. To demonstrate such characteristics, a model in the form of the Ramberg-Osgood equation is proposed to simulate the healing curve:

$$\hat{h} = \dot{h}_2 \Delta t + \frac{(\dot{h}_1 - \dot{h}_2) \Delta t}{1 + \frac{(\dot{h}_1 - \dot{h}_2) \Delta t}{h_\beta}} \quad [199]$$

where; \hat{h} = predicted healing based on three parameters, \dot{h}_1 , \dot{h}_2 , and h_β ; \dot{h}_1 = initial healing rate, or short-term healing rate, representing the healing speed of the material at the initial stage of healing, \dot{h}_2 is the ultimate healing rate, or long-term healing rate, indicating the healing speed of the material after a long rest time, and h_β is the healing scale, reflecting the overall ability of the material to heal.

Prediction of Healing Environmental Effects. Healing parameters can be predicted using undamaged material properties, surface bond energy and relaxation modulus, and a mixture design parameter, the air void content, as shown in the equations below (Luo *et al.*, 2012). They indicate how the environmental conditions influence the healing properties as demonstrated by the change of the bond energy components, aging, and temperature.

$$\dot{h}_1 = a_1 \left(\frac{1}{\Delta G^{LW} E_1} \right)^{b_1 \kappa} \quad [200]$$

$$-\log(\dot{h}_2) = a_2 \left[-\log \left(\frac{\Delta G^{AB}}{E_1} \right) \right]^{b_2 \kappa} \quad [201]$$

$$h_\beta = a_\beta \left(\frac{\Delta G^{AB}}{\Delta G^{LW} E_1^2} \right)^{(1-h_0) b_\beta \kappa} \quad [202]$$

where; ΔG^{LW} = non-polar surface bond energy, ΔG^{AB} = polar surface bond energy, E_1 and κ = fitting parameters for the relaxation modulus of undamaged asphalt mixtures, ϕ_0 is the initial damage density, or the air void content, a_1 and b_1 = fitting parameters for \dot{h}_1 , a_2 and b_2 = fitting parameters for \dot{h}_2 and a_β and b_β are fitting parameters for h_β .

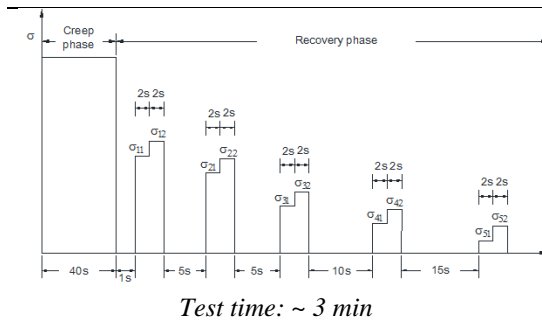
Testing Equipment and Implementation

The DCH parameters are characterized using material properties determined by experimentation. Table 10 summarizes the test method and required time (independent of any conditioning time) for the DCH model.

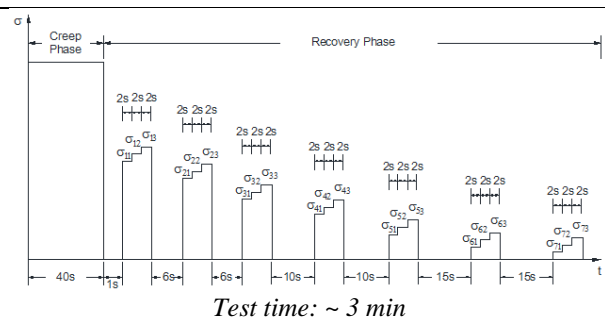
Testing Protocol and Time. The CSR test is conducted using a Material Test System (MTS). Every asphalt mixture specimen is subjected to two consecutive CSR tests: one is considered to be nondestructive and the other is destructive.

Table 10. Testing Protocols and Time in DCH Model.

Nondestructive Test	Destructive Test
---------------------	------------------



Step	Step-Load Number				
	1	2	3	4	5
1	25% P _N	20% P _N	12.5% P _N	7% P _N	3% P _N
2	50% P _N	35% P _N	25% P _N	15% P _N	6% P _N



Step	Step-Load Number						
	1	2	3	4	5	6	7
1	15% P _D	10% P _D	7% P _D	5% P _D	2.5% P _D	1.5% P _D	1% P _D
2	25% P _D	15% P _D	12.5% P _D	8% P _D	7% P _D	3% P _D	2% P _D
3	35% P _D	20% P _D	15% P _D	12.5% P _D	10% P _D	6% P _D	4% P _D

Implementation. The prediction formulas can be used to determine the environmental effects on healing. In the prediction equations of the healing parameters, bond energy can be measured directly in the endurance limit test (Luo *et al.*, 2014b). With the prediction of the short-term healing rate, the selection of a binder for heavy and light traffic pavement materials design require the smallest non-polar bond energy for heavy traffic conditions, and the largest polar bond energy for light traffic conditions.

Summary

The DCH model is developed based upon the principle that healing is predictable using undamaged tensile properties of a mixture and a knowledge of the bond energy components. The equations presented above can be used for a variation of the effects of rest periods, aging, air void content and temperature. Varying the bond energy with moisture allows that mechanism to be considered as well. Combined use of Paris' Law (fracture) and healing rest period (depending on traffic rate) will permit realistic estimate of the fatigue life of a pavement. Both Paris' Law coefficients and healing rate equations can be adjusted systematically to reflect the progressive effects of environmental conditioning. Together they predict the cumulative growth of the lost area.

8. Going Forward

As stated at the beginning of this document, the intent of this synthesis is not to promote a single experimental test or numerical model. It is meant to be a resource for readers to gain a deeper understanding about the important dates in the development of tools we have to quantify fatigue cracking of asphalt mixtures. What the synthesis does show is that there exists a great deal of information and expertise with respect to experiments and approaches to investigate fatigue cracking. Going forward one must ask if the future will bring still additional experiments to characterize fatigue in asphalt concrete, or if the field, with all of the expertise that this document clearly shows exists, is in a position to move forward. This document does not advocate for one strategy or another, but based on the synthesis some important broadly disseminated gaps in our knowledge exist.

8.1. Origins of Material Behavior

Much of the work identified in the preceding sections has focused on characterizing the fatigue behavior of asphalt concrete mixtures and binders. Conversely, relatively little work has been done to identify, characterize, and exploit the underlying mechanisms that drive the fatigue cracking process. During the summer of 2016, the National Science Foundation hosted a workshop in Beijing, China, that explored the concept of a material genome, and how this can be applied to asphalt materials. The term "genome" refers to the composition, microstructure, and inherent defects of a material. The proceeding sections show how there is not a consensus on any of these genome components. For example, much research on asphalt materials assumes that all PG64-22 binder is the same. While the binder may grade to the same binder type in the Superpave binder grading system, it is well known that not only the source of the crude oil influences the characteristics of the binder, but also the refining process. In recent years,



refineries have had to deal with the daily changing of crude oil sources, making it very difficult to produce consistent asphalt binder. This very basic perspective does not take into account polymer modification, the additional of supplementary binder materials such as Recycled Asphalt Pavement or Recycled Asphalt Shingles, or any chemical modifications for Warm Mix Asphalt or anti-stripping modification. Changes like these highlight how limited studies that only provide information on the response of materials to a particular loading condition can be. Failing to explain underlying and basic material behaviors means that as technologies change the findings from experimental and analytical studies however advanced they may be, will not be translatable.

The struggle continues when considering the microstructure of asphalt materials. In undergraduate courses, the students are taught that asphalt materials consist of aggregate, asphalt binder, and air. However, this is not true. Research has recognized that there is no such thing as pure asphalt binder in the mixture, it is a mastic that consists of very fine aggregate particles floating in the binder. There has been bulk characterization of this material, either in small cylinder form or even in the parallel plates of the dynamic shear rheometers, but it is treated as a bulk material, not as a heterogeneous mixture. The physical and chemical properties of the very fine aggregate, usually assumed to be P200 material, are not examined. Yet it is known that P200 gradation varies significantly based on aggregate source and the crushing technique used in the quarry. In addition, the chemical nature of the aggregate is not often accounted for, as all 12.5mm NMAS mixtures are assumed to be “the same.”

Finally, the concept of inherent defects is a source of question as well. Are inherent defects the air voids within a compacted asphalt mixture, or some weak spot in the mixture, caused either by material, production, or construction issues? At the end of the day, we know that cracks start by two surfaces opening, yet there is little to no work done at the atomic scale, as surfaces are simply a collection of atoms. Instead, elaborate tests and models are based on mixtures that can be compacted and tested in the laboratory, utilizing all the assumptions discussed in the previous two paragraphs.

This discussion is not meant to be discouraging, but should be a platform for discussion on the best path forward. Should we continue testing bulk material, or should we start drilling into the fundamental material properties of mixtures? Should we continue refining elaborate models based off bulk materials, or should we start exploring fundamental aggregate and asphalt binder adhesion and cohesion principles? What we have done in the previous chapters has led to a much stronger understanding of asphalt materials than we had twenty years ago, but there is more work to do.

8.2. Sensitivity

In addition to understanding the material genome of asphalt mixtures, there is also a high level of understanding of the sensitivity of both the tests and the numerical models. For example, it is common to accept 10-15% coefficient of variation for tests of asphalt mixtures, and this level often goes up to 30% or even 40% before questions are asked about the repeatability of tests. With this high level of repeatability, questions should be asked about the source of this variability. Does it come from the fact that asphalt mixtures are a heterogeneous material with a high level of inherent variability? For example, cracking tests often discuss how cracks sometimes move through aggregates and sometimes around, and depending on where specific aggregates are located within the sample, an energy value gained from a cracking test can have a high level of variation. Or, does the variability come from the machine? There is compliance in load frames, so labs aim to use external LVDT's to capture displacement. However, what sort of compliance does that introduce, and does the compliance also influence the load being recorded? These are just two examples, but it is apparent that a stronger understanding of variability in testing would be beneficial.

Along with testing, there is a significant lack of understanding of the reliability in models. This reliability can be both analytical reliability and ability to rely on the accuracy of resultant predictions. Both aspects are important. So many models that have been developed are not only based on a relatively small set of mixtures (perhaps a handful of gradations, some binders, and maybe some innovative materials or designs), but there is no follow through to see if long term the models are producing expected results in the field. With the exception of Pavement ME models, which are robustly investigated by state agencies, most research grade models do not have a high level of rigor associated with long-term reliability. Since the discipline of asphalt mixtures is so highly dependent of field performance, this is a significant shortcoming of many of the proposed models.

8.3. Case Studies, Specific Examples and Comparing Models across Technologies

Quite possibly, the largest shortcoming is the lack of comparison of these tests and models against each other. With some relatively rare exceptions, such as RILEM's fatigue cracking synthesis (Di Benedetto et al., 2004), Molennar's review (Molennar, 2007), Mogawer *et al.* (2015), and NCHRP's 9-57 (Zhou et al., 2016), very few labs



have attempted a comprehensive review of fatigue cracking tests. This is in part because of the immense need of capital to obtain the equipment, but also the vested interest that academics have in keeping tests developed in their lab salient in academic discussions. In addition, results from these tests have not been compared extensively across technologies. For example, the change in fatigue performance of the four-point bending beam test has not been compared to the trapezoidal test when 25% RAP has been added to the same mixture. If both of these tests product accurate fatigue cracking characterization, the influence of the addition of 25% should be the same. The same argument can be made for the models as well, as the influence of RAP has not been robustly compared between energy fatigue analysis and continuum damage models. Thus, in addition to the continual development and refining of these models, there should be a conscious effort to ensure that the models are telling the same story, and the tests are producing the same trends, as if they are not, they should be carefully vetted to determine the best path forward.



9. References

Section 1

- Di Benedetto, H., de La Roche, C., Baaj, H., Pronk, A., Lundström, R. (2004). Fatigue of bituminous mixtures. *Materials and Structures*, Vol. 37, pp. 202-216.
- Miller, J., Bellinger, W. (2003). Distress identification manual for the long-term pavement performance program. *Federal Highway Administration*, 4th Edition, FHWA-RD-03-031.
- Molenaar, A. (2007). Prediction of fatigue cracking in asphalt pavements, do we follow the right approach? *Transportation Research Record*, No.2001, pp. 155-162.
- Monosmith, C. (1994). Fatigue Response of Asphalt-Aggregate Mixes. *Strategic Highway Research Program*, SHRP-A-404, National Research Council, Washington, DC.
- Monosmith, C., Brown, S. (1999). Developments in the Structural Design and Rehabilitation of Asphalt Pavements over Three Quarters of a Century. *J. Assn. Asphalt Paving Technologists*, Vol. 68A, pp. 128-251.
- Zhou, F., Newcomb, D., Gurganus, C., Banihashemrad, S., Park, E., Sakhaeifar, M., Lytton, R. (2016). Experimental design for field validation of laboratory tests to assess cracking resistance of asphalt mixtures. *National Cooperative Highway Research Program*, NCHRP 9-57, draft final report.

Section 2

- Aguiar-Moya, J. P., Salazar-Delgado, J., Baldi-Sevilla, A., Leiva-Villacorta, F., and Loria-Salazar, L., "Effect of Aging on Adhesion Properties of Asphalt Mixtures with the Use of Bitumen Bond Strength and Surface Energy Measurement Tests," *Transportation Research Record: Journal of the Transportation Research Board*, Vol 2505, 2015, pp. 57-65.
- Arabani, M. and Hamed, G.H., "Using the Surface Free Energy Method to Evaluate the Effects of Polymeric Aggregate Treatment on Moisture Damage in Hot-Mix Asphalt," *Journal of Materials in Civil Engineering*, Vol. 23, No. 6, 2010, pp. 802-811.
- Cong, L., Peng, J., Guo, Z., and Wang, Q., "Evaluation of Fatigue Cracking in Asphalt Mixtures Based on Surface Energy," *Journal of Materials in Civil Engineering*, In Press. 2016.
- Bhasin, A., Masad, E., Little, D., and Lytton, R. (2006). "Limits on Adhesive Bond Energy for Improved Resistance of Hot-Mix Asphalt to Moisture Damage," *Transportation Research Record: Journal of the Transportation Research Board*, Vol 1970, 2006, pp. 3-13.
- Bhasin, A., Little, D., Vasconcelos, K., and Masad, E., "Surface Free Energy to Identify Moisture Sensitivity of Materials for Asphalt Mixes," *Transportation Research Record: Journal of the Transportation Research Board*, Vol 2001, 2007, pp. 37-45.
- Grenfell, J., Apeagyei, A., and Airey, G., "Moisture Damage Assessment using Surface Energy, Bitumen Stripping and the SATS Moisture Conditioning Procedure," *International Journal of Pavement Engineering*, Vol. 16, No. 5, 2015, pp. 411-431.
- Little, D.N., Bhasin, A., and Hefer, A.W., "Using Surface Energy Measurements to Select Materials for Asphalt Pavement," Report 316, National Cooperative Highway Research Program, Washington, D.C., 2006.
- Soenen, H., De La Roche, C and Redelius, P., "Fatigue Behavior of Bituminous Materials: From Binders to Mixes," *Road Material and Pavement Design*, Vol. 4, No. 1, 2003, pp. 7-27.
- Wasiuddin, N. M., Fogle, C. M., Zaman, M. M., and O'Rear, E. A. (2006). "Effect of Antistrip Additives on Surface Free Energy Characteristics of Asphalt Binders for Moisture-Induced Damage Potential," *Journal of Testing and Evaluation*, Vol. 35, No. 1, 2006, pp. 1-9.
- Wei, J., Dong, F., Li, Y., and Zhang, Y., "Relationship Analysis Between Surface Free Energy and Chemical Composition of Asphalt Binder," *Construction and Building Materials*, Vol. 71, 2014, pp. 116-123.

Section 2.1.1

- Anderson, D. A., Le Hir, Y. M., Marasteanu, M. O., Planche, J.-P., Martin, D., and Gauthier, G. (2001). "Evaluation of fatigue criteria for asphalt binders." *Transportation Research Record*, No.1766, 48-55.
- Andriescu, A., Hesp, S. A. M., and Youtcheff, J. S. (2004). "Essential and plastic works of ductile fracture in asphalt binders." *Transportation Research Record*, No.1875, 1-8.
- Bahia, H. U., Hanson, D. I., Zeng, M., Zhai, H., Khatri, M. A., and Anderson, R. M. (2001). *Characterization of Modified Asphalt Binders in Superpave Mix Design*, NCHRP Report 459, National Academy Press.
- Bahia, H. U., Zhai, H., Zeng, M., Hu, Y., and Turner, P. (2002). "Development of binder specification parameters based on characterization of damage behavior." *Journal of the Association of Asphalt Paving Technologists*, Vol. 70, 442-470.




- Bonnetti, K. S., Nam, K., and Bahia, H. U. (2002). "Measuring and defining fatigue behavior of asphalt binders." *Transportation Research Record*, No.1810, 33-43.
- Kim, Y. R., Little, D. N., D'Angelo, J., Davis, R., Rowe, G., Reinke, G., Marasteanu, M., Masad, E., Roque, R., Tashman, L., and Lytton, R. L. (2002). "Use of dynamic mechanical analysis (DMA) to evaluate the fatigue and healing potential of asphalt binders in sand asphalt mixtures." *J. Assn. Asphalt Paving Technologists*, Vol. 71, 176-206.
- Kim, Y., Lee, H. J., Little, D. N., and Kim, Y. R. (2006). "A simple testing method to evaluate fatigue fracture and damage performance of asphalt mixtures." *J. Assn. Asphalt Paving Technologists*, Vol. 75, 755-788.
- Kutay, M. E., Shenoy, A., and Qi, X., (2007). "Full-Scale Accelerated Performance Testing for Superpave and Structural Validation." Federal Highway Administration Turner-Fairbank Highway Research Center.
- Martono, W., and Bahia, H. U. (2008). "Developing a surrogate test for fatigue of asphalt binders." *Proceedings from the 87th Annual Meeting of the Transportation Research Board*, Vol.
- Martono, W., Bahia, H. U., and D'Angelo, J. (2007). "Effect of testing geometry on measuring fatigue of asphalt binders and mastics." *Journal of Materials in Civil Engineering*, Vol.19, No.9, 746-752.
- Pell, P. S. (1962). "Fatigue Characteristics of Bitumen and Bituminous Mixes." *Proceedings, International Conference on the Structural Design of Asphalt Pavements*, Vol. 1, 310.
- Shenoy, A. (2002). "Fatigue testing and evaluation of asphalt binders using the dynamic shear rheometer." *Journal of Testing and Evaluation*, Vol.30, No.4, 303-312.

Section 2.1.2

- Andriescu, A., Hesp, S.A.M., and Youtcheff, J.S. (2004). "Essential and Plastic Works of Ductile Fracture in Asphalt Binders," *Transportation Research Record 1875*, Transportation Research Board, National Research Council, Washington, DC.
- Broberg, K.B. (1975). "On Stable Crack Growth," *Journal of the Mechanics and Physics of Fatigue Fracture Using Double Edge Notched Tension Test (DENT)*," *MTO Laboratory Testing Manual*, Ontario Ministry of Transportation, Downsview, ON.
- Cotterell, B. and Reddel, J.K. (1977). "The Essential Work of Plane Stress Ductile Fracture." *International Journal of Fracture*, Vol. 13, Issue 3.
- Gibson, N., Qi, X., Shenoy, A., Al-Khateeb, G., Kutay, M.E., Andriescu, A., Stuart, K., Youtcheff, J. and Harman, T., (2012). *Performance testing for Superpave and structural validation* (No. FHWA-HRT-11--45).
- Huber, G. (2009). *Evaluation of Low Temperature Cracking of Hot Mix Asphalt Pavements in Ontario*, A report prepared for The Ministry of Transportation of Ontario and Ontario Hot Mix Producers Association, Ontario, Canada.
- Mai, Y.W. and Cotterell, B. (1980). "Effects of Pre-Strain on Plane Stress Ductile Fracture in a brass," *Journal of Materials Science*, Vol. 15, No. 9.
- MOT LS-299. (2009). "Method of Test for Determining of Asphalt Cement's Resistance to Ductile Failure Using Double Edge Notched Tension (DENT), Ministry of Transportation, Ontario, Laboratory Testing Manual, Rev. No. 27.
- Zhou, F., Li, H., Chen, P., & Scullion, T. (2014). Laboratory Evaluation of Asphalt Binder Rutting, Fracture, and Adhesion Tests. In *Report No. FHWA/TX-14/0-6674-1*. Texas A&M Transportation Institute College Park, TX.
- Zhou, F., Mogawer, W., Li, H., Andriescu, A. and Copeland, A., (2012). Evaluation of fatigue tests for characterizing asphalt binders. *Journal of Materials in Civil Engineering*, 25(5), pp.610-617.

Section 2.1.3

- Andriescu, A., Hesp, S. A. M., and Youtcheff, J. S. (2004). Essential and plastic works of ductile fracture in asphalt binders. *Transportation Research Record 1875*, pp. 1-8.
- Gibson, N., Qi, X., Shenoy, A., Al-Khateeb, G., Kutay, M. E., Andriescu, A., Stuart, K., Youtcheff, J., Harman, T. (2012). Performance testing for Superpave and structural validation. *FHWA-HRT-11-045 Final Report*. Office of Infrastructure Research and Development. Washington, DC: U.S. Department of Transportation, Federal Highway Administration.
- Hintz, C., Velasquez, R., Johnson, C., and Bahia, H. (2011a). Modification and validation of the linear amplitude sweep test for binder fatigue specification. *Transportation Research Record 2207*, pp. 99-106.
- Hintz, C., Velasquez, R., Li, Z., and Bahia, H. (2011b). Effect of oxidative aging on binder fatigue performance. *J. Assoc. Asphalt Paving Technologists*, Vol. 80, pp. 527-548.
- Hoare, T. R., Hesp, S. A. M. (2000). Low-temperature fracture testing of asphalt binders. *Transportation Research Record 1728*, pp. 36-42.


- 
- Johnson, C. M. (2010). Estimating asphalt binder fatigue resistance using an accelerated test method. *Ph.D. Dissertation*, Madison, Wisconsin: University of Wisconsin-Madison.
- Johnson, C. M., Bahia, H. U., and Wen, H. (2009). Practical Application of Viscoelastic Continuum Damage Theory to Asphalt Binder Fatigue Characterization. *J. Assoc. Asphalt Paving Technologists*, Vol. 78, pp. 597–638.
- Niu, T., Roque, R. and Lopp, G. (2014). Development of a binder fracture test to determine fracture energy. *Road Materials and Pavement Design*, Vol. 15, Supplement 1, pp. 219–238.
- Ponniah, J. E., Cullen, R. A., Hesp, S. A. M. (1996). Fracture energy specifications for modified asphalts. Preprints of papers, Vol. 41 (4). 212th National Meeting of the American Chemical Society (ACS). Orlando, Florida, 25–30 August.
- Roque, R., Birgisson, B., Drakos, C. and Dietrich, B. (2004). Development and field evaluation of energy-based criteria for top-down cracking performance of hot mix asphalt. *J. Assoc. Asphalt Paving Technologists*, Vol. 73, pp. 229–260.
- Yan, Y., Cocconcelli, C., Roque, R., Nash, T., Zou, J., Hernando, D. and Lopp, G., (2015). Performance evaluation of alternative polymer modified asphalt binders. *Road Material and Pavement Design*, Vol. 16, Supplement 1, pp. 389–403.
- Yan, Y., Chun, S., Roque, R., and Kim, S., (2016). Effects of Alternative Polymer Modifications on Cracking Performance of Asphalt Binders and Resultant Mixtures, *Construction and Building Materials*, Vol.121, pp. 569–575.
- Zhou, F., Mogawer, W., Li, H., Andriescu, A., and Copeland, A., (2013). Evaluation of fatigue tests for characterizing asphalt binders. *Journal of Materials in Civil Engineering*, Vol. 25, pp. 610–617.

Section 2.2.1

- Blankenship, P., Anderson, M., King, G., Hanson, D., “A Laboratory and Field Investigation to Develop Test Procedures for Predicting Non-Load Associated Cracking of Airfield HMA Pavements,” Final Report Airfield Asphalt Pavement Technology Program, AATP Project 06-01. 2011.
- Deacon, J., Harvey, J., Tayebali, A., and Monismith, C., “Influence of Binder Loss Modulus on the Fatigue Performance of Asphalt Concrete Pavements,” *Journal of the Association of Asphalt Paving Technologists*, Vol. 66, 1997, pp. 633–685.
- Doyle, P. C., “Cracking Characteristics of Asphalt Cement,” *Journal of the Association of Asphalt Paving Technologists*, Vol. 27, 1958, pp. 581–597
- Glover, C.J., Davison, R.R., Domke, C.H., Ruan, Y., Juristyarini, P. Knorr, D.B., and Jung, S.H., “Development of a New Method for Assessing Asphalt Binder Durability with Field Validation,” Final Report FHWA/TX-03/1872-2, Texas Transportation Institute, College Station, TX, 2005.
- Hubbard, P., and Gollomb, H. “The Hardening of Asphalt with Relation to Development of Cracks in Asphalt Pavements,” *Proceedings of the Association of Asphalt Paving Technologists*. 1937.
- Kandhal, P.S., and Wenger, M.E., “Asphalt Properties in Relation to Pavement Performance,” *Transportation Research Record: Journal of the Transportation Research Board*, Vol 544, 1975, pp. 1–13.
- Kandhal, P.S., “Low-Temperature Ductility in Relation to Pavement Performance,” In ASTM STP 628: *Low-Temperature Properties of Bituminous Materials and Compacted Bituminous Paving Mixtures*, C.R. Marek (Ed.), American Society for Testing and Materials, Philadelphia, PA, 1977, pp. 95–106.
- Kandhal, P.S., and Koehler, W.C., (1984) “Significant Studies on Asphalt Durability: Pennsylvania Experience,” *Transportation Research Record: Journal of the Transportation Research Board*, Vol 999, 1984, pp. 41–50.
- Lee, D.Y., Asphalt Durability Correlation in Iowa, *Transportation Research Record: Journal of the Transportation Research Board*, Vol 468, 1973, pp. 43–60.
- Reese, R.E. and Goodrich, J.L., “California Desert Test Road-A Step Closer to Performance Based Specifications,” *Journal of the Association of Asphalt Paving Technologists*, Vol. 62, 1993, pp. 247–313.
- Skog, J., “Setting and Durability Studies on Paving Grade Asphalts,” *Journal of the Association of Asphalt Paving Technologists*, Vol. 36, 1967, pp. 387–420.
- Tayebali, A., Deacon, J., Coplantz, J., Harvey, J., Finn, F., & Monismith, C., “Fatigue Response of Asphalt-Aggregate Mixes: Part I Test Method Selection; Part II Extended Test Program; Part III Mix Design and Analysis,” Strategic Highway Research Program Report No. A-404, National Research Council, Washington, D.C., 1994.

Section 2.2.2

- Bahia, H. U., Hanson, D.I., Zeng, M., Zhai, H., Khatri, M.A., and Anderson, R.M.. (2001). *Characterization of Modified Asphalt Binders in Superpave Mix Design*, National Cooperative Highway Research Program Report 459, National Research Council, Washington, D.C.
- Bahia, H. U., Zhai, H., Zeng, M., Hu, Y., and Turner, P. (2002). "Development of binder specification parameters based on characterization of damage behavior." *J. Assn. Asphalt Paving Technologists*, Vol. 70, 442-470.
- Gibson, N., Qi, Z., Shenoy, A., Al-Khateeb, G., Kutay, M.E., Andriescu, A., Stuart, K., Youtcheff, J., and Harmon, T., *Performance Testing for Superpave and Structural Validation*, Federal Highway Administration Report No. FHWA-HRT-11-045, Washington, D.C., 2012.
- Hintz, C. and Bahia, H. U., "Simplification of Amplitude Sweep Test and Specification Parameter" *Transportation Research Record*, No. 2370, 2013, pp. 10-16.
- Hintz, C., Velasquez, R., Johnson, C., and Bahia, H., "Modification and Validation of the Linear Amplitude Sweep Test for Binder Fatigue Specification," *Transportation Research Record*, No. 2207, 2012, pp. 99-106.
- Johnson, C. and Bahia, H.U., "Evaluation of an Accelerated Procedure for Fatigue Characterization of Asphalt Binders," *Road Materials and Pavement Design*, 2011.
- Johnson, C. M., Bahia, H. U., and Wen, H., "Practical Application of Viscoelastic Continuum Damage Theory to Asphalt Binder Fatigue Characterization," *Journal of the Association of Asphalt Paving Technologists*, Vol. 78, 2009, pp. 597-638.
- Kim, Y., Lee, H. J., Little, D. N., and Kim, Y. R. (2006). "A simple testing method to evaluate fatigue fracture and damage performance of asphalt mixtures." *Journal of the Association of Asphalt Paving Technologists*, Vol. 75, 755-788.
- Lee, J.S. and Kim, Y.R., "Performance-Based Moisture Susceptibility Evaluation of Warm-Mix Asphalt Concrete through Laboratory Tests," *Transportation Research Record*, No. 2446, 2014, pp. 17-28.
- Motamed, A., Bhasin, A., and Liechti, K.M., 2012. Interaction nonlinearity in asphalt binders. *Mechanics of Time-Dependent Materials*, 16(2), 145-167.
- Motamed, A., Bhasin, A., and Liechti, K.M., 2013. Constitutive modeling of the nonlinearly viscoelastic response of asphalt binders; incorporating three-dimensional effects. *Mechanics of Time-Dependent Materials*, 17(1), 83-109.
- Narayan, S.P.A., Krishnan, J.M., Deshpande, A.P., and Rajagopal, K.R., 2012. Nonlinear viscoelastic response of asphalt binders: an experimental study of the relaxation of torque and normal force in torsion. *Mechanics Research Communications*, 43, 66-74.
- Narayan, S.P.A., Little, D.N., and Rajagopal, K.R., 2013. A nonlinear viscoelastic model for describing the response of asphalt binders within the context of a Gibbs-potential based thermodynamic framework. *Journal of Engineering Mechanics*, In Press.
- Rajagopal, K.R. and Srinivasa, A.R., 1998. Mechanics of the inelastic behavior of materials. Part I, theoretical underpinnings. *International Journal of Plasticity*, 14(10-11), 945-967.
- Rajagopal, K.R. and Srinivasa, A.R., 2004. On the thermomechanics of materials that have multiple natural configurations part I: viscoelasticity and classical plasticity. *Zeitschrift fur angewandte Mathematik und Physik ZAMP*, 55(5), 861-893.
- Safaei, F., and Castorena, C., "Temperature Effects in Linear Amplitude Sweep Testing and Analysis," In Press, *Transportation Research Record*, 2016.
- Safaei, F., Castorena, C., and Kim, Y.R., "Linking asphalt binder fatigue to asphalt mixture fatigue performance using viscoelastic continuum damage modeling," *Mechanics of Time Dependent Materials*, Vol. 20, No. 3, 2016, pp. 299-323.
- Safaei, F., Lee, J., Nascimento, L. A. H., Hintz, C., and Kim, Y.R., "Implications of Warm-Mix Asphalt on Long Term Oxidative Aging and Fatigue Performance of Asphalt Binders and Mixtures," *Journal of the Association of Asphalt Paving Technologists*, Vol. 83, 2014, pp.143-170.
- Schapery, R. A. (1975). "A theory of crack initiation and growth in viscoelastic media. III- Analysis of continuous growth." *International Journal of Fracture*, Vol.11, 549-562.
- Schapery, R.A., 1966. A theory of non-linear thermoviscoelasticity based on irreversible thermodynamics. *Proceedings 5th U.S. National Congress of Applied Mechanics*, 511-530.
- Schapery, R.A., 1969. On the characterization of nonlinear viscoelastic materials. *Polymer Engineering and Science*, 9(4), 295-310.

- 
- Tsai, B.-W., Monismith, C. L., Dunning, M., Gibson, N., D'Angelo, J., Leahy, R., King, G., Christensen, D., Anderson, D., Davis, R., and Jones, D. (2005). "Influence of asphalt binder properties on the fatigue performance of asphalt concrete pavements." *J. Assn. Asphalt Paving Technologists*, Vol. 74, 733-789.
- Underwood, B. S. (2016). A continuum damage model for asphalt cement and asphalt mastic fatigue. *International Journal of Fatigue*, 82, 387-401.
- Underwood, B. S., & Kim, Y. R. (2015). Nonlinear viscoelastic analysis of asphalt cement and asphalt mastics. *International Journal of Pavement Engineering*, 16(6), 510-529.
- Underwood, B.S., "A continuum damage model for asphalt cement and asphalt mastic fatigue," *International Journal of Fatigue*, Vol. 82, 2016, pp. 387-401.
- Underwood, B.S., Kim, Y.R. and Guddati, M.N., "Improved Calculation Method of Damage Parameter in Viscoelastic Continuum Damage Model," *International Journal of Pavement Engineering*, Vol. 11, No. 6, 2010, pp. 459-476.
- Wang, C., Castorena, C., Zhang, J., and Kim, Y.R., "Unified Failure Criterion for Asphalt Binder Under Cyclic Fatigue Loading," *Journal of the Association of Asphalt Paving Technologists*, Vol. 84, 2015, pp. 125-148.
- Wen, H., and Bahia, H., "Characterizing Fatigue of Asphalt Binders with Viscoelastic Continuum Damage Mechanics," *Transportation Research Record*, No. 2126, 2008, pp. 55-62.

Section 3

- Kim, Y. R. (2009). Modeling of asphalt concrete. American Society of Civil Engineers Press, McGraw Hill,
- Miller, J., Bellinger, W. (2003). Distress identification manual for the long-term pavement performance program. *Federal Highway Administration*, 4th Edition, FHWA-RD-03-031.
- Teymourpour, P., Bahia, H. (2014). Effects of binder modification on aggregate structure and thermovolumetric properties of asphalt mixtures. *Transportation Research Record*, No.2445, pp. 21-28.

Section 4

- Braham, A., Buttlar, W. (2009). Mode II cracking in asphalt concrete. *Advanced Testing and Characterization of Bituminous Materials*, Rhodes, Greece, Eds. Loizos, Patrl, Scarpas, and Al-Qadi, CRC Press Taylor and Francis Group, New York, ISBN: 978-0-415-55854-9, Vol. 2, pp.699-706.
- Braham, A., Buttlar, W., Ni, F. (2010). Fracture characteristics of asphalt concrete in mixed-mode. *Road Materials and Pavement Design*, Vol 11/4, pp. 947-968.
- Huang, Y. (1993). Pavement analysis and design. Prentice Hall,
- Molenaar, A. (2004). Prediction of fatigue cracking in asphalt pavements, do we follow the right approach? *Transportation Research Record*, No.2001, pp. 155-162.
- Roque, R, Zou, J., Kim, Y.R. *et al.* (2010). Top-down cracking of hot-mix asphalt layers: models for initiation and propagation. *National Cooperative Highway Research Program*, web only document 162.
- Tangella, S., Craus, J., Deacon, J., Monosmith, C. (1990). Summary report on fatigue response of asphalt mixtures, *Strategic Highway Research Program*, Project A-003A, TM-UCB-A-003A-89-3.

Section 5.1.1

- AASHTO, "Method for Determining the Fatigue Life of Compacted Hot-Mix Asphalt (HMA) Subjected to Repeated Bending," AASHTO TP8-94, 1994. (Reapproved 1996 and reconfirmed in January 2001).
- AASHTO, "Standard Method of Test for Determining the Fatigue Life of Compacted Asphalt Mixtures Subjected to Repeated Flexural Bending," AASHTO T 321-03, August 2003.
- AASHTO, "Standard Method of Test for Determining the Fatigue Life of Compacted Asphalt Mixtures Subjected to Repeated Flexural Bending," AASHTO T 321-07, January 2007. (Reconfirmed 2011).
- AASHTO, "Standard Method of Test for Determining the Fatigue Life of Compacted Asphalt Mixtures Subjected to Repeated Flexural Bending," AASHTO T 321-14, August 2014.
- Asphalt Institute, "Research and Development of the Asphalt Institute's Thickness Design Manual (MS-1) Ninth Edition," Research Report No. 82-2, August 1982.
- ASTM, "Standard Test Method for Determining Fatigue Failure of Compacted Asphalt Concrete Subjected to Repeated Flexural Bending," ASTM Designation D7460 – 10, ASTM International, 100 Barr Harbor Drive, PO Box C700, West Conshohocken, PA 19428-2959. United States. 2010.
- Claessen, A.I.M., Edwards, J.M., Sommer, P. and Ugé, P., "Asphalt Pavement Design, The Shell Method," *Proceedings, Forth International Conference on the Structural Design of Asphalt Pavements*, Ann Arbor, Michigan, 1977, pp. 39-74.



- Deacon, J.A., "Fatigue of Asphalt Concrete," Graduate Report, *The Institute of Transportation and Traffic Engineering*, University of California, Berkeley, 1965.
- Epps, J.A. and Monismith, C.L., "Influence of Mixture Variables on the Flexural Fatigue Properties of Asphalt Concrete, Proceedings, *Association of Asphalt Paving technologists*, Los Angeles, 1969, pp. 423 to 464.
- Finn, F., Saraf, C., Kulkarni, R., Nair, K., Smith, W. and Abdullah, "The Use of Distress Prediction Subsystems for the Design of Pavement Structures," Proceedings, *Forth International Conference on the Structural Design of Asphalt Pavements*, Ann Arbor, Michigan, 1977, pp. 3 to 38.
- Kingham, R.I., "Failure Criteria from AASHTO Road Test Data," Proceedings, *Third International Conference on the Structural Design of Asphalt Pavements*, London, 1972, pp. 656 to 669.
- Monismith, C. L., Secor, K. E. and Blackmer, W., "Asphalt Mixture Behavior in Repeated Flexure," Proceedings, *Association of Asphalt Paving Technologists*, Volume 30, 1961, pp 188 to 222.
- Monismith, C.L., "Flexibility Characteristics of Asphalt Paving Mixtures," Proceedings, *Association of Asphalt Paving technologists*, Quebec, Canada, 1958, pp.74 to 106.
- Monismith, C.L., Epps, J.A., Kasianchuk, D.A. and McLean, D.B., "Asphalt Mixture Behavior on Repeated Flexure. Report No. TE 70-5 to Federal Highway Administration, University of California, Berkeley, 1971.
- Monismith, C.L., Symposium on Flexible Pavement Behavior as Related to Deflection, Part II – Significance of Pavement Deflections," Proceedings, *Association of Asphalt Paving Technologists*, Volume 31, 1962, pp. 231 to 260.
- Pell, P.S., "Fatigue Characteristics of Bitumen and Bituminous Mixes," Proceedings, *First International Conference on the Structural Design of Asphalt Pavements*, Ann Arbor, Michigan, 1962.
- Pronk, A.C. and Huurman, M., "Shear deflection in 4PB tests," 2nd Workshop on Four Point Bending, University of Minho, 2009.
- Rao Tangell, S.C.S., Craus, J., Deacon, J.A. and Monismith, C.L., "Summary Report on Fatigue Response of Asphalt Mixtures," UCB Report TM-UCB-A-003A-89-3, Prepared for *Strategic Highway Research Program Project A-003-A (SHRP-A-312)*, February 1990.
- Rowe, G.M., Blankenship, P. and Bennert, T., "Fatigue assessment of conventional and highly modified asphalt materials with ASTM and AASHTO standard specifications," Proceedings of the *Third Conference on Four Point Bending* (Editors J. Pais and J. Harvey), Davis, CA, 17-18 September 2012, pp. 113–122.
- Saal, R. N. J. and Pell, P.S., "Fatigue of bituminous road mixes," *Kolloid-Zeitschrift*, Vol. 171, No. 1, pp 61-71, 1960.
- Santucci and Schmidt, "The Effect of Asphalt Properties on the Fatigue Cracking of Asphalt Concrete on the Zaca-Wigmore Test Project," Proceedings, *Association of Asphalt Paving Technologists*, Volume 38, 1969, pp. 39 to 64.
- Vallerga, B., Finn, F.N. and Hicks, R.G., "Effect of Aging on the Fatigue Properties of Asphalt Concrete," Second *International Conference on the Structural Design of Asphalt Pavements*, Ann Arbor, Michigan, 1967, pp. 595 to 617.
- Way, G. B., Kaloush, K.E. and Sousa J.M.B., "Four point bending beam tests in Arizona and relationship to asphalt binder properties, Proceedings, *Four-Point Bending* (Edited by Pais & Harvey), Taylor & Francis Group, London, ISBN 978-0-415-64331-3, 2012.
- Witczak, M.W., "Design of Full-Depth Asphalt Airfield Pavements," Proceedings, *Third International Conference on the Structural Design of Asphalt Pavements*, London, 1972, pp. 550 to 567.
- Witczak, M.W., "Fatigue Behavior of a Trinidad Epuré Mix," *Consulting Report*, July 1980.

Section 5.1.2

- AASHTO TP 107 (2014). Determining the Damage Characteristic Curve of Asphalt Concrete from Direct Tension Cyclic Fatigue Tests (Provisional standard). Washington, DC.
- Chehab, G.R., O'Quinn, E., and Kim, Y.R., "Specimen Geometry Study for Direct Tension Test Based on Mechanical Tests and Air Void Variation in Asphalt Concrete Specimens Compacted by SGC," *Transportation Research Record: Journal of the Transportation Research Board*, Vol 1723, 2000, pp. 125-133.
- Christensen, D.W., and Bonaquist, R.F., "Analysis of HMA Fatigue Data Using the Concepts of Reduced Loading Cycles and Endurance Limit," *Journal of the Association of Asphalt Paving Technologists*, Vol 78, 2009, pp. 377-416.

- 
- Daniel, J.S., and Kim, Y.R. "Development of a Simplified Fatigue Test and Analysis Procedure Using a Viscoelastic, Continuum Damage Model," *Journal of the Association of Asphalt Paving Technologists*, Vol 71, 2002, pp. 619-650.
- Diefenderfer, B. K., B. F. Bowers, and S. D. Diefenderfer. *Asphalt Mixture Performance Characterization Using Small-Scale Cylindrical Specimens*, Report No. VCTIR 15-R26, 2015.
- Gudipudi, P. P. and Underwood, B.S., "Development of Modulus and Fatigue Test Protocol for Fine Aggregate Matrix for Axial Direction of Loading," *ASCE Journal of Testing and Evaluation*, Vol. 45, No. 2, 2016.
- Kim, Y.R., Lee, H.J., and Little, D.N., "Fatigue Characterization of Asphalt Concrete Using Visco-elasticity and Continuum Damage Theory," *Journal of the Association of Asphalt Paving Technologists*, Vol 66, 1997, pp. 520-569.
- Kutay, M.E., Gibson, N., Youtcheff, J., and Dongre, R., "Use of Small Samples to Predict Fatigue Lives of Field Cores; Newly Developed Formulation Based on Viscoelastic Continuum Damage Theory," *Transportation Research Record: Journal of the Transportation Research Board*, Vol 2127, 2009, pp. 90-97.
- Lee, H.J. and Kim, Y.R., "A Uniaxial Viscoelastic Constitutive Model for Asphalt Concrete under Cyclic Loading," *ASCE Journal of Engineering Mechanics*, Vol 124, No 1, 1998a, pp. 32-40.
- Lee, H.J. and Kim, Y.R., "A Viscoelastic Continuum Damage Model of Asphalt Concrete with Healing," *ASCE Journal of Engineering Mechanics*, Vol 124, No 11, 1998b, pp. 1224-1232.
- Li, X., and Gibson, N., "Using Small Scale Specimens for AMPT Dynamic Modulus and Fatigue Tests," *Journal of the Association of Asphalt Paving Technologists*, Vol 82, 2013, pp. 579-615.
- N. Li. "Asphalt Mixture Fatigue Testing- Influence of Test Type and Specimen Size," *Ph.D Dissertation*, Delft University of Technology, Netherlands, 2013.
- Park, H. J., Eslaminia, M., and Kim, Y. R., "Mechanistic Evaluation of Cracking in In-Service Asphalt Pavements," *Materials and Structures*, Vol. 47, No. 8, 2014, pp. 1339-1358.
- Pell, P. S. and Brown, S. F., "The Characteristics of Materials for the Design of Flexible Pavement Structures," *Proceedings of the Third International Conference on the Structural Design of Asphalt Pavements*, Michigan, USA, 1972, pp. 326 – 342.
- Pell, P. S. and Cooper, K. E. "The Effect of Testing and Mix Variables on the Fatigue Performance of Bituminous Materials," *Journal of the Association of Asphalt Paving Technologists*, Vol. 44, 1975, pp. 1-37.
- Raithby, K. D. and Sterling, A. B., "Some Effects of Loading History on the Performance of Rolled Asphalt," *TRRL-LR 496*, 1972, Crowthorne, England.
- Soltani, A., and Anderson, D.A., "New Test Protocol to Measure Fatigue Damage in Asphalt Mixtures," *Journal of Road Materials and Pavement Design*, Vol. 6, 2005, pp. 485-514.
- Soltani, A., Solaimanian, M., and Anderson, D.A., "An Investigation of the Endurance Limit of Hot-Mix Asphalt Concrete Using a New Uniaxial Fatigue Protocol," Final Report, Report Number FHWA-HIF-07-002, *Federal Highway Administration (FHWA)*, 2006, Washington, D.C.
- Underwood, B. S., Kim, Y. R., and Guddati, M. N., "Improved Calculation Method of Damage Parameter in Viscoelastic Continuum Damage Model," *International Journal of Pavement Engineering*, Vol. 11, No. 6, 2010, pp. 459-476.
- Zeida, W.A., Kaloush, K.E., Underwood, B.S., and Mamlouk, M.S. (2016). "Development of Test Protocol to Measure Axial Fatigue Damage and Healing," *Transportation Research Record: Journal of the Transportation Research Board*, Vol 2576, 2016, In Press.

Section 5.1.3

- Behnia, B., Dave, E.V., Ahmed, S., Buttlar, W.G., Reis, H. (2011) Effects of Recycled Asphalt Pavement Amounts on Low-Temperature Cracking Performance of Asphalt Mixtures Using Acoustic Emissions. *Journal of the Transportation Research Record*, vol. 2208, pp. 64-71.
- Behnia, B., Kebede, N., Hill, B.C., Buttlar, W.G. (2013) Developing A New Mechanical Performance Test for Asphalt Mixtures. *Presented at the 12th U.S. National Congress for Computational Mechanics*, July 2013, Raleigh, N.C.
- Bower, N., Wen, H., Wu, S., Willoughby, K., Weston, J., and DeVol, J., "Evaluation of the Performance of Warm Mix Asphalt in Washington State," *International Journal of Pavement Engineering*, Vol. 17, No. 5, 2016, pp. 423-434.
- Braham, A.F., Buttlar, W.G., Clyne, T.R., Marasteanu, M.O., Turos, M.I. (2009) The Effect of Long-Term Laboratory Aging on Asphalt Concrete Fracture Energy. *Journal of the Association of Asphalt Paving Technologists*, vol. 78, pp. 417-454.



- Buttlar, W.G., Roque, R. (1994) Development And Evaluation Of The Strategic Highway Research Program Measurement And Analysis System For Indirect Tensile Testing At Low Temperatures. *Transportation Research Record*, vol. 1454, pp. 163-171.
- Buttlar, W.G., Wang, H. (2016) Laboratory Investigation of Illinois Tollway Stone Matrix Asphalt Mixtures with Varied Levels of Asphalt Binder Replacement. Final Report, *Illinois Tollway Authority*.
- Chang, H.S., Lytton, R.L., Carpenter, S.H. (1976) Prediction of Thermal Reflection Cracking in West Texas. Research Report No. TTI-2-8-73-18-3, *Texas Transportation Institute*, Texas A&M University, College Station, Texas, March, 1976.
- Dave, E.V., Ahmed, S., Buttlar, W.G., Bausano, J.P., Lynn, T. Investigation of Strain Tolerant Mixture Reflective Crack Relief Systems: an Integrated Approach. *Journal of the Association of Asphalt Paving Technologists*, vol. 79, pp. 119-156.
- Dinegda, Y.H., Birgisson, B. (2016) Reliability-Based Design Procedure for Fatigue Cracking in Asphalt Pavements. *Transportation Research Board Compendium of Papers*, pp. 1-16.
- Hill, B.C., Behnia, B., Hakimzadeh, S., Buttlar, W.G., Reis, H. (2012) Evaluation of Low-Temperature Cracking Performance of Warm-Mix Asphalt Mixtures. *Journal of the Transportation Research Record*, vol. 2294, pp. 81-88.
- Hill, B.C., Behnia, B., Buttlar, W.G., Reis, H. (2013A) Evaluation of Warm Mix Asphalt Mixtures Containing Reclaimed Asphalt Pavement through Mechanical Performance Tests and an Acoustic Emission Approach. *ASCE Journal of Materials in Civil Engineering*, vol. 25 (12), pp. 1887-1897.
- Hill, B.C., Oldham, D., Behnia, B., Fini, E.H. Buttlar, W.G., Reis, H. (2013B) Low-Temperature Performance Characterization of Biomodified Asphalt Mixtures That Contain Reclaimed Asphalt Pavement. *Journal of the Transportation Research Record*, vol. 2371, pp. 49-57.
- Hill, B.C., Oldham, D., Behnia, B., Fini, E.H. Buttlar, W.G., Reis, H. (2016) Evaluation of Low Temperature Viscoelastic Properties and Fracture Behavior of Bio-Asphalt Mixtures. *International Journal of Pavement Engineering*, pp. 1-8.
- Hiltunen, D.R., Roque, R. (1994) A Mechanics-Based Prediction Model for Thermal Cracking of Asphaltic Concrete Pavements. *Journal of the Association of Asphalt Paving Technologists*, vol. 63, pp. 81-108.
- Kebede, N. (2012) Development of an Alternative Test to Obtain Asphalt Mixture Creep Compliance at Low Temperatures. *Master's Thesis*, University of Illinois at Urbana-Champaign.
- Kim, M., Buttlar, W.G., Baek, J., Al-Qadi, I.L. (2009) Field and Laboratory Evaluation of Fracture Resistance of Illinois Hot-Mix Asphalt Overlay Mixtures. *Journal of the Transportation Research Record*, vol. 2127, pp. 146-154.
- Lytton, R., Uzan, J., Fernando, E.G., Roque, R., Hiltunen, D., Stoffels, S.M. (1993). Development and Validation Of Performance Prediction Models And Specifications For Asphalt Binders And Paving Mixes. *Strategic Highway Research Program - A357*. Washington, D.C.
- Marasteanu, M., Buttlar, W.G., Bahia, H., Williams, R.C. (2012) Investigation of Low Temperature Cracking in Asphalt Pavements, National Pooled Fund Study - Phase II. Final Report 2012-23, *Minnesota Department of Transportation*.
- Roque, R., Buttlar, W.G. (1992) The Development of a Measurement and Analysis System to Accurately Determine Asphalt Concrete Properties using the Indirect Tensile Mode. *Journal of the Association of Asphalt Paving Technologists*, vol. 61, pp. 304-332.
- Roque, R., Hiltunen, D.R., Buttlar, W.G. (1995) Thermal Cracking Performance and Design of Mixtures using Superpave. *Journal of the Association of Asphalt Paving Technologists*, vol. 64, pp. 718-735.
- Roque, R., Birgisson, B., Zhang, Z., Sangpetngam, B., Grant, T. (2002) Implementation of SHRP Indirect Tension Tester to Mitigate Cracking in Asphalt Pavements and Overlays. Final Report, *Florida Department of Transportation*.
- Roque, R., Birgisson, B., Drakos, C., Dietrich, B. (2004) Development and Field Evaluation of Energy-Based Criteria for Top-down Cracking Performance of Hot Mix Asphalt. *Journal of the Association of Asphalt Paving Technologists*, vol. 73, pp. 229-260.
- Roque, R., Zou, J., Kim, Y.R., Baek, C., Thirunavukkarasu, S., Underwood, B.S., Guddati, M.N. Top-Down Cracking of Hot-Mix Asphalt Layers: Models for Initiation and Propagation. Final Report, *National Cooperative Highway Research Program*, 1-42A, Washington, D.C.
- Shen, S., Wu, S., Zhang, W., Mohammad, L.N., Wen, H. Bahadori, A., and Muhunthan, B., "Performance of WMA Technologies: Stage II – Long-term Field Performance," Draft final report for NCHRP, *Transportation Research Board of the National Academies*, Washington, D.C., 2016.




- Wagoner, M.P., Buttlar, W.G., Paulino, G.H., Blankenship, P. (2006) Laboratory Testing Suite for Characterization of Asphalt Concrete Mixtures Obtained from Field Cores. *Journal of the Association of Asphalt Paving Technologists*, vol. 75, pp. 815-851.
- Wen, H. and Kim, Y.R., "Simple Performance Test for Fatigue Cracking and Validation with WesTrack Mixtures," *Transportation Research Record: Journal of the Transportation Research Board*, Vol. 1789, 2002, pp. 66-72.
- Wen, H., "Use of Density of fracture work Obtained from Indirect Tensile Testing for the Mix Design and Development of a Fatigue Model," *International Journal of Pavement Engineering*, Vol. 14, No. 6, 2013, pp. 1-8.
- Wu, S., Zhang, K., Wen, H., DeVol, J., and Kelsey, K., "Performance Evaluation of Hot Mix Asphalt Containing Recycled Asphalt Shingles in Washington State," *Journal of Materials in Civil Engineering*, Vol. 28, No. 1, 2016.
- Wu, S., Wen, H., Chaney, S., Littleton, K., and Muench, S., "Evaluation of Long-Term Performance of Stone Matrix Asphalt in Washington State," *Journal of Performance of Constructed Facilities*, 2016, In Press.
- Wu, S., Wen, H., Zhang, W., Shen, S., Faheem, A., and Mohammad, L.N., "Long-term Field Performance of Transverse Cracking for Warm Mix Asphalt Pavement and Identification of Significant Material Property for Transverse Cracking," *Transportation Research Record: Journal of Transportation Research Board (TRB)*, 2016.
- Zhang, W., Shen, S., Basak, P., Wen, H., Wu, S., Faheem, A., and Mohammad, L.N., "Development of Predictive Models for the Initiation and Propagation of Field Transverse Cracks". *Transportation Research Record: Journal of Transportation Research Board*, Vol. 2524, 2015, pp.92-99.

Section 5.1.4

- Bonnot, J., "Asphalt aggregate mixtures," *Transportation Research Record*, Vol 1096, 1986, pp. 42-51.
- Chompton, Doan, Harlin & Kennel, "Journées d'information. Bitumes et enrobés bitumineux," *Laboratoire Central des Ponts et Chaussées*, 1972, Paris, France. Ministère de L'équipement et du logement.
- Francken, L. and Verstraeten, J., "Methods for predicting moduli and fatigue laws of bituminous road mixes under repeated bending," *Transportation Research Record*, Vol 515, 1974, pp. 114-123.
- INVIAS, "Especificaciones generales de construcción de carreteras," *Ministerio de Transporte*, 2013, Bogotá, Colombia.
- LCPC, "French design manual for pavement structures," *Laboratoire Central des Ponts et Chaussées*, 1997, Paris, France.
- Rowe, G.M., "Performance of asphalt mixtures in the trapezoidal fatigue test", *Journal of the Association of Asphalt Paving Technologists*, Vol 62, 1993, pp. 344-384.
- The British Standards Institution, "BS EN 12697-24:2012. Bituminous mixtures — test methods for hot mix asphalt. Part 24: Resistance to fatigue," *The British Standards Institution*, 2012.
- Witczak, M., Mamlouk, M., Souliman, M. and Zeiada, W., "Project no. NCHRP 9-44 A. Validating an endurance limit for hot-mix asphalt (hma) pavements: Laboratory experiment and algorithm development. Appendix 1: Integrated predictive model for healing and fatigue endurance limit for asphalt concrete," *National Cooperative Highway Research Program*, 2013.

Section 5.1.5

- Bennert, T. and A. Maher (2008). Field and Laboratory Evaluation of a Reflective Cracking Interlayer in Jew Jersey, *Transportation Research Record: Journal of the Transportation Research Board*, Vol. 2084, pp. 114-123.
- Bennert, T., F. Fee, E. Sheehy, R. Blight, and R. Sauber (2012). Implementation of Performance-Based HMA Specialty Mixtures in New Jersey. *Journal of the Association of Asphalt Paving Technologists*, Vol. 80, 2011, pp. 719-740.
- Bennert, T., J. Daniel, and W. Mogawer (2014). Strategies for Incorporating Higher Recycled Asphalt Pavement Percentages-Review of Implementation Trials in Northeast States, *Transportation Research Record: Journal of the Transportation Research Board*, Vol. 2445, pp. 83-93.
- Button, J. W. and J. A. Epps (1982). *Evaluation of Fabric Interlayers*, Research report 261-2, Texas Transportation Institute, College Station, Texas, 1982.
- Button, J. W. and R. L. Lytton (1987). Evaluation of Fabrics, Fibers, and Grids in Overlays, *Proceedings of 6th international conference on structural design of asphalt pavements*, The university of Michigan, Michigan, USA, 1987, Vol. 1, 925-934.

- 
- Cleveland, G. S., R. L. Lytton, and J. W. Button (2003). Reinforcing Benefits of Geosynthetic Materials in Asphalt Concrete Overlays Using Pseudo Strain Damage Theory, 2003 *Transportation Research Board* conference commendium of papers.
- Germann, F. P. and R. L. Lytton (1979). Methodology for Predicting the Reflective Cracking Life of Asphalt Concrete Overlays, Research report FHWA/TX-79/09+207-5, *Texas Transportation Institute*, Texas.
- Gu, F., Y. Zhang, X. Luo, R. Luo, and R. L. Lytton (2015a). Improved Methodology to Evaluate Fracture Properties of Warm Mix Asphalt Using Overlay Test. *Transportation Research Record: Journal of the Transportation Research Board*, No. 2506, pp. 8-18.
- Gu, F., X. Luo, Y. Zhang, and R. L. Lytton (2015b). Using Overlay Test to Evaluate Fracture Properties of Field-Aged Asphalt Concrete. *Construction and Building Materials*, Vol. 101, pp. 1059-1068.
- Koochi, Y., R. Luo, R. L. Lytton, and T. Scullion (2013). New Methodology to Find the Healing and Fracture Properties of Asphalt Mixes Using Overlay Tester. *Journal of Materials in Civil Engineering*, Vol. 25, No. 10, pp. 1386-1393.
- Luo, X., R. Luo, and R. L. Lytton (2013). Modified Paris' Law to Predict Entire Crack Growth in Asphalt Mixtures. *Transportation Research Record: Journal of the Transportation Research Board*, No. 2373, pp. 54-62.
- Lytton, R. L., F. Tsai, S. I. Lee, R. Luo, S. Hu, and F. Zhou (2010). Models for Predicting Reflection Cracking of Hot-Mix Asphalt Overlays. NCHRP Report 669, *Transportation Research Board of the National Academies*, Washington, D.C.
- Ma, W., N. H. Tran, A. Taylor, J. R. Willis, and M. Robbins (2015), Comparison of Laboratory Cracking Test Results and Field Performance, *Journal of Association of Asphalt Paving Technologists*, Vol. 84, pp.243-268.
- Paris, P. C., and F. Erdogan (1963). A Critical Analysis of Crack Propagation Laws. *Journal of Basic Engineering*, Vol. 85, No. 4, pp. 528-533.
- Pickett, D. L. and R. L. Lytton (1983). Laboratory evaluation of selected fabrics for reinforcement of asphaltic concrete overlays, Research report 261-1, *Texas Transportation Institute*, Texas.
- Schapery, R. A. (1975). A Theory of Crack Initiation and Growth in Viscoelastic Media II. Approximate Methods of Analysis. *International Journal of Fracture*, Vol. 11, No. 3, pp. 369-388.
- TxDOT Designation: TEX-248-F. Overlay Test. Construction Division, *Texas Department of Transportation*, 2009.
- Walubita, L. F., A. N. Faruk, G. Das, H. A. Tanvir, J. Zhang, and T. Scullion (2012). The Overlay Tester: A Sensitivity Study to Improve Repeatability and Minimize Variability in the Test Results. Report No. FHWA/TX-12/0-6607-1, *Texas A&M Transportation Institute*, College Station, Texas.
- Zhou, F., and T. Scullion (2004). Upgraded Overlay Tester and Its Application to Characterize Reflection Cracking Resistance of Asphalt Mixtures, FHWA/TX-04/0-4467-1, *Texas Transportation Institute*, Texas, p. 44.
- Zhou, F., E. Fernando, and T. Scullion (2010b). Development, Calibration, and Validation of Performance Prediction Models for the Texas M-E Flexible Pavement Design System, FHWA/TX-10/0-5798-2, *Texas Transportation Institute*, Texas, p.216.
- Zhou, F., S. Hu, and T. Scullion (2010a). Advanced Asphalt Overlay Thickness Design and Analysis System, *Journal of Association of Asphalt Paving Technologists (AAPT)*, Vol. 79, Sacramento, CA.
- Zhou, F., S. Hu, T. Scullion, and R. Lee (2014). Balanced RAP/RAS Mix Design System for Project-Specific Conditions”, *Journal of Association of Asphalt Paving Technologists*, Vol. 83, Atlanta, Ga.
- Zhou, F., S. Hu, T. Scullion, et al. (2007a). Development and Verification of the Overlay Tester Based Fatigue Cracking Prediction Approach, *Journal of Association of Asphalt Paving Technologists*, Vol. 76, pp. 627-662.
- Zhou, F., S. Hu, T. Scullion, M. Mikhail, and L. Walubita (2007b). A Balanced HMA Mix Design Procedure for Overlays, *Journal of the Association of Asphalt Paving Technologists*, Vol. 76, pp. 823-850.


Section 5.1.6

- Bolzan, P. E. and Huber, G. (1993) “Direct Tension Test Experiments,” SHRP-A-641, Strategic Highway Research Program, Transportation Research Board, National Research Council, Washington, D.C.
- Buttlar, W G, Wagoner, M P, You, Z, Brovold, S T. (2004). Simplifying the Hollow Cylinder Tensile Test Procedure through Volume-Based Strain. *Journal of the Association of Asphalt Paving Technologists*, Vol. 73, pp. 367-399.
- Buttlar, W. G. and Roque, R. (1994) “Development and Evaluation of the Strategic Highway Research Program Measurement and Analysis System for Indirect Tensile Testing at Low Temperatures,” In *Transportation Research Record: Journal of the Transportation Research Board*, No. 1454, National Research Council, National Academy Press, Washington, D. C., pp. 163-171.

- 
- Buttlar, W. G., Al-Khateeb, G. G., and Bozkurt, D. (1999). "Development of a Hollow Cylinder Tensile Tester to Obtain Mechanical Properties of Bituminous Paving Mixtures," *Journal of the Association of Asphalt Paving Technologists*, Vol. 68, pp. 369-403.
- Haas, R. C. G. (1973) "A Method for Designing Asphalt Pavements to Minimize Low -Temperature Shrinkage Cracking". The *Asphalt Institute Research Report* 73-1 (RRR-73-1).
- Huang, B., Shu, X., and Tang, Y. (2005) Comparison of Semi-Circular Bending and Indirect Tensile Strength Tests for HMA Mixtures. *Advances in Pavement Engineering*: pp. 1-12.
- Kim Y.R., Daniel, J.S., Wen, H. (2002) Fatigue Performance Evaluation of WesTrack Asphalt Mixtures Using Viscoelastic Continuum Damage Approach. *Final Report of North Carolina Department of Transportation*, North Carolina State University, Raleigh, NC.
- Koh C. (2009) "Tensile Properties of Open Graded Friction Course (OGFC) Mixture to Evaluate Top-Down Cracking Performance" *PhD Dissertation*, University of Florida.
- Koh, C., Roque, R. (2010). "Use of Nonuniform Stress-State Tests to Determine Fracture Energy of Asphalt Mixtures Accurately," *Transportation Research Record: Journal of the Transportation Research Board*, Vol. 2181, pp. 55-66
- Li, X. and Marasteanu, M. (2004). "Evaluation of the Low Temperature Fracture Resistance of Asphalt Mixtures Using the Semi Circular Bend Test," *Journal of the Association of Asphalt Paving Technologists*, Vol. 73, pp. 401-426.
- Roque, R. and Buttlar, W. G. (1992) "The Development of a Measurement and Analysis System to Accurately Determine Asphalt Concrete Properties Using the Indirect Tensile Mode," *Journal of the Association of Asphalt Paving Technologists*, Vol. 61, pp. 304-332, 1992.
- Roque, R., Buttlar, W. G., Ruth, B. E., Tia, M., Dickson, S. W., and Reid, B., "Evaluation of SHRP Indirect Tension Tester to Mitigate Cracking in Asphalt Pavements and Overlays," *Final Report of Florida Department of Transportation*, University of Florida, Gainesville, FL, August 1997.
- Roque, R, Koh, C., Chen, Y., Sun, X., Lopp, G. (2009) "Introduction of Fracture Resistance to the Design and Evaluation of Open Graded Friction Courses in Florida," *FDOT Final Report UF Project No.: 00054539*, pp. 100-133.

Section 5.1.7

- Aschenbrener, T. (1994). Comparison of results obtained from the LCPC rutting tester with pavements of known field performance. *Transportation Research Record: Journal of the Transportation Research Board*, Vol. 1454, pp. 66-73.
- Aschenbrener, T. (1995). Evaluation of Hamburg wheel-tracking device to predict moisture damage in hot-mix asphalt. *Transportation Research Record: Journal of the Transportation Research Board*, Vol. 1492, pp. 193-201.
- Bhattacharjee, S., Gould, J. S., Mallick, R. B., and Hugo, F. (2004). An Evaluation of use of Accelerated Loading Equipment for Determination of Fatigue Performance of Asphalt Pavement in Laboratory. *International Journal of Pavement Engineering*, 5(2), pp. 61-79.
- Bhattacharjee S. (2005) "Use of Accelerated Loading Equipment for Fatigue Characterization of Hot Mix Asphalt in the Laboratory", *Ph.D. dissertation*, Worcester Polytechnic Institute.
- Collins, R., Shami, H., and Lai, J. (1996). Use of Georgia loaded wheel tester to evaluate rutting of asphalt samples prepared by Superpave gyratory compactor. *Transportation Research Record: Journal of the Transportation Research Board*, Vol. 1545, pp. 161-168.
- Cooley, L. A., Kandhal, P. S., Buchanan, M. S., Fee, F., and Epps, A. (2000). Loaded wheel testers in the United States: State of the practice. *Transportation Research Circular E-C016*, Transportation Research Board.
- Huang, B., Shu, X., and Wu, H. (2016). U.S. Patent No. 9,234,825. Washington, DC: *U.S. Patent and Trademark Office*.
- Shen, S. "Dissipated energy concepts for HMA performance: Fatigue and healing". *Ph.D. Thesis*, University of Illinois at Urbana-Champaign, Urbana, IL, 2006.
- West, R. C., Zhang, J., and Cooley, L. A. (2004). "Evaluation of the asphalt pavement analyzer for moisture sensitivity testing," Rep. No. 04-04, *National Center for Asphalt Technology (NCAT)*, Auburn Univ., Auburn, AL.
- Wu, H. (2011). "Investigating properties of pavement materials utilizing loaded wheel tester (LWT)." *Ph.D. dissertation*, Univ. of Tennessee, Knoxville, TN.



Wu, H., Huang, B., and Shu, X. (2013). Characterizing fatigue behavior of asphalt mixtures utilizing loaded wheel tester. *Journal of Materials in Civil Engineering*, 26(1), pp. 152-159.

Section 5.2.1

- Biligiri, K.P., Said, S., and Hakim, H. (2012) "Asphalt Mixture's Crack Propagation Assessment using Semi-Circular Bending Tests," *International Journal of Pavement Research and Technology*, Vol. 5, No. 4, pp. 209-217.
- Cao, W., Mohammad, L.N., Elseifi, M., and Cooper, S.B. III (2016a) "Asphalt Pavement Fatigue Performance Prediction Based on Semi-Circular Bend Test at Intermediate Temperature," *Transportation Research Record: Journal of the Transportation Research Board*, submitted.
- Cao, W., Mohammad, L.N., Elseifi, M. (2016b) "Assessing the Effects of RAP/RAS and Warm-Mix Technologies on Fatigue Performance of Asphalt Mixtures and Pavements Using the Viscoelastic Continuum Damage Approach," *Road Materials and Pavement Design*, submitted.
- Cooper, S.B. Jr., Mohammad, L.N., and Elseifi, M.A. (2014) "Laboratory Performance of Asphalt Mixtures Containing Recycled Asphalt Shingles," *Transportation Research Record: Journal of the Transportation Research Board*, No. 2445, pp. 94-102.
- Cooper, S.B. Jr., Mohammad, L.N., Elseifi, M.A., and Medeiros, M.S. Jr. (2015a) "Effect of Recycling Agents on the Laboratory Performance of Asphalt Mixtures Containing Recycled Asphalt Shingles," *Transportation Research Record: Journal of the Transportation Research Board*, No. 2506, pp. 54-61.
- Cooper, S.B. Jr., Negulescu, I., Balamurugan, S.S., Mohammad, L.N., and Daly, W.H. (2015b) "Binder Composition and Intermediate Temperature Cracking Performance of Asphalt Mixtures Containing RAS," *Road Materials and Pavement Design*, Vol. 16, No. S2, pp. 275-295.
- Cooper, S.B. Jr., Negulescu, I., Balamurugan, S.S., Mohammad, L.N., and Daly, W.H., and Baumgardner, G.L. (2016) "Asphalt Mixtures Containing RAS and/or RAP: Relationships amongst Binder Composition Analysis and Mixture Intermediate Temperature Cracking Performance," *Presented at the 91th Annual Meeting of Association of Asphalt Paving Technologists*, Indianapolis, IN.
- Elseifi, M.A., Mohammad, L.N., Ying, H., and Cooper, S. III (2012) "Modeling and Evaluation of the Cracking Resistance of Asphalt Mixtures Using the Semi-Circular Bending Test at Intermediate Temperatures," *Road Materials and Pavement Design*, Vol. 13, No. S1, pp. 124-139.
- Kim, M., Mohammad, L.N., Elseifi, M.A., "Characterization of Fracture Properties of Asphalt Mixtures as Measured by Semicircular Bend Test and Indirect Tension Test," *Transportation Research Record: Journal of the Transportation Research Board*, No. 2296, 2012, pp. 115-124.
- Li, X.J., and Marasteanu, M.O. (2010), "Using Semi Circular Bending Test to Evaluate Low Temperature Fracture Resistance for Asphalt Concrete," *Journal of Experimental Mechanics*, Vol. 50, pp. 867-876.
- Louisiana Standard Specifications for Roads and Bridges, DOTD Specifications for roads and Bridges, 2016 Edition, Baton Rouge, Louisiana.
- Mohammad, L.N., Kim, M., and Challa, H., (2016) Development of Performance-Based Specifications for Louisiana Asphalt Mixtures. Report No. FHWA/LA.14/558. *Louisiana Transportation Research Center*, Baton Rouge, Louisiana.
- Mohammad, L.N., Wu, Z., and Mull, M.A. (2004) "Characterization of Fracture and Fatigue Resistance on Recycled Polymer-Modified Asphalt Pavements," *Proc., 5th RILEM International Conference on Cracking in Pavements*, France, pp. 375-382.
- Mull, M.A., Othman, A., and Mohammad, L.N. (2005), "Fatigue Crack Propagation Analysis of Chemically Modified Crumb Rubber-Asphalt Mixtures," *Journal of Elastomers and Plastics*, Vol. 37, pp. 73-87.
- Mull, M.A., Stuart, K., and Yehia, A. (2002) "Fracture Resistance Characterization of Chemically Modified Crumb Rubber Asphalt Pavement," *Journal of Materials Science*, Vol. 37, pp. 557-566.
- Paris, P.C., and Erdogan, F. (1963) "A Critical Analysis of Crack Propagation Laws," *Journal of Basic Engineering ASME*, Vol. 85, No. 4, pp. 528-534.
- Rice, J.R. (1968) "A Path Independent Integral and the Approximate Analysis of Strain Concentration by Notches and Cracks," *Journal of Applied Mechanics*, Vol. 35, pp. 379-386.

Section 5.2.2

- AASHTO TP124-16 (2016). "Determining the fracture potential of asphalt mixtures using semicircular bend geometry (SCB) at intermediate temperature." *Washington, DC: American Association of State Highway and Transportation Officials*.



- Al-Qadi, I. L., Ozer, H., Lambros, J., El Khatib, A., Singhvi, P., Khan, T., and Doll, B. (2015). "Testing protocols to ensure performance of high asphalt binder replacement mixes using RAP and RAS." Report No. *FHWA ICT-15-07*. Rantoul, IL: Illinois Center for Transportation.
- Bazant, Z. P. (1996). "Analysis of Work-of-Fracture Method for Measuring Fracture Energy of Concrete." *Journal of Engineering Mechanics*, Vol. 122, No.2, pp.138-144.
- Hillerborg, A. (1985). "The Theoretical Basis of a Method to Determine the Fracture Energy of Concrete." *Materials and Structures*, Vol 18, No.4, pp. 291-296.
- Ozer, H., Al-Qadi, I. L., Lambros, J., El-Khatib, A., Singhvi, P., & Doll, B. (2016a). "Development of the fracture-based flexibility index for asphalt concrete cracking potential using modified semi-circle bending test parameters." *Construction and Building Materials*, 115, 390-401. doi:10.1016/j.conbuildmat.2016.03.144
- Ozer, H., Singhvi, P., Kahn, T., Rivera, J., & Al-Qadi, I. L. (2016b). "Fracture characterization of asphalt mixtures with RAP and RAS using the Illinois semi-circular bending test method and flexibility index." *Transportation Research Record: Journal of the Transportation Research Board* (in press).
- Ozer, H., Al-Qadi, I. L., Singhvi, P., Bausano, J., Carvalho, R., Li, X., and Gibson, N. (2017). "Assessment of Asphalt Mixture Performance Tests to Predict Fatigue Cracking in an Accelerated Pavement Testing Trial" *International Journal of Pavement Engineering* (submitted).

Section 5.2.3

- Ahmed, S., Dave, E., Buttlar, W., Behnia, B. (2012) "Compact tension test for fracture characterization of thin bonded asphalt overlay systems at low temperature," *Materials and Structures*, Vol. 45, pp. 1207-1220.
- ASTM D7313-13. (2013) "Standard Test Method for Determining Fracture Energy of Asphalt-Aggregate Mixtures using the Disk-Shaped Compact Tension Geometry," *ASTM International*, West Conshohocken, PA, www.astm.org.
- Behnia, B., Ahmed, S., Dave, E., Buttlar, W. (2010) "Fracture Characterization of Asphalt Mixtures with Reclaimed Asphalt Pavement," *International Journal of Pavement Research and Technology*, Vol. 3, , pp. 72-78.
- Lee, K., Soupharath, N., Shukla, A., Franco, C., Manning, F. (1999) "Rheological and Mechanical Properties of Blended Asphalts Containing Recycled Asphalt Pavement Binders," *Asphalt Paving Technology*, Vol. 68, pp. 89-128.
- Marasteanu, M., Buttlar, W., Bahia, H., Williams, C. (2012) "Investigation of Low Temperature Cracking in Asphalt Pavements, National Pooled Fund Study-Phase II," *Minnesota Department of Transportation*, MN/RC 2012-23.
- Marasteanu, M., Zofka, A., Turos, M., Li, X., Velasquez, R., Li, X., Buttlar, W., ...McGraw, J. (2007) "Investigation of Low Temperature Cracking in Asphalt Pavements, National Pooled Fund Study 776," *Minnesota Department of Transportation*, MN/RC 2007-43.
- Wagoner, M., Butlar, W., Paulino, G. (2005a) "Disk-shaped Compaction Tension Test for Asphalt Concrete Fracture," *Society for experimental mechanics*, 45(3), pp. 270-277.
- Wagoner, M., Butlar, W., Paulino, G. (2005b) "Investigation of the Fracture Resistance of Hot-Mix Asphalt Concrete Using a Disk-Shaped Compact Tension Test," *Transportation Research Record: Journal of the Transportation Research Board*, No 1929, Washington, D.C, pp 183-192.

Section 5.2.4

- Bhurke, A., Shin, E., Drzal, L. (1997). Fracture morphology and fracture toughness measurement of polymer-modified asphalt concrete, *Transportation Research Record: Journal of the Transportation Research Board*, Vol. 1590, pp. 23-33.
- Braham, A., Buttlar, W., Ni, F. (2010). Fracture Characteristics of Asphalt Concrete in Mixed-Mode. *Road Materials and Pavement Design*, Vol 11, No. 4, pp. 947-968.
- Hossain, M., Swartz, S., Hoque, E. (1999). Fracture and tensile characteristics of asphalt-rubber concrete, *ASCE Journal of Materials in Civil Engineering*, Vol. 11, No. 4, pp. 287-294.
- Kim, H., Wagoner, M., Buttlar, W. (2009). Micromechanical fracture modeling of asphalt concrete using a single-edge notched beam test, *Materials and Structures*, Vol. 42, pp. 677-689.
- Kim, K., El Hussein, H. (1997). Variation of fracture toughness of asphalt concrete under low temperatures, *Construction and Building Materials*, Vol. 11, Nos. 7-8, pp. 403-411.
- Majidzadeh, K., Kauffmann, E., Ramsamooj, D. (1971). Application of fracture mechanics in the analysis of pavement fatigue, *Journal of the Association of Asphalt Paving Technologists*, Vol. 40, pp. 227-246.
- Marasteanu, M., Dai, S., Labuz, J., Li, X. (2002). Determining the low-temperature fracture toughness of asphalt



mixtures, *Transportation Research Record: Journal of the Transportation Research Board*, Vol. 1789, pp. 191-199.

Mobasher, B., Mamlouk, M., Lin, H. (1997). Evaluation of crack propagation properties of asphalt mixtures, *ASCE Journal of Transportation Engineering*, Vol. 123, No. 5, pp. 405-413.

Ramsamooj, D. (1991). Fatigue cracking of asphalt concrete pavements, *Journal of Testing and Evaluation*, Vol. 19, No. 3, pp. 231-239.

Wagoner, M., Buttlar, W., Paulino, G. (2005). Development of a Single-Edge Notched Beam test for asphalt concrete mixtures, *Journal of Testing and Evaluation*, Vol. 33, No. 6, pp.452-460.

Section 5.2.5

Barenblatt, G. I., "The Mathematical Theory of Equilibrium Cracks in Brittle Fracture," *Advanced Applied. Mech.* Vol. 7, 1962, pp. 55-129.

Bazant, Z.P. and Xu, K., "Size Effect in Fatigue Fracture of Concrete," *ACI Materials Journal*, Vol. 88, No. 4, 1991, pp. 390-399.

Bazant, Z. P. and Schell, W. F., "Fatigue Fracture of High Strength Concrete and Size Effect," *ACI Materials Journal*, Vol. 90, No. 5, 1993, pp. 472-478.

Cedolin, L., Dei Poli, S., and IoTi, L. "Experimental Determination of the Fracture Process Zone in Concrete," *Cement and Concrete Research*, Vol. 13, No. 4, 1983, pp. 557-567.

Chehab, G., Seo, Y., Kim, Y.R., "Viscoelastoplastic Damage Characterization of Asphalt-Aggregate Mixtures Using Digital Image Correlation," *International Journal of Geomechanics*, Vol. 7, No. 2, 2007, pp. 111-118.

Dugdale, D.S. "Yielding of Steel Sheets Containing Slits," *Journal of the Mechanics and Physics of Solids*, Vol. 8, 1960, pp. 100-108.

Hillerborg, A., Modeer, M., and Petersson, P.E., "Analysis of Crack Formation and Crack Growth in Concrete by means of Fracture Mechanics and Finite Elements," *Cement and Concrete Research*, Vol. 6, No. 6, 1976, pp. 773-782.

Jenq, Y.S., and Perng, J.D., Analysis of Crack Propagation in Asphalt Concrete Using a Cohesive Crack Model, *Transportation Research Record: Journal of the Transportation Research Board*, Vol 1317, 1996, pp. 90-99.

Krstulovic-Opara, N., "Fracture Process Zone Presence and Behavior in Mortar Specimens," *ACI Materials Journal*, Vol. 90, No. 6, 1993, pp. 618-626.

Paris, P.C. and Erdogan, F., "Critical Analysis of Propagation Laws," *Transactions of ASME, Journal of Basic Engineering*, Vol. 85, 1963, pp. 528-534.

Petersson, P.E., "Crack Growth and Development of Fracture Process Zone in Plain Concrete and Similar Materials," Report No. TVBM-1006, Lund Institute of Technology, Lund, Sweden, 1981.

Popelar, S.F., Chengalva, M.K., Popelar, C.H., "Accelerated Performance Evaluation for Polyimide Films," *Time-Dependent Failure of Polymers: Experimental Study*, ASME, Vol. 155, 1992, pp. 15-22.

Seo, Y., Kim, Y.R., Witczak, M., Bonaquist, R., "Application of Digital Image Correlation Method to Mechanical Testing of Asphalt-Aggregate Mixtures," *Transportation Research Record: Journal of the Transportation Research Board*, Vol 1789, 2002, pp. 162-172.

Seo, Y., Kim, Y.R., Schapery, R., Witczak, M., Bonaquist, R., "A Study of Crack-Tip Deformation and Crack Growth in Asphalt Concrete Using Fracture Mechanics," *Journal of the Association of Asphalt Paving Technologists*, 73, pp. 200-228.

Section 6.1

Coffin, L. (1954). A study of the effects of cyclic thermal stresses on a ductile metal. *Transactions of the American Society of Mechanical Engineers*, Vol. 76, pp. 931-950.

Forsyth, P. (1961). A two stage process of fatigue growth. *Crack Propagation Symposium*, Cranfield, Vol. 1, pp. 76-94.

Manson, S. (1954). Behavior of materials under conditions of thermal stress. *National Advisory Committee for Aeronautics*, NACA Technical Report 1170, NACA-TR-1170.

Miner, M. (1945). Cumulative damage in fatigue. *Journal of Applied Mechanics*, Vol. 12, No. 3, pp. A159-A164.

Paris, P., Erdogan, F. (1963). A critical analysis of crack propagation laws. *Journal of Basic Engineering*, Transactions of the American Society of Mechanical Engineers, December 1963, pp.528-534.

Stubbington, C. (1963). Some observations on air and corrosion fatigue fracture surfaces of Al-7.5 Zn-2.5 Mg. *Royal Aircraft Establishment*, RAE report CPM4.

Wood, W. (1958). Recent observations on fatigue fracture in metals, *American Society of Testing Materials*, ASTM STP 237, pp. 110-121.




Section 6.2.1

- Ajideh, H., Bahia, H. and Earthman, J. (2010) "Damage Resistance and Performance Evaluations of Engineered Asphalt Materials and Asphalt-Aggregate Mixtures with High Percentage of RAP," *Research Report, City of Los Angeles and the University of California, Irvine and the University of Wisconsin, Madison*.
- Ajideh, H., Bahia, H. and Earthman, J. (2012) "Measuring Fatigue Damage Propagation of Asphalt Mixes Using Scanning Laser Detection (SLD) System," *91st Annual Meeting of the Transportation Research Board*, Washington, D.C., January 22-26.
- Chomton, G. and Valayer, P.J. (1972), "Applied Rheology of Asphalt Mixes - Practical Applications," *Proceedings, Third International Conference on the Structural Design of Asphalt Pavements*, London, England, pp. 214-225.
- Claessen, A.I.M., Edwards, J.M., Sommer, P. and Ugé, P. (1977) "Asphalt Pavement Design, The Shell Method," *Proceedings, Forth International Conference on the Structural Design of Asphalt Pavements*, Ann Arbor, Michigan, pp. 39-74.
- Deacon, J.A., Tayebali, A.A., Coplantz, J.S., Finn F.N. and Monismith C.L. (1994) "Fatigue Response of Asphalt - Aggregate Mixes: Part III Mix Design and Analysis," *Strategic Highway Research Program*, National Research Council, Washington, D.C.
- Hopman, P.C., Kunst P.A.J.C and Pronk A.C. (1989), "A Renewed Interpretation Method for Fatigue Measurement, Verification of Miner's Rule," *4th Eurobitume Symposium*, Volume 1, Madrid, 4-6 October, pp 557-561.
- Martin, J.S., Harvey, J.T., Long, F., Lee E., Monismith, C.L. and Herritt, K. (2001), "Long-Life Rehabilitation Design and Construction, I-710 Reeway, Long Beach, California," *Transportation Research Board/National Research Council, Transportation Research Circular, Number 503*, December, pp. 50-65.
- Rowe, G.M. and Boulidin, M.G. (2000), "Improved Techniques to Evaluate the Fatigue Performance of Asphaltic Mixtures," *Eurobitume - Book 1*, September, pp.754-763.
- Rowe, G.M. (1996), "Application of the Dissipated Energy Concept to Fatigue Cracking in Asphalt Pavements," *Ph.D. Thesis, University of Nottingham*, January.
- Rowe, G.M., (1993) "Performance of Asphalt Mixtures in the Trapezoidal Fatigue Test," *Journal, Association of Asphalt Paving Technologists*, Technical Sessions, Austin, Texas, March, Volume 62, pp 344-384.
- Rowe, G.M., Bennert, T., Blankenship, P., Criqui, W., Mamlouk, M., Willes, J.R., Steger, R. and Mohammad, L. (2012) "The Bending Beam Fatigue Test Improvements to test procedure definition and analysis," Presentation to the *Asphalt Mixture Expert Task Group*, Baton Rouge, LA, March 19 -20.
- Tayebali, A.A., Deacon, J.A, Coplantz, J.S. and Monismith, C.L. (1993), "Modeling Fatigue Response of Asphalt Aggregate Mixtures," *Journal, Association of Asphalt Paving Technologists*, Technical Sessions, Austin, Texas, March, Volume 62, pp 385-421.
- van Dijk, W. and Visser, W. (1977) "The Energy Approach to Fatigue for Pavement Design," *Proceedings, Association of Asphalt Paving Technologists*, Technical Sessions, San Antonio, Texas, February, Volume 46, pp 1-40.
- van Dijk, W. (1975) "Practical Fatigue Characterisation of Bituminous Mixes," *Proceedings, Association of Asphalt Paving Technologists*, Technical Sessions, Phoenix, Arizona, February, Volume 44, pp 38-74.
- van Dijk, W., Moreaud, H., Quedeveille, A. and Ugé, P. (1972) "The Fatigue of Bitumen and Bituminous Mixes," *Proceedings, Third International Conference on the Structural Design of Asphalt Pavements*, London, pp. 355-366.

Section 6.2.2

- Birgisson, B. *et al.*, "Determination of Fundamental Tensile Failure Limits of Mixtures", *Journal of the Association of Asphalt Paving Technologists*, Vol. 76, 2007, pp. 303-344.
- Isola, M. *et al.*, "Development and Validation of Laboratory Conditioning Procedures to Simulate Mixture Property Changes Effectively in the Field", *Transportation Research Record: Journal of the Transportation Research Board*, No. 2447, 2014, pp. 74-82.
- Kim, B. and Roque, R., "Evaluation of Healing Property of Asphalt Mixtures", *Transportation Research Record: Journal of the Transportation Research Board*, No. 1970, 2006, pp. 84-91.
- Kim, S. *et al.*, "Performance of Polymer-Modified Asphalt Mixtures with Reclaimed Asphalt Pavement", *Transportation Research Record: Journal of the Transportation Research Board*, No. 2126, 2009, pp. 109-114.
- Roque, R. *et al.*, "Development and Field Evaluation of Energy-Based Criteria for Top-Down Cracking Performance of Hot Mix Asphalt", *Journal of the Association of Asphalt Paving Technologists*, Vol. 73, 2004, pp. 229-260.
- Roque, R. *et al.*, "Hot Mix Asphalt Fracture Mechanics: a Fundamental Crack Growth Law for Asphalt Mixtures", *Journal of the Association of Asphalt Paving Technologists*, Vol. 71, 2002, pp. 816-827.

- 
- Roque, R. *et al.*, *Evaluation of SHRP Indirect Tension Tester to Mitigate Cracking in Asphalt Pavements and Overlays*, Final Report of Florida Department of Transportation, Gainesville, University of Florida, 1997.
- Roque, R. *et al.*, *Top-Down Cracking of HMA Layers: Models for Initiation and Propagation*, NCHRP Web-Only Document 162, National Cooperative Highway Research Program, Transportation Research Board of the National Academies, 2010.
- Sangpetngam, B., *Development and Evaluation of a Viscoelastic Boundary Element Method to Predict Asphalt Pavement Cracking*, Ph.D. Dissertation, Gainesville, University of Florida, 2003.
- Timm, D. H. *et al.*, “Forensic Investigation and Validation of Energy Ratio Concept”, *Transportation Research Record: Journal of the Transportation Research Board*, No. 2127, 2009, pp. 43-51.
- Yan, Y. *et al.*, “Evaluation of Cracking Performance for Polymer-Modified Asphalt Mixtures with High RAP Content”, *Journal of the Association of Asphalt Paving Technologists*, 2016, Accepted.
- Zhang, Z. *et al.*, “Identification and Verification of a Suitable Crack Growth Law”, *Journal of the Association of Asphalt Paving Technologists*, Vol. 70, 2001, pp. 206–241.
- Zou, J. and Roque, R., “Top-down Cracking: Enhanced Performance Model and Improved Understanding of Mechanisms”, *Journal of the Association of Asphalt Paving Technologists*, Vol. 80, 2011, pp. 255–287.
- Zou, J. *et al.*, “Effect of HMA Aging and Potential Healing on Top-Down Cracking Using HVS”, *Road Materials and Pavement Design*, Vol. 13(3), 2012, pp. 518–533.
- Zou, J. *et al.*, “Impact of Hydrated Lime on Cracking Performance of Asphalt Mixtures with Oxidation and Cyclic Pore pressure”, *Transportation Research Record: Journal of the Transportation Research Board*, 2016, Accepted.
- Zou, J. *et al.*, “Long-Term Field Evaluation and Analysis of Top-Down Cracking for Superpave Projects”, *Road Materials and Pavement Design*, Vol. 14(4), 2013, pp. 831-846.

Section 6.2.3

- Bonnetti, K.S., Nam, K., and Bahia, H.U., “Measuring and Defining Fatigue Behavior of Asphalt Binders,” *Transportation Research Board 81st Annual Meeting*, Jan., 2002, Washington, D.C.
- Carpenter, S. H., and Jansen, M. “Fatigue Behavior under New Aircraft Loading Conditions,” *Proceedings of Aircraft Pavement Technology in the Midst of Change*, 1997, pp. 259-271.
- Carpenter, S. H., and Shen, S. “A Dissipated Energy Approach to Study HMA Healing in Fatigue,” *Transportation Research Record: Journal of the Transportation Research Board*, 2006, pp. 178-185.
- Carpenter, S., Ghuzlan, K., and Shen, S. “Fatigue Endurance Limit for Highway and Airport Pavements,” *Transportation Research Record: Journal of the Transportation Research Board*, Vol. 1832, 2003, pp. 131-138.
- Daniel, J. and Bisirri, W. “Characterizing Fatigue in Pavement Materials Using a Dissipated Energy Parameter,” *Advances in Pavement Engineering*, ASCE, 2005, pp. 1-10.
- Daniel, J.S., Bisirri, W., and Kim, Y.R. “Fatigue Evaluation of Asphalt Mixtures Using Dissipated Energy and Viscoelastic Continuum Damage Approaches,” *Asphalt Paving Technology: Association of Asphalt Paving Technologists-Proceedings of the Technical Sessions*, Vol. 73, 2004, pp. 557-583.
- Ghuzlan, K. A., and Carpenter, S. H. “Fatigue Damage Analysis in Asphalt Concrete Mixtures Using the Dissipated Energy Approach,” *Canadian Journal of Civil Engineering*, Vol. 33, No. 7, 2006, pp. 890-901.
- Ghuzlan, K., and Carpenter, S. “Energy-Derived, Damage-Based Failure Criterion for Fatigue Testing,” *Transportation Research Record: Journal of the Transportation Research Board*, Vol. 1723, 2000, 141-149.
- Hopman, P.C., Kunst, P.A.J.C., and Pronk, A.C.. “A Renewed Interpretation Method for Fatigue Measurement, Verification of Miner’s Rule”, *4th Eurobitume Symposium*, Volume 1, Madrid, 4-6 October, 1989, pp. 557-561.
- Huang, B., Shu, X., and Vukosavljevic, D. “Laboratory Investigation of Cracking Resistance of Hot-Mix Asphalt Field Mixtures Containing Screened Reclaimed Asphalt Pavement,” *Journal of Materials in Civil Engineering*, Vol. 23, No. 11, 2011, pp. 1535-1543.
- Maggiore, C., Airey, G., and Marsac, P., “A Dissipated Energy Comparison to Evaluate Fatigue Resistance Using 2-Point Bending,” *Journal of Traffic and Transportation Engineering (English Edition)*, Vol. 1, No. 1, 2014, pp. 49–54.
- Nejad, F., Notash, M., and Forough, S. “Evaluation of Healing Potential in Unmodified and SBS-Modified Asphalt Mixtures Using a Dissipated-Energy Approach,” *Journal of Material Civil Engineering*, Vol. 27, No. 2, 2015.
- Pronk, A.C., and Hopman, P.C., “Energy Dissipation: The Leading Factor of Fatigue,” *In Highway Research: Sharing the Benefits (J. Porter, ed.)*, T. Telford, London, 1991.
- Prowell, B., Brown, E.R., Anderson, R.M., Shen, S., and Carpenter, S.H. “Endurance Limit of Hot Mix Asphalt Mixtures to Prevent Bottom-Up Fatigue Cracking,” *Journal of the Association of the Asphalt Paving Technologists*, Vol. 79, 2010, pp. 519-560.

- 
- Prowell, B.D., Brown, E.R., Anderson, R.M., Daniel, J.S., Von Quintus, H., Shen, S., Carpenter, S., Bhattacharjee, S., and Maghsoodloo, S. "Validating the Fatigue Endurance Limit for Hot Mix Asphalt," *NCHRP Report 646*, National Cooperative Highway Research Program, Washington, D.C., 2010.
- Rowe, G. M. "Performance of Asphalt Mixtures in the Trapezoidal Fatigue Test," *Journal of the Association of the Asphalt Paving Technologists*, Vol. 62, 1993, pp. 344-384.
- Shen, S. "Dissipated Energy Concepts for HMA Performance: Fatigue and Healing". *Ph.D. Dissertation*. Department of Civil and Environmental Engineering, University of Illinois at Urbana-Champaign, 2006.
- Shen, S. and Sutharsan, T. "Quantification of Cohesive Healing of Asphalt Binder and its Impact Factors Based on Dissipated Energy Analysis," *International Journal of Road Materials and Pavement Design*, Vol. 12, No. 3, 2011, pp. 525-546.
- Shen, S. and Xin Lu. "Energy Based Laboratory Fatigue Failure Criteria for Asphalt Materials," *ASTM Journal of Testing and Evaluation*, Vol. 39, No. 3, 2010.
- Shen, S., Airey, G.D., Carpenter, S.H., and Huang, H. "A Dissipated Energy Approach to Fatigue Evaluation". *International Journal of Road Materials and Pavement Design*, Vol. 7, No. 1, 2006, pp. 47-69.
- Shen, S., and Carpenter, S. "Application of the Dissipated Energy Concept in Fatigue Endurance Limit Testing," *Transportation Research Record Journal of the Transportation Research Board*, Vol. 1929, 2005, pp. 165-173.
- Shen, S., and Carpenter, S. H., "Development of an Asphalt Fatigue Model Based on Energy Principles," *Journal of the Association of the Asphalt Paving Technologists*, Vol. 76, 2007, pp. 525-573.
- Shen, S., Chiu, H. M., and Huang, H. "Characterization of Fatigue and Healing in Asphalt Binders," *ACSE Journal of Materials in Civil Engineering*, Vol. 22, No. 9, 2010, pp. 846-852.
- Shu, X., Huang, B., and Vukosavljevic, D. "Laboratory Evaluation of Fatigue Characteristics of Recycled Asphalt Mixture," *Construction & Building Materials*, Vol. 22, No. 7, 2008, pp. 1323-1330.
- Song, W., Shu, X., Huang, B., and Woods, M. "Laboratory Investigation of Interlayer Shear Fatigue Performance between Open-graded Friction Course and Underlying Layer," *Construction and Building Materials*, Vol. 115, No. 15, 2016, pp. 381-389.
- Wu, H., Huang, B., and Shu, X. "Characterizing Fatigue Behavior of Asphalt Mixtures Utilizing Loaded Wheel Tester". *Journal of Materials in Civil Engineering*, Vol. 26, No. 1, 2014, pp. 152-159.

Section 6.2.4

- Di Benedetto, H., Partle, M., Francken, L., La Roche, C. (2001) "Stiffness testing for bituminous mixtures, RILEM TC 182-PEB, Performance Testing and Evaluation of Bituminous Materials," *Materials and Structures/Matériaux et Constructions*, Vol. 34, pp 66-70.
- Hopman, P.C., et al., A Renewed Interpretation Method for Fatigue Measurement, Verification of Miner's Rule, 4th Eurobitume Symposium, Volume 1, Madrid, 4-6 October, London, 1989.
- Pronk, A. C., and P. C. Hopman, Energy Dissipation: The Leading Factor of Fatigue. In *Highway Research: Sharing the Benefits* (J. Porter, ed.), T. Telford, London, 1990.
- Pronk, A.C., Partial Healing: A new approach for the damage process during fatigue testing of asphalt specimen, *Proceedings of the Symposium American Society of Civil Engineering*, Baton Rouge, USA, 1995.
- Pronk, A.C., Evaluation of the dissipated energy concept for the interpretations of fatigue measurements in the crack initiation phase, *Internal report, Road and Hydraulic Engineering Division, Ministry of Transport, Public Work and Water management*, Delft, The Netherlands, 1995.
- Pronk, A.C. and Cocurullo, A., Investigation of the PH model as a prediction tool in fatigue bending tests with rest periods, *RILEM Conference Advanced Testing and Characterization of Bituminous Materials* (pp. 761-772). London: Taylor & Francis Group, 2009.
- Pronk, A.C. Analytical investigation of the correctness of formulas used in bending beam test. *Proceedings 4th International Gulf Conference on Roads*, CRC Press/Balkema, Taylor & Francis group, Doha, Qatar, 2009.
- Pronk, A.C. and Molenaar, A.A.A., The modified partial healing model used as a prediction tool for the complex stiffness modulus evolutions in four point bending fatigue tests based on the evolutions in uni-axial push-pull tests, *The 11th international conference on asphalt pavements* (pp. 1-10). Nagoya, Japan, 2010.
- Pronk, A.C., Description of a procedure for using the Modified Partial Healing model (MPH) in 4PB test in order to determine material parameters, *Proceedings of the 3rd 4PB Workshop*, Davis California, USA., 17 & 18 September 2012.
- Pronk, A.C. et al. Prediction of Wöhler curve using only one 4PB fatigue test. Is it Possible ?, *4PB Platform*, <http://www.civil.uminho.pt/4pb/acp-f-model.htm>, 2015.

- Pronk, A.C., Pseudo Healing due to thixotropy in 4PB tests with rest periods, *4PB Platform*, <http://www.civil.uminho.pt/4pb/acp-f-model.htm>, 2016.
- van Dijk, W. and Visser, W., The Energy Approach to Fatigue for Pavement Design, *Proceedings, Association of Asphalt Paving Technologists*, Technical Sessions, San Antonio, Texas, Volume 46, pp 1-40, 1977.

Section 6.3

- Kachanov, L. M., "On the Creep Rupture Time," *Izv. AN SSSR, Otd. Tekhn. Nauk*, Vol 8, 1958, pp. 26–31.
- Krajcinovic, D. K., "Continuum damage mechanics," *Applied Mathematics Reviews*, Vol 37, No 1, 1984, pp. 16.
- Lemaitre, J. and Chaboche, J. L., "Aspect Phénoménologique de la Rupture Par Endommagement," *Journal Méc Appl*, Vol 2, No 3, 1978, pp. 317-365.
- Murakami, S., "Notion of Continuum Damage Mechanics and its Application to Anisotropic Creep Damage Theory," *Journal of Engineering Materials and Technology*, Vol 105, No 2, 1983, pp. 99-105.
- Murzewski, J., "Une Théorie Stastique du Corps Fragile Quasi-Homogène," *IX-e Congrès International de Méchanique Appliquée. Univ. de Bruxelles*, Vol. 5, 1957, pp 313-320.
- Rabotnov, Y. N., "Mechanism of Long-Term Fracture," *Problems of Strength of Materials and Structures*, 1959, pp. 5–7.

Section 6.3.1

- Chehab, G. R., Kim, Y. R., Schapery, R. A., Witczack, M. and Bonaquist, R., "Time-Temperature Superposition Principle for Asphalt Concrete Mixtures with Growing Damage in Tension State," *Journal of the Association of Asphalt Paving Technologists*, Vol. 71, 2002, pp. 559-593.
- Daniel, J. S. and Kim, Y. R., "Development of a Simplified Fatigue Test and Analysis Procedure Using a Viscoelastic Continuum Damage Model," *Journal of the Association of Asphalt Paving Technologists*, Vol. 71, 2002, pp. 619-650.
- Gibson, N., "A Viscoelastoplastic Continuum Damage Model for the Compressive Behavior of Asphalt Concrete," *Ph.D. Dissertation*, University of Maryland, College Park, MD, 2006.
- Hou, E.T., Underwood, B. S., and Kim, Y.R., "Fatigue Performance Prediction of North Carolina Mixtures Using the Simplified Viscoelastic Continuum Damage Model," *Journal of the Association of Asphalt Paving Technologists*, Vol. 79, 2010, pp. 35-80.
- Kim, Y.R. and Little, D. N., "One-Dimensional Constitutive Modeling of Asphalt Concrete," *ASCE Journal of Engineering Mechanics*, Vol. 116, No. 4, 1990, pp. 751-772.
- Kim, Y. R., Allen, D., and Little, D. N., "Computational Model to Predict Fatigue Damage Behavior of Asphalt Mixtures under Cyclic Loading," *Transportation Research Record: Journal of the Transportation Research Board*, Vol. 1970, 2006, pp. 196-206.
- Kim, Y. R., Baek, C., Underwood, B. S., Subramanian, V., Guddati, M. N. and Lee, K., "Application of Viscoelastic Continuum Damage Model Based Finite Element Analysis to Predict the Fatigue Performance of Asphalt Pavements," *KSCE Journal of Civil Engineering*, Vol. 12, No. 2, 2008, pp. 109-120.
- Kim, Y. R., Guddati, M. N., Choi, Y. T., Kim, D., Norouzi, A., and Wang, Y., Hot Mix Asphalt Performance-Related Specifications (HMA-PRS) Based on Viscoelastoplastic Continuum Damage (VEPCD) Models, Final Report to Federal Highway Administration, Project No. DTFH61-08-H-00005, 2016.
- Kutay, M.E., Gibson, N., and Youtcheff, J., "Conventional and Viscoelastic Continuum Damage (VECD) Based Fatigue Analysis of Polymer Modified Asphalt Pavements," *Journal of the Association of Asphalt Paving Technologists*, Vol. 77, 2008, pp. 395-434.
- Lacroix, A. T., "Performance Prediction of the NCAT Test Track Pavements Using Mechanistic Models," *Ph.D. Dissertation*, North Carolina State University, Raleigh, NC, 2013.
- Lee, H.J. and Kim, Y.R., "A Uniaxial Viscoelastic Constitutive Model for Asphalt Concrete under Cyclic Loading," *ASCE Journal of Engineering Mechanics*, Vol. 124, No. 1, 1998a, pp. 32-40.
- Lee, H.J. and Kim, Y.R., "A Viscoelastic Continuum Damage Model of Asphalt Concrete with Healing," *ASCE Journal of Engineering Mechanics*, Vol. 124, No. 11, 1998b, pp. 1224-1232.
- Lundström, R. and Isacsson, U., "Linear viscoelastic and fatigue characteristics of styrene-butadiene-styrene modified asphalt mixtures," *Journal of materials in civil engineering*, Vol. 16, No. 6, 2004, pp. 629-638.
- Nascimento, L.A.H.D., "Implementation and Validation of the Viscoelastic Continuum Damage Theory for Asphalt Mixture and Pavement Analysis in Brazil," *Ph.D. Dissertation*, North Carolina State University, Raleigh, NC, 2015.
- Norouzi, A. and Kim, Y. R., "Mechanistic Evaluation of Fatigue Cracking in Asphalt Pavements," *International Journal of Pavement Engineering*, Vol. 1, No. 17, 2015, pp. 1-17.



- Sabouri, M. and Kim, Y. R., "Development of a Failure Criterion for Asphalt Mixtures Under Different Modes of Fatigue Loading," *Transportation Research Record: Journal of the Transportation Research Board*, Vol. 2447, 2014, pp. 117-125.
- Sabouri, M., Bennert, T., Daniel, J. S., and Kim, Y. R., "A Comprehensive Evaluation of the Fatigue Behaviour of Plant-Produced RAP Mixtures," *Road Materials and Pavement Design*, Vol. 16, 2015, pp. 29-54.
- Schapery, R. A., "Effect of Cyclic Loading on the Temperature in Viscoelastic Media with Variable Properties," *AIAA Journal*, Vol. 2, No. 5, 1964, pp. 827-835.
- Schapery, R. A., "A theory of crack initiation and growth in viscoelastic media," *International Journal of Fracture*, Vol. 11, No. 1, 1975, pp. 141-159.
- Schapery, R.A., "On Viscoelastic Deformation and Failure Behavior of Composite Materials with Distributed Flaws," *Advances in Aerospace Structures and Materials*, ASME, New York, 1981, pp. 5-20.
- Schapery, R.A., "Deformation and Fracture Characterization of Inelastic Composite Materials using Potentials," *Polymer Engineering and Science*, Vol. 27, No. 1, 1987, pp. 63-76.
- Schapery, R. A., "Nonlinear Viscoelastic and Viscoplastic Constitutive Equations Based on Thermodynamics," *Mechanics of Time-Dependent Materials*, Vol. 1, No. 2, 1997, pp. 209-240.
- Schapery, R.A., "Nonlinear Viscoelastic and Viscoplastic Constitutive Equations with Growing Damage," *International Journal of Fracture*, Vol. 97, No. 1, 1999, pp. 33-66.
- Underwood, B. S., Kim, Y. R., and Guddati, M. N., "Characterization and Performance Prediction of ALF Mixtures Using a Viscoelastoplastic Continuum Damage Model," *Journal of the Association of Asphalt Paving Technologists*, Vol. 75, 2006, pp. 577-636.
- Underwood, B. S., Kim, Y. R., and Guddati, M. N., "Improved Calculation Method of Damage Parameter in Viscoelastic Continuum Damage Model," *International Journal of Pavement Engineering*, Vol. 11, No. 6, 2010, pp. 459-476.
- Wang, Y., Norouzi, A. and Kim, Y. R., "Comparison of Fatigue Cracking Performance of Asphalt Pavements Predicted by Pavement ME and LVECD Programs," *Transportation Research Record: Journal of the Transportation Research Board*, Vol. 2590, 2016, pp. 44-55.
- Xie, Z. and Shen, J., "Fatigue Performance of Rubberized Stone Matrix Asphalt by a Simplified Viscoelastic Continuum Damage Model," *Journal of Materials in Civil Engineering*, Vol. 28, No. 4, 2015,
- Yun, T., Underwood, B. S. and Kim, Y. R., "Time-Temperature Superposition for HMA with Growing Damage and Permanent Strain in Confined Tension and Compression," *Journal of Materials in Civil Engineering*, Vol. 22, No. 5, 2009, pp. 415-422.
- Zhang, J., Sabouri, M., Guddati, M. N., and Kim, Y. R., "Development of a Failure Criterion for Asphalt Mixtures under Fatigue Loading," *Road Materials and Pavement Design*, Vol 14, 2013, pp. 1-15.
- Zhao, Y. and Kim, Y. R., "Time-Temperature Superposition for Asphalt Mixtures with Growing Damage and Permanent Deformation in Compression," *Transportation Research Record: Journal of the Transportation Research Board*, Vol. 1832, 2003, pp. 161-172.

Section 6.3.2

- AFNOR. NF EN 12697-24 (2012). Méthodes d'essai pour mélange hydrocarboné à chaud – Partie 24 : résistance à la fatigue.
- AFNOR. NF P98-086 (2011). Dimensionnement structurel des chaussées routières – Application aux chaussées neuves.
- Bodin, D. (2002) Modèle d'endommagement cyclique : Applications à la fatigue des enrobés bitumineux. *PhD, EC Nantes*, University of Nantes.
- De la Roche C., Charrier J., Marsac P., Molliard J.-M. (2001) Evaluation de l'endommagement par fatigue des enrobés bitumineux, apport de la thermographie infrarouge. *Bulletin des laboratoires des Ponts et Chaussées* 232.
- De la Roche C., Odeon H., Simoncelli J.-P., Spornol A. (1994) Study of the fatigue of asphalt mixes using the circular test track of the laboratoire Central des Pont et Chaussées in Nantes. *Transportation Research Record: Journal of the Transportation Research Board*, Vol. 1436, pp. 17-27.
- De la Roche C., Rivière N. (1997) Fatigue behavior of asphalt mixes – Influence of test procedures on Laboratory Fatigue Performances. *8th International Conference on Asphalt Pavement*, Seattle, WA, pp. 889-917.
- Di Benedetto H, Nguyen QT, Sauzéat C (2011) Nonlinearity, heating, fatigue and thixotropy during cyclic loading of asphalt mixtures. *Road Materials and Pavement Design*, 12(1), pp. 129–158.
- Di Benedetto H, Soltani A., Chaverot P. (1996). Fatigue damage for bituminous mixtures: a pertinent approach. *Journal of the Association of Asphalt Paving Technologists*, Vol. 65, pp. 142-158.



- Di Benedetto H., de la Roche C., Baaj H., Pronk H., Lundstrom R. (2004) Fatigue of bituminous mixtures. *Materials and Structures*, Vol 37, Issue 3, pp. 202-216.
- Doan T. H. (1977) Les études de fatigue des enrobés bitumineux au LCPC. Bulletin de liaison des laboratoires des ponts et Chaussées, n° special : *Bitume et enrobés bitumineux*.
- Francken L., Hopman P., Partl M., de la Roche C. (1996) Rilem interlaboratory tests on bituminous mixes in repeated loadings. Teachings and recommendations. *1st Eurasphalt & Eurobitume Congress*.
- Mangiafico S., Sauzeat C., Di Benedetto H., Pouget S., Olard F., Planque L. (2015) Quantification of biasing effects during fatigue tests on asphalt mixes: non-linearity, self-heating and thixotropy. *Road Materials and Pavement Design*, Vol.16 Special Issue, pp. 73-99.
- Miner M. A. (1945) Cumulative damage in fatigue. *Journal Applied Mechanics*, Vol. 12, pp. A156-A164..
- Moutier F. (1991) Etude statistique de la composition des enrobes bitumineux sur leur comportement en fatigue complexe. *Bulletin de liaison des laboratoires des Ponts et Chaussées* 172.
- Nguyen Q. T., Di Benedetto H. & Sauzéat C. (2012) Determination of thermal properties of asphalt mixtures as another output from cyclic tension-compression test. *Road Materials and Pavement Design*, Vol. 13, pp. 85-103.
- Nguyen Q.T., Di Benedetto H., Sauzéat C. (2015) Effect of fatigue cyclic loading on linear viscoelastic properties of bituminous mixtures. *Journal of Materials in Civil Engineering*, 27(8), C4014003.
- Odéon H., Caroff G. (1997) Asphalt mix fatigue behaviour: experimental structures and modelling. *8th International Conference on Asphalt Pavement*, Seattle, WA, pp. 881-897.
- SETRA. (1994) Guide technique de conception et des dimensionnements des structures de chaussées. *SETRA/LCPC*.
- Tapsoba N, Sauzéat C., Di Benedetto H. (2013) Analysis of fatigue test for bituminous mixtures. *Journal of Materials in Civil Engineering*, 25(6), pp. 701–710.
- Tapsoba N., Sauzeat C., Di Benedetto H., Baaj H., Ech M. (2015) Three-dimensional analysis of fatigue tests on bituminous mixtures. *Fatigue & Fracture of Engineering*, 38(6), pp. 730-741.

Section 6.3.3

- Christensen, D. W. and Bonaquist, R. F. (2012) “Modeling of Fatigue Damage Functions for Hot Mix Asphalt and Applications to Surface Cracking,” *Journal of the Association of Asphalt Paving Technologists*, Vol. 81, pp. 241-271.
- Christensen, D. W., and Bonaquist, R. F. (2006) “Practical Application of Continuum Damage Theory to Fatigue Phenomena in Asphalt Concrete Mixtures,” *Journal of the Association of Asphalt Paving Technologists*, Vol. 74, pp. 963-1002.
- Christensen, D. W., and Bonaquist, R. F. (2014) Design Guidance for Fatigue and Rut Resistant Mixtures, *Asphalt Research Consortium Report U*.
- Christensen, D. W., and Bonaquist, R. R., (2009) “Analysis of HMA Fatigue Data Using the Concepts of Reduced Loading Cycles and Endurance Limit,” *Journal of the Association of Asphalt Paving Technologists*, Vol. 78, pp. 377-400.
- Kim, Y. R., Little, D. N., and Lytton, R. L. (2012), “Use of Dynamic Mechanical Analysis (DMA) to Evaluate the Fatigue and Healing Potential of Asphalt Binders in Sand Asphalt Mixtures,” *Journal of the Association of Asphalt Paving Technologists*, Vol. 71, pp. 176-199.

Section 6.3.4

- Abu Al-Rub, R.K., Darabi, M.K., 2012. A thermodynamic framework for constitutive modeling of time- and rate-dependent materials, Part I: Theory. *International Journal of Plasticity*, Vol. 34, 61-92.
- Abu Al-Rub, R.K., Darabi, M.K., Little, D.N., Masad, E.A., 2010. A micro-damage healing model that improves prediction of fatigue life in asphalt mixes. *International Journal of Engineering Science*, Vol. 48, No. 11, 966-990.
- Caro, S., Castillo, D., Darabi, M., Masad, E., 2016. Influence of different sources of microstructural heterogeneity on the degradation of asphalt mixtures. *International Journal of Pavement Engineering*, 1-15.
- Castillo, D., Caro, S., Darabi, M., Masad, E., 2016. Modelling moisture-mechanical damage in asphalt mixtures using random microstructures and a continuum damage formulation. *Road Materials and Pavement Design*, 1-21.
- Coleman, B.D., 1964. Thermodynamics of materials with memory. *Archive for Rational Mechanics and Analysis* 17, 1-46.



- Darabi, M.K., Abu Al-Rub, R.K., Little, D.N., 2012 (b). A Continuum damage mechanics-based framework for modeling micro-damage healing. *International Journal of Solids and Structures*, Vol. 49, No. 3-4, 492-513.
- Darabi, M.K., Abu Al-Rub, R.K., Masad, E. A., Little, D.N., 2013. Constitutive modeling of fatigue damage response of asphalt concrete materials with consideration of micro-damage healing. *International Journal of Solids and Structures*, Vol. 50, 2901-2913.
- Darabi, M.K., Abu Al-Rub, R.K., Masad, E.A., Huang, C.W., Little, D.N., 2012(a). A modified viscoplastic model to predict the permanent deformation of asphaltic materials under cyclic-compression loading at high temperatures. *International Journal of Plasticity*, Vol. 35, 100-134, 2012 (a).
- Darabi, M.K., Abu Al-Rub, R.K., Masad, E.A., Little, D.N., 2011. A thermo-viscoelastic-viscoplastic-viscodamage constitutive model for asphaltic materials. *International Journal of Solids and Structures*, Vol. 48, No. 1, 191-207.
- Dessouky, S.H., 2005. Multiscale approach for modeling hot mix asphalt. *Ph.D. Dissertation*, Texas A&M University.
- Kachanov, L.M., 1958. On time to rupture in creep conditions (in russian). *Izvestia Akademii Nauk SSSR, Otdelenie Tekhnicheskikh Nauk* 8, 26-31.
- Little, D.N., Bhasin, A., 2007. Exploring mechanisms of healing in asphalt mixtures and quantifying its impact. In: van der Zwaag, S. (Ed.). *Self healing materials*. Springer, Dordrecht, The Netherlands, 205-218.
- Masad, E., Tashman, L., Little, D., Zbib, H., 2005. Viscoplastic modeling of asphalt mixes with the effects of anisotropy, damage and aggregate characteristics. *Mechanics of Materials* 37, 1242-1256.
- Perzyna, P., 1971. Thermodynamic theory of viscoplasticity. *Advances in Applied Mechanics* 11, 313-354.
- Rushing, J.F., Darabi, M.K., Rahmani, E., Little, D.N., 2015. Comparing rutting of airfield pavements to simulations using Pavement Analysis using Nonlinear Damage Approach (PANDA), *International Journal of Pavement Engineering*, DOI: 10.1080/10298436.2015.10390074.
- Schapery, R.A., 1969. Further development of a thermodynamic constitutive theory: Stress formulation. Purdue University, *Purdue Research Foundation*, Lafayette, IN.
- Tashman, L., Masad, E., Little, D., Zbib, H., 2005. A microstructure-based viscoplastic model for asphalt concrete. *International Journal of Plasticity* 21, 1659-1685.

Section 6.4.1

- Griffith, A. 1920. The phenomena of rupture and flow in solids. *Philosophical Transactions. Series A*, Vol. 221, pp. 163-198.
- Inglis, C. 1913. Stresses in a plate due to the presence of cracks and sharp corners. *Transactions of the Institute of Naval Architects*, Vol. 55, pp. 219-241.
- Irwin, G. 1957. Analysis of stresses and strains near the end of a crack traversing a plate. *Journal of Applied Mechanics*, Vol. 24, pp. 361-364.
- Majidzadeh, K. Kauffmann, E., Saraf, C. 1972. Analysis of fatigue of paving mixtures from the fracture mechanics viewpoint, *Fatigue of Compacted Bituminous Aggregate Mixtures*, ASTM STP 508, American Society for Testing and Materials, pp. 67-83.
- Sneddon, I. 1946. The distribution of stress in the neighbourhood of a crack in an elastic solid. *Proceedings, Royal Society of London*, Vol. A-189, pp. 229-260.
- Sulaiman, S., Stock, A. 1995. The use of fracture mechanics for the evaluation of asphalt mixes, *Journal of the Association of Asphalt Paving Technologists*, Vol. 64, pp. 417-454.
- Westergaard, H. 1939. Bearing pressures and cracks. *Journal of Applied Mechanics*, Vol. 6, pp. 49-53.
- Williams, M. 1957. On the stress distribution at the base of a stationary crack. *Journal of Applied Mechanics*, Vol. 24, pp. 109-114.

Section 6.4.2

- Glover, C., X. Luo, A. Rose, R.L. Lytton (2016). "On Fundamentals-Based Modeling of Binder Oxidative Hardening in Pavements and Its Effects on Mixture Durability." *Proceedings of 2016 International Society for Asphalt Pavements Symposium*, Jackson Hole, Wyoming, July 18-21.
- Luo, R., and R. L. Lytton (2010). "Characterization of the Tensile Viscoelastic Properties of an Undamaged Asphalt Mixture." *Journal of Transportation Engineering*, 136(3), 173-180.
- Luo, X., R. Luo, and R.L. Lytton (2013a). "Characterization of Asphalt Mixtures Using Controlled-Strain Repeated Direct Tension Test." *Journal of Materials in Civil Engineering*, Vol. 25, No. 2, pp.194-207.
- Luo, X., R. Luo, and R.L. Lytton (2013b). "Characterization of Fatigue Damage in Asphalt Mixtures Using Pseudo Strain Energy." *Journal of Materials in Civil Engineering*, Vol. 25, No. 2, pp.208-218.



- Luo, X., R. Luo, and R.L. Lytton (2013c). "Energy-Based Mechanistic Approach to Characterize Crack Growth of Asphalt Mixtures." *Journal of Materials in Civil Engineering*, Vol. 25, No. 9, pp.1198-1208.
- Luo, X., R. Luo, and R.L. Lytton (2013d). "A Modified Paris' Law to Predict Entire Crack Growth in Asphalt Mixtures." *Transportation Research Record: Journal of the Transportation Research Board*, No. 2373, pp. 54–62.
- Luo, X., R. Luo, and R.L. Lytton (2014a). "Energy-Based Mechanistic Approach for Damage Characterization of Pre-Flawed Visco-Elasto-Plastic Materials." *Mechanics of Materials*, Vol. 70, pp.18-32.
- Luo, X., R. Luo, and R.L. Lytton (2014b). "Energy-Based Crack Initiation Criterion for Visco-Elasto-Plastic Materials with Distributed Cracks." *Journal of Engineering Mechanics*, Vol.141, No. 2, p. 04014114.
- Luo, X., Y. Zhang, and R.L. Lytton (2016). "Implementation of Pseudo J-Integral Based Paris' Law for Fatigue Cracking in Asphalt Mixtures and Pavements." *Materials and Structures*, Vol. 49, No. 9, pp. 3713-3732.
- Schapery, R.A. (1975). "A Theory of Crack Initiation and Growth in Viscoelastic Media I. Theoretical Development." *International Journal of Fracture*, 11(1), 141-159.
- Schapery, R.A. (1984). "Correspondence Principles and a Generalized J Integral for Large Deformation and Fracture Analysis of Viscoelastic Media." *International Journal of Fracture*, 25, 195-223.
- Zhang, Y., R. Luo, and R.L. Lytton (2012). "Characterizing Permanent Deformation and Fracture of Asphalt Mixtures by Using Compressive Dynamic Modulus Tests." *Journal of Materials in Civil Engineering*, 24(7), 898-906.
- Zhang, Y., R. Luo, and R.L. Lytton (2013). "Mechanistic Modeling of Fracture in Asphalt Mixtures under Compressive Loading." *Journal of Materials in Civil Engineering*, 25(9), 1189-1197.
- Zhang, Y., X. Luo, R. Luo, and R.L. Lytton (2014). "Crack Initiation in Asphalt Mixtures under External Compressive Loads." *Construction and Building Materials*, 72, 94-103.
- Zhang, Y., F. Gu, B. Birgisson, and R.L. Lytton (2016). "Coupled Modelling of Deformation and Cracking of Asphalt Mixtures." *Proceeding of ISAP 2016 Symposium*, Wyoming, USA, July 18-21.

Section 6.4.3

- Abdulshafi, A. and Kaloush, K. (1988) "Modifiers for Asphalt Concrete, ESL-TR-88-29", *Air Force Engineering and Technical Services Center*, Tyndall Air Force Base, Florida.
- Abdulshafi, O. (1992) "Effect of Aggregate on Asphalt Mixture Cracking Using Time-Dependent Fracture Mechanics Approach". *Effects of aggregate and Mineral Fillers on Asphalt Mixture Performance*, ASTM STP1147-EB, American Society for Testing and Materials, Philadelphia.
- Abdulshafi, O. (1983) "Rational Material Characterization of Asphaltic Concrete Pavements," *Ph.D. Dissertation*, The Ohio State University.
- Anderson, T.L. (2005) *Fracture Mechanics 3rd Edition, Fundamentals and Applications*. Boca Raton, FL: *Taylor and Francis*.
- Kaloush, K., Biligiri, K., Zeiada, W., Rodezno, M., & Reed, J. (2010) "Evaluation of Fiber-Reinforced Asphalt Mixtures Using Advanced Material Characterization Tests." *ASTM Journal of Testing and Evaluation*, 38(4), pp. 1-12.
- Landes, J.D. & Begley, J. (1976), "A Fracture Mechanics Approach to Creep Crack Growth." *Mechanics of Crack Growth; Proceedings of the Eighth National Symposium on Fracture Mechanics*, 590, pp. 128-148.
- Stempihar, Jeffrey J. (2013) "Development of the C* Fracture Test for Asphalt Concrete Mixtures," *Ph.D. Dissertation*, Arizona State University.
- Vinson, T.S, Janoo, V. & Haas, R. (1989) Low Temperature and Thermal Fatigue Cracking, *SHRP-A-306, Strategic Highway Research Program*, Transportation Research Board, Washington D.C.
- Wu, D., Christian, E.M. & Ellison E.G. (1984), "Evaluation of Creep Crack C* Integrals." *Journal of Strain Analysis*, 19 (3), pp. 185-195.

Section 7.0


- Ayar, P., Moreno-Navarro, F. and Rubio-Gámez, M. C., "The Healing Capability of Asphalt Pavements: a State of the Art Review," *Journal of Cleaner Production*, Vol 113, 2016, pp. 28-40.
- Balbissi, A.H., "A comparative Analysis of the Fracture and Fatigue Properties of Asphalt Concrete and Sulphex," *Ph.D. Dissertation*, Texas A&M University, College Station, Texas, 1983.
- Bazin, P. and Saunier, J., "Deformability, Fatigue and Healing Properties of Asphalt Mixes," *Intl Conf Struct Design Asphalt Pvmnts*, 1967, January



- Bommavaram, R., Bhasin, A. and Little, D., "Determining Intrinsic Healing Properties of Asphalt Binders: Role of Dynamic Shear Rheometer," *Transportation Research Record: Journal of the Transportation Research Board*, Vol 2126, 2009, pp. 47-54.
- Carpenter, S. and Shen, S., "Dissipated Energy Approach to Study Hot-Mix Asphalt Healing in Fatigue," *Transportation Research Record: Journal of the Transportation Research Board*, Vol 1970, 2006, pp. 178-185.
- Finn, F., Sarf, C., Kulkarni, K., Smith, W. and Adullah, A., "The use of Prediction Subsystems for the Design of Pavement Structures, in Proceedings," *Fourth International Conference on Structural Design of Asphalt Pavements*, (1977), pp. 3-38.
- Kim, B. and Roque, R., "Evaluation of Healing Property of Asphalt Mixtures," *Transportation Research Record: Journal of the Transportation Research Board*, Vol 1970, 2006, pp. 84-91.
- Kim, Y.R., Little, D.N. and Benson, F.C., 1990, "Chemical and Mechanical Evaluation on Healing Mechanism of Asphalt Concrete," *Journal of the Association of Asphalt Paving Technologists*, 59, pp. 240-275.
- Lee, H. J. and Kim, Y. R., "Viscoelastic Continuum Damage Model of Asphalt Concrete with Healing," *Journal of Engineering Mechanics*, Vol 124, No 11, 1998, pp. 1224-1232.
- Little, D. N., Lytton, R. L., Williams, D. and Kim, Y. R., "Propagation and Healing of Microcracks in Asphalt Concrete and their Contributions to Fatigue," In: *Asphalt Science and Technology*, Ed. A.M. Usmani, 1997, pp. 149-195. Marcel Dekker, New York.
- Little, D.N., Lytton, R.L., Williams, A.D. and Chen, C.W., "Microdamage Healing in Asphalt and Asphalt Concrete, Vol I: Microdamage and Microdamage Healing," Final report: *FHWA-RD-98-141*, Texas Transportation Institution, College Station, Texas, 2001.
- Little, D. N. and Bhasin, A., "Exploring Mechanism of Healing in Asphalt Mixtures and Quantifying its Impact," *Self Healing Materials*, 2007, pp. 205-218. Springer Netherlands.
- Lytton, R., Uzan, J., Fernando, E.G., Roque, R. and Hiltunen, D., "Development and Validation of Performance Prediction Models and Specifications for Asphalt Binders and Paving Mixes," *Report No. SHRP-A-357. Strategic Highway Research Program*, 1993.
- Raithby, K. D. and Sterling, A. B., "Some Effects of Loading History on the Performance of Rolled Asphalt," *Transport and Road Research Laboratory, Report TRRLR496, Crowthorne, England*, 1972.
- Witzak, M. W., "Pavement Performance Models; Repeated Load Fracture of Pavement Systems," *Report No. FAA-RD-75-2771. U.S. Army Engineer Waterways Experiment Station*, Vol 1, 1976.
- Wool, R.P. and O'Connor, K.M., "A Theory of Crack Healing in Polymers," *Journal of Applied Physics*, Vol 52, No 10, 1981, pp. 5953-5963.

Section 7.1

- Ashouri, M., "Modeling Microdamage Healing in Asphalt Pavements Using Continuum Damage Theory," *Ph.D. Dissertation*, North Carolina State University, Raleigh, NC, 2014.
- Carpenter, S. and Shen, S., "Dissipated Energy Approach to Study Hot-Mix Asphalt Healing in Fatigue," *Transportation Research Record: Journal of the Transportation Research Board*, Vol 1970, 2006, pp. 178-185.
- Daniel, J. S. and Kim, Y. R., "Laboratory Evaluation of Fatigue Damage and Healing of Asphalt Mixtures," *ASCE Journal of Materials in Civil Engineering*, Vol 13, No 6, 2001, pp. 434-440.
- Kim, B. and Roque, R., "Evaluation of Healing Property of Asphalt Mixtures," *Transportation Research Record: Journal of the Transportation Research Board*, Vol 1970, 2006, pp. 84-91.
- Kim, Y. R., Little, D. N. and Lytton, R. L., "Fatigue and Healing Characterization of Asphalt Mixtures," *ASCE Journal of Materials in Civil Engineering*, Vol 15, No1, 2003, pp. 75-83.
- Kim, Y. R., Little, D. N. and Lytton, R. L., "Use of Dynamic Mechanical Analysis (DMA) to Evaluate the Fatigue and Healing Potential of Asphalt Binders in Sand Asphalt Mixtures," *Journal of the Association of Asphalt Paving Technologists*, Vol 71, 2002, pp. 176-206.
- Kim, Y. R., "Evaluation of Healing and Constitutive Modeling of Asphalt Concrete by Means of the Theory of Nonlinear Viscoelasticity and Damage Mechanics," *Ph.D. Dissertation*, Texas A&M University, College Station, TX, 1988.
- Kim, Y.R., Little, D.N. and Benson, F.C., 1990, "Chemical and Mechanical Evaluation on Healing Mechanism of Asphalt cConcrete," *Journal of the Association of Asphalt Paving Technologists*, 59, pp. 240-275.
- Karki, P., "An Integrated Approach to Measure and Model Fatigue Damage and Healing in Asphalt Composites," *Ph.D. Dissertation*, University of Texas-Austin, TX, 2014.
- Lee, H. J. and Kim, Y. R., "Viscoelastic continuum damage model of asphalt concrete with healing," *Journal of Engineering Mechanics*, Vol 124, No 11, 1998, pp. 1224-1232.

- 
- Roque, R., Zou, J., Kim, Y. R., Baek, C., Thirunavukkarasu, S., Underwood, B. S. and Guddati, M. N., “Top-Down Cracking of Hot-Mix Asphalt Layers: Models for Initiation and Propagation,” Final Report NCHRP 1-42A, National Cooperative Highway Research Program, *Transportation Research Board of the National Academies*, 2010.
- Underwood, B.S. and Zeiada, W., “Characterization of Microdamage Healing in Asphalt Concrete with a Smeared Continuum Damage Approach,” *Transportation Research Record: Journal of the Transportation Research Board*, Vol 2447, 2014, pp. 126-135.

Section 7.2

- Ahlquist, C. N. and W. D. Nix (1971). “The Measurement of Internal Stresses during Creep of Al and Al-Mg Alloys.” *Acta Metallurgica*, Vol. 19, No. 4, pp.373-385.
- Luo, X., R. Luo, and R.L. Lytton (2013a). “Characterization of Recovery Properties of Asphalt Mixtures.” *Construction and Building Materials*, Vol. 48, pp. 610-621.
- Luo, X., R. Luo, and R.L. Lytton (2013b). “Characterization of Fatigue Damage in Asphalt Mixtures Using Pseudo Strain Energy.” *Journal of Materials in Civil Engineering*, Vol. 25, No. 2, pp.208-218.
- Luo, X., R. Luo, and R.L. Lytton (2014a). “Energy-Based Mechanistic Approach for Damage Characterization of Pre-Flawed Visco-Elasto-Plastic Materials.” *Mechanics of Materials*, Vol. 70, pp.18-32.
- Luo, X., R. Luo, and R.L. Lytton (2014b). “Energy-Based Crack Initiation Criterion for Visco-Elasto-Plastic Materials with Distributed Cracks.” *Journal of Engineering Mechanics*, Vol.141, No. 2, p. 04014114.
- Luo, X., R. Luo, and R.L. Lytton (2015a). “Mechanistic Modeling of Healing in Asphalt Mixtures Using Internal Stress.” *International Journal of Solids and Structures*, Vol. 60-61, pp. 35-47.
- Luo, X., and R.L. Lytton (2015b). “Characterization of Healing of Asphalt Mixtures Using Creep and Step-loading Recovery Test.” *Journal of Testing and Evaluation*, doi:10.1520/JTE20150135.
- Teoh, S. H, C. L. Chuan, and A. N. Poo (1987). “Application of a Modified Strain Transient Dip Test in the Determination of the Internal Stresses of PVC under Tension.” *Journal of Materials Science*, Vol. 22, No. 4, pp.1397-1404.

Section 8

- Di Benedetto, H., de La Roche, C., Baaj, H., Pronk, A., Lundström, R. (2004). Fatigue of bituminous mixtures. *Materials and Structures*, Vol. 37, pp. 202-216.
- Molenaar, A. (2007). Prediction of fatigue cracking in asphalt pavements, do we follow the right approach? *Transportation Research Record*, No.2001, pp. 155-162.
- Mogawer, W. S., Austerman, A., Roque, R., Underwood, S., Mohammad, L., & Zou, J. (2015). Ageing and rejuvenators: evaluating their impact on high RAP mixtures fatigue cracking characteristics using advanced mechanistic models and testing methods. *Road Materials and Pavement Design*, 16(sup2), pp. 1-28.
- Zhou, F., Newcomb, D., Gurganus, C., Banihashemrad, S., Park, E., Sakhaeifar, M., Lytton, R. (2016). Experimental design for field validation of laboratory tests to assess cracking resistance of asphalt mixtures. *National Cooperative Highway Research Program*, NCHRP 9-57, draft final report.